UNIVERSITÉ DE STRASBOURG

ÉCOLE DOCTORALE DES SCIENCES CHIMIQUES ED222
Institut Charles Sadron – CMP

THÈSE présentée par :

Olga SISCAN

soutenue le : **19 février 2015**

pour obtenir le grade de : **Docteur de l'université de Strasbourg**
Discipline/ Spécialité : Chimie des Polymères

Single-chain technology using sequence-controlled precursors

THÈSE dirigée par :

[M. LUTZ Jean-François]	Directeur de Recherche CNRS, ICS, Strasbourg

RAPPORTEURS :

[M. MEIER Michael]	Professeur, Karlsruhe Institute of Technology
[M. WOISEL Patrice]	Professeur, Université Lille1

EXAMINATEURS :

[M. GRANDE Daniel]	Directeur de Recherche CNRS, ICMPE Paris-Est
[M. BOUQUEY Michel]	Maitre de Conférences, ICS, Strasbourg
[Mme MOULIN Emilie]	Chargée de Recherche CNRS, ICS, Strasbourg

ACKNOWLEDGEMENTS

I would like to express my gratitude to all the people who contributed in some way to the work described in this thesis. Foremost, I sincerely thank my academic advisor, Dr. Jean-François Lutz, for accepting me into the PMC group. You gave me fascinating projects, contributed to my development as a chemist (and more generally, as a scientist) and supported my attendance at various conferences. Furthermore, I express my gratitude to Pr. David Leigh, Pr. Marc A. Gauthier, Pr. Hans Börner, and Dr. Guillaume De Bo for their collaboration, for involving me into interesting projects and providing insightful discussions about the research.

This thesis could not see the light without the members of my PhD jury, Pr. Patrice Woisel, Pr. Michael Meier, Dr. Daniel Grande, Dr. Michel Bouquey and Dr. Emilie Moulin. I thank you for spending time to evaluate the manuscript carefully, for your helpful suggestions and thoughtful questions.

I am very grateful to all PMC members, especially to Dr. Delphine Chan-Seng: you are an inexhaustible source of scientific knowledge. I thank you for getting my endless questions (scientific and not only ☺) answered. I wish I could be as zen and wise as you are. I am also very thankful to Dr. Nezha Badi for the evaluation of the manuscript. I deeply appreciate the technical support and useful lab tips of Laurence Oswald. I thank as well Alexandre Collard for his abilities to find anything anywhere and for creating a lively atmosphere in the lab. I am also grateful to Dr. Paul Baxter and Dr. Pierre Lutz for the fruitful discussions and material support.

The PMC group became truly one more family for me! My sincere thanks to my first teacher at the ICS, Dr. Mirela Zamfir: you were uniting all of us, encouraging us and sharing energy ~~at any moment of day and night~~, and you became a true friend. Anechka (Dr. Anna Meszynska), I can entirely rely on you, and there are no words to express how important are your whatever-happens-positive mood and empathy. Our friendship went out from the institute walls and, I believe, will be continued (you can tell Romain that adventures are waiting!). I was very lucky with office- and lab mates who created a cooperative and friendly atmosphere. Ma chère Tâm (Dr. Tam Trinh Thanh), we shared not just the space nearby, but emotions, successes and difficulties. I am really happy to continue meeting you and Maxime. Dear "petite" Fair (Dr. Sansanee Srichan), I profoundly appreciate your buddhistic way of being and diplomatic skills. We will greet the dawn together in Thailand soon, won't we? Special thank you to Dr. Gladys Pozza and Chloé Laure for your friendliness and French lessons. I am also very grateful to Aziz (Dr. Al Ouahabi Abdelaziz) for your encouragement, kindness and understanding. We could discuss anything, from chemistry and new tendencies in the industry to cultural differences and travelling. I won't forget either my passionate and smiley friend, Meryem Amrane, for your special ability to transform rainy days into sunny ones. I am thankful to Dr. Raj Kumar Roy, Dr. Dalila Chouikhi, Dr. Maria Kaliva, Dr. Hatice Mutlu and Véronique Divry for your support and good mood.

I appreciate the help of the SEC characterization platform, especially of Dr. Mélanie Legros and Odile Gavat for their professionalism and useful advices. Thank you, Mélanie, for spending your time to share the knowledge about SEC measurements. I am also thankful to Dr. Jean-Marc Strub, Dr. Eric Busseron and Dr. Eric Lutz for MALDI and mass spectroscopy measurements.

Cristinushka (Dr. Christina Misuraca), my italian lunch mate, you are one of the most “naturaleza íntegra” I have ever met. Once you helped me to make a choice that changed my life. Thank you for your precious advices and encouragement. I am grateful to Dr. Yves Ruff for the inspiring discussions and his ability to put complex ideas into simple terms. В радости и в горе you are with me, my amazing friends, Artem Osypenko and Anushka Demchenko. We shared so much – is there need to say how dear, how important are you for me? Обнимаю вас, родные! We were discovering Strasbourg together with a wonderful Australian guy Tom (Dr. Thomas Ellis). Thank you for being nearby in this great trip. I also thank Dr. Rémi Merindol and Dr. Alexandru Sarbu for their active participation in the social life of the institute. Alexandre, Natasha, Iuliia, Pierre, Valentina, Adrian, Dasha, Quan, Marek, Liosha and many-many other, thank you for the coffee breaks, parties, hiking trips and all great moments spent together. You made my stay at the Institut Charles Sadron and in France an unforgettable and very important period in my life. I also thank the wonderful staff at the ICS for being so helpful and friendly.

I know I always have my family to count on. I express my deep gratitude to my dear parents, Natalia and Alexandr. You transmitted me a free spirit, curiosity and love for adventures. Thank you for your love and supporting me at any moment of my life. Люблю вас очень сильно, даже если не всегда показываю. Big thank you to my sister, Valiusha, for the understanding, thoughtfulness and her magic ability to listen. Je remercie de tout mon cœur les familles Reb et Lutz. Mes beaux-parents, Laurence et Christian, vous partagez tous les moments heureux et difficiles avec moi et Eric. Vos aides précieuses et votre soutien moral ont fortement facilité la traversée des moments pénibles. Merci beaucoup et plein de bisous à Benjamin, Brigitte, Virginie, Fabienne et Marlène.

Solnyshko, my Love, my soul mate, I owe you my deepest gratitude for your encouragement, advices and extraordinary patience. Your faith in me and my abilities was the water which could move the rock. We say in Russian that people need to pass water, fire and copper pipes to be together. We passed two theses together – does it count as a proof ? Thank you for the manuscript evaluation (for all your time spent on understanding my very special style and correcting it), all warm words and indispensable hugs (and kicks ☺). « Aqui se queda la clara, la entrañable transparencia… »

All my life through, the new sights of Nature made me rejoice like a child.

…il faut avoir de la persévérance, et surtout de la confiance en soi. Il faut croire que l'on est doué pour quelque chose, et que, cette chose, il faut l'atteindre coûte que coûte.

Maria Skłodowska-Curie

TABLE OF CONTENTS

ABBREVIATIONS AND SYMBOLS A

LIST OF FIGURES G

LIST OF SCHEMES Q

LIST OF TABLES S

INTRODUCTION GENERALE - 1 -

GENERAL INTRODUCTION - 7 -

CHAPTER I. BIBLIOGRAPHY - 13 -

I.1. INTRODUCTION - 15 -

I.2. MONOMER SEQUENCE CONTROL BY CHAIN-GROWTH POLYMERIZATION - 16 -

- I.2.1. Monoinsertion - 16 -
- I.2.2. Template Synthesis in Controlled Radical Polymerization - 19 -
- I.2.3. Multiblock Copolymer - 21 -
- 1.2.4. Kinetic Approach - 24 -

I.3. OTHER CHEMICAL APPROACHES TO CONTROL MONOMER SEQUENCE - 30 -

- I.3.1. Metal Coordination - 30 -
- I.3.2. Step Growth Polymerization - 32 -
- I.3.3. Iterative Synthesis (Multistep Growth) - 34 -
- I.3.4. Molecular Machines - 39 -

I.4. COMPACTION AND FOLDING OF POLYMER CHAINS THROUGH THE FORMATION OF INTRAMOLECULAR LINKS - 41 -

- I.4.1. Compaction of Single Polymer Chains by Covalent Interactions - 42 -
  - I.4.1.A. Single Chain Polymer Nanoparticles (SCPNs) - 42 -
  - I.4.1.B. Compartmentalization of Single Polymer Chains - 48 -
  - I.4.1.C. Topological Polymers - 49 -
    - I.4.1.C.1. Cyclic Structures - 49 -
    - I.4.1.C.2. Synthesis of Complex Architectures Based on Cyclic Polymers - 51 -
    - I.4.1.C.3. Positionable Covalent Bridges - 52 -
- I.4.2. Compaction/Folding of Single Polymer Chains by Non-Covalent Interactions - 56 -
  - I.4.2.A. Isotropic Compaction - 56 -
    - I.4.2.A.1. Folding of Polymer Chains by Hydrogen Bonding - 56 -
    - I.4.2.A.2. Metal Coordination - 57 -
    - I.4.2.A.3. Host-Guest Interactions - 59 -
  - I.4.2.B. Anisotropic Compaction - 59 -

I.5. CONTROLLED/LIVING RADICAL POLYMERIZATION TECHNIQUES - 63 -

- I.5.1. Introduction - 63 -
- I.5.2. Reversible Thermal Cleavage of Weak Covalent Bonds - 65 -
  - I.5.2.1. Nitroxide-Mediated Polymerization - 65 -

I.5.3. Metal-Catalyzed Living Radical Polymerizations - 69 -
I.5.3.1. Atom Transfer Radical Polymerization - 69 -
I.5.3.2. SET-LRP, or SARA ATRP - 71 -
CHAPTER II. PRECISE POSITIONING OF AMINO ACID MOIETIES IN POLYMER CHAINS - 75 -
II.1. INTRODUCTION. ORIGINS AND MAIN IDEA OF THE PROJECT - 77 -
II.2. DESIGN AND SYNTHESIS OF MALEIMIDES - 80 -
II.2.1. Synthesis of *N*-Hydroxybenzyl Maleimide I - 82 -
II.2.2. Synthesis of *N*-Substituted Maleimides II-V - 83 -
II.2.3. Synthesis of the Maleimide with Fluorenyl Moiety VI - 86 -
II.3. SYNTHESIS OF SEQUENCE-CONTROLLED POLYMERS USING A CONVENTIONAL STRATEGY - 87 -
II.3.1. Conditions for ATRP - 87 -
II.3.2. Positioning of a Single Amino Acid Moiety in Polymer Chains - 89 -
II.3.3. Insertion of Several Maleimide Units into a Polymer Chain - 94 -
II.4. SYNTHESIS OF SEQUENCE-CONTROLLED POLYMERS USING ULTRA-PRECISE METHODOLOGY - 96 -
II.4.1. Origins and Main Features of the Ultra-Precise Methodology - 96 -
II.4.2. Model Polymers - 98 -
II.4.3. Ultra-Precise Insertion of Amino Acid Moieties in Polymer Chains - 101 -
II.5. REMOVAL OF THE TRIMETHYLSILYL GROUP - 105 -
II.6. CONCLUSIONS - 107 -
CHAPTER III. SINGLE-CHAIN TOPOLOGIES FORMED BY POSITIONABLE DISULFIDE BRIDGES - 109 -
III.1. INTRODUCTION. GENERAL IDEA - 111 -
III.2. DESIGN OF LINEAR POLYMER CONJUGATES. GENERAL SCHEME - 113 -
III.3. SYNTHESIS OF LINEAR POLYMER CONJUGATES - 115 -
III.3.1. Synthesis of Polymers with Positioned Pentafluorophenyl Ester Groups - 115 -
III.3.2. Synthesis of Polymer Conjugates with Protected Cysteine-Arginine-Cysteine Motifs - 119 -
III.3.3. Polymer Conjugates with CRC Fragments. Removal of Protecting Groups - 122 -
III.4. INTRAMOLECULAR FORMATION OF DISULFIDE BRIDGES - 125 -
III.5. CONCLUSIONS - 128 -
CHAPTER IV. SINGLE-CHAIN POLYMER METAL COMPLEXES - 129 -
IV.1. METAL-LIGAND INTERACTIONS DRIVING POLYMER COMPACTION - 131 -
IV.1.1. Introduction - 131 -
IV.1.2. Selection of Metals and Ligands - 132 -
IV.1.3. General Strategy - 133 -
IV.2. SEQUENCE-CONTROLLED POLYMERS CONTAINING PHENANTHROLINE MOIETIES- 135 -
IV.2.1. Direct Synthesis of Sequence-controlled Polymers Containing Phenanthroline - 135 -

IV.2.1. Synthesis of 1,10-Phenanthrolin-5-maleimide X - 135 -
IV.2.2. Sequence-controlled Polymers Containing Phenanthroline Groups - 135 -
IV.2.2. Post-Polymerization Modification using 1,10-Phenanthrolin-5-amine - 141 -
IV.3. POLYMER METAL COMPLEXES - 142 -
IV.3.1. Polymer Ruthenium(II) Complexes - 142 -
IV.3.2. Polymer Palladium(II) Complexes - 145 -
IV.4. CONCLUSIONS AND PERSPECTIVES - 146 -
GENERAL CONCLUSIONS AND PERSPECTIVES - 149 -
EXPERIMENTAL PART - 153 -
1. CHEMICALS - 155 -
2. CHARACTERIZATION METHODS - 157 -
3. SYNTHESIS OF COMPOUNDS I - X - 159 -
4. SYNTHESIS OF POLYMERS - 169 -
REFERENCES - 199 -
ADDITIONAL DATA (ANNEX) - 217 -

ABBREVIATIONS AND SYMBOLS

<G>	compaction parameter
AA	amino acid
Ac_2O	acetic anhydride
AcOEt	ethyl acetate
AcONa	sodium acetate
AFM	atomic force microscopy
AIBN	2,2-azoisobutyronitrile
Ala	alanine
ARGET ATRP	activator regenerated by electron-transfer for atom transfer radical polymerization
ATRA	atom transfer radical addition
ATRP	atom transfer radical polymerization
BCB	benzocyclobutene
bipy	bipyridine
BlocBuilder MA®	*N*-(*tert*-butyl)-*N*-(1-diethylphosphono-2,2-dimethylpropyl) -*O*-(2-carboxylprop-2-yl)-hydroxylamine
Boc	*tert*-butyloxycarbonyl
BTA	benzene-1,3,5-tricarboxamide
$^{\circ}$C	celsius degree
CB[8]	cucurbit[8]uril
CD	circular dichroism
CH_2Cl_2	dichloromethane
CH_3CN	acetonitrile
$CHCl_3$	chloroform
CLRP	controlled/living radical polymerization
CO_2Cl_2	oxalyl chloride
Cons.	consumption
Conv.	conversion
CRC	cysteine-arginine-cysteine
CRP	controlled radical polymerization
Cu(0)	copper powder

CuAAC	copper-catalyzed azide-alkyne cycloaddition
CuBr	copper (I) bromide
$CuBr_2$	copper (II) bromide
CXC	cysteine-*any amino acid*-cysteine
DCC	*N*,*N*'-dicyclohexylcarbodiimide
DEA	*N*,*N*-diethylacrylamide
DEAD	diethyl azodicarboxylate
DGA	diglycolic anhydride
DIC	*N*,*N*′-diisopropylcarbodiimide
DIPEA	*N*-diisopropylethylamine
DLS	dynamic light scattering
DMA	*N*,*N*-dimethylacrylamide
DMAP	4-dimethylaminopyridine
DMF	dimethylformamide
DMPA	2,2-dimethoxy-2-phenylacetophenone
DMSO	dimethylsulfoxide
DNA	deoxyribonucleic acid
DNBP	4,4′-di(5-nonyl)-2,2′-bipyridine
DOSY	difusion ordered spectroscopy
DP_n	degree of polymerization
DSC	differential scanning calorimetry
EHA	2-ethyl hexyl acrylate
ESI-MS	electrospray ionization-mass spectrometry
Et_3N	triethylamine
Eq., eq.	equivalent
exp.	experimental
F_c	fraction of cyclized regions
FT-IR	Fourier transform infrared spectroscopy
HOBt	1-hydroxybenzotriazole hydrate
HPLC	high performance liquid chromatography
i-PrOH	*i*-propanol
J	coupling constant
k	reaction rate constant

k_a	activation constant
k_d	deactivation constant
k_p	propagation constant
k_t	termination constant
$K_{eq.}$	equilibrium constant
LCMS	liquid chromatography–mass spectrometry
Leu	leucine
$LiBH_4$	lithium borohydride
LiBr	lithium bromide
M	mol/L
M_1, M_2, …	first monomer, second monomer, …
MA	methacrylate
MALDI-TOF-MS	matrix-assisted laser desorption/ionization time-of-flight mass spectrometry
MALS	multi angle light scattering
Me6-TREN	tris(2-aminoethyl)amine
MeOH	methanol
MI	*N*-substituted maleimide
MI-Bz	*N*-benzyl maleimide
MI-PFP	pentafluorophenyl ester maleimide
MI-Pr	*N*-propyl maleimide
mL	millilitre
MMA	methyl methacrylate
M_n	mumber average molecular weight
M_p	molecular weight at chromatogram peak
M_w/M_n	molecular weight distribution
v	frequency
NAM	4-acryloylmorpholine
NBVE	n-butyl vinyl ether
NIPAM	*N*-isopropylacrylamide
nm	nanometer
NMP	nitroxide-mediated polymerization
NMR	nuclear magnetic resonance

Pbf	2,2,4,6,7-pentamethyl dihydrobenzofuran-5-sulfonamide
Pd (II)	palladium (II)
PDI	polydispersity index
PEG	polyethyleneglycol
PFP	pentafluorophenyl
Ph_3P	triphenylphosphine
Phe	phenylalanine
phen	1,10-phenanthroline
PMDETA	*N*,*N*,*N′*,*N′*,*N″*-pentamethyldiethylenetriamine
PMMA	poly(methyl methacrylate)
PNBVE	poly(n-butyl vinyl ether)
ppm	parts per million
PRE	persistant radical effect
PS	polystyrene
PyBOP	benzotriazol-1-yl-oxytripyrrolidinophosphonium hexafluorophosphate
PyBroP	bromotripyrrolidinophosphonium hexafluorophosphate
r	reactivity ratio
RAFT	reversible addition-fragmentation chain transfer
ROMP	ring-opening metathesis polymerization
ROP	living ring-opening copolymerization
RT	room temperature
Ru (II)	ruthenium (II)
S	styrene
SA	symmetric anhydride
SARA ATRP	supplemental activator and reducing agent atom transfer radical polymerization
SAXS	small-angle X-ray scattering
SCNP	single-chain polymer nanoparticle
SDP	diphenylphosphinostyrene
SEC	size-exclusion chromatography
SET-LRP	single-electron transfer living radical polymerization
SG1	*N*-tert-butyl-*N*-(1-diethylphosphono-2,2-dimethylpropyl)
TBAF	tetra-n-butylammonium fluoride

*t*BuA	*tert*-butyl acrylate
TEM	transmission electron microscopy
TEMPO	(2,2,6,6-tetramethylpiperidin-1-yl)oxy, or (2,2,6,6-tetramethylpiperidin-1-yl)oxidanyl
TFA	trifluoroacetic acid
T_g	glass transition temperatures
THF	tetrahydrofuran
TIPNO	2,2,5-trimethyl-4-phenyl-3-azahexane-*N*-oxyl
TIPS-PMI	triisopropylsilyl protected *N*-propagylmaleimide
TIS	triisopropylsilane
TMS	trimethylsilyl
Trt	trityl
Tyr	tyrosine
Upy	2-ureidopyrimidinine
UV-*vis*	ultraviolet-visible
VA-044	2,2'-azobis[2-(2-imidazolin-2-yl)propane]dihydrochloride
VE	vinyl ether
V_p	elution volume at chromatogram peak
$Zn(OAc)_2$	zinc acetate
$[Pd(CH_3CN)_4(BF_4)_2]$	tetrakis(acetonitrile)palladium(II) tetrafluoroborate
$[Ru(II)Cl_2(DMSO)_4]$	dichlorotetrakis(dimethyl sulfoxide) ruthenium(II)
$[\eta]$	intrinsic viscosity

LIST OF FIGURES

Figure 1 | Recapitulative scheme of the thesis. (A) Sequence-controlled polymers carrying amino acid and a terminal fluorenyl moieties synthesized by time-controlled additions of *N*-substituted maleimides into growing polystyrene chains (chapter I). (B) Synthesis of cyclic topologies by twin positionable disulfide bridges using cysteine-arginine-cysteine sequences (chapter II). (C) Complexation of polymers carrying phenanthroline moieties in the presence of Ru(II) or Pd(II) metals (chapter III). .... - 9 -

Figure 2 | Single addition in living cationic polymerization of *n*-butyl vinyl ether........... - 17 -

Figure 3 | Post-polymerization modification of PNBVE with BocVE unit (A) either quenching the polymer chain end with $LiBH_4$ followed by deprotection of Boc-groups, or (B) quenching the polymer chain end with sodium diethyl malonate followed by deprotection of malonate- and Boc-groups. .... - 17 -

Figure 4 | Consecutive addition of acrylic monomers by RAFT leading to sequence-controlled acrylate oligomers.. - 18 -

Figure 5 | Schematic representation of the synthesis of sequence-controlled polymers using allyl alcohol and post-modifications. .... - 19 -

Figure 6 | (A) Template-assisted living radical polymerization. (B) Radical addition of methacrylic acid using a template initiator. Reprinted with permission from reference [23]. Copyright © 2009, American Chemical Society. .... - 20 -

Figure 7 | Schematic representation of the synthesis of the block copolymer containing three different repeating sequences of around three units each and molecular weight distributions for successive block extensions of this block copolymer. Reprinted with permission from [25]. Copyright © 2013, Rights managed by Nature Publishing Group. .... - 23 -

Figure 8 | (A) Monomer conversions of styrene and maleic anhydride, determined by ^{1}H NMR, as a function of time. (B) Schematic representation of NMP copolymerization of styrene with maleic anhydride. Reprinted with permissions from [62]. Copyright © 2000, American Chemical Society. .... - 27 -

Figure 9 | Concept of the sequential copolymerization of styrene and various *N*-substituted maleimides. Reprinted with permissions from [20]. Copyright © 2007, American Chemical Society... - 28 -

Figure 10 | Automated preparation of complex monomer sequence patterns. Reprinted with permissions from [63]. Copyright © 2012 WILEY-VCH Verlag GmbH & Co. KGaA, Weinheim.. - 29 -

Figure 11 | Alternating copolymerization of diglycolic anhydride (DGA) and various epoxides. .... - 31 -

Figure 12 | Alternating copolymerization of enantiopure β-lactones in the presence of a syndiospecific catalyst [70].. - 31 -

Figure 13 | (A) Step-growth azide-alkyne cycloaddition of heterotelechelic oligomer and (B) homotelechelic oligomer prepared by ATRP [71]. (C) Synthesis of alternating polymers by

step-growth polymerization of two bifunctional symmetrical monomers with azide and alkyne terminal groups. - 33 -
Figure 14 | Sequence-defined ABC-type copolymers prepared by step-growth metal-catalyzed polymerization [18] - 34 -
Figure 15 | Iterative synthesis of a sequence-specific polypeptoid on a solid support [76].- 35 -
Figure 16 | Schematic representation of the synthesis of sequence-defined encoded oligomers. Reprinted with permission from [77]. Copyright © 2013 WILEY-VCH Verlag GmbH & Co. KGaA, Weinheim. - 36 -
Figure 17 | Synthesis of ABC-sequenced copolymer [79] - 37 -
Figure 18 | Synthesis of sequence-defined tetramer starting from stearic acid (1a) or sequence-defined polymer starting from *O*-methyl-*O'*-succinylpolyethylene glycol (1b) by iterative use of Passerini three-component reaction followed by thiol-ene “click” chemistry. Adapted with permission from [81]. Copyright © 2014 WILEY-VCH Verlag GmbH & Co. KGaA, Weinheim. - 38 -
Figure 19 | Assembly of oligomer containing five precisely positioned functional moieties [80]. - 39 -
Figure 20 | Assembled rotaxane-based molecular machine 1 [11]. - 40 -
Figure 21 | Proposed mechanism for sequence-specific peptide synthesis by small-molecule machine. *Reaction conditions*: (*i*) 20% TFA in CH_2Cl_2, RT, 2 hours. (*ii*) DIPEA, $(HO_2CCH_2CH_2)_3P$ in 3:1 CH_3CN : DMF, 60°C, 36 hours. (*iii*) 30% TFA in 3:1 CH_2Cl_2 : H_2O, RT, 18 hours. Reprinted with permission from [11]. Copyright © 2013, American Association for the Advancement of Science. - 41 -
Figure 22 | Schematic representation of the intramolecular collapse of a random copolymer with benzocyclobutene units [3]. - 43 -
Figure 23 | Synthesis of a water-soluble single-chain nanoparticle for imaging [91]. - 45 -
Figure 24 | Reversible single-chain nanoparticle formation through intramolecular disulfide bond. Adapted with permission from [5]. Copyright © 2012, Royal Society of Chemistry.- 47 -
Figure 25 | Sequence-controlled copolymer synthesized by time-controlled additions of pentafluorophenyl 4-maleimidobenzoate (1) and TIPS-protected *N*-propargyl maleimide (2). Double compaction of the sequence-controlled copolymer. Reprinted with permission from [95]. Copyright © 2014, American Chemical Society. - 48 -
Figure 26 | Synthesis of linear precursors by ATRP, RAFT and ROP, and modification of the chain-ends followed by intramolecular cyclization. - 50 -
Figure 27 | Synthesis of a tadpole-shaped polymer. Reprinted with permission from [112]. Copyright © 2006 WILEY-VCH Verlag GmbH & Co. KGaA, Weinheim. - 51 -
Figure 28 | “Programmed” polymer folding of bridged dicyclic and *spiro* tricyclic polymers. Reprinted with permission from [115]. Copyright © 2011, American Chemical Society. - 52 -
Figure 29 | Covalent folding of linear polymer chains leading to a variety of controlled shapes. Reprinted with permission from [8]. Copyright © 2011, Rights Managed by Nature Publishing Group. - 53 -

Figure 30 | Chromatograms of linear (dashed line) and folded by covalent link (straight line) polymers. Reprinted with permission from [8]. Copyright © 2011, Rights Managed by Nature Publishing Group. .... - 54 -
Figure 31 | Folding of polystyrene chains using asymmetric covalent bridges in three steps: (*i*) THF, RT, overnight; (*ii*) TBAF, THF, RT, overnight; (*iii*) CuBr/bipy, 80°C, DMF, dilute conditions. Reprinted with permission from [9]. Copyright © 2011, Royal Society of Chemistry. .... - 55 -
Figure 32 | Schematic representation of the microstructure of the linear precursors exploited for the synthesis of α-shaped polymers. ^{a}Compaction parameter <G> is shown for folded polymers. Reprinted with permission from [9]. Copyright © 2011, Royal Society of Chemistry. .... - 55 -
Figure 33 | UV irradiation induced the collapse of a single polymer chain into a nanoparticle *via* supramolecular cross-linking. Reprinted with permission from [119]. Copyright © 2010, American Chemical Society. .... - 57 -
Figure 34 | General idea of metal-containing single chain nanoparticles synthesis [6]...... - 58 -
Figure 35 | Idealized picture of metallo-folded single-chain nanoparticle [7]................... - 58 -
Figure 36 | Folding of polymer chains by host-guest interactions on the example of CB[8] – viologen or naphtyl-modified polyacrylamide.. - 59 -
Figure 37 | Compaction of polymer coils due to the self-assembly of BTA moieties upon irradiation and cleavage of *o*-nitrobenzyl groups. Reprinted with permission from [126]. Copyright © 2011 WILEY-VCH Verlag GmbH & Co. KGaA, Weinheim. .... - 60 -
Figure 38 | Orthogonal self-assembly leading to the formation of a SCPN by directional hydrogen bonding. Reprinted with permission from [129]. Copyright © 2013, American Chemical Society. .... - 61 -
Figure 39 | Single-chain folding caused by self-assembly of BTA groups of a polymer containing catalytic units (SDP with ruthenium), hydrophilic (PEG chains) and hydrophobic parts (BTA substituents) [130].. - 62 -
Figure 40 | Cyclization of single polymer chain driven by metal-ligand interactions [33].- 63 -
Figure 41 | a) The semilogarithmic plot of the dependence of monomer concentration on time; b) the dependence of molecular weight on conversion. Reprinted with permission from [133]. Copyright © 2001, American Chemical Society. .... - 64 -
Figure 42 | Synthetic pathways to prepare alkoxyamines [137]. .... - 67 -
Figure 43 | SARA ATRP and SET-LRP model mechanisms. Reprinted with permission from [153]. Copyright © 2014, Royal Society of Chemistry. .... - 72 -
Figure 44 | (A) Schematic representation of the precise positioning of a small amount of *N*-functionalized maleimide in a polymer chain. (B) Two main types of chain-to-chain deviation.. - 78 -
Figure 45 | Assembled molecular machine for a sequence-specific peptide synthesis based on the use of a polymer track connected to a rotaxane synthon. .... - 79 -
Figure 46 | Schematic representation of the sequence-defined polymer track with several precisely positioned amino acids and a terminal fluorenyl building block prepared by the CRP of styrene with *N*-functionalized maleimides.. - 80 -

Figure 47 | Possible maleimide designs in comparison with the rotaxane macrocycle of the molecular machine (RM). AA – amino acid moiety. Confirmed by three-dimensional molecular models [156] by Leigh group. - 81 -
Figure 48 | Maleimides (MI) II-V structure. - 81 -
Figure 49 | Probable microstructures and corresponding semi-logarithmic plots of comonomer conversions in function of time recorded for sequence-controlled polymers synthesized by the ATRP of styrene with maleimide IV (A, P11) added at the beginning of the polymer chain and (B, P12) at the end of polymerization. - 92 -
Figure 50 | Evolution of the size exclusion chromatograms of polymers carrying an amino acid moiety, in THF. (A) SEC data for P11 (with phenylalanine precisely positioned at the beginning of polymer chain) before maleimide addition (blue line), after partial incorporation of maleimides (green line), after full maleimide consumption (orange line) and for the purified polymer (black line). (B) SEC data for P12 (with phenylalanine precisely positioned at the end of polymer chain) after partial incorporation of maleimides (green line), after full maleimide consumption (orange line) and for the purified polymer (black line). - 93 -
Figure 51 | ^{1}H NMR spectrum of P12 (similar to P11) with phenylalanine moiety, in $CDCl_3$. - 94 -
Figure 52 | Synthesis of sequence-controlled polymers P16 and P17. Semi-logarithmic plots of comonomer conversions *versus* time and probable microstructures for (A) P16 and (B) P17. - 95 -
Figure 53 | (A) Semi-logarithmic plot of comonomer conversions *versus* time and (B) probable microstructure for P18. - 96 -
Figure 54 | General concept of the ultra-precise synthesis of sequence-controlled polymers. - 97 -
Figure 55 | Ultra-precise synthesis of sequence-controlled polymers using controlled radical copolymerization (SET-LRP) of styrene with *N*-substituted maleimides. - 97 -
Figure 56 | Ultra-precise synthesis of a sequence-controlled polymer P19 with two maleimides MI-Bz and MI-Pr. (A) Probable microstructure of P19. (B) Semi-logarithmic plot of comonomer conversions *versus* time (calculated from ^{1}H NMR spectra). (C) Size-exclusion chromatograms after consumption of MI-Bz (red curve) and of the purified polymer (black curve), in THF. - 99 -
Figure 57 | Ultra-precise synthesis of the sequence-controlled polymer P20 with three positioned model maleimides MI-Pr, MI-Bz and MI-PPF. (A) Probable microstructure of P20. (B) Semi-logarithmic plot of comonomer conversions *versus* time (calculated from ^{1}H NMR spectra). (C) Size-exclusion chromatograms after consumption of MI-Pr (green curve), MI-Bz (red curve), MI-PFP (pink curve) and of the purified polymer (black). - 100 -
Figure 58 | Synthesis of a sequence-controlled polymer P21 with four positioned model maleimides MI-Bz, MI-Pr added twice and MI-PPF by combination of ultra-precise and conventional methods. (A) Probable microstructure of P21. (B) Semi-logarithmic plot of comonomer conversions *versus* time (calculated from ^{1}H NMR spectra). (C) Size-exclusion chromatograms after consumption of the first added MI-Pr (solid green curve), the second

added MI-Pr (dash green curve), MI-PFP (pink curve) and of the purified polymer (black).... - 101 -
Figure 59 | Ultra-precise synthesis of a sequence-controlled polymer P22 with two positioned maleimides V and VI. (A) Probable microstructure of P22. (B) Semi-logarithmic plot of comonomer conversions *versus* time (calculated from ^{1}H NMR spectra). (C) Size-exclusion chromatograms after consumption of V (red curve) and of the purified polymer (black curve). .... - 102 -
Figure 60 | Ultra-precise synthesis of the sequence-controlled polymer P23 with three positioned maleimides IV, III and VI. (A) Probable microstructure of P23. (B) Semi-logarithmic plot of comonomer conversions *versus* time (calculated from ^{1}H NMR spectra). (C) Size-exclusion chromatograms after consumption of IV (green curve), III (orange curve) and of the purified polymer (black curve). .... - 103 -
Figure 61 | Ultra-precise synthesis of a sequence-controlled polymer P24 with four positioned maleimides III, IV, V and VI. (A) Probable microstructure of P24. (B) Semi-logarithmic plot of comonomer conversions *versus* time (calculated from ^{1}H NMR spectra). (C) Size-exclusion chromatograms after consumption of III (orange), IV (green), V (red), VI (purple) and of the purified polymer (black). .... - 104 -
Figure 62 | ^{1}H NMR spectrum of the polymer P24, in $CDCl_3$.. - 105 -
Figure 63 | ^{1}H NMR spectra of P1 before and after deprotection: (A) after synthesis by ATRP and purification; (B) after TBAF treatment. *Reaction conditions*: 0.01 M solution of TBAF (10 Eq.) in THF to 1 Eq. of TMS-group (P1), RT, 12 hours. .... - 106 -
Figure 64 | ^{1}H NMR spectra for a α-alkyne functional polymer P9 with *N*-Boc-protected leucine moieties: (A) after synthesis by ATRP and purification and (B) after TBAF treatment. *Reaction conditions*: 0.01 M solution of TBAF (2 Eq.) in THF to 1 Eq. of TMS-group (P9), RT, 1 hour. .... - 107 -
Figure 65 | Oxidation of two CXC motifs into a 22-units macrocycle containing two disulfide bonds. Only one of the two possible cycles is shown. .... - 112 -
Figure 66 | General scheme of the project. (A) The synthesis of sequence-controlled precursors by copolymerization of styrene with pentafluorophenyl 4-maleimidobenzoate. (B) Synthesis of polymer conjugates by *1*) attachment of cysteine-arginine-cysteine fragments (CRC) with protected amino acid groups by activated ester/amine chemistry followed by *2*) the removal of the protecting groups. (C) *3*) Intramolecular oxidation of the cysteine residues leading to a single-polymer chain folded by precisely positioned orthogonal disulfide bridges. .... - 114 -
Figure 67 | (A) Synthesis of “asymmetric” sequence-controlled precursor by the NMP of styrene with MI-PFP in the presence of BlocBuilder®. (B) Synthesis of “symmetric” sequence-controlled precursor by NMP of styrene with MI-PFP in the presence VIII. (C) The structures of BlocBuilder® and bifunctional alkoxyamine VIII. .... - 117 -
Figure 68 | (A) ^{1}H NMR spectrum of the polymer with PFP ester moieties P27 and (B) ^{19}F NMR spectrum of P27, in CD_2Cl_2. .... - 118 -

Figure 69 | (A) ^{1}H NMR spectrum of P27 containing pentafluorophenyl ester moieties, (B) the resulting polymer P33 after the reaction with IX and (C, D) the corresponding ^{19}F NMR spectra for P27 and P33, in CD_2Cl_2. .... - 120 -
Figure 70 | (A) FT-IR spectrum of P27 with PFP ester moieties and (B) FT-IR spectrum of the resulting polymer with CRC fragment P33........ - 121 -
Figure 71 | Size-exclusion chromatograms of P27 with PFP ester moieties (dashed line) and the resulting polymer after reaction with the oligomer IX (solid line), in DMF with 0.1 M LiBr. .... - 122 -
Figure 72 | Normalized UV spectra of polymers with CRC motifs, on the example of P33 (solid line) and in the presence of the Ellman's reagent (dashed line), MeOH (UV) / THF (UV) and a drop of DIPEA. .... - 124 -
Figure 73 | (A) ^{1}H NMR spectrum of P33 containing CRC motifs with Trt-cysteine and Pbf-arginine protected residues and (B) the resulting polymer P37 after the removal of protecting groups, in CD_2Cl_2........ - 124 -
Figure 74 | Size-exclusion chromatograms of P33 with cysteine (Trt)-arginine (Pbf)-cysteine (Trt) motifs (dashed line) and the resulting polymer after the deprotection of amino acid residues P37 (solid line), in CH_2Cl_2........ - 125 -
Figure 75 | SEC chromatograms for two polymers before and after oxidation. (A) Size-exclusion chromatograms of the polymers with CRC motifs (dashed line) P37 and the resulting polymers after oxidation of the thiol group (solid line) P40 in CH_2Cl_2. (B) Size-exclusion chromatograms of the polymers with CRC motifs P38 and the resulting polymers after oxidation of the thiol group (solid line) P41, in CH_2Cl_2. .... - 127 -
Figure 76 | General strategy of the project. (A) Synthesis of sequence-controlled precursors by copolymerization of styrene with 1,10-phenanthrolin-5-maleimide (MI-phen). (B) Intramolecular complexation leading to a single-polymer chain folded by metal-ligand interactions. .... - 134 -
Figure 77 | Synthesis of sequence-controlled polymer by NMP of styrene with 1,10-phenanthrolin-5-maleimide X added at the end of the polymerization in the presence of the bifunctional alkoxyamine VIII. (A) Estimated microstructure of P44. (B) Corresponding semi-logarithmic plot of comonomer conversions *versus* time for P44. .... - 137 -
Figure 78 | Calculation of styrene reactivity ratio r_S (Jaacks plots). (A) Logarithmic plot of styrene S monomer conversion *versus* maleimide X monomer conversion for P44. (B) Logarithmic plot of styrene S monomer conversion *versus* maleimide X monomer conversion for P46........ - 138 -
Figure 79 | SEC analysis of P43 with one phenanthroline moiety. (A) Chromatogram in THF. (B) Chromatogram in CH_2Cl_2. .... - 139 -
Figure 80 | SEC analysis of the polymers with two phenanthroline moieties, in *N*-methylpyrrolidone with 0.1 M LiBr. (A) Chromatogram of P44. (B) Chromatogram of P45. . - 140 -
Figure 81 | ^{1}H NMR spectrum of P44, in $CDCl_3$. .... - 140 -

Figure 82 | ^{1}H NMR spectra of P43 and its complexes with Ru(II). (A) ^{1}H NMR spectrum of P43; (B) ^{1}H NMR spectrum of Ru(II) polymer complex P48, (P43/Ru(II) = 1/1 molar ratio), in $CDCl_3$. - 143 -
Figure 83 | SEC analysis of Ru(II) polymer complexes. (A) Chromatograms of P43 (solid black line) and P48 (dash-dot red line), in CH_2Cl_2. (B) Chromatograms of P44 (solid black line) and P49 (dash violet line), in *N*-methylpyrrolidone with 0.1 M LiBr. - 144 -
Figure 84 | SEC analysis of Pd(II) polymer complexes. (A) Chromatograms of P43 (solid) and P50 (dash), in CH_2Cl_2. (B) Chromatograms of P44 (solid) and P51 (dash), in *N*-methylpyrrolidone with 0.1 M LiBr. - 146 -
Figure 85 | Monomer conversion (a) and semi-logarithmic plot of monomer conversion *versus* time (b) for P1. - 170 -
Figure 86 | Monomer conversion (a) and semi-logarithmic plot of monomer conversion *versus* time (b) for P2. - 170 -
Figure 87 | Monomer conversion (a) and semi-logarithmic plot of monomer conversion *versus* time (b) for P3. - 171 -
Figure 88 | Monomer conversion (a) and semi-logarithmic plot of monomer conversion *versus* time (b) for P4. - 171 -
Figure 89 | Monomer conversion (a) and semi-logarithmic plot of monomer conversion *versus* time (b) for P5. - 172 -
Figure 90 | Monomer conversion (a) and semi-logarithmic plot of monomer conversion *versus* time (b) for P6. - 172 -
Figure 91 | Characterization of P7: a) Semi-logarithmic plot of monomer conversion versus time for ATRP of styrene (squares) with II (dots) added at the beginning of the polymerization; b) Size exclusion chromatogram of the copolymer, in THF. - 174 -
Figure 92 | Characterization of P8: a) Semi-logarithmic plot of monomer conversion versus time for ATRP of styrene (squares) with II (dots) added at the end of the polymerization; b) Size exclusion chromatogram of the copolymer, in THF. - 174 -
Figure 93 | Characterization of P9: a) Semi-logarithmic plot of monomer conversion versus time for ATRP of styrene (squares) with III (dots) added at the beginning of the polymerization; b) Size exclusion chromatogram of the copolymer, in THF. - 175 -
Figure 94 | Characterization of P10: a) Semi-logarithmic plot of monomer conversion versus time for ATRP of styrene (squares) with III (dots) added at the end of the polymerization; b) Size exclusion chromatogram of the copolymer, in THF. - 175 -
Figure 95 | Characterization of P13: a) Semi-logarithmic plot of monomer conversion versus time for ATRP of styrene (squares) with MI-Bz added in the middle (dots) and at the end (triangles) of the polymerization; b) Size exclusion chromatogram of the copolymer, in THF.- 177 -
Figure 96 | Characterization of P14: a) Semi-logarithmic plot of monomer conversion versus time for ATRP of styrene (squares) with MI-Bz added in the middle (dots) and at the end (triangles) of the polymerization; b) Size exclusion chromatogram of the copolymer, in THF.- 177 -

Figure 97 | Characterization of P15: a) Semi-logarithmic plot of monomer conversion versus time for ATRP of styrene (squares) with MI-Bz added in the middle (dots) and at the end (triangles) of the polymerization; b) Size exclusion chromatogram of the copolymer, in THF.- 178 -
Figure 98 | Characterization of P17: a) Semi-logarithmic plot of monomer conversion versus time for ATRP of styrene (squares) with III added at the beginning (dots), in the middle (rhomb) and at the end (triangles) of the polymerization; b) Size exclusion chromatogram of the copolymer, in THF. .... - 179 -
Figure 99 | Normalized UV spectra of P24 (solid line) and VI (dashed line), in THF (UV). ... - 185 -
Figure 100 | Characterization of P25: a) Semi-logarithmic plot of monomer conversion versus time for NMP of styrene (squares) with MI-PFP added at the beginning of the polymerization (dots) and at 3/4 of the chain (triangles); b) Size exclusion chromatogram of the copolymer, in THF. .... - 186 -
Figure 101 | Characterization of P26: a) Semi-logarithmic plot of monomer conversion versus time for NMP of styrene (squares) with MI-PFP added at the beginning of the polymerization (dots) and at the end of polymer chain (triangles); b) Size exclusion chromatogram of the copolymer, in THF. .... - 187 -
Figure 102 | Size exclusion chromatograms of P27: a) in THF; b) in DMF with 0.1M LiBr. .. - 187 -
Figure 103 | Characterization of P28: a) Semi-logarithmic plot of monomer conversion versus time for the NMP of styrene (squares) with MI-PFP added at ~ 1/4 (dots) and ~3/4 of the polymer chain (triangles); b) Size exclusion chromatogram of the copolymer, in THF. . - 188 -
Figure 104 | (A) ^{1}H NMR spectrum of P29, in CD_2Cl_2. (B) ^{19}F NMR spectrum of P29, in CD_2Cl_2.. - 189 -
Figure 105 | a) Size exclusion chromatogram of P29, in THF; b) Size exclusion chromatogram of P29, in DMF with 0.1M LiBr. .... - 189 -
Figure 106 | Characterization of P30: a) Semi-logarithmic plot of monomer conversion versus time for NMP of styrene (squares) with MI-PFP added close to the ends of the polymer chain (dots); b) Size exclusion chromatogram of the copolymer, in THF. .... - 190 -
Figure 107 | Characterization of P31: a) Semi-logarithmic plot of monomer conversion versus time for NMP of styrene (squares) with MI-PFP added close to the ends of the polymer chain (dots); b) Size exclusion chromatogram of the copolymer, in THF. .... - 190 -
Figure 108 | Size-exclusion chromatograms of P29 with PFP ester moieties (dashed line) and (B) the resulting polymer P34 after reaction with oligomer IX (solid line), in DMF with 0.1 M LiBr. .... - 191 -
Figure 109 | (A) ^{1}H NMR spectra of P29 containing pentafluorophenyl ester moieties and (B) the resulting polymer P34 after the reaction with IX and (C, D) the corresponding ^{19}F NMR spectra for P29 and P34, in CD_2Cl_2. .... - 192 -
Figure 110 | Size-exclusion chromatograms of the polymers with CRC protected moieties P33 (dashed line). The resulting polymers P37 after removal of Trt- and Pbf-protecting groups (solid line), in DMF with 0.1 M LiBr. .... - 193 -

Figure 111 | (A), (B) Size-exclusion chromatograms of the polymers conjugates with CRC motifs P39 (dashed line). (A) The resulting polymer after the oxidation of thiol groups for 2 days in *N*-methylpyrrolidone (solid line), in CH_2Cl_2. (B) The resulting polymer after the oxidation of thiol groups for 2 days in *N*-methylpyrrolidone with added DIPEA (solid line). . - 193 -
Figure 112 | a) Characterization of P43; b) Characterization of P46. Semi-logarithmic plot of monomer conversion versus time for NMP of styrene (squares) with MI-phen X added close to the ends of the polymer chain (dots). .... - 194 -
Figure 113 | SEC analysis of Ru(II) polymer complexes. Chromatograms of P43 (solid) and P48 (dash), in THF. .... - 195 -
Figure 114 | ^{1}H NMR spectra of P44 and its complex with Ru(II). (A) ^{1}H NMR spectrum of P44; (B) ^{1}H NMR spectrum of Ru(II) polymer complex P49, in $CDCl_3$. .... - 196 -
Figure 115 | ^{1}H NMR spectra of P43 and its complex with Pd(II). (A) ^{1}H NMR spectrum of P43; (B) ^{1}H NMR spectrum of Pd(II) polymer complex P50, in $CDCl_3$. .... - 196 -
Figure 116 | ^{1}H NMR spectra of P44 and its complex with Pd(II). (A) ^{1}H NMR spectrum of P44; (B) ^{1}H NMR spectrum of Pd(II) polymer complex P51, in $CDCl_3$. .... - 197 -
Figure 117 | ^{1}H NMR spectrum of I, in CD_3OD. .... - 217 -
Figure 118 | ^{1}H NMR spectrum of II, in $CDCl_3$. .... - 217 -
Figure 119 | ^{1}H NMR spectrum of III in $CDCl_3$. .... - 218 -
Figure 120 | ^{1}H NMR spectrum of IV, in $CDCl_3$. .... - 218 -
Figure 121 | ^{1}H NMR spectrum of V, in $CDCl_3$. .... - 219 -
Figure 122 | ^{1}H NMR spectrum of VI, in $CDCl_3$. .... - 219 -
Figure 123 | ^{1}H NMR spectrum of VII in $CDCl_3$. .... - 220 -
Figure 124 | ^{1}H NMR spectrum of X, in $CDCl_3$. .... - 220 -
Figure 125 | ^{1}H NMR spectrum of P7, in $CDCl_3$. .... - 221 -
Figure 126 | ^{1}H NMR spectrum of P8, in $CDCl_3$. .... - 221 -
Figure 127 | ^{1}H NMR spectrum of P9 in $CDCl_3$. .... - 222 -
Figure 128 | ^{1}H NMR spectrum of P10, in $CDCl_3$. .... - 222 -
Figure 129 | ^{1}H NMR spectrum of P11, in $CDCl_3$. .... - 223 -
Figure 130 | ^{1}H NMR spectrum of P12, in $CDCl_3$. .... - 223 -
Figure 131 | ^{1}H NMR spectrum of P16, in $CDCl_3$. .... - 224 -
Figure 132 | ^{1}H NMR spectrum of P17, in $CDCl_3$. .... - 224 -
Figure 133 | ^{1}H NMR spectrum of P20, in $CDCl_3$. .... - 225 -
Figure 134 | ^{1}H NMR spectrum of P22, in $CDCl_3$. .... - 225 -
Figure 135 | ^{1}H NMR spectrum of P23, in $CDCl_3$. .... - 226 -
Figure 136 | ^{1}H NMR spectrum of P24, in $CDCl_3$. .... - 226 -
Figure 137 | MALDI-TOF spectrum of the deprotected polymer P10. .... - 227 -
Figure 138 | MALDI-TOF spectrum of P11. .... - 228 -
Figure 139 | ^{1}H NMR spectrum of P26, in $CDCl_3$. .... - 228 -
Figure 140 | ^{1}H NMR spectrum of P27, in $CDCl_3$. .... - 229 -
Figure 141 | ^{1}H NMR spectrum of P29, in $CDCl_3$. .... - 229 -

LIST OF SCHEMES

Scheme 1 | Various combinations between propagating chain end and a monomer that can take place during polymerization. - 25 -
Scheme 2 | Classification of the olefins used for copolymerization of *N*-substituted maleimides with various olefins [61]. - 26 -
Scheme 3 | Synthesis of one of block-polymers PT-*b*-PF-*b*-PS from six possible combinations [17]. - 32 -
Scheme 4 | Metal-catalyzed radical polyaddition of ester-linked monomers [19]. - 34 -
Scheme 5 | Synthesis of linear precursors and their intramolecular cross-linking to form a nanoparticle [4]. - 46 -
Scheme 6 | Schematic representation of dynamic equilibrium in reversible thermal cleavage of weak covalent bonds. - 65 -
Scheme 7 | Activation-deactivation equilibrium in nitroxide-mediated polymerization: a) bicomponent initiating system; b) monocomponent initiating system [137]. - 66 -
Scheme 8 | Possible chain end degradation during NMP of styrene. Reprinted with permissions from [142]. Copyright © 2001, American Chemical Society. - 68 -
Scheme 9 | Schematic representation of the dynamic equilibrium in transition metal catalyzed processes. - 69 -
Scheme 10 | General scheme for the synthesis of *N*-substituted maleimide from maleic anhydride and an amine. - 82 -
Scheme 11 | Synthesis of *N*-hydroxybenzyl maleimide (I). *Reaction conditions*: *a*) maleic anhydride (1.2 Eq.), 4-hydroxybenzylamine (1 Eq.), AcOEt, RT, 10 hours; quantitative yield; *b*) Ia (1 Eq.), $Zn(OAc)_2$ (0.04 Eq.), toluene/DMF = 10/1, 125°C, 12 hours; 27% yield. - 82 -
Scheme 12 | Synthesis of *N*-hydroxybenzyl maleimide (c) by the Mitsunobu reaction [164]. *Reaction conditions*: maleimide a (1 Eq.), 4-hydroxybenzyl alcohol b (1.5 Eq.), THF, -78°C → RT, 2 hours. - 83 -
Scheme 13 | Unsuccessful trials to synthesize maleimide III by the esterification of *N*-hydroxybenzyl maleimide I with *N*-Boc-protected leucine (AAIII). *Reaction conditions*: I (1 Eq.), AAIII (1.1 Eq.), RT, *a*). DIC (1.2 Eq.), DMAP (10 % mol.), CH_2Cl_2, DMF, 0°C → RT; *b*). HOBt (1.1 Eq.), PyBOP (1.1 Eq.), DIPEA (2 Eq.), CH_2Cl_2, DMF, RT; *c*). PyBOP (1.5 Eq.), DIPEA (3 Eq.), CH_2Cl_2, DMF, RT; *d*). HOBt (1.1 Eq.), DIC (1.2 Eq.), CH_2Cl_2, DMF, RT. - 84 -
Scheme 14 | Synthesis of the maleimide III by esterification of *N*-hydroxybenzyl maleimide I with *N*-Boc protected leucine AAIII. *Reaction conditions*: I (1 Eq.), *N*-Boc-leucine AAIII (1.3 Eq.), PyBroP (1.4 Eq.), DIPEA (3 Eq.), CH_2Cl_2/DMF ~ 5/1, RT, 1 day. - 85 -
Scheme 15 | A possible mechanism of an amino acid activation by PyBroP [170]. - 85 -
Scheme 16 | Synthesis of maleimides II to V by esterification of *N*-hydroxybenzyl maleimide I with the *in situ* formed corresponding symmetric anhydrides SA of amino acids AA. *Reaction conditions*: *a*) AA (2.3 Eq.), DCC (1.15 Eq.), CH_2Cl_2, 0ºC → RT, 2 hours; *b*). I (1 Eq.), DIPEA (2 Eq.), CH_2Cl_2/DMF ~ 10/1, RT, 1 day; 40-50% yield over the 2 steps. - 86 -

Scheme 17 | Synthesis of maleimide VI by esterification of *N*-hydroxybenzyl maleimide I with fluorenyl methyl acyl chloride. *Reaction conditions*: *a*) fluorenyl methyl carboxylic acid (1 Eq.), oxalyl chloride CO_2Cl_2 (5 Eq.), CH_2Cl_2, RT, 3 hours; *b*) fluorenyl methyl acyl chloride (1.2 Eq.), I (1 Eq.), Et_3N (2 Eq.), THF anhydrous, RT, 5 hours. - 87 -

Scheme 18 | Synthesis of the alkyne-functionalized initiator VII [173]. *Reaction conditions*: 2-bromoisobutyryl bromide (1.5 Eq.), 3-trimethylsilyl-2-propyn-1-ol (1 Eq.), Et_3N (1.5 Eq.), THF, 0°C → RT, 1 hour; 27% yield. - 88 -

Scheme 19 | ATRP of styrene in the presence of alkyne-functionalized initiator VII and Cu(I)Br/PMDETA. 1. Initiation, 2. Propagation reaction, 3. Equilibrium with dormant species and termination reaction; k_a – activation constant, k_d – deactivation constant, k_p – propagation constant, k_t – termination constant; P_t – products of termination reaction. - 88 -

Scheme 20 | Structures of MI-Bz, MI-Pr and MI-PFP. - 98 -

Scheme 21 | Synthesis of polymer conjugates with a cysteine-arginine-cysteine motif (P32 to P35) by modification of polymers with PFP ester moieties (P26, P27, P29 and P30) with IX. *Reaction conditions*: polymer with PFP moieties (1 Eq.), IX (1.2 Eq.), *N*-methylpyrrolidone, RT, 10 hours, 70% yield. - 119 -

Scheme 22 | Removal of Trt- and Pbf-protecting groups from the polymers P32 to P36. *Reaction conditions*: a polymer with CRC protected moieties (10^{-2} mmol), 2.5 mL of TFA / THF / H_2O / TIS = 60/45/4/1 (v/v) mixture, RT, 0.5 hour (2 hours for P38, P39), 70% yield. - 123 -

Scheme 23 | Oxidation of the polymers with CRC fragments. *Reaction conditions*: a polymer with a CRC motif ($C = 10^{-4}$ M in *N*-methylpyrrolidone), O_2 (atmospheric), DIPEA (0.1-0.5% v/v), DMSO (1-5% v/v), RT, 1.5 days. - 126 -

Scheme 24 | Modification of dichlorotetrakis(dimethyl sulfoxide) ruthenium(II) $[Ru(II)Cl_2(DMSO)_4]$ complex with monodentate N-donor (L) and bidentate N_2 ligands [216]. - 132 -

Scheme 25 | Tetrakis(acetonitrile)palladium(II) tetrafluoroborate $[Pd(CH_3CN)_4(BF_4)_2]$. - 133 -

Scheme 26 | Synthesis of 1,10-phenanthrolin-5-maleimide X. *Reaction conditions*: *a*) maleic anhydride (3 Eq.), 1,10-phenanthrolin-5-amine (1 Eq.), CH_2Cl_2, 40ºC, 10 hours; *b*) AcONa (12 Eq.), Ac_2O, 100ºC, 3 hours; total yield 60%. - 135 -

Scheme 27 | Trials to synthesize the polymers with phenanthroline ligand P(S-phen) by modification of P47 or P29 with 1,10-phenantrolin-5-amine. *Reaction conditions*: P29 or P47 (1 Eq. of PFP ester groups or succinic anhydride), 1,10-phenantrolin-5-amine (3 Eq.) *a*). THF, 1 day, RT; *b*). THF anhydrous, 5 days, 60°C; *c*). DMF, 1 day, 70°C; *d*). DMAP (1 Eq.), DMF, 1 day, 70°C. - 141 -

LIST OF TABLES

Table 1 | ATRP copolymerization of styrene with the maleimides II to IV positioned once in the polymer chain. ..... - 90 -
Table 2 | A. Kinetic data recorded for the nitroxide-mediated polymerization (NMP) of styrene with pentafluorophenyl 4-maleimidobenzoate (MI-PFP) using BlocBuilder®. ..... - 116 -
Table 3 | Kinetic data recorded for the nitroxide-mediated polymerization of styrene with pentafluorophenyl 4-maleimidobenzoate (MI-PFP) using VIII. ..... - 118 -
Table 4 | Kinetic data recorded for the NMP of styrene with MI-phen X using VIII. ..... - 136 -
Table 5 | ATRP of styrene with varied concentration of metal catalyst Cu(I)Br/PMDETA and temperature of polymerization. ..... - 169 -
Table 6 | Reactivity ratios r_s for P7 to P12. ..... - 174 -
Table 7 | ATRP of styrene with *N*-benzyl maleimide (MI-Bz) added at certain conversion of styrene, with varied concentration of metal catalyst Cu(I)Br/PMDETA. ..... - 176 -

INTRODUCTION GÉNÉRALE

Les polymères à séquences contrôlées sont des macromolécules avec un arrangement défini de leurs unités monomères [1]. Le contrôle de la « structure primaire » (c'est-à-dire, la séquence de monomères dans la chaîne polymère et leur composition chimique) est une clé de voûte des biomacromolécules (polypeptides et polynucléotides), parce qu'elle influence fortement leur organisation spatiale et leurs propriétés telles que l'autoréplication ou la reconnaissance moléculaire. Bien que les biomacromolécules ayant des structures primaires contrôlées soient présentes partout dans la nature, les méthodes pour préparer les macromolécules synthétiques à séquences contrôlées sont toujours sous-explorées. Réguler la séquence de monomères permet le contrôle du repliement et l'auto-assemblage des polymères, ainsi que l'imitation du compactage de l'ADN et l'assemblage de chaînes polypeptides dans les structures tertiaires. De plus, les polymères à séquences contrôlées peuvent être potentiellement utilisés comme un moyen de stockage de données. Leurs propriétés macroscopiques comme la biodégradabilité, le comportement en solution, la conductivité peuvent aussi être définies selon la séquence [1].

L'étude des macromolécules synthétiques en tant qu'objets discrets est une autre direction de recherche émergente en science des polymères [2]. De nombreuses applications pour les systèmes de polymères à chaîne unique pourraient être envisagées, telles que la miniaturisation de dispositifs, en catalyse, en optique, *etc*. [2]. Les différents polymères ayant une architecture moléculaire contrôlée pouvant être considérés comme des objets à chaîne polymère unique sont, par exemple, les dendrimères, les polymères en forme d'étoiles et les polymères hyperbranchés. D'autres possibilités de former des objets macromoléculaires à chaîne unique sont le repliement de chaînes uniques de polymères ou la synthèse de nanoparticules formées d'une seule chaîne. Le compactage ou le repliement de polymères peut être effectué en faisant réagir des fonctions chimiques préalablement placées soit aléatoirement dans la chaîne de polymère, soit aux extrémités de la chaîne. La formation de nanoparticules à chaîne unique peut être réalisée en utilisant des copolymères statistiques [3-7]. Cependant, des topologies à chaîne unique comprenant des liaisons intramoléculaires positionnables peuvent être réalisées uniquement en utilisant des polymères à séquences contrôlées portant des groupes fonctionnels précisément placés [8, 9].

L'objectif de cette thèse consiste en la synthèse d'objets à chaîne unique basés sur des polymères linéaires à séquences contrôlées. Dans cette thèse, de nouveaux systèmes macromoléculaires ont été conçus et synthétisés dans le but de former de nouvelles structures complexes basées sur des systèmes à chaîne polymère unique (Schéma 1). Dans la première partie de ce projet, des chaînons contenant des groupements fonctionnels positionnés de manière précise ont été préparés avec succès dans le but de former des machines moléculaires de type rotaxane (Schéma 1, **A**). Dans la seconde étude, des origamis macromoléculaires repliés ont été étudiés, et plus particulièrement des chaînes uniques à topologies complexes telles que des composés pseudocycliques ou noué (Schéma 1, **B**, **C**). Ces topologies ont été obtenus en utilisant des ponts disulfures pouvant être positionnés à divers endroits de la chaîne polymère et grâce à des auto-associations intramoléculaires de type métal-ligand. Le placement des groupements fonctionnels et des ponts intramoléculaires dans les chaînes polymères a été rendu possible par le contrôle des séquences de monomères, en s'appuyant sur la cinétique de copolymérisation de monomères styrèniques (donneurs d'électrons) avec des monomeres de type maléimides *N*-substitués (accepteurs). En effet, l'ajout de maléimides *N*-substitués à des temps contrôlés dans la chaîne de polystyrène en croissance, au moyen de techniques de polymérisations radicalaires contrôlées (vivantes) s'est avéré être une stratégie efficace et rapide pour la régulation de la séquence de monomères dans la chaîne polymère.

Cette thèse est composée de quatre parties et s'ouvre sur un **chapitre bibliographique** évoquant, premièrement, les principales stratégies permettant d'insérer des séquences de monomères de manière organisée au sein de chaînes macromoléculaires, et, deuxièmement, les progrès récents dans le domaine de la technologie à chaîne unique. Les avantages et les inconvénients de la polymérisation radicalaire en chaîne pour la synthèse de polymères à séquences contrôlées sont décrits en début de chapitre. Des approches alternatives pour contrôler la séquence de monomères sont également décrits (tels que la coordination de métal, la polymérisation par étape, la synthèse itérative et l'utilisation de machines moléculaires). Ensuite, les développements récents dans le domaine du compactage et du repliement de chaînes polymères par la formation de liaisons intramoléculaires, soit par des liaisons covalentes ou soit par des interactions non covalentes, sont présentés. À la fin de ce chapitre, une brève analyse des principales méthodes de polymérisation radicalaire contrôlée est proposée.

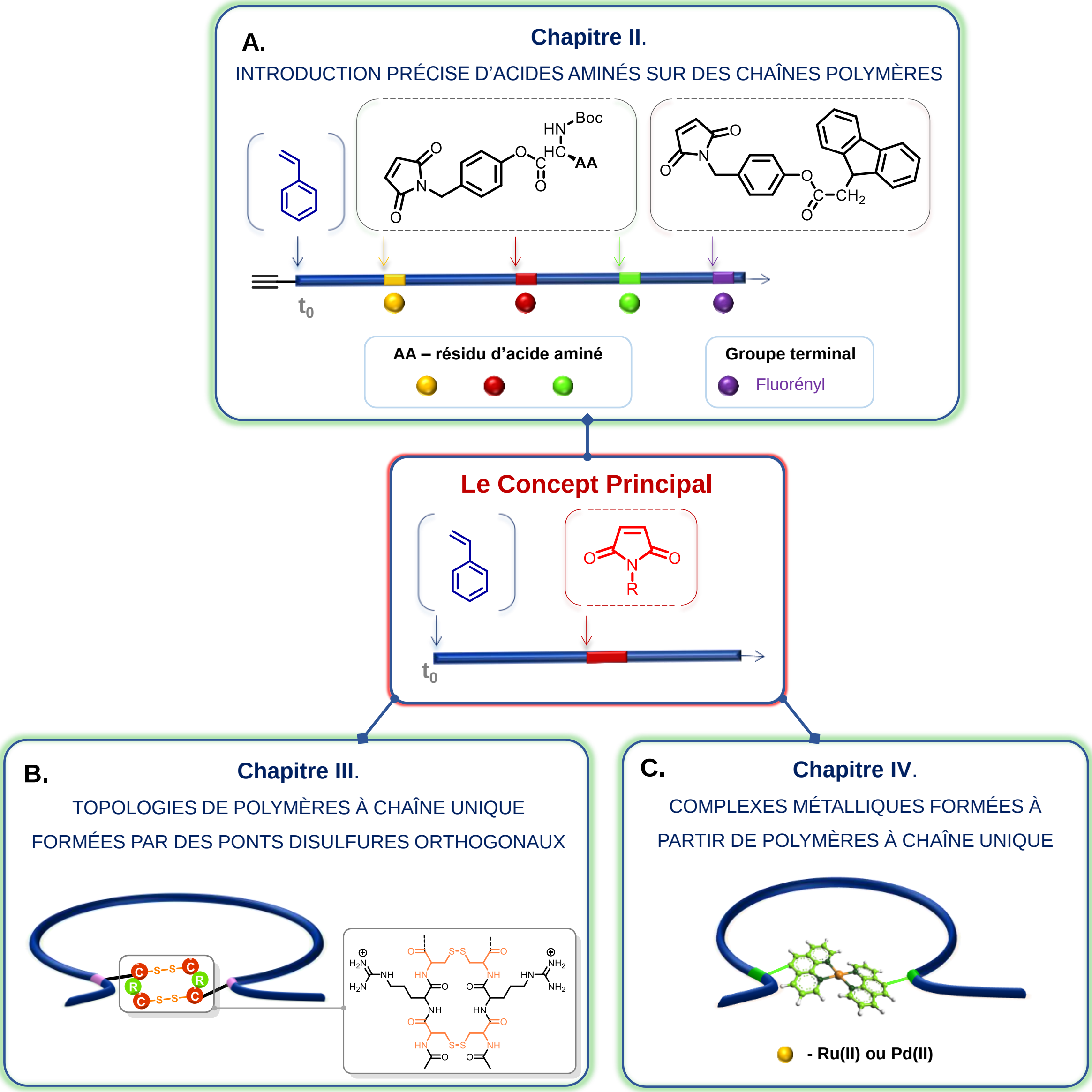
A.
Chapitre II.
INTRODUCTION PRÉCISE D'ACIDES AMINÉS SUR DES CHAÎNES POLYMÈRES
HN
Boc
HC
AA
O
N
C
CH_2
t_0
AA – résidu d'acide aminé
Groupe terminal
Fluorényl
Le Concept Principal
O
N
R
t_0
B.
Chapitre III.
TOPOLOGIES DE POLYMÈRES À CHAÎNE UNIQUE
FORMÉES PAR DES PONTS DISULFURES ORTHOGONAUX
C
R
S–S
H_2N
NH
HN
S-S
NH_2
C.
Chapitre IV.
COMPLEXES MÉTALLIQUES FORMÉES À
PARTIR DE POLYMÈRES À CHAÎNE UNIQUE
- Ru(II) ou Pd(II)

Schéma 1 | Schéma récapitulatif de la thèse. (**A**) Les polymères à séquences contrôlées portant des fonctions acides aminés et un groupe terminal fluorényl sont synthétisés par des additions à temps contrôlé de maléimides *N*-substitués dans les chaînes de polystyrène en croissance (chapitre II). (**B**) Synthèse de topologies cycliques par création de ponts disulfures orthogonaux intramoléculaires en utilisant des séquences cystéine-arginine-cystéine (chapitre III). (**C**) Complexation de polymères portant des groupements phénanthrolines en présence de Ru (II) ou Pd (II) (chapitre IV).

Le **deuxième chapitre** est dédié à l'élaboration des axes polymères à base de polystyrène comportant sur leur partie latérale un enchaînement prédéfini d'acides aminés. Ces polymères sont destinés à être utilisés comme l'axe d'une machine moléculaire artificielle en collaboration avec l'équipe du Pr. Leigh à Manchester [10, 11], qui a rapporté la synthèse peptidique d'une séquence donnée par une petite machine moléculaire basée sur un rotaxane [11]. Bien que l'oligopeptide préparé par leur machine moléculaire soit monodisperse et contient la séquence d'acides aminés souhaitée, la synthèse de leur axe (contenant des acides aminés) est complexe et se déroule en plusieurs étapes (7-9) avec un rendement total faible (2-3%). Durant ma thèse, les avantages de la polymérisation radicalaire ont été utilisés pour synthétiser des axes macromoléculaires avec de meilleurs rendements et une durée globale de la synthèse plus courte. De plus, jusqu'à 4 groupes fonctionnels ont été positionnés avec précision dans la chaîne polymère. Les deux méthodologies, la classique et l'ultra-précise [12] (récemment développée dans notre équipe), ont été étudiées pour la copolymérisation du styrène avec des maléimides fonctionnels. La séquence peptidique finale est contrôlée par l'ordre d'insertion des maléimides fonctionnalisés (portants les groupes d'acides aminés) dans les chaînes macromoléculaires. Finalement, l'intégration de l'axe polymère dans une machine moléculaire *via* une réaction de Huisgen a été envisagée à l'aide d'un amorceur d'ATRP porteur d'une fonction alcyne protégée (Schéma 2).

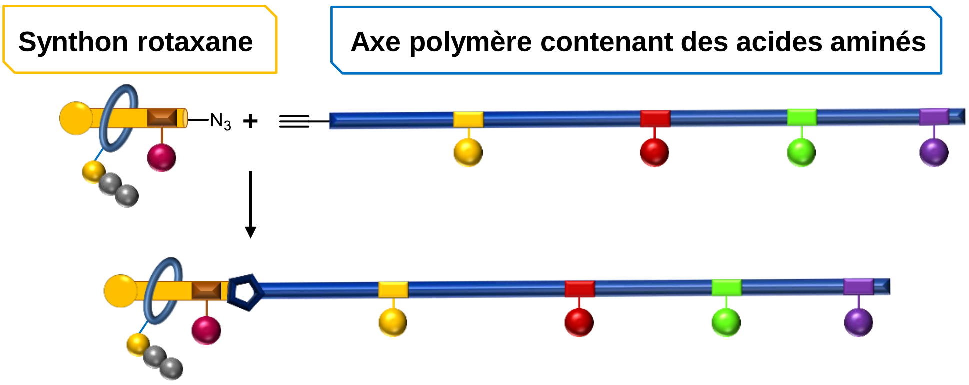

Schéma 2 | Assemblage de la machine moléculaire basé sur l'utilisation d'un axe polymère lié à un synthon rotaxane.

Le **troisième chapitre** a trait à l'élaboration de structures macromoléculaires cycliques en utilisant des liaisons covalentes intramoléculaires, plus précisément des ponts disulfures. Ce travail a été inspiré par la possibilité d'imiter le repliement de protéines, car la structure tertiaire de ces dernières est stabilisée par des ponts disulfures. L'originalité de cet étude a consisté en l'utilisation de motifs «cystéine-un acide aminé-cystéine» (CXC) pour déclencher le repliement de la chaîne polymère. Ces motifs, récemment décrits par Gauthier, Leroux et leurs collaborateurs [13], sont capable de se dimériser et ainsi de former un pont intramoléculaire cyclique en milieu oxydant. Dans mon travail, deux motifs oligopeptidiques de type cystéine-arginine-cystéine (CRC) ont été précisément introduit en trois étapes sur des chaînes polystyrènes (Schéma 3). D'abord, des polymères à séquence contrôlée portant deux fonctions esters activées de type pentafluorophényle ont été préparées par la copolymérisation radicalaire en présence de nitroxydes de styrène avec un maléimide *N*-substitué, pentafluorophényl 4-maléimido benzoate, (Schéma 3, **A**) suivi par le greffage des motifs peptidiques *via* un couplage avec un dérivé monoaminé protégé du tripeptide CRC (Schéma 3, **B**, 1.). Après déprotection des fonctions amine et thiol (Schéma 3, **B**, 2.), la présence de groupes thiols a été confirmée par un résultat négative au test d'Ellman, et la formation de dérivés cycliques en milieu oxydant été démontrée par chromatographie d'exclusion stérique (CES). Une augmentation du volume d'élution après la cyclodimérisation, liée à une diminution du volume hydrodynamique, a été observée. Ainsi, des polymères à chaînes uniques ont pu être pliés grâce à l'oxydation des groupes thiol du motif CRC conduisant à la formation de liaisons disulfures intramoléculaires orthogonales [14] (Schéma 3, **C**).

Dans le **quatrième chapitre,** des structures cycliques ont été élaborées à partir de liaisons non-covalentes de type métal-ligand. Bien que la formation de nanoparticules basée sur une chaîne polymère unique utilisant ce type d'interaction ait été récemment rapportée [6, 7], ce domaine n'est pas suffisamment exploré. Dans cette thèse, les couples ligand/métal 1,10-phenanthroline/Ru(II) et 1,10-phenanthroline/Pd(II) ont été choisis. La première étape a consistée en la synthèse de polystyrènes avec deux motifs de reconnaissance moléculaire phénanthroline introduit en façon précise. Pour cela, le maléimide fonctionnalisé par une entité phénanthroline a été synthétisé et inséré aux bouts des chaînes polystyrènes. Ensuite, le repliement intramoléculaire de polystyrènes portant des motifs phénanthroline en présence d'un métal, Ru(II) ou Pd(II), a été examiné. Des analyses RMN attestent de la présence de ces motifs au sein des chaines macromoléculaires et la formation de complexes phénanthroline/métal. Néanmoins, la caractérisation par CES de ces polymères s'est avérée délicate à cause de l'affinité de la phénanthroline envers la phase chromatographique. Les premières études menées en CES sur les complexes montrent de légères variations de volume d'élution pouvant être liées à un compactage des chaînes macromoléculaires. Cependant, ces résultats ont besoin d'être confirmés en utilisant d'autres systèmes d'éluent en CES.

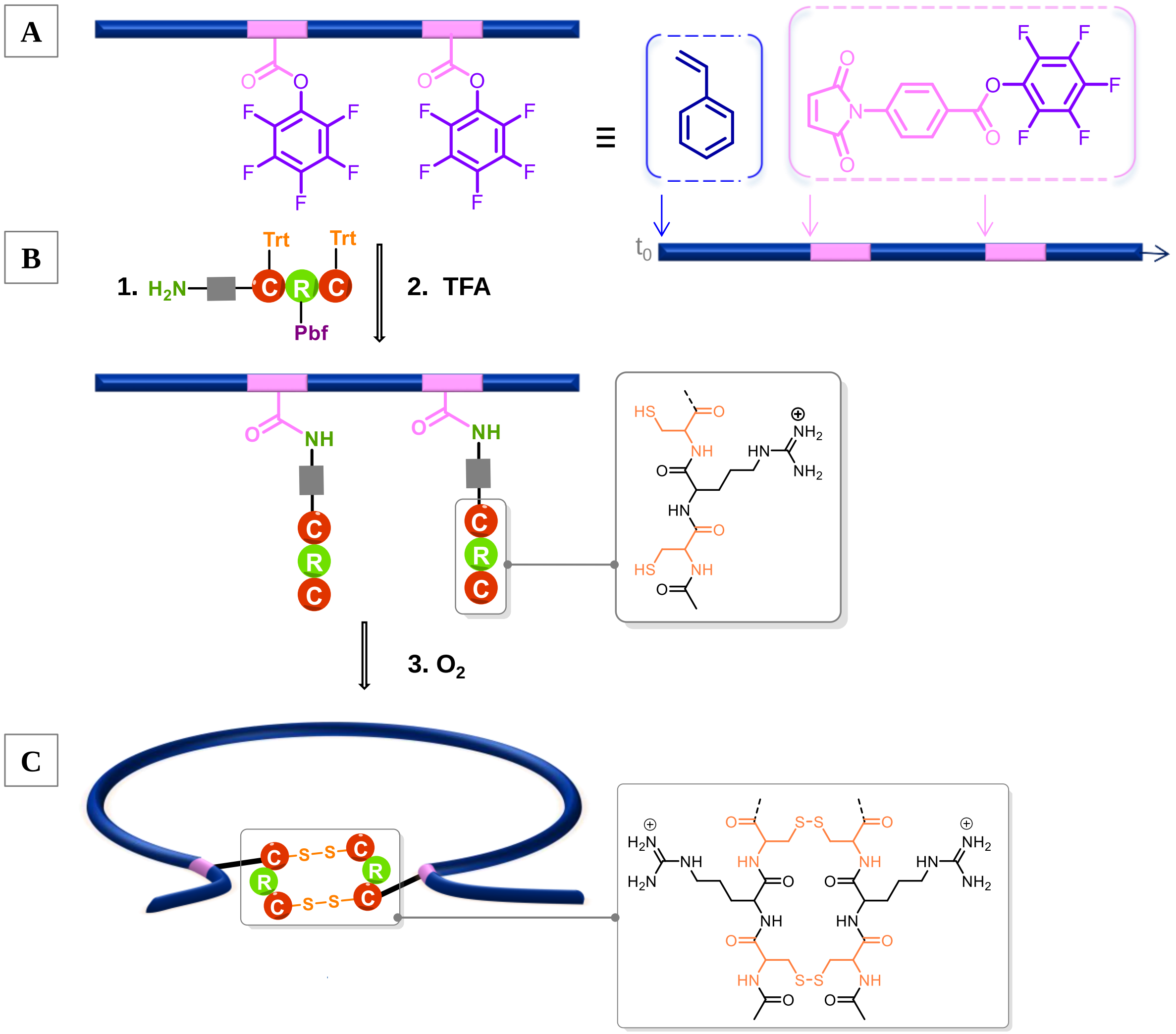

Schéma 3 | Schéma général du chapitre III. (**A**) Synthèse des précurseurs à séquence contrôlée par copolymérisation de styrène avec du pentafluorophényl 4-maléimido benzoate. (**B**) Introduction de deux motifs oligopeptidiques de type cystéine-arginine-cystéine (CRC) sur les chaînes polymères par 1) couplage entre le pentafluorophényl benzoate et un dérivé monoaminé protégé du tripeptide CRC et 2) déprotection des cystéines et arginines. (**C**) 3) Oxydation intramoléculaire des thiols des cystéines conduisant à la formation de liaisons disulfures intramoléculaires orthogonales et obtention des topologies cycliques.

GENERAL INTRODUCTION

Sequence-controlled polymers are macromolecules with a defined arrangement of their monomer units [1]. The control of "primary structure" (*i.e.*, the sequence of the monomers in the polymer chain and their chemical composition) is a keystone for biomacromolecules (*i.e.*, polypeptides and polynucleotides), since it strongly influences their spatial organization and properties such as self-replication or molecular recognition. Although biomacromolecules with controlled monomer sequence are everywhere present in nature, methods to prepare synthetic macromolecules with precisely controlled microstructure are still underexplored. The ability to regulate monomer sequences permits the control of polymer folding and self-assembly, and also to mimic important naturally occurring processes such as DNA packaging, assembly of polypeptide chains into tertiary structure, *etc*. Moreover, sequence-controlled polymers can be potentially used as a medium for data storage. Their macroscopic properties such as biodegradability, behavior in solution, conductivity can also be tuned according to the sequence [1].

Various strategies using synthetic chemistry have been investigated for monomer sequence control. Iterative synthesis [15] consisting in the attachment of the monomers one by one to a support is, perhaps, the simplest approach. However, it is time-demanding and it is not convenient for the synthesis of complex macromolecular architectures (because of the limited accessibility of the reaction sites in the resin). Metal coordination [16, 17] and step-growth polymerizations [18, 19] using specially designed monomers carrying functional groups proposed an alternative way for the synthesis of sequence-controlled polymers. Nevertheless, these strategies led mostly to alternating or periodic copolymers. The control of primary structure by means of chain-growth polymerization [20-22] is another fast-paced approach due to the development of controlled/living radical polymerization (CLRP) techniques, easier to handle than ionic polymerizations and that allow synthesizing polymers with well-defined structures and narrow molecular weight distributions. This latter polymerization technique has some advantages such as its practical ease and the broad range of polymerizable monomers, although some challenges still remain because of the statistical nature of radical polymerization. Some interesting strategies were proposed for the monomer sequence control using either CLRP or living ionic polymerization such as template synthesis [23], monoinsertion (*i.e.*, selective single monomer additions) and synthesis of multiblock copolymers [24-30]. Although these strategies broadened the opportunities of the primary structure control, they did not allow positioning of a functional group multiple times at any chain-locations by means of a straightforward, fast one-pot synthesis strategy.

In the present work, a precise placement of functional moieties at any targeted position in polymer chains was performed using strategies previously developed in our group [31]. The monomer sequence is controlled by the use of specific comonomer pair electron-donor styrene and electron-acceptor *N*-substituted maleimide (Figure 1, Main concept), *via* atom transfer radical polymerization (ATRP) or nitroxide-mediated polymerization (NMP). CLRP provides simultaneous growth of polymer chains, control over molecular weight and chain-end functionalities. As the reactivity ratios of most styrene/maleimide comonomer pair are close to 0, the comonomers tend to cross-propagation rather than homopolymerization. In non-stoichiometric conditions, when a small amount (1-3 Eq.) of *N*-substituted maleimide is added in the polymerization medium containing styrene, the maleimide is locally incorporated in growing polystyrene chains. A big advantage of this method is the possibility to use a broad library of *N*-substituted maleimides [21] and styrene derivatives [32], and, therefore, various polymers with precisely positioned functional groups are available.

Investigation of synthetic macromolecules as discrete objects is another emerging research direction in polymer science [2]. Broad applications of single-chain technology could be envisioned, for example, miniaturization of devices composed of a single chain, applications in catalysis, optics, *etc*. [2]. Various polymers with controlled molecular architecture are considered as single-chain objects such as dendrimers, star and hyperbranched polymers. However, the objective of this thesis consisted in the synthesis of single-chain objects based on linear polymers. The compaction/folding of polymers can be performed using self-associations either randomly positioned in polymer chains or at chain ends. For instance, the formation of single-chain nanoparticles can be performed using statistical copolymers [3-7], and cyclic topologies can be synthesized by chain-end modifications in dilute solution [33]. However, the formation of single-chain topologies with positionable intramolecular bridges can be realized only using sequence-controlled polymers carrying precisely placed functional groups [8, 9].

Thus, the principal objectives of this thesis were: ***1***) synthesis of sequence-controlled polymers carrying various functional groups using time-controlled additions of N-substituted maleimides in growing polystyrene chains by ATRP or NMP; and ***2***) positioning of intramolecular bridges in sequence-controlled polymers containing precisely introduced functional moieties leading to the formation of single-chain topologies, using covalent and non-covalent interactions.

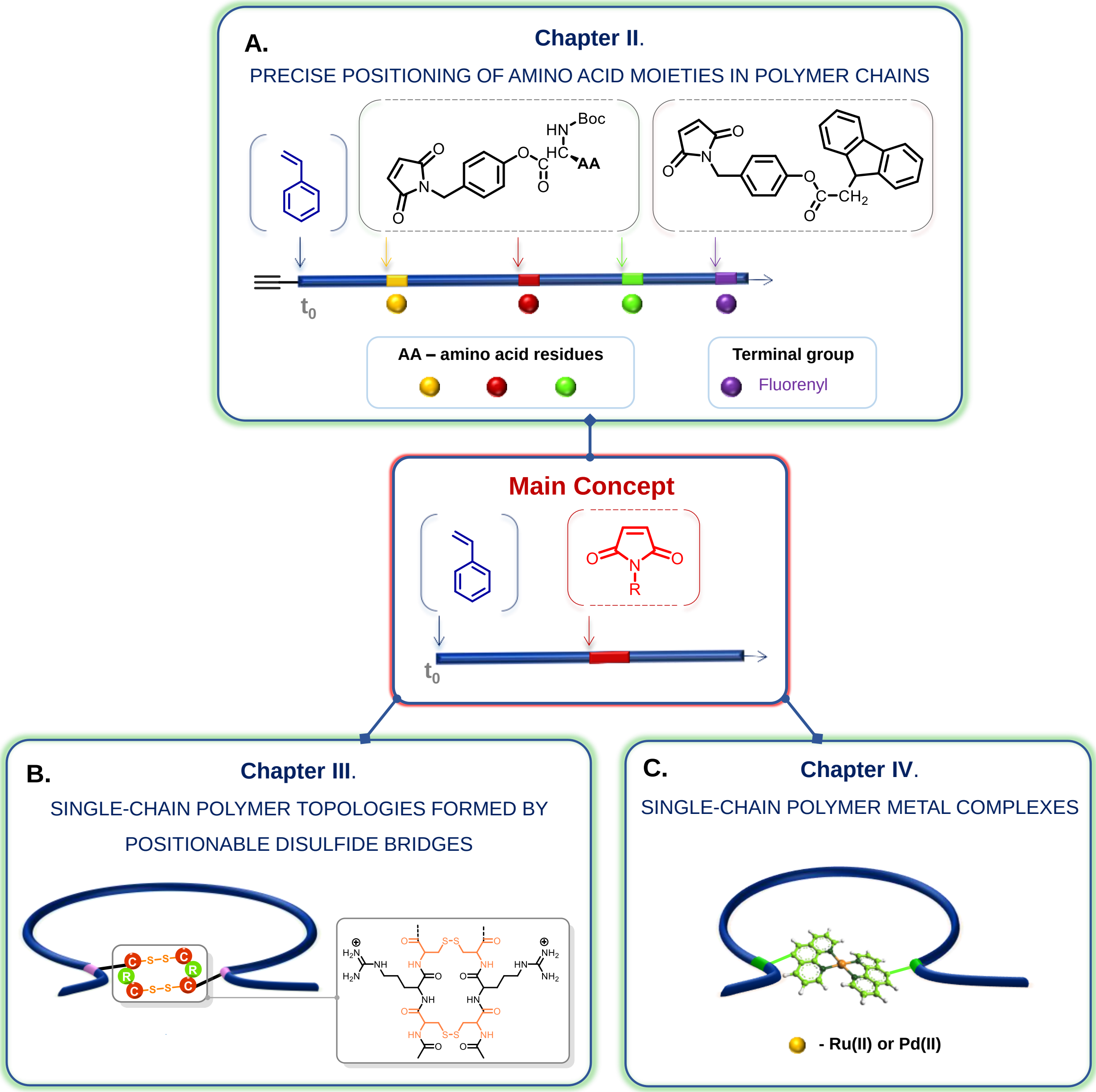
A.
Chapter II.
PRECISE POSITIONING OF AMINO ACID MOIETIES IN POLYMER CHAINS
HN
Boc
HC
AA
N
O
C
CH2
t0
AA – amino acid residues
Terminal group
Fluorenyl
Main Concept
N
R
t0
B.
Chapter III.
SINGLE-CHAIN POLYMER TOPOLOGIES FORMED BY POSITIONABLE DISULFIDE BRIDGES
C
S–S
R
H2N
NH2
NH
HN
C.
Chapter IV.
SINGLE-CHAIN POLYMER METAL COMPLEXES
- Ru(II) or Pd(II)

Figure 1 | Recapitulative scheme of the thesis. (**A**) Sequence-controlled polymers carrying amino acid and a terminal fluorenyl moieties synthesized by time-controlled additions of *N*-substituted maleimides into growing polystyrene chains (chapter I). (**B**) Synthesis of cyclic topologies by twin positionable disulfide bridges using cysteine-arginine-cysteine sequences (chapter II). (**C**) Complexation of polymers carrying phenanthroline moieties in the presence of Ru(II) or Pd(II) metals (chapter III).

In the **first chapter** ("Bibliography"), recent progress in the field of sequence-controlled polymers and single-chain technology is reported. In the present work, the monomer sequence is controlled using chain-growth polymerization. The advantages and limitations of this type of polymerization for the synthesis of sequence-controlled polymers are described at the beginning of the chapter. Alternative approaches for the monomer sequence regulation such as metal coordination, step-growth polymerization, iterative synthesis and the use of molecular machines are described afterwards. Then, development in the field of compaction and folding of polymer chains through the formation of intramolecular bonds is discussed, with the help of both covalent and non-covalent interactions. Lastly, the NMP and ATRP techniques are briefly presented.

Chapter II consisted of the preparation of sequence-controlled polymers with precisely positioned amino acid moieties *via* ATRP using the comonomer pair styrene – *N*-substituted maleimide. Such polymers are aimed to be used as a "track" for an artificial molecular machine in collaboration with the Leigh group in Manchester [10, 11], who reported in 2013 a sequence-specific peptide synthesis by a rotaxane-based small-molecule machine [11]. Although the oligopeptide prepared by their molecular machine is monodisperse and has the desired sequence of amino acids, the synthesis of the "track" (*i.e.*, thread containing amino acid building blocks) is complex and proceeds in several steps (from 7 to 9) with a low total yield (2-3 %). In my work, the advantages of radical polymerization were used for the synthesis of improved "tracks" (better yields and shorter overall synthesis time), and up to 4 functional groups could be precisely positioned in the polymer chain. Both conventional and "ultra-precise" methodologies [12] (recently developed in our group) were studied for the copolymerization of styrene with maleimides.

In **Chapter III** we focused on the synthesis of single polymer chain topologies through the formation of intramolecular covalent links (disulfide bridges). Disulfide bridges are present in Nature and stabilize the tertiary structure of proteins. This work was inspired by the possibility to mimic important natural processes such as protein folding. The originality of my study consisted in the use of the "cysteine-*any amino acid*-cysteine" (CXC) sequence to trigger the folding of the molecule. This motif, recently reported by Gauthier, Leroux and coworkers [13], led to a much more specific and efficient disulfide bridge formation compared to the sequence containing only a single cysteine residue. The control of the monomer sequence gives the opportunity to regulate the polymer topology [34]. Sequence-controlled polystyrenes with precisely positioned functional groups were synthesized by the copolymerization of styrene with *N*-substituted maleimide carrying reactive moieties (*i.e.*, pentafluorophenyl activated ester). CXC fragments were introduced by post-polymerization modifications; the pentafluorophenyl activated ester was substituted by the primary amine moiety of the CXC derivative, yielding the desired polymer conjugate. Finally, polymer chains were folded by the oxidation of thiol groups leading to the formation of intramolecular orthogonal disulfide bonds [14].

The synthesis of single-chain topologies using coordination chemistry was investigated in **Chapter IV**. Although the formation of single chain polymer nanoparticles by means of metal-ligand interactions was recently reported [6, 7], this field is insufficiently explored. The present study consisted in the synthesis of sequence-controlled polymers carrying precisely positioned ligands (*i.e.*, 1,10-phenanthroline) followed by the intramolecular folding in the presence of metal, Ru(II) or Pd(II), complexes. Thus, the copolymerization of styrene with phenanthroline-bearing maleimide was firstly performed, and afterwards the possibility to form single chain polymer metal complexes was examined.

CHAPTER I. BIBLIOGRAPHY

I.1. INTRODUCTION

Sequence-controlled polymers are constituted of precisely arranged monomer units along polymer chain leading to controlled microstructure (“primary structure”) – similarly to precise sequences of amino acids in a peptide chain or nucleotides in a DNA chain. The primary structure of biomacromolecules determines their complex organization and such significant natural processes as self-replication or molecular recognition. Initially the interest to sequence-controlled polymers was due to the ability to reproduce or mimic biomacromolecules. Therefore, solid-phase and liquid-phase iterative synthesis [35, 36] became broadly exploited methods for the preparation of natural and non-natural sequence-defined macromolecules such as oligocarbamates [37], oligoureas [38], oligoesters [39] and polyamides [40].

Nowadays the idea of sequence control progressed toward the ability to synthesize polymers with new properties since monomer sequence strongly influences some macroscopic properties [1]. For example, the hydrolysis of a poly(lactic-*co*-glycolic acid) copolymer was notably different for a random compared to a sequence-controlled copolymer [41]. Another interesting developing direction is data storage at molecular level [31, 42, 43]. As described by Church *et al*. [44], the information can be successfully encoded and stored in nucleic acid chains with further recovery of data. By analogy to DNA which codes biological information, sequence-controlled synthetic polymers can be also considered as potential data storage containers.

Another emerging direction is the application of single-chain technology, through compaction and folding of single polymer chains, for mimicking complex biomacromolecules and/or the preparation of single-chain devices [2, 45]. The main advantage of the use of single-chain technology relies in the miniaturization [2]. Non-covalent and covalent intermolecular interactions are used to compact a single-polymer chain into a complex structure. Various topologies and ordered structures were designed and synthesized. Among them are non-natural foldable oligomers and polymers [46] mimicking the folding of peptides chains and single-chain nanoparticles compacted by covalent or non-covalent links [45, 47]. Precise positioning of intramolecular covalent bridges in a polymer chain is another strategy for single-chain technology [8, 9].

I.2. MONOMER SEQUENCE CONTROL BY CHAIN-GROWTH POLYMERIZATION

Controlling monomer sequence of polymers is important since monomer ordering strongly influences polymer properties. Several strategies to regulate monomer sequence are investigated, the main ones being iterative synthesis, step-growth polymerization and chain-growth polymerization. This latter polymerization technique is under very fast development thanks to the broad range of polymerizable monomers and its practical ease. However, some challenges remain since chain-growth polymerization is a statistical process, and deals with ions and radicals, mostly leading to random microstructures. Controlled/living radical polymerization techniques (CLRP) that are easier to handle compared to ionic polymerizations allow synthesizing polymers with well-defined structures and narrow molecular weight distributions, thus explaining its increasing use for the synthesis of sequence-controlled polymers. Various methods to control monomer sequence, mainly by CLRP techniques, are presented below with their advantages and limitations.

I.2.1. Monoinsertion

One of the important features of controlled/living polymerizations, *i.e.*, control over growing polymer length and chain-ends, was used to realize monoinsertion of a functional monomer. The ability to “restart” the CRP was used in some studies to perform multiple monoinsertions, and, thereby, prepare sequence-controlled polymers.

An example of selective single monomer addition at polymer chain end using living cationic polymerization was proposed by Sawamoto and coworkers [48]. Poly(*n*-butyl vinyl ether) (PNBVE) was prepared by living cationic polymerization in the presence of $SnCl_4$ as a catalyst (Figure 2). Afterwards, a specific monomer that deactivated the polymer chain-end of PNBVE was added. Such “end-capped” chain-end could be re-activated only by increasing the temperature or by addition of more active catalyst. From several tested monomers di-*tert*-butyl (*N*-(2-(vinyloxy)ethyl)imido)dicarboxylate (BocVE) revealed the selective “end-capping” and specific addition of one unit. This particular result was proven by matrix-assisted laser desorption/ionization time-of-flight mass spectrometry (MALDI-TOF-MS). The selectivity of BocVE was explained by electronic and steric factors, consisting in intramolecular stabilization of the growing carbocation through a double carbonyl coordination, and hindrance of two bulky Boc-groups, preventing another monomer to approach.

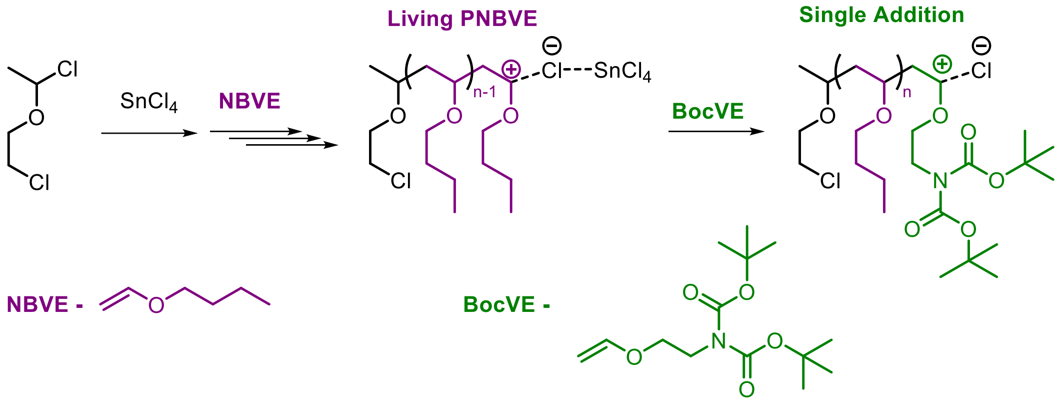

Figure 2 | Single addition in living cationic polymerization of *n*-butyl vinyl ether.

The chain-end with BocVE was stable against NBVE propagation. There were two possibilities for post-polymerization modification either deprotection of BocVE terminal unit to obtain an amine-capped PNBVE, or modification by an active compound to receive PNBVE with another functional end-group. Quenching the polymer with methanol and $LiBH_4$ followed by deprotection of Boc-groups led to an amino-functionalized polymer (Figure 3, **A**). Electrophilic reaction of terminal BocVE with sodium diethyl malonate with subsequent double deprotection of malonate- and Boc-groups resulted in a polymer with terminal amine and carboxylic groups (Figure 3, **B**).

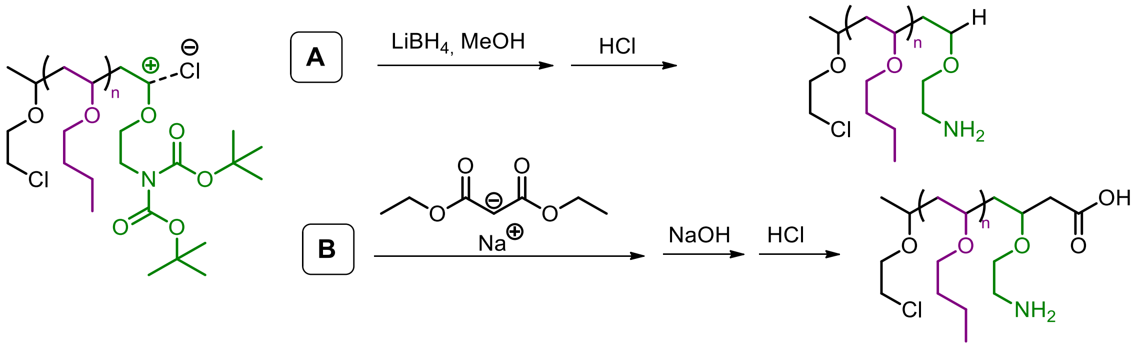

Figure 3 | Post-polymerization modification of PNBVE with BocVE unit (**A**) either quenching the polymer chain end with $LiBH_4$ followed by deprotection of Boc-groups, or (**B**) quenching the polymer chain end with sodium diethyl malonate followed by deprotection of malonate- and Boc-groups.

Although the described strategy was not versatile and used a specifically designed monomer for the single addition, it showed the possibility to insert a single functional group at the chain-end leading after several modifications to the polymers with only amine or amine and carboxylic terminal functional groups.

The combination of CRP and automated purification techniques was used for the synthesis of sequence controlled oligomers by Junkers and coworkers [49]. Consecutive monomer additions were performed *via* reversible addition fragmentation radical transfer (RAFT) technique leading to oligomers with a precisely tuned order. The product after each addition was isolated by purification by automated recycling size-exclusion chromatography (SEC). The first monomer *n*-butyl acrylate (*n*BuA) was inserted into the RAFT agent (2-cyano-2-propyl dodecyl trithiocarbonate). Very short reaction time of 10 min. and 10 eq. of *n*BuA to 1 eq. of RAFT agent were used that allowed high trithiocarbonate end group retention for the addition of next monomer and led to three products with single, double and triple *n*BuA insertions. The single adduct was isolated after two cycles of recycling SEC with 55% yield. Subsequent addition of 2-ethylhexyl acrylate (EHA), *tert*-butyl acrylate (*t*BuA) and *n*BuA to the purified *n*BuA single adduct **1** resulted in the oligoacrylate RAFT agent **2** with a precise sequence of monomers (Figure 4). The yield of the last step was 10-15%, and it required higher amount of cycles.

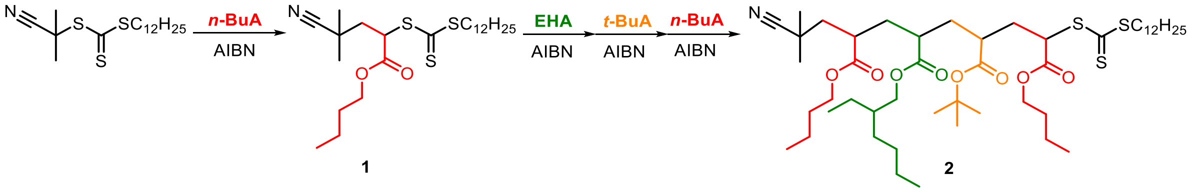

Figure 4 | Consecutive addition of acrylic monomers by RAFT leading to sequence-controlled acrylate oligomers.

This approach demonstrated the use of RAFT for a straightforward synthesis of sequence-controlled oligomers that was proved by APT ^{13}C NMR spectroscopy, SEC and MS analyses. However, the further extension of the sequence to longer oligomers is restricted, since higher cycle times are required, and the yields are low.

Another study used atom transfer radical polymerization (ATRP) for the sequence regulation. Huang and coworkers reported a strategy consisting in the repetition of monoinsertion at polymer chain-end followed by chemical modification cycles [50] (Figure 5). Poly(methyl methacrylate) (PMMA) synthesized by ATRP was chosen as a first block. Afterwards, a low activity vinyl monomer (allyl alcohol) possessing low propagation rate constant, was added to the PMMA with bromine chain-end in the presence of Cu/$CuBr_2$/Me_6-TREN *via* atom transfer radical addition (ATRA). By oxidation of the alcohol into carboxylic group in the presence of TEMPO, KBr and NaOCl and consequent esterification by a functional alcohol (Figure 5, R_1-OH), a specific side group (Figure 5, R_1) was introduced in the polymer chain. A new batch of monomer was added to the esterified product, and a cycle of post-polymerization modifications (*i.e.* ATRA of allyl alcohol followed by oxidation of alcohol to carboxylic group and esterification by a functional alcohol R-OH) was performed. Thereby, functional moieties were placed at aimed position in polymer chain. The intermediary and final polymers were analyzed by mass spectroscopy and revealed the quantitative oxidation of hydroxyl groups and esterification, but a loss of bromine groups (less than 20 %) after the mono addition of allyl alcohol was detected. Although this strategy still has to be optimized, it presented a new alternative for the synthesis of sequence-controlled polymers.

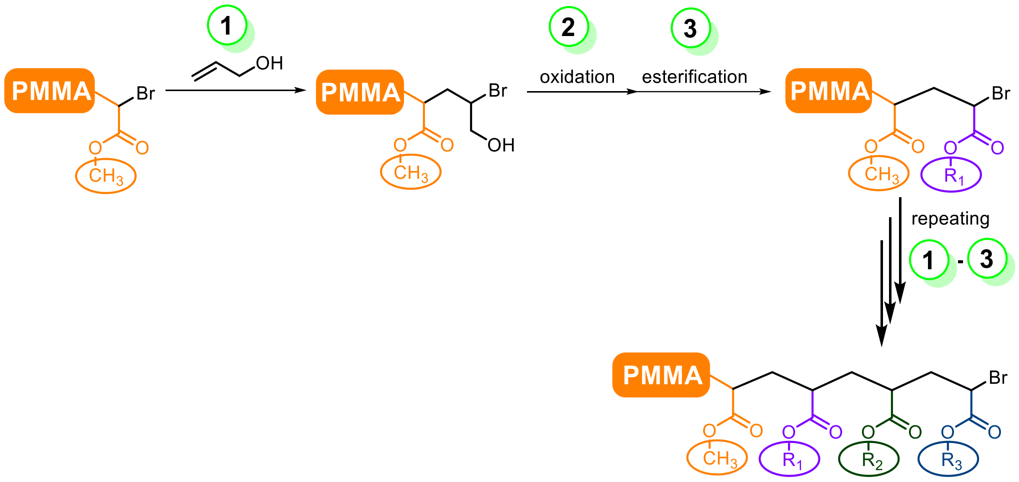

Figure 5 | Schematic representation of the synthesis of sequence-controlled polymers using allyl alcohol and post-modifications.

I.2.2. Template Synthesis in Controlled Radical Polymerization

This part is dedicated to the synthesis of polymers in the presence of a macromolecular template. This approach is inspired by some natural processes such as DNA replication, transcription and translation when biomacromolecules with a defined sequence are synthesized using templates (*i.e.*, mRNA). Sawamoto and coworkers [23] designed a template initiator (Figure 6, **1**) bearing in *ortho*-positions of aromatic ring two different initiating sites (C-Cl): a haloether part that can initiate living cationic polymerization and a haloester part that can initiate living radical polymerization (Figure 6, **A**).

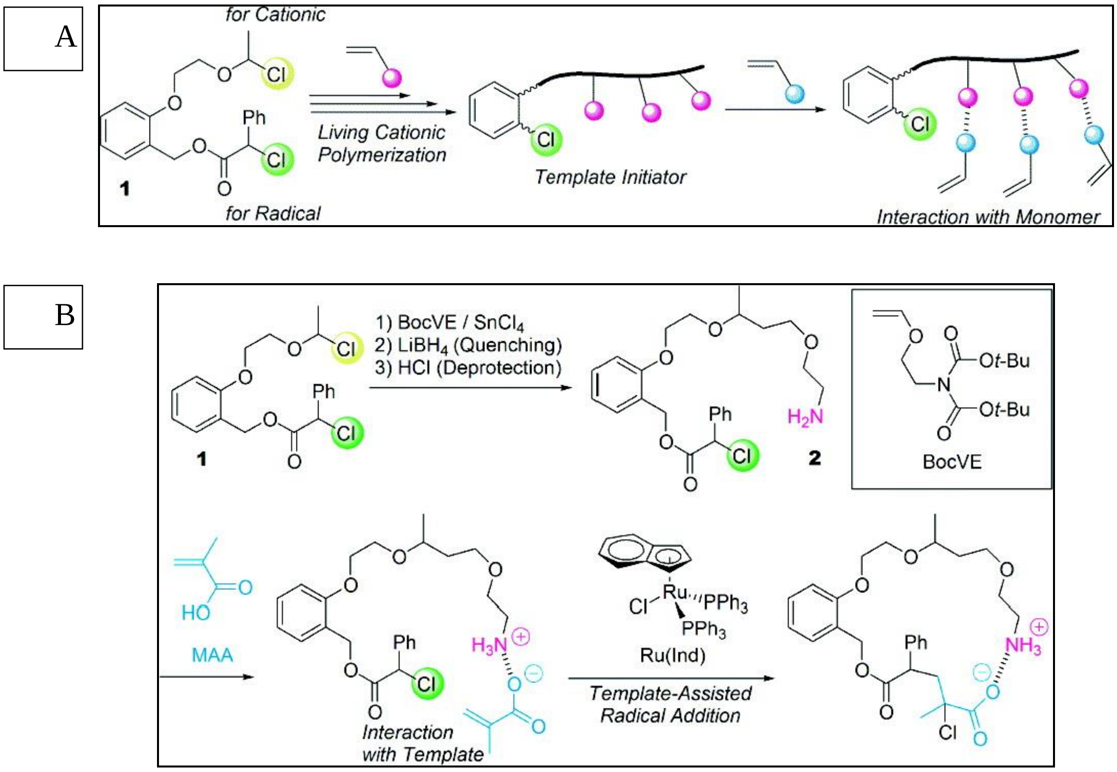
A
for Cationic
Cl
Ph
Cl
1
for Radical
Living Cationic Polymerization
Template Initiator
Interaction with Monomer
B
1) BocVE / SnCl4
2) LiBH4 (Quenching)
3) HCl (Deprotection)
H2N
2
O-t-Bu
N
O-t-Bu
BocVE
HO
MAA
H3N
Interaction with Template
Cl
Ru
PPh3
PPh3
Ru(Ind)
Template-Assisted Radical Addition
NH3

Figure 6 | (**A**) Template-assisted living radical polymerization. (**B**) Radical addition of methacrylic acid using a template initiator. Reprinted with permission from reference [23]. Copyright © 2009, American Chemical Society.

In order to prove the template effect [23], the initiator haloether site was modified into amine **2**, and a radical addition of methacrylic acid was initiated with ruthenium complex catalyst in toluene at 80°C (Figure 6, **B**). Methacrylic acid monomer bearing carboxylate group (in acidic conditions) was “recognized” by the ammonium of the initiator leading to formation of a 1:1 adduct as evidenced by ^{1}H NMR and electrospray ionization-mass spectrometry (ESI-MS). In addition, a radical addition in the presence of methacrylic acid and methyl methacrylate (1 to 1 molar ratio) was checked out with the template initiator **2** and a template-free initiator, and revealed more than 10 times slower incorporation of methyl methacrylate in the presence of template initiator than in the presence of template-free initiator. More detailed investigation and design of the initiators were performed by

Sawamoto and coworkers [51-53] toward sequence control with such template initiators. Although only the first steps in this direction were demonstrated, the use of template initiator predetermining the order of covalently attached monomers might be a promising approach in the future.

I.2.3. Multiblock Copolymer

During the last few years interesting approaches for controlling the block-sequence of multiblock copolymers have been reported. Such polymers consist of repeating homopolymer units connected by covalent link. Along with conventional AB-type diblock and ABA-type triblock copolymers, block copolymers with additional number of blocks and chemically distinct block types can be prepared that broaden the number of unique sequences [24-26]. Multiblock copolymers were first synthesized using living anionic polymerization [27]. A variety of synthetic strategies were investigated afterwards [54-56], however a straightforward one-pot synthesis of multiblock copolymers with varied block sequence and length was reported by Coates and coworkers only recently [28]. They used living polymerization techniques to prepare a monodisperse (PDI = 1.12) hexablock copolymer containing hydrophilic, lipophilic and fluorophilic blocks (polycarbonate derivatives). Block copolymers can be nowadays synthesized by controlled radical, ring-opening, and metal-catalyzed polymerizations using various strategies, such as chain-coupling strategies or sequential addition of distinct monomers to an active polymer chain [25, 29, 30]. Some novel strategies proposing easy and straightforward synthesis of multiblock copolymers are described below.

The synthesis of hexablock and octablock copolymers by single-electron transfer living radical polymerization (SET-LRP) was described by Whittaker and coworkers [30, 57]. These polymers were obtained by successive additions of monomers (methyl methacrylate derivatives) until their full conversion, without any intermediate purification. Due to the use of SET-LRP in the presence of Cu(II), the loss of chain-end groups was minimal. It allowed the successful preparation of well-controlled copolymers with very short blocks (3 monomer units). Although side reactions (with formation of dead chains) occurred, the vast majority of chains had a bromine terminal group that was confirmed by mass spectrometry.

Junkers and coworkers showed the application and advantages of the use of a micro-flowreactor for the preparation of well-defined acrylate multiblock copolymers [58]. The first block, poly(*n*-butyl acrylate) with a narrow polydispersity (PDI 1.14), synthesized by RAFT polymerization, served as a macro RAFT agent. The polymerizations were carried out at 100ºC during a short period of time of 5-10 minutes. Successive addition of different acrylate monomers (2-ethylhexyl acrylate, *t*-butyl acrylate and *n*-butyl acrylate) yielded copolymers with four and five consecutive blocks with PDI 1.32 and 1.46, respectively. However, the approach was limited by the number of blocks, and the isolation of the polymer should be performed after each block formation.

Recently a facile synthetic route providing polymers with a large number of blocks, each with identical monomer units, was proposed by Perrier and coworkers [25]. Multiblock copolymers with a polydispersity inferior to 1.4 were obtained by RAFT in a one-pot reaction. Several acrylamide derivatives such as *N*,*N*-dimethylacrylamide (DMA), 4-acryloylmorpholine (NAM), *N*,*N*-diethylacrylamide (DEA) and *N*-isopropylacrylamide (NIPAM) with high propagation rate constants and ease of functionalization were selected. Rapidly propagating monomers that allowed fast consumption of the starting monomer and subsequent incorporation of a new block were used. Block copolymers containing repeating four and five different sequences were synthesized by RAFT in the presence of chain transfer agent 2-(((butylthio)-carbonothiolyl)thio)propanoic acid and 2,2-azoisobutyronitrile (AIBN) as initiator in dioxane at 65°C. A new monomer was added after each 24 hours period to prepare a new block. Initiator was also added as around 80% of it was consumed after 24 hours. Monomer conversions for each block were high, around 97-100%, and molecular weight distributions were monomodal.

Another block copolymer containing three different repeating sequences of around three units each was obtained with accurately adjusted synthetic conditions [25]. The initiator 2,2'-azobis[2-(2-imidazolin-2-yl)propane]dihydrochloride (VA-044) was employed since it decomposes at around 90% in 2 hours. The initiator did not influence the control of polymerization, but increased the reaction rate. Water was used as solvent because it increases the propagation rate constant of acrylamide monomers. As it is demonstrated on the Figure 7, the sequence $PNAM_3$, $PDMA_3$, $PNAM_3$ and $PDEA_3$ was repeated five times using poly(NAM) of DP_n 10 as a macro chain transfer agent. The evolution of chromatograms after each new block addition is presented (Figure 7).

Although it is possible to analyze by mass spectroscopy the signals of the first five added blocks, the following addition of more blocks could not be analyzed by mass spectroscopy due to signal overlapping. The mass spectra of the first five blocks confirmed the extension at each step, and molecular weight of the final copolymer was close to the theoretical. Although this approach does not ideally provide sequence-controlled polymers, it shows a synthetically simple and scalable strategy for the primary structure regulation.

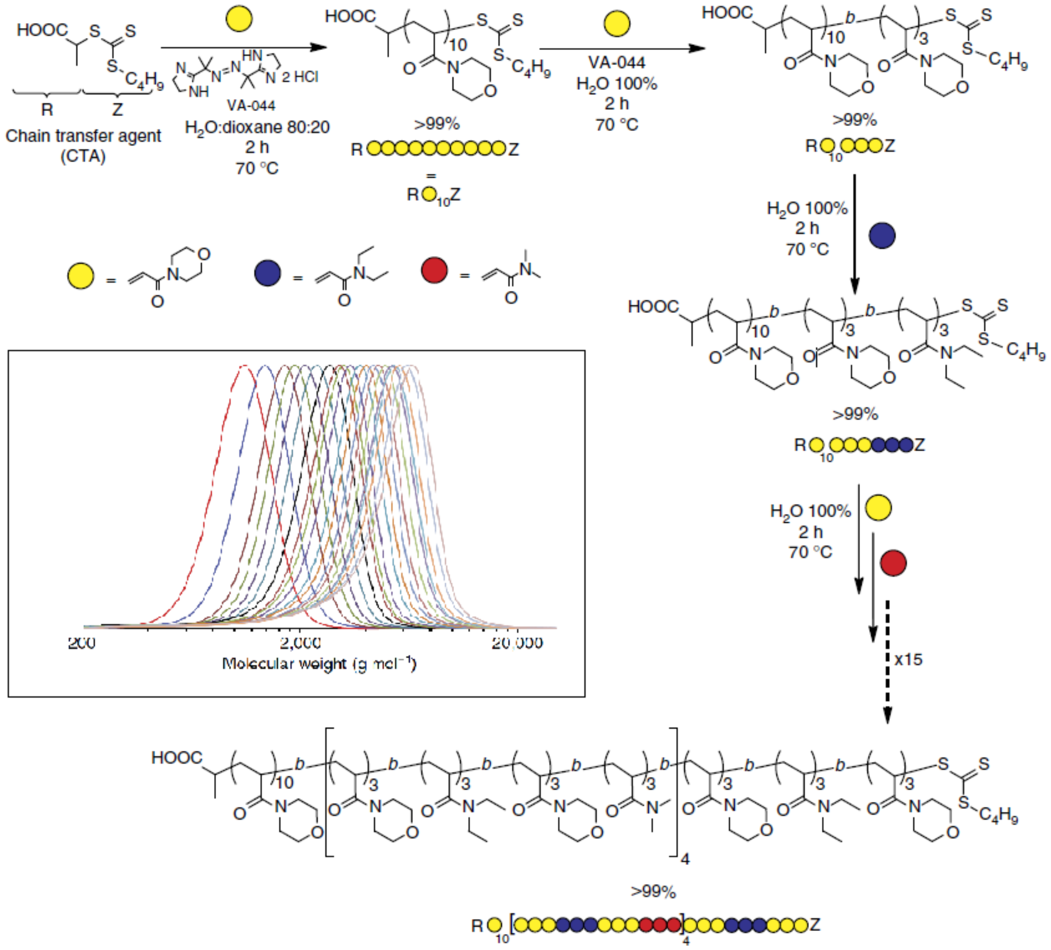
HOOC
R
Z
Chain transfer agent (CTA)
VA-044
2 HCl
H2O:dioxane 80:20
2 h
70 °C
>99%
R○○○○○○○○○○Z
=
R○10Z
VA-044
H2O 100%
2 h
70 °C
H2O 100%
2 h
70 °C
x15
200
2,000
20,000
Molecular weight (g mol−1)
R○10[○○○●●●○○○●●●]4○○○●●●○○○Z

Figure 7 | Schematic representation of the synthesis of the block copolymer containing three different repeating sequences of around three units each and molecular weight distributions for successive block extensions of this block copolymer. Reprinted with permission from [25]. Copyright © 2013, Rights managed by Nature Publishing Group.

Another interesting example combining block and gradient copolymers was presented by Sawamoto and coworkers [26]. This approach is based on the combining ruthenium-catalyzed living radical polymerization and *in situ* transesterification of methacrylates (MA). Transesterification of carboxylate esters can be performed in the presence of alcohols using metal alkoxides as catalysts. At the same time, well-defined polymers can be synthesized by ruthenium-catalyzed polymerization in alcohol media, wherein metal alkoxides serve as additives. The authors first investigated if some mandatory conditions for this tandem polymerization were fulfilled: a) the selective transesterification of monomer ester moieties in the presence of the polymers, independently of the monomer concentration, and b) the absence of influence of transesterification on the polymerization. When suitable conditions were found, gradient triblock copolymers were obtained *via* three iterative addition of methyl methacrylate (MMA) and the use of different alcohols in the polymerization media. First, MMA was polymerized in the presence of a ruthenium catalyst, $Ti(O\textit{i}\text{-}Pr)_4$, and *i*-propanol (*i*-PrOH), thus leading to a MMA/*i*-PrMA gradient block. Afterwards, two other gradient blocks were prepared: MMA/ethyl MA and MMA/benzyl MA. The molecular weight distribution was monomodal, and the PDI of the final copolymer was 1.36. The use of commercially available reagents, efficient and versatile catalysts, and straightforward synthetic route has made this approach convenient for the design of tailor-made sequence-controlled copolymers.

1.2.4. Kinetic Approach

By a right selection of comonomer pairs, the sequence can be self-controlled to some extent. One of the well-studied examples is the synthesis of alternating copolymers of AB-type when two monomers are regularly following each other, thus leading to a defined microstructure [59]. The use of electron-donor and electron-acceptor comonomer pairs that tend to copolymerize rather than homopolymerize, is one of the ways to obtain alternating copolymers. Maleic anhydride, most *N*-substituted maleimides, sulfur dioxide and pentafluorostyrene are powerful electron-acceptors and are difficult to homopolymerize, but easy to copolymerize with electron-donating monomers such as styrene derivatives, vinyl ethers and isobutylene [59].

The reactivity ratio r [60] was introduced to characterize the tendency of comonomers for homo- and copolymerization. Different combinations of propagating radical and monomer can occur during copolymerization (Scheme 1) according to the terminal model (reaction rate constant k only depends on the terminal monomer). Every stage has its reaction rate constant k [60], and reactivity constant is defined as a ratio of reaction rate constant of homopolymerization to copolymerization for each couple of monomers (M_1 and M_2).

Consequently, when $r_1 = r_2 \approx 0$, monomers do not tend to homopolymerize, thus leading to favorable conditions to obtain alternating copolymers.

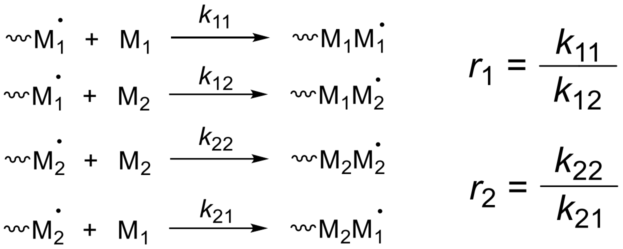

Scheme 1 | Various combinations between propagating chain end and a monomer that can take place during polymerization.

Along with various AB systems [61], the synthesis of AAB-sequence copolymerization was described [22, 61] by Kamigaito and coworkers [22] using *N*-substituted maleimide (A) and limonene (B). They showed that not only the nature of comonomers has an influence on the obtained monomer sequence, but also the polymerization conditions. The copolymerization of limonene was examined with *N*-phenyl and *N*-cyclohexyl maleimides in the presence of 2,2-azoisobutyronitrile (AIBN) as radical initiator and *N*-butyl cumyl trithiocarbonate as chain transfer agent in various solvents (DMF, CH_2Cl_2, cumyl alcohol and fluorinated cumyl alcohol). When fluorinated cumyl alcohol was used as solvent, a 2 to 1 ratio of maleimide to limonene was detected by NMR spectroscopy despite the initial monomer feed ratios. This result was explained by the interaction of the fluorinated alcohol with the carbonyl group of maleimide and by steric interactions caused by the bulky structure of limonene. The copolymers were characterized by MALDI-TOF-MS which confirmed the expected ratio of limonene units. Only minor series of peaks corresponding to an additional maleimide were detected in the mass spectra. Those results can be explained by earlier termination of the polymer chain with chain transfer agent. Thus, the proposed strategy allowed preparing copolymers with a highly-controlled AAB-sequence.

The work on the synthesis of AB- and AAB-sequences was expanded by Matsumoto and coworkers [61] who investigated the copolymerization of *N*-substituted maleimides with olefins and polyisobutene macromonomers. It was shown that the copolymer sequence depended on the olefin structures. Planar and conjugated olefins (Scheme 2, type **a**) as well as less-hindered and non-conjugated olefins (Scheme 2, type **b**) led to AB alternating copolymers, whereas hindered and non-conjugated olefins with saturated or unsaturated substituents led (Scheme 2, type **c**) to AAB alternating copolymers with maleimide.

1:1 Alternating copolymerization under terminal control	**2:1 Alternating copolymerization under penultimate unit control**
Type a: conjugate olefins 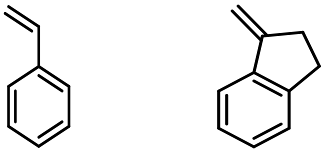	**Type c**: hindered / non-conjugated olefins 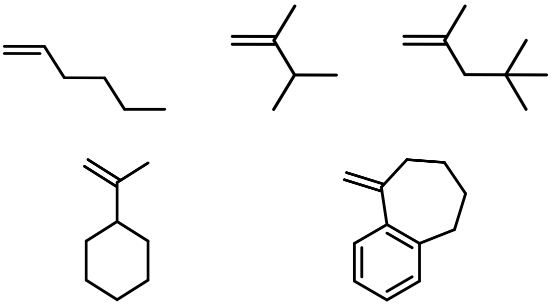
Type b: less-hindered non-conjugated olefins 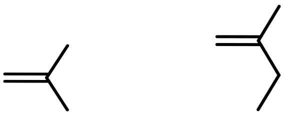	

Scheme 2 | Classification of the olefins used for copolymerization of *N*-substituted maleimides with various olefins [61].

N-alkyl and *N*-phenylmaleimides were investigated in this work. The expanded model of monomer reactivity ratios determination ("Penultimate unit model") was explored [22] and took into consideration the influence of penultimate unit on the propagation chain-end. The nature of comonomers and microstructure affected copolymer properties: for example, the copolymers with a 2:1 composition of *N*-methylmaleimide and the olefins turned out to have high glass transition temperatures (T_g), while the copolymers of *N*-(2-ethylhexyl)maleimide with isobutene oligomers revealed to be low T_g-copolymers. The introduction of bulkier substituents into the α-position of the olefin (Scheme 2, type **c**) led to the suppressed dynamic chain motion, and, consequently, to an increase in the T_g value of the copolymers.

Various initial ratios of electron-acceptor (maleic anhydride or *N*-substituted maleimide) to electron-donor monomer (olefin) were also used. But what happens if a discrete amount of electron-acceptor compared to electron-donor monomer is used? Benoit *et al*. [62] decided to prepare block-copolymers via CRP using a 9 to 1 initial mixture of styrene to maleic anhydride. Neither nitroxide-mediated polymerization (NMP) using TEMPO, nor Cu-, Ni-, Fe-based atom transfer radical polymerization (ATRP) showed living character of styrene-maleic anhydride copolymerization. However, when a 5 mol. % of free nitroxide **II** (Figure 8) was added to alkoxyamine **I**, copolymers with high conversion and low PDI (1.1-1.2) were obtained by NMP. Afterwards, the kinetics of monomer conversions *versus* time were examined (Figure 8). The preferential incorporation of maleic anhydride took place at initial stage of polymerization until it was fully consumed, the conversion of styrene at that moment reached around 25-30%. Consequently, a block copolymer with an alternating poly(styrene-*alt*-maleic anhydride) and a pure polystyrene parts was prepared with a molecular mass M_n = 5000 g•mol-1 and a PDI ~ 1.2. Two glass transition temperatures corresponding to styrene/maleic anhydride and polystyrene blocks were measured by differential scanning calorimetry (DSC).

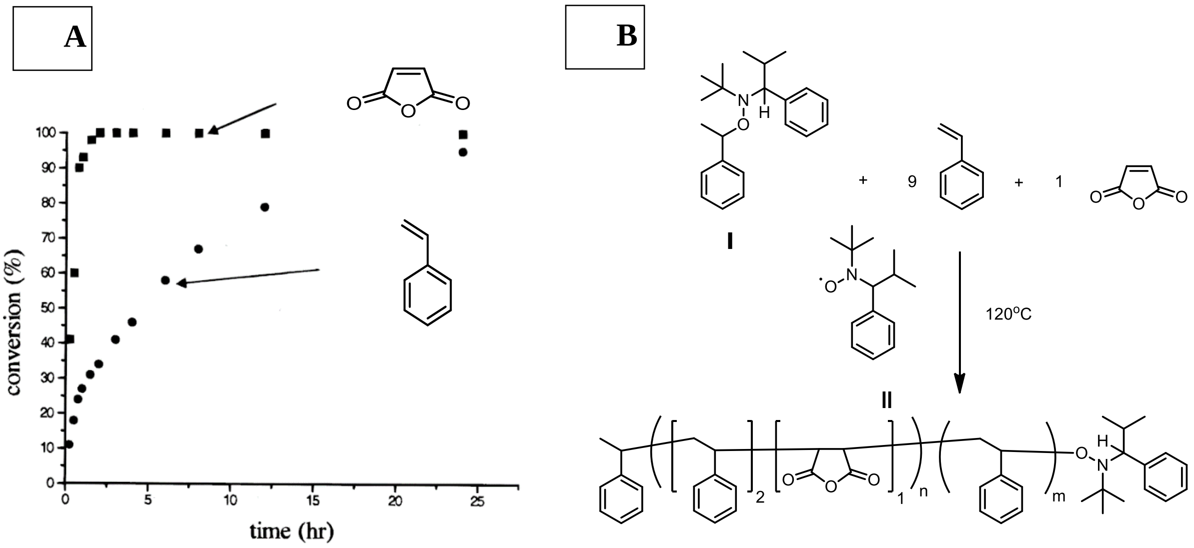

Figure 8 | (**A**) Monomer conversions of styrene and maleic anhydride, determined by ^{1}H NMR, as a function of time. (**B**) Schematic representation of NMP copolymerization of styrene with maleic anhydride. Reprinted with permissions from [62]. Copyright © 2000, American Chemical Society.

This strategy was further developed by Lutz and coworkers [20] who described the copolymerization of two monomers forming alternating polymers: styrene with a small amount of *N*-substituted maleimide (100 Eq. to 3 Eq.). ATRP was used as an efficient method to control the copolymerization of styrene. Various *N*-substituted maleimides (Figure 9) were added in the reaction medium at a defined time and, consequently, at defined conversion rates of styrene. Their incorporation in the polymer chain was proved by the disappearance of characteristic peaks in ^{1}H NMR spectra of each maleimide. The final polymer had a narrow polydispersity (PDI 1.16) and molecular mass close to the theoretical one. Although the monomer sequence in the polymer chain is not strictly defined and polymer chains contain defects (some chains contain higher or lower number of maleimides than it was added in the reaction mixture), this study reveals a new and elegant approach for the synthesis of polymers with controlled sequence [21, 60, 63].

Indeed, N-substituted maleimides were chosen as electron-acceptor monomers as they can be rather easily functionalized, and a library of *N*-functionalized maleimides was presented by Pfeifer *et al*. [21], allowing the introduction of various functional groups at any position of the polymer chain. With analogy to the library of electron-acceptor *N*-substituted maleimides, a range of electron-donor styrenic monomers were prepared and used in the copolymerization with N-functionalized maleimides by nitroxide mediated polymerization (NMP) [32]. It was shown that strong donor substituents (*tert*-butoxy, for example) at the para-position of styrene derivatives led to more precise sequence-controlled polymerization.

Other applications based on the pair *N*-functionalized maleimide – styrene derivatives were explored by the Lutz team. Polystyrenes with precisely positioned functional dendrons [64], or multifunctional single-chain hexose arrays that interact specifically with complementary lectins were synthesized [65]. Moreover, copolymers containing poly(ethylene glycol) (PEG) side chains with precisely positioned fluorescent and reactive functionalities were prepared [66] to add water-soluble and fluorescent properties.

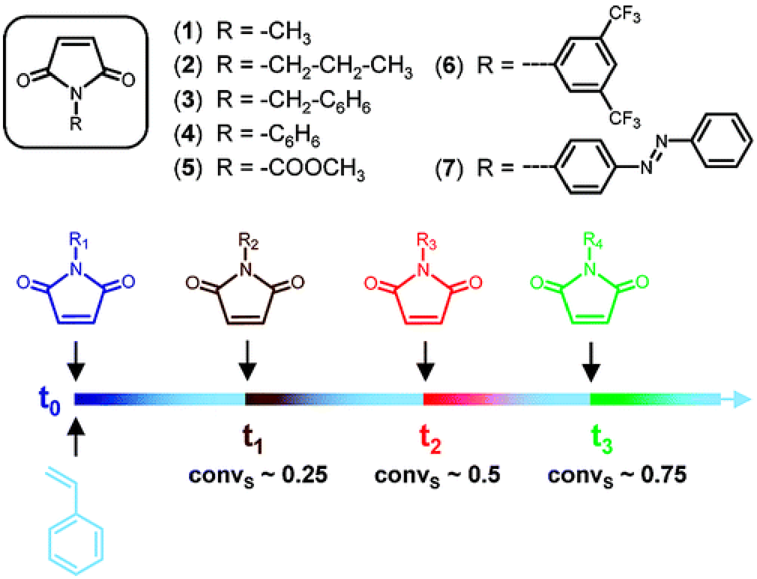

Figure 9 | Concept of the sequential copolymerization of styrene and various *N*-substituted maleimides. Reprinted with permissions from [20]. Copyright © 2007, American Chemical Society.

Chan-Seng *et al*. investigated the synthesis of more complex microstructures by the automatization of this method [63]. In order to prepare polymers with a maximum incorporation of different maleimides, an automated platform was exploited. NMP copolymerization of styrene with different chain lengths (degree of polymerization DP_n = 20, 50, 100) with *N*-functionalized maleimides was investigated. Each functionalized maleimide should be incorporated separately in order to not intersect functional zones. As copolymer should have "separate zones" of functions (maleimides) and thereby possess a perfectly regulated sequence, each new addition of maleimide should be made after the full conversion of a previous one. It was shown that four additions of maleimide in the polymer chain can be performed maximally if DP_n = 20, seven additions in the case DP_n = 50, and eight additions if DP_n = 100. Afterwards, complex monomer sequence patterns were obtained using polystyrene with DP_n = 100 and different combinations of four *N*-substituted maleimides (Figure 10). Therefore, using only four different functions and eight possible opportunities to position them into a polymer chain, 48 possible microstructures can be prepared.

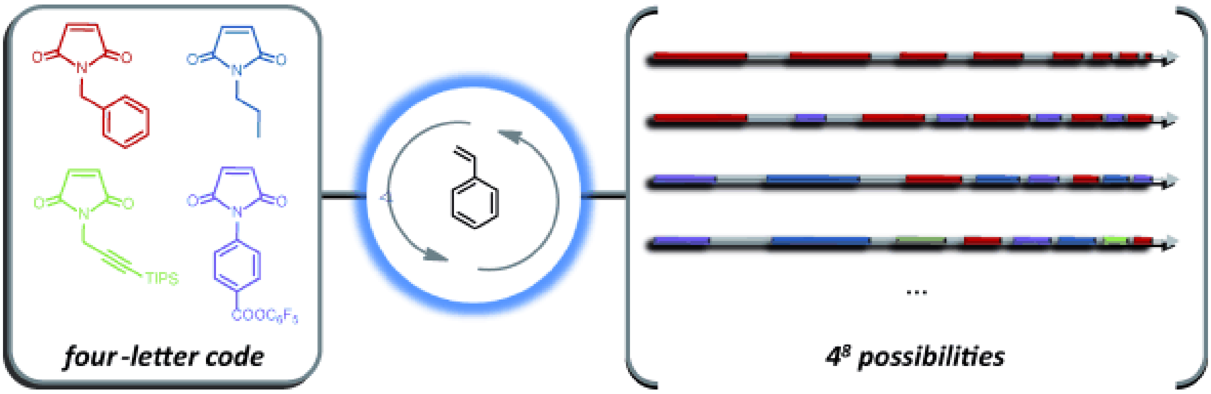

Figure 10 | Automated preparation of complex monomer sequence patterns. Reprinted with permissions from [63]. Copyright © 2012 WILEY-VCH Verlag GmbH & Co. KGaA, Weinheim.

Recently the ability to control monomer sequence by applying a kinetic approach was described by the use of ring-opening metathesis polymerization (ROMP) of *exo*- and *endo*-norbornenes [67]. O'Reilly and coworkers took advantage of the rapid ROMP of *exo*-norbornenes in the presence of a ruthenium-based catalyst and the slow polymerization kinetics of *endo*-norbornenes due to steric interactions. Firstly, kinetics of copolymerization of the model monomers *exo*- and *endo*-norbornenes (10 Eq. of 7-coumarinyl-*exo*-5-norbornene-2-carboxylate to 50 Eq. of N-hexyl-*endo*-norbornene-5,6-dicarboximide) were investigated. It was shown that *endo*-norbornene was consumed 30-100 times slower than *exo*-norbornene. Secondly, a polymer containing four different functional moieties at relatively known positions was synthesized. The incorporation of *exo*-norbornenes in the *endo*-norbornene chain was monitored by ^{1}H NMR spectroscopy, and the final polymer was characterized by size-exclusion chromatography (SEC) and UV spectroscopy.

I.3. OTHER CHEMICAL APPROACHES TO CONTROL MONOMER SEQUENCE

The progress in the synthesis of sequence-defined polymers by other chemical approaches will be reported in this subchapter. Four main approaches will be described; among them are metal coordination, step-growth polymerization, iterative synthesis (multistep growth) and the use of molecular machines.

I.3.1. Metal Coordination

Coordination polymerization using metal complexes is another tool in the synthesis of sequence-controlled polymers. Alternating [16] and block [17] copolymers were synthesized by careful choice of metal catalyst and monomer pairs. Although alternating and block copolymers can be synthesized by the strategies previously described, metal-catalyzed polymerization allows broadening the range of used monomers leading to polymers with controlled molecular weight.

Aida and Inoue [68] showed the alternating character of a polyester copolymer on the example of copolymerization of phthalic anhydride as cyclic anhydride with epoxide in the presence of (porphynato)aluminium alkoxide as a catalyst. Copolymers with a low molecular weight were synthesized. Aliphatic polyesters with high molecular weight values (up to $55 \cdot 10^{3}$ g·mol^{-1}) and narrow molecular weight distribution (1.1-1.3) were prepared by Coates and coworkers [69]. In their study, epoxides and cyclic anhydrides were copolymerized in the presence of a highly active catalyst β-diiminate zinc acetate ((BDI)ZnOAC). First, the copolymerizations of diglycolic anhydride (DGA) with a range of epoxides (cyclohexene oxide, *trans*-(*R*)-limonene oxide, *cis*-butene oxide, propylene oxide and isobutylene oxide) were explored (Figure 11). The alternating character of the copolymer was confirmed by ^{1}H NMR spectra as no consecutive

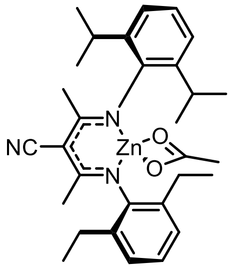

(BDI)ZnOAc

anhydride or epoxide sequences were observed. The polyesters with alicyclic backbones had a T_g close to the one of poly(lactic acid). Other cyclic anhydrides, succinimic and maleic anhydrides, were copolymerized with the above mentioned epoxides and also led to polyesters with narrow molecular weight distributions (1.1-1.3).

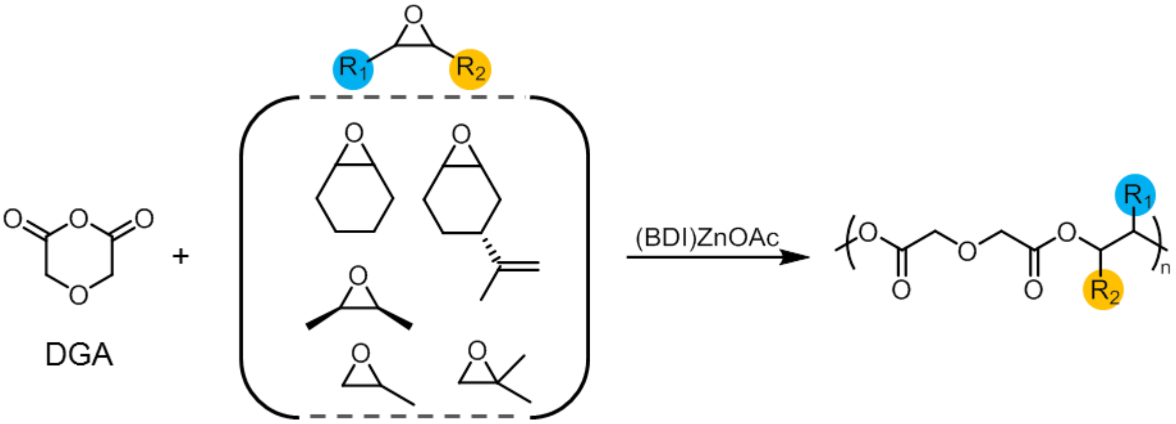

Figure 11 | Alternating copolymerization of diglycolic anhydride (DGA) and various epoxides.

Another way to prepare alternating copolymers was inspired by stereochemical control using racemic monomers. In this case, stereoisomerism of the last inserted monomer influences the catalyst to interact with a monomer of the opposite stereochemistry. Thus, the monomers are alternating during the copolymerization process. Thomas, Coates and coworkers studied a slightly different approach where they used two enantiomerically pure and different monomers instead of racemic monomers [70] (Figure 12). A syndiospecific catalyst (based on the complex of yttrium with a tetradentate phenoxyamine ligand) was examined for the copolymerization in either benzene-d_6, or THF-d_8. The monomers were consumed at the same rate, and the percentage of alternation determined by ^{1}H and ^{13}C NMR appeared to be high, around 90-94 %. The final copolymers had narrow molecular weight distributions, and their sequence was well controlled.

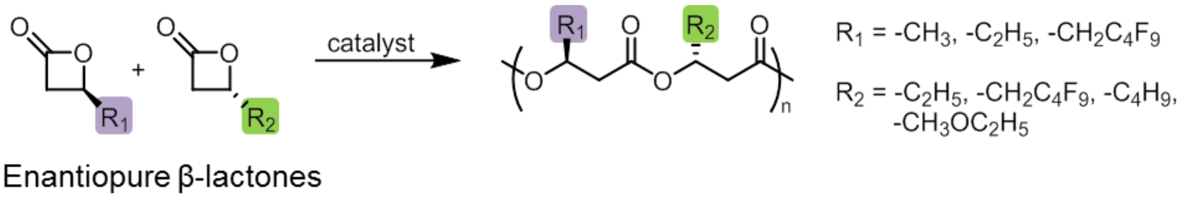

R_1 = $-CH_3$, $-C_2H_5$, $-CH_2C_4F_9$

R_2 = $-C_2H_5$, $-CH_2C_4F_9$, $-C_4H_9$, $-CH_3OC_2H_5$

Figure 12 | Alternating copolymerization of enantiopure β-lactones in the presence of a syndiospecific catalyst [70].

The formation of another type of sequence-controlled polymer prepared by chain-growth polymerization in the presence of metal catalyst was investigated by Koeckelberghs and coworkers [17]. ABC-block copolymer comprising three different blocks poly(3-hexylthiophene)-*block*-poly(9,9-dioctylfluorene)-*block*-poly(3-octylselenophene) **PT-*b*-PF-*b*-PS** (Scheme 3) was synthesized in the presence of palladium-based catalyst Pd(RuPhos). ABC block-polymers were obtained by sequential monomer addition in a one-pot synthesis. The sequence of the added monomers was varied, thus six different combinations of block-copolymers were prepared. The synthesized copolymers were characterized by SEC, ^{1}H NMR, UV-*vis* and fluorescence spectroscopies. The order of monomers influenced the emission of the polymers according to fluorescence measurements.

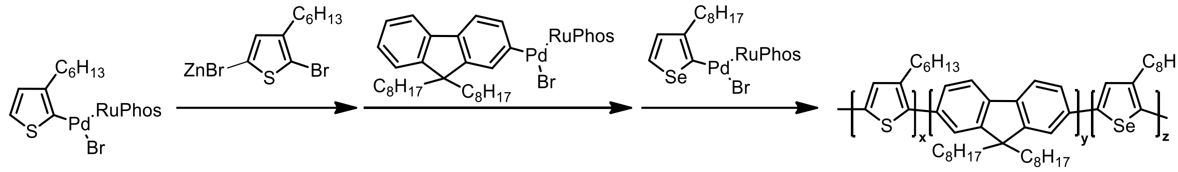

Scheme 3 | Synthesis of one of block-polymers PT-*b*-PF-*b*-PS from six possible combinations [17].

I.3.2. Step Growth Polymerization

An important characteristic of step-growth polymerization is that reaction progresses due to the presence of functional reactive groups at each step. Non-controlled character of step-growth polymerization is usually leading to polymers with broad polydispersities. Mainly alternating or periodic polymers are prepared by this approach.

Matyjaszewski and coworkers [71] combined ATRP and step-growth polymerizations to yield high-molecular weight polystyrenes. First, homo- and heterotelechelic polystyrene oligomers were prepared by ATRP of styrene in the presence of α-alkyne-ω-bromine- or di-bromine-functionalized initiator, respectively, followed by the transformation of bromine-groups into azide. Afterwards, azide-alkyne cycloaddition of the synthesized oligomers was performed (Figure 13, **A**, **B**) leading to polystyrenes with molecular weights around $20 \cdot 10^3$ $g \cdot mol^{-1}$ and broad molecular weight distributions (3.3-4.8). It was noticed that a cyclized polymer was formed as a by-product.

Although this strategy is not leading to sequence-defined macromolecules, the use of two different blocks with symmetrically positioned azide- and alkyne-functional groups (Figure 13, **C**) inspired by symmetrically functionalized polystyrene (Figure 13, **B**) led to an alternating polymer and, consequently, to the sequence regulation. Obviously, other couples of reactive groups and various monomers can be used. However, the poor control restricts the broad use of step-growth polymerization for the synthesis of sequence-defined polymers.

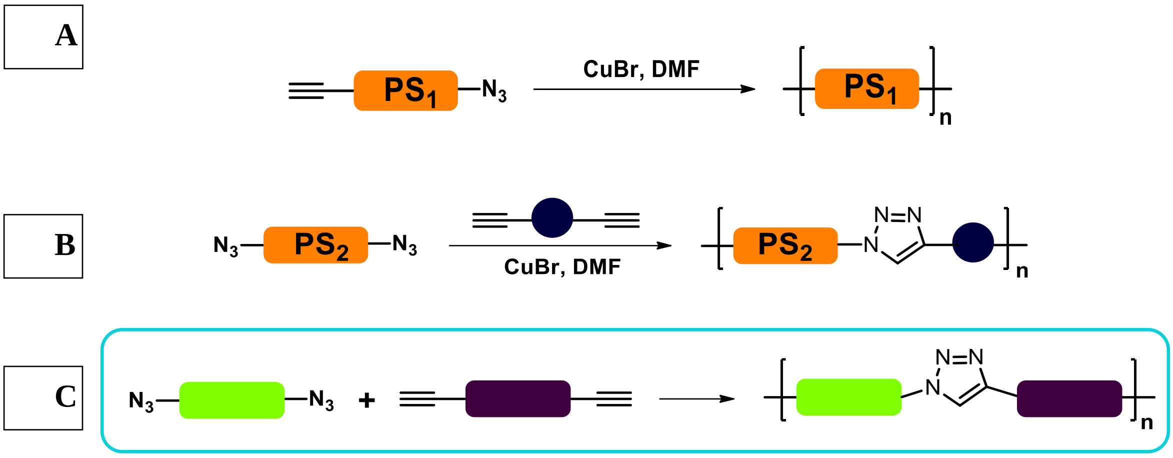

Figure 13 | (A) Step-growth azide-alkyne cycloaddition of heterotelechelic oligomer and (**B**) homotelechelic oligomer prepared by ATRP [71]. (**C**) Synthesis of alternating polymers by step-growth polymerization of two bifunctional symmetrical monomers with azide and alkyne terminal groups.

Periodic polymers can be also prepared by step-growth polymerization using monomers with selected reactivities. The main strategy is to polymerize a block consisting of several monomer units and containing two terminal reactive groups. Kamigaito and coworkers [18] proposed a novel strategy to form sequence-regulated vinyl copolymers through metal-catalyzed step-growth radical polymerization of specifically designed ABC-type monomers (Figure 14). Such monomers possessed unconjugated double C=C bond, reactive C-Cl end group, phenyl and an ester moiety containing functional groups.

Due to the adjacent carbonyl group, C-Cl bond in the monomer was active in the catalysis, and when it was interacting with a metal catalyst, radical species were generated (Figure 14). In turn, carbon radical was reacting with the double bond of the monomer resulting in the formation of a carbon-carbon bond as the main chain, along with inactive to metal catalyst C-Cl bond. The formed species possessed an active C-Cl bond, and the metal-catalyzed addition could be repeated. Thus, a sequence-defined polymer was prepared by this step-growth metal-catalyzed radical polymerization.

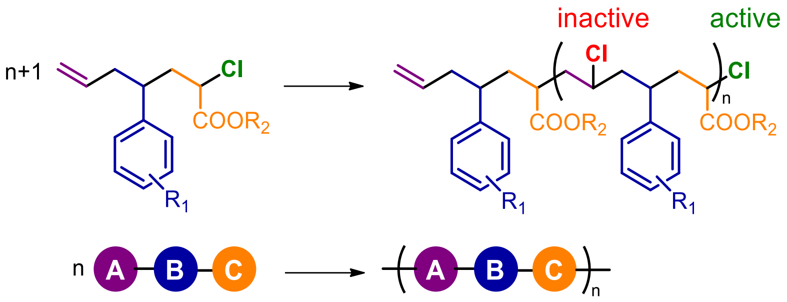
inactive
active
n+1
Cl
COOR2
R1
Cl
Cl
COOR2
COOR2
n
R1
R1
n
A
B
C
A
B
C
n

Figure 14 | Sequence-defined ABC-type copolymers prepared by step-growth metal-catalyzed polymerization [18].

Along with ABC-copolymers, cyclized polymers were synthesized. Their content decreased if bulky ester substituents were used (Scheme 4, R_2 = *i*-propyl). It was also shown that the use of ABCC-type monomer bearing two ester moieties reduced significantly intramolecular cyclization. The ABC- and ABCC-type polymers were characterized by SEC, MALDI-TOF-MS, ^{1}H and ^{13}C NMR spectroscopies confirming the formation of the described polymers.

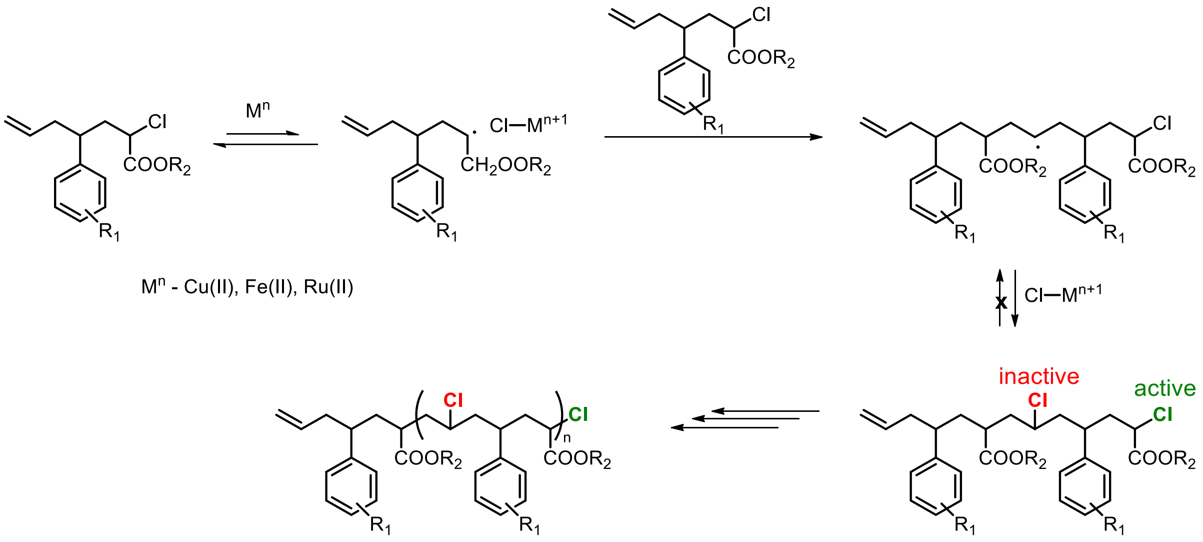
Cl
COOR2
R1
Mn
Cl—Mn+1
CH2OOR2
R1
Cl
COOR2
R1
Cl
COOR2
COOR2
R1
R1
Mn - Cu(II), Fe(II), Ru(II)
x
Cl—Mn+1
Cl
Cl
n
COOR2
COOR2
R1
R1
inactive
Cl
active
Cl
COOR2
COOR2
R1
R1

Scheme 4 | Metal-catalyzed radical polyaddition of ester-linked monomers [19].

I.3.3. Iterative Synthesis (Multistep Growth)

Iterative synthesis implies stepwise addition of monomers, and the most known and used technique is solid-phase synthesis. This methodology consists of the addition of a monomer with one protected to a support (resin) followed by deprotection, and the process of “Addition/deprotection” is repeated *n*-times with subsequent cleavage of the product from the support. This strategy developed by Merrifield [35] was first used to prepare peptides [72]. More recently, it allowed the synthesis of oligoamides with a highly controlled sequence [73]. Solid-phase was found to be efficient to obtain oligomers, but it is not convenient for the synthesis of complex macromolecular architectures because of limited accessibility of the reaction sites in the resin. Solid phase allows up to 50 monomers to be added, but the use of bigger amount of monomers is challenging. Chemical conjugation can be a solution for the synthesis of longer chains.

Other types of oligomers synthesized by multistep growth approach were investigated such as synthetic polyamide nucleic acids [74] and peptoids [75]. Peptoids is a class of pseudo-peptides prepared by solid-phase synthesis. The monomer units in peptoids are connected by *N*-substituted amide links in contrast to natural peptides. They are usually prepared by a two-step addition of monomers containing carboxylic end-groups and protected secondary amine functions. As an example, a sequence specific polypeptoids was synthesized by Zuckermann and coworkers [76] (Figure 15). This strategy allowed avoiding protecting groups in the main chain. The first step included acylation of the resin-connected amine moiety with bromoacetic acid. The second step consisted in introducing one unit possessing a *N*-substituted amine. Both steps demanded mild conditions, consequently the synthesis could be automatized. As readily and/or commercially available reactants were used, a broad range of sequence-specific polypeptoids could be synthesized.

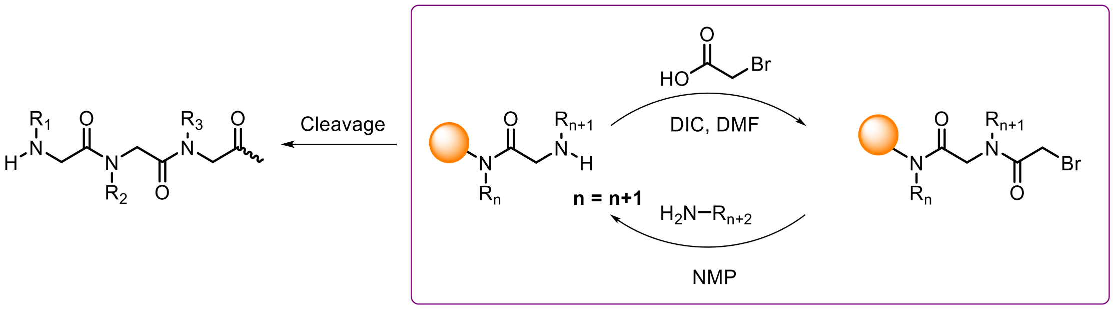

Figure 15 | Iterative synthesis of a sequence-specific polypeptoid on a solid support [76].

Oligoamides, peptoids and other sequence-defined oligomers like natural peptides are able to form complex secondary structures. But the facilities and applications of iterative synthesis on solid supports can be expanded to the synthesis of “molecularly encoded oligomers” [77] and thereby connecting polymer sequence with encoded information. Trinh *et al.* prepared a sequence-controlled oligomers library where two monomers where put in three different positions [77] (Figure 16). Two organic acids, 4-pentynoic acid and 2-methyl-4-pentynoic acid, were chosen as "coding" monomers. They were connected by a spacer with azide- and amine- chain ends (1-amino-11-azido-3,6,9-trioxaundecane) using the reactions of azide-alkyne cycloaddition and amidification, respectively. The final oligomers presenting various sequences of three units were cleaved from a Wang resin in the presence of TFA. All obtained sequence-defined oligomers were characterized by MALDI-TOF-MS and were found to be monodisperse.

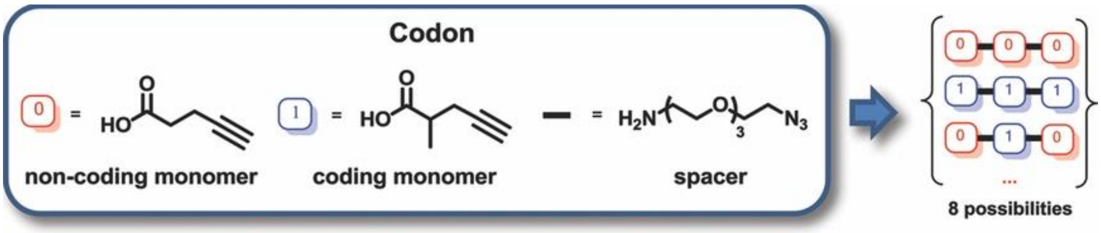

Figure 16 | Schematic representation of the synthesis of sequence-defined encoded oligomers. Reprinted with permission from [77]. Copyright © 2013 WILEY-VCH Verlag GmbH & Co. KGaA, Weinheim.

All above described strategies were using solid-phase iterative synthesis. However, this technique has some limitations such as accessibility of the functional moieties and difficulties with oligomer characterization at each step without cleavage from the support. The use of soluble supports [36] overcomes these difficulties while keeping some advantages of solid phase synthesis, such as the easy isolation of the intermediate products. One of the recent studies describing the synthesis of a model oligopeptide using soluble supports was reported by Amrane *et al*. [78]. A soluble polystyrene support with a Rink cleavable linker was prepared by ATRP of styrene and further modification by a linker with a *N*-Fmoc-amine group. Removal of the Fmoc-group of the polystyrene support was followed by amidification with a *N*-Fmoc-protected amino acid. This cycle was repeated three more times with various *N*-Fmoc-protected amino acids. The advantage of this strategy was the monitoring of every step by SEC and ^{1}H NMR. The last step, *i.e.* the cleavage of the Rink linker, leading to the tetrapeptide, was performed in mild acidic conditions.

In another recent study [79], You and coworkers proposed to prepare a short sequence consisting of three units with a polymerizable moiety and then to polymerize it. ABC-copolymer was synthesized by a two-step selective one-pot reaction followed by polymerization (Figure 17). First, 2-aminoethanethiol (B) was added to allyl methacrylate (A) resulting in the modification of the methacrylate group by thiol group in mild conditions. Neither amine, nor thiol reacted with allyl group in these conditions. Afterwards, thiolactone (C) was added to the prepared AB sequence bearing an amine group leading to ABC sequence with allyl and thiol end-groups. This second step was followed by a thiol-ene "click" reaction *via* UV irradiation in the presence of 2,2-dimethoxy-2-phenylacetophenone. ^{1}H NMR spectrum of the obtained product revealed only trace signals of the double bond and the PDI of the ABC-copolymer was 1.57 according to SEC. This strategy was extended to longer sequences based on the same reactions. For example, DCBABCDE-sequence was prepared starting with a symmetric bifunctional methacrylate ethylene dimethacrylate (A unit) followed by the series of modifications with 2-aminoethanethiol (B), thiolactone (C), bromomaleimide (D). The last step consisting in nucleophilic addition of a propyl diamine to thiolmaleimide resulted in DCBABCDE-sequenced copolymer with a molecular weight M_n = 25600 g·mol^{-1} and a PDI = 1.24. The complete nucleophilic addition was confirmed by ^{1}H NMR spectroscopy.

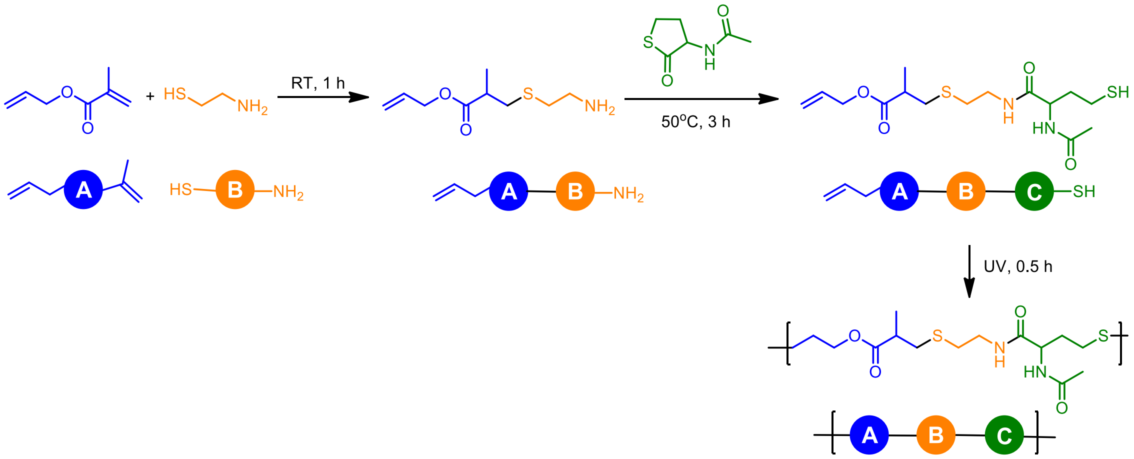

Figure 17 | Synthesis of ABC-sequenced copolymer [79].

Further development in the synthesis of sequence-controlled polymers by iterative synthesis led to the application of selective reactions and functional groups with not equal reactivities that allow avoiding protecting group chemistry [79-81]. Solleder and Meier demonstrated that multicomponent reaction combined with thiol-ene "click" chemistry can be a convenient and simple method for the synthesis of sequence-ordered oligomers and polymers [81]. Sequence-defined tetramer and pentamer blocks were synthesized by this group. The first block was synthesized by Passerini three component reaction (Passerini 3-CR). Either stearic acid, or *O*-methyl-*O*′-succinylpolyethylene glycol were chosen as units carrying carboxylic group. The use of isocyanides **3a-e** (Figure 18) provided the introduction of functional moieties, and the use of undec-10-enal allowed employing aldehyde group for Passerini 3-CR and vinyl group for further thiol-ene addition. The second step consisted in the "regeneration" of the carboxylic group by thiol-ene click chemistry of the terminal vinyl group of the formed block with 3-thiol-propanoic acid. Iterative application of Passerini 3-CR to introduce a functional group followed by thiol-ene addition to introduce carboxylic moiety led to sequence-defined tetramer (when isocyanides **3a-d** (Figure 18) were used). Proton NMR spectra and SEC data confirmed that every step was successful. However, the isolation of the product at each step demanded a purification by column. PEG derivative **1b** (Figure 18) was used in order to simplify the isolation of the product by straightforward precipitation. The final polymer carrying five precisely positioned functional moieties was prepared without the use of protecting groups and activating reagents with 34% overall yield.

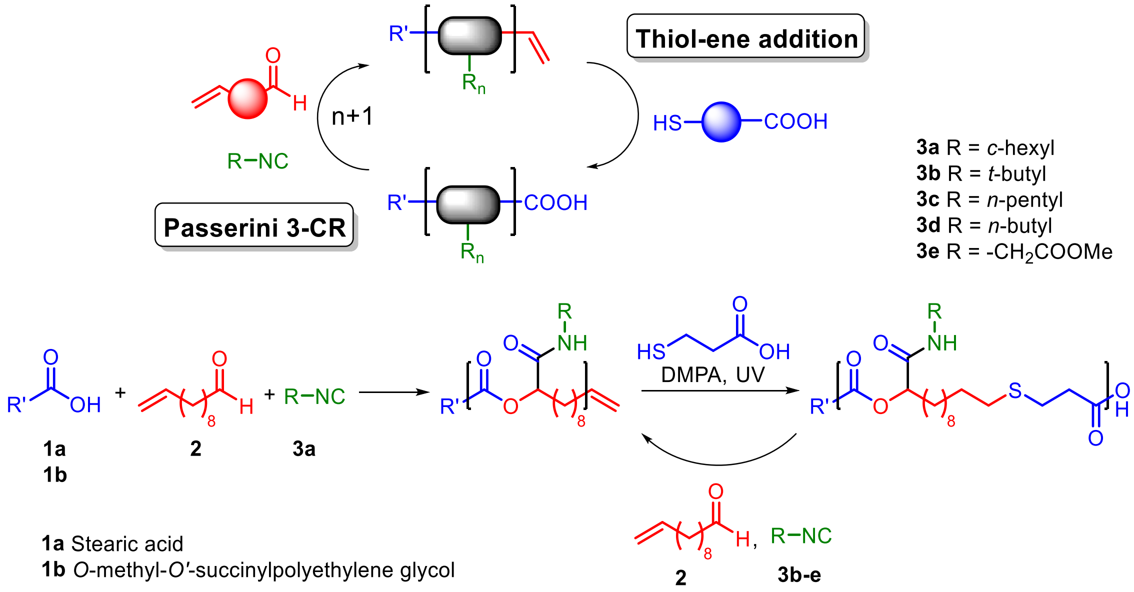

Thiol-ene addition
Passerini 3-CR
n+1
R–NC
HS–COOH
R'
Rn
COOH
3a R = c-hexyl
3b R = t-butyl
3c R = n-pentyl
3d R = n-butyl
3e R = -CH2COOMe
R'
OH
H
8
3a
1a
1b
2
DMPA, UV
HS
NH
S
2
3b-e
1a Stearic acid
1b O-methyl-O′-succinylpolyethylene glycol

Figure 18 | Synthesis of sequence-defined tetramer starting from stearic acid (**1a**) or sequence-defined polymer starting from *O*-methyl-*O*′-succinylpolyethylene glycol (**1b**) by iterative use of Passerini three-component reaction followed by thiol-ene "click" chemistry. Adapted with permission from [81]. Copyright © 2014 WILEY-VCH Verlag GmbH & Co. KGaA, Weinheim.

The use of two orthogonal reactive sites of allyl acrylamide combined with a dithiol were shown by Porel and Alabi as another tool for the synthesis of sequence-defined polymers [80]. Allyl group underwent photo-initiated thiol-ene addition whereas acrylamide group reacted with thiols by phosphine-catalyzed Michael addition. These reactions had fast kinetics (90-300 s) at room temperature. Application of fluorous tags with allyl group as a support for the iterative synthesis allowed combining advantages of solution-phase and solid-phase synthesis. Fluorous tags are soluble in common organic solvents and in the fluorocarbon medium resulting in the near complete recovery of the compound with fluorous "tail". Moreover, they have fast solution phase kinetics, are inert in a big range of reaction conditions, and allow reaction monitoring by common spectroscopic techniques. Thereby, a sequence-defined oligomer (10-mer) with five positioned functional moieties was synthesized by repeating thiol-ene and Michael additions followed at the last step by the cleavage from the fluorous polymer (Figure 19). ^{1}H NMR spectra and liquid chromatography/mass spectrometry (LCMS) data confirmed the stepwise formation of the oligomer.

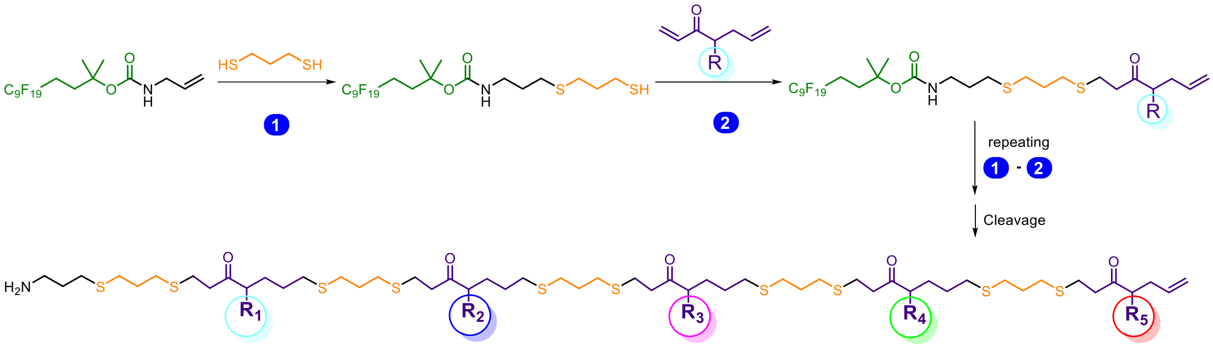

Figure 19 | Assembly of oligomer containing five precisely positioned functional moieties [80].

I.3.4. Molecular Machines

Recently, a conceptually new approach for the synthesis of sequence-defined oligoamides was described [11]. Lewandowski *et al*. proposed to prepare a sequence of amino acids by an artificial small-molecule machine, inspired by a "biological molecular machine", *i.e.* the ribosome. Rotaxane-based small-molecule machine was fixed on a strand carrying amino-acid moieties in a predetermined order. The molecular machine was blocked from one side by a terminal bulky tertiary group, and by amino acid building block from another side. After fixation of a "reactive arm" with a cysteine-protected moiety on the rotaxane-based machine, the conjugate **1** (Figure 20) was ready to operate.

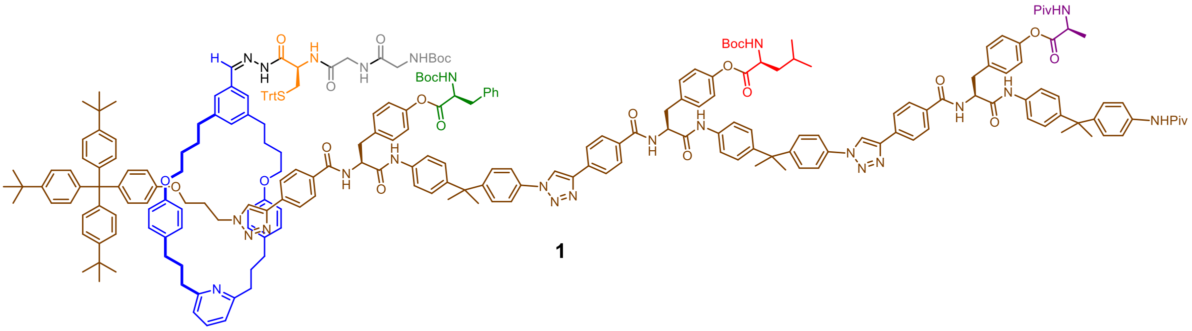

1

Figure 20 | Assembled rotaxane-based molecular machine **1** [11].

When the thiol of cysteine bore trityl (Trt) protected group, the machine **1** was stable. Acid-catalyzed cleavage of trityl- and Boc-protecting groups activated the molecular machine (Figure 21, **2a**). The thiolate groups on the cycteine residue attacked carboxyl group of the first amino acid residue on the strand (Figure 21, **2b**). After transacylation reaction, amino acid of the formed phenyl alanine thioester was transferred to glycine-glycine amino acid group by native chemical ligation [82] (Figure 21, **2c**) through 11-membered ring transition state. Afterwards, thiolate could again react with the next amino acid (leucine). Through native chemical ligation leucine was transferred to phenylalanyne unit allowing thiolate group reacting with the following amino acid moiety on the track. When the last amino acid group was transferred to the end of the growing peptide, molecular machine was deatached from the strand (Figure 21, **3**). After hydrolysis of hydrozone link connecting rotaxane and peptide, a sequence-specified peptide was formed (Figure 21, **4**). The amino acid sequence was analyzed by mass spectrometry confirming the intended sequence. It was shown that peptide sequence could be extended to four amino acid blocks assembled by a molecular machine [10].

Although the synthesis of sequence-defined peptide by artificial molecular machines proposed a novel approach to the synthesis of peptides, it had a number of limitations. The reaction times were long (around 12 hours) compared to conventional peptide synthesis (around 0.5-2 hours) for each amide bond. Moreover, the increase of peptide size can be limited by the ring size of transition state.

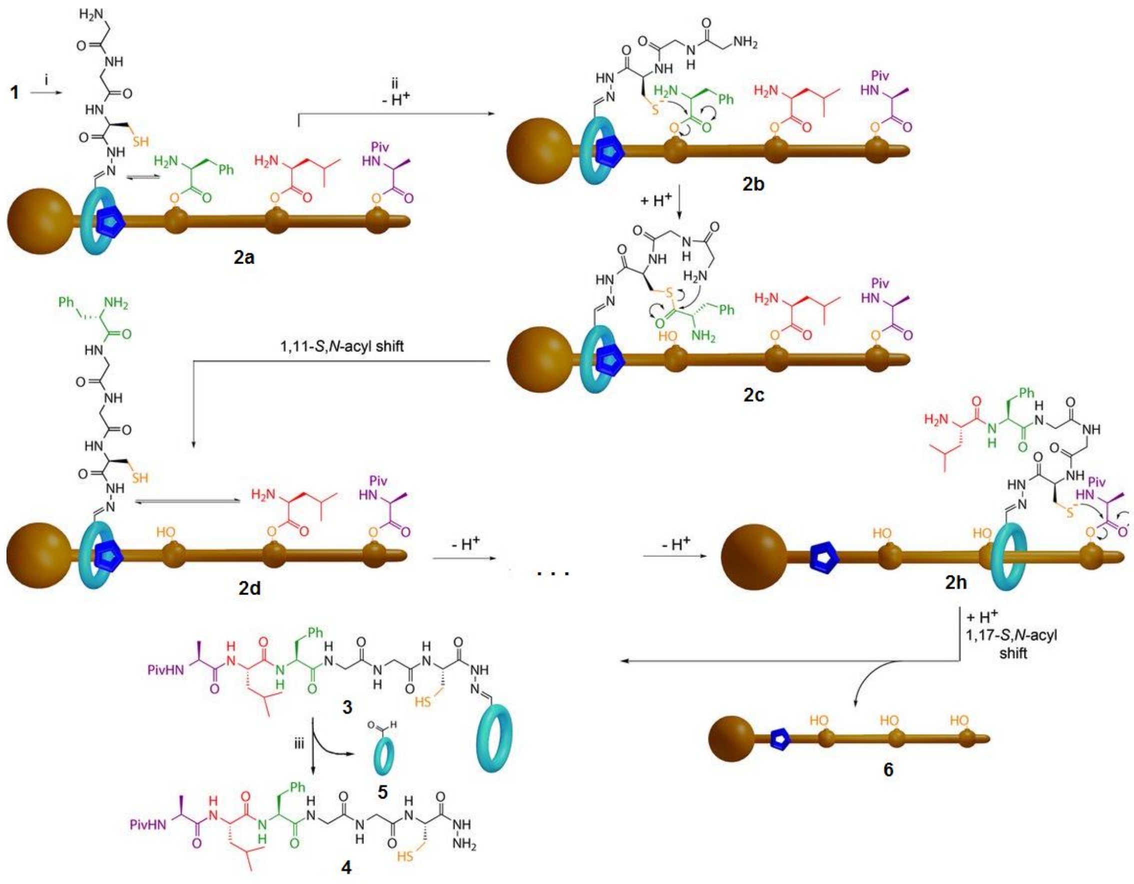

Figure 21 | Proposed mechanism for sequence-specific peptide synthesis by small-molecule machine. *Reaction conditions*: (*i*) 20% TFA in CH_2Cl_2, RT, 2 hours. (*ii*) DIPEA, $(HO_2CCH_2CH_2)_3P$ in 3:1 CH_3CN : DMF, 60°C, 36 hours. (*iii*) 30% TFA in 3:1 CH_2Cl_2 : H_2O, RT, 18 hours. Reprinted with permission from [11]. Copyright © 2013, American Association for the Advancement of Science.

I.4. COMPACTION AND FOLDING OF POLYMER CHAINS THROUGH THE FORMATION OF INTRAMOLECULAR LINKS

The motivation for the development of controlled single-chain folded/compacted polymers is to mimic important natural processes such as protein folding, and DNA packing. Primary structure (*i.e.* sequence of amino acids for proteins) determines folding of biomacromolecules driven by non-covalent and/or covalent interactions. Foldamers that can be considered as the closest to mimic peptides [46, 83], mostly present oligomers with a regular structure [84, 85]. The field of high-molecular weight foldable macromolecules is less advanced compared to foldamers, and helical macromolecules are one of the examples [86, 87]. Conformational properties of such macromolecular structures are of the main interest, and stereoregularity is determining the folding [88].

Although the primary structure plays an important role in the folding, it was shown that single synthetic polymer chains can be organized into unimolecular structures using intramolecular self-associations [2, 89]. The opportunity to perform folding/compaction of polymer chains is possible today due to the development of CRP (controlled radical polymerization) techniques that provides polymers with well-defined structures and narrow molecular weight distributions. Random (isotropic) or directional (anisotropic) interactions can be used to transform polymer coils into globular shapes. The formed objects are called “single-chain polymer (nano)particles”. The cyclization of polymer chains is another approach toward polymer folding. However, it provides a unique topology. The synthesis of complex unimolecular structures and shapes will be described based on cyclic polymers and positioning of intramolecular bridges.

Either covalent, or non-covalent interactions will be used for the synthesis of ordered structures by single-chain technology. Firstly, the compaction of random coils into globular shapes and the placement of intramolecular bridges leading to different topologies will be illustrated by means of covalent link. Secondly, the use of non-covalent interactions will be described for the compaction of random polymer chains.

I.4.1. Compaction of Single Polymer Chains by Covalent Interactions

Disulfide bridges between cysteine residues that maintain tertiary structure in some proteins is one of the most widely exploited and inspiring example of the use of covalent interaction for polymer chain folding. Covalent bonds are stronger than non-covalent interactions, and they are fixing the polymer geometry. However, some covalent bonds can be reversible influencing the “dynamics” of compaction.

I.4.1.A. Single Chain Polymer Nanoparticles (SCPNs)

One of the driving forces for the investigation and creation of nanoparticles is the possibility to use them as building blocks for various nanotechnological applications, for example, as vectors for drug and DNA delivery systems. Different strategies have been developed for the synthesis of particles of 20-200 nm size range, but the ability to prepare nanoparticles of smaller size is limited. The approach involving the use of collapse and intramolecular coupling of single-polymer chains is one of the solutions of this problem. Another problem is to find simple and readily accessible polymers for efficient intramolecular coupling under mild conditions. Some progresses in this field are described below.

Hawker and coworkers proposed to prepare SCPN at high concentrations (0.1-1 M) [3]. A linear polymer, containing latent functions along the backbone that could be thermally activated, was slowly added to a heated solvent (Figure 22). The choice of the functional group was important as it should be selectively activated and react rapidly and irreversibly. The benzocyclobutene (BCB) – a latent Diels-Alder reagent – corresponds to above mentioned demands. BCB-functionalized polystyrene was synthesized by NMP, and incorporation of BCB units was monitored by ^{1}H NMR (specific chemical shift present at 3.10 ppm). It was shown that even under high diluted conditions ($5{\cdot}10^{-5}$ M) an increase of the molecular weight value was observed due to the intermolecular coupling. Therefore, it was decided to change the strategy: a concentrated solution (0.2 M) of BCB-functionalized polymer was continuously added to a high-boiling solvent (dibenzyl ether) at 250°C with a final concentration of 0.05 M. The successful formation of only intramolecular bonds was observed.

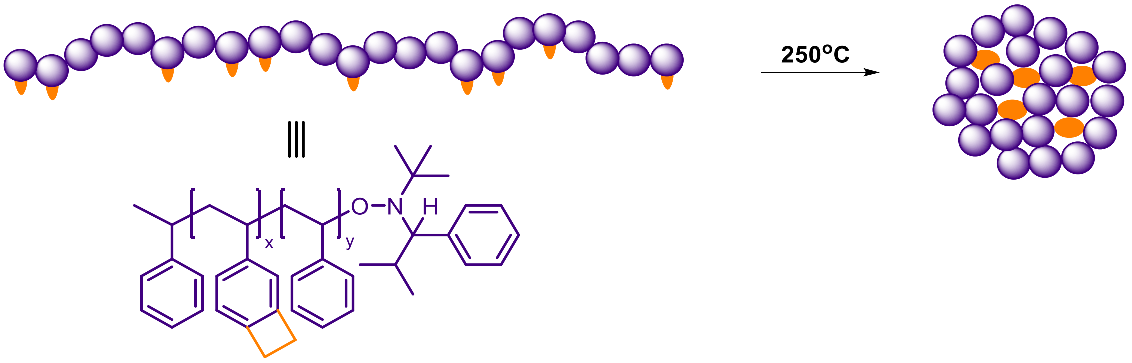

Figure 22 | Schematic representation of the intramolecular collapse of a random copolymer with benzocyclobutene units [3].

The SCPNs were characterized by various techniques including ^{1}H NMR spectroscopy, SEC, dynamic light scattering (DLS), and DSC. The decrease of the hydrodynamic radius from 8.7 to 6.6 nm was observed in DLS (for the polymer with a molecular weight of $95{\cdot}10^3$ $g{\cdot}mol^{-1}$). The decrease of the hydrodynamic volume of the obtained SCPN was evidenced by

SEC. A change in the glass transition temperature also indicated the formation of the nanoparticle. Hawker and coworkers extended the present study to the synthesis of hybrid copolymers containing the above SCNP conjugated with a linear poly(n-butyl acrylate) [90].

Harth and coworkers aimed at synthesizing water-soluble SCPN that could be further used for magnetic resonance imaging [91]. Such particles were prepared from ABA triblock copolymers. Fluorene monomer was chosen for long-term fluorescence tracking, and its modification by ethylene oxide (EO) pendant moieties provided water-soluble properties. A telechelic macroinitiator was prepared from fluorene monomer with EO moieties and served as block B (Figure 23, **1**). Thus, a ABA triblock (Figure 23, **2**) copolymer was synthesized by polymerization of *t*-butyl acrylate using fluorene macroinitiator with nitroxide chain-ends. Every step was characterized by SEC and ^{1}H NMR confirming 2:1:2 ratio of acrylate to fluorene to acrylate blocks. In parallel, a linear precursor with carboxylic and crosslinking groups was prepared by removal of *t*-butyl protecting groups and introduction of a small amount (~ 5%) of cross-linker 2-(1,2-dihydrocyclobutabenzen-1-yloxy)-ethanamine. The intramolecular chain collapse of the final polymer was performed by a slow addition of the linear precursor into a solution of DMF at diluted conditions (~ 10^{-5} M) and at 150°C. Significant shift in retention time to a bigger value for the nanoparticle compared to linear precursor confirmed the presence of a compound with smaller hydrodynamic volume and the formation of intramolecular link. The size of the collapsed particle was measured as 35 ± 2 nm by DLS. Absorption and emission peaks were observed at 370 and 438nm using UV-vis and fluorescence spectroscopies, respectively. Further modification of the acrylic acids groups by amine-functional units led to a broader range of applications. The introduction of catechol moieties, for example, provided nanoparticle with metal complexing units.

An effective intra-chain cross-linking strategy was recently proposed by Berda and coworkers [92] for the synthesis of SCPN of sub-20 nm size. Linear precursors were based on methyl methacrylate copolymers with various percentage of incorporated anthracenyl moieties (10-46%). The authors chose anthracene because of its ability to form photosensitive and thermally responsive materials. Indeed, anthracene can form photodimers at a wavelength of 350 nm or thermally (> 180°C). The photodimerization can be realized reversibly, when wavelength below 300 nm are used. The nanoparticles were synthesized by irradiation of the linear precursors (concentration ~ 10^{-7} M) with 350 nm UV light in THF. The reaction was monitored by UV-vis spectroscopy to detect the disappearance of the characteristic absorption peak at ~ 360 nm and by SEC to observe the changes in the hydrodynamic volume. Despite the high dilution, SEC with MALS detector measurements revealed a small degree of intermolecular coupling. This inter-chain coupling was more pronounced for the precursor with the biggest amount of anthracene moieties. Reduction of the hydrodynamic volume and the intrinsic viscosity confirmed the coil to nanoparticle transition. Interesting data were observed by TEM showing that nanoparticles had ellipsoid form. The authors assumed that the interparticle aggregation was due to anthracene stacking, or dimerization by ambient light.

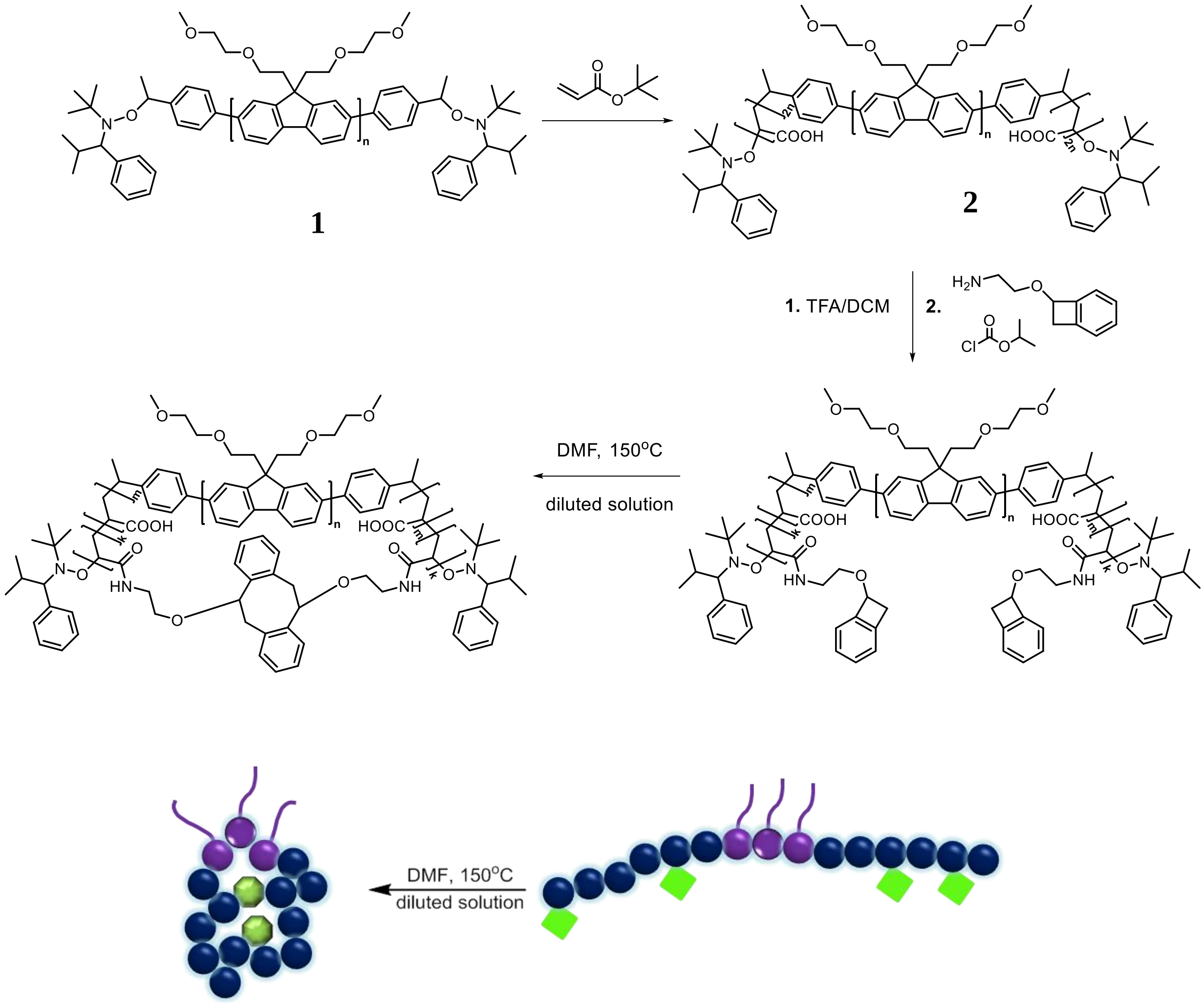

Figure 23 | Synthesis of a water-soluble single-chain nanoparticle for imaging [91].

Another synthetic route using intramolecular self-crosslinking of macromolecules by covalent bond in ultra-dilute solution was proposed by Miller and coworkers [4]. Copolymers containing pendant acryloyl and methacryloyl functional groups which are potentially crosslinkable were used. Polyesters were prepared by living ring-opening copolymerization

(ROP) of 4-acryloyloxy caprolactone with either *ε*-caprolactone (Scheme 5) or L,L-lactide. Subsequently, the unimolecular particles were synthesized in the presence of a radical initiator AIBN at 65°C in dilute solution ($4 \cdot 10^{-4}$ M). The disappearance of the vinyl signals observed on the ^{1}H NMR spectrum confirmed the self-crosslinking reaction. Due to the appearance of a new covalent internal bond, the size of the macromolecule decreased as proved by the decrease of the hydrodynamic volume of the nanoparticle in SEC compared to the linear precursor. Finally, the nanoparticles were characterized by DLS that showed a very small nanoparticle size (3.8-13.1 nm).

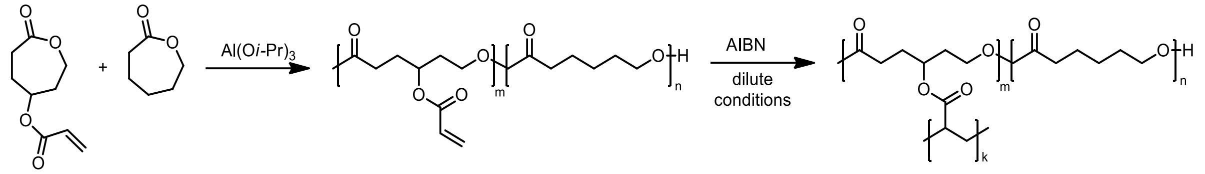

Scheme 5 | Synthesis of linear precursors and their intramolecular cross-linking to form a nanoparticle [4].

Dynamic Covalent Interactions

Although it exists a variety of dynamic covalent bonds such as disulfide, alkoxyamine, imine, and hydrazone, their exploration for single polymer chain compaction/folding has emerged only recently. The use of dynamic covalent bonds supplies structured polymers with responsiveness to the external stimuli making reversible the transformation of a polymer coil into a compact unimolecular object.

Berda and coworkers [5] showed an interesting example of a transition from a coil to a particle through disulfide bond formation and cleavage. Poly(norbornene-*exo*-anhydride) **P1** synthesized *via* ring-opening metathesis polymerization (ROMP) and *p*-aminophenyl disulfide were chosen as linear precursor and difunctional cross-linker with disulfide bond, respectively (Figure 24). As every monomer unit along **P1** backbone was reactive, the variation of the collapse degree was dependent on the amount of cross-linker added. SCPNs were obtained under diluted conditions (1 mg·mL^{-1}). The coil to particle transition was characterized by the reduction of the hydrodynamic volume in SEC. Disassembly of the SCPN was performed by the reductive cleavage of disulfide bonds with dithiothreitol. This step was followed by SEC. An increase of the hydrodynamic volume to the original value confirmed unfolding. The assembly of the individual polymer chains to SCPN was repeated by oxidation with a catalytic amount of $FeCl_3$ at high dilution. This resulted in a shift to smaller SEC hydrodynamic volume. The authors also used SEC coupled to a MALS and differential viscometer for the full characterization of SCPNs.

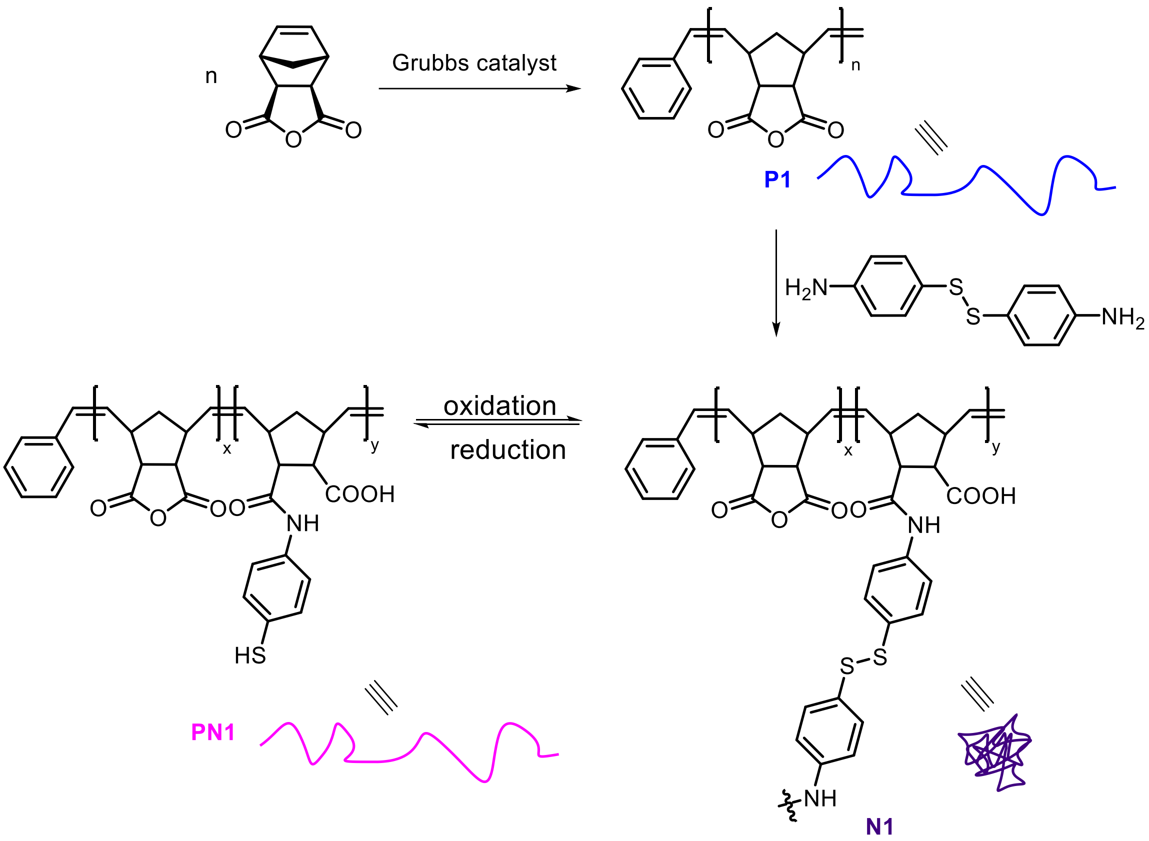

Figure 24 | Reversible single-chain nanoparticle formation through intramolecular disulfide bond. Adapted with permission from [5]. Copyright © 2012, Royal Society of Chemistry.

Single-chain polymer nanoparticles (SCPN) were synthesized through the formation of acylhydrazone bond. Chain collapse of linear polymer poly(vinylbenzaldehyde) (PVBA) took place when a bis-hydrazide cross-linker was added in the presence of TFA as catalyst [93]. The amount of cross-linker influenced the cross-linking density. The remaining aldehyde units were functionalized with a variety of hydrazides and alkoxyamines in order to obtain SCPN with a very high functionality density. The authors also showed the dynamic nature of hydrazone bond. Indeed, linear polymers containing hydrazone moieties were collapsed to a SCPN through an exchange with bis-hydrazide linker. Thereby, the adaptability of single polymer chain architecture by the use of dynamic chemistry was demonstrated for the first time.

I.4.1.B. Compartmentalization of Single Polymer Chains

The reactive functional groups for intramolecular cross-linking were positioned randomly in the above described examples of SCPNs. The compaction process was only controlled by the amount of cross-linker, the number of reactive sites, the changes of concentration or the reaction duration. Pomposo and coworkers investigated the behavior of various SCPNs in solution and showed that SCPNs are “sparse” objects at large scales, with, probably, local compact (globular) domains [94]. The use of sequence-controlled polymers with periodically positioned (self-)reactive moieties could allow better control of the compaction.

Roy and Lutz described the preparation of a sequence-controlled linear precursor that was intramolecularly cross-linked by two consecutive orthogonal reactions [95]. It led to a polymer with two terminal “structured compartments” (Figure 25). The linear precursor was synthesized by sequence-controlled nitroxide-mediated copolymerization of styrene with pentafluorophenyl 4-maleimidobenzoate (**1**) and TIPS-protected *N*-propargyl maleimide (**2**). The first step of intramolecular compaction was performed by modification of reactive pentafluorophenyl groups with a cross-linker ethylenediamine at diluted conditions in THF. The second step of intramolecular compaction was realized by deprotection of alkyne groups followed by Eglinton coupling using copper(II) acetate in dilute THF solution. Each stage of the double compaction was confirmed by SEC by the significant decrease of the apparent hydrodynamic volume and ^{1}H NMR spectroscopy.

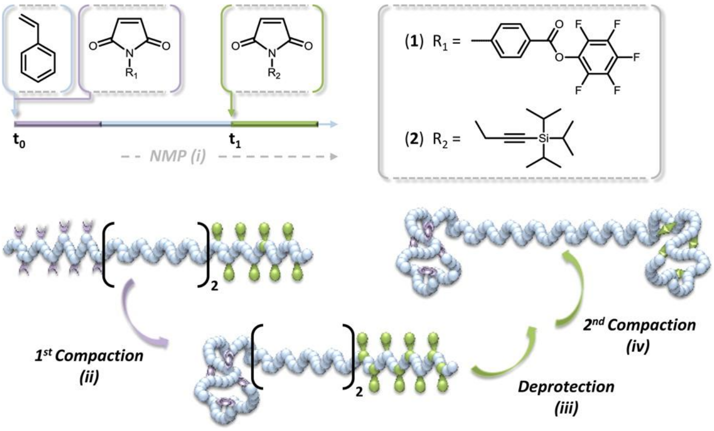

Figure 25 | Sequence-controlled copolymer synthesized by time-controlled additions of pentafluorophenyl 4-maleimidobenzoate (**1**) and TIPS-protected *N*-propargyl maleimide (**2**). Double compaction of the sequence-controlled copolymer. Reprinted with permission from [95]. Copyright © 2014, American Chemical Society.

I.4.1.C. Topological Polymers

In chapter I.4.1.A, random polymers were used as linear precursors leading to undefined primary structure, and, consequently, random distribution of covalent intramolecular bridges in SCPN. The control of polymer shape will be reported in the present paragraph based on cyclization of polymer chains and precise positioning of covalent bridges.

I.4.1.C.1. Cyclic Structures

Cyclic macromolecular structures can be prepared either by modification of the polymer chain-ends, or taking advantage of ring-chain equilibrium [96-100]. The advantage of the first method is that various well-defined polymers with functional chain-ends can be synthesized [97, 101, 102]. These polymers are usually prepared by radical polymerization with the development of CRP techniques and by ionic polymerizations. Therefore, a variety of monomers and post-modification reactions were explored for the formation of polymers folded by covalent link [101, 102]. It was reported that the properties of linear polymers can significantly differ from the cyclic polymers [100, 103-105].

A general idea of the synthesis of folded polymers with end-functional groups using various polymerization techniques and monomers is illustrated on the example of azide-alkyne "click" chemistry (copper-catalyzed Huisgen 1,3-dipolar cycloaddition) [101] (Figure 26). An initiator containing alkyne and bromine functional groups is usually exploited in ATRP (Figure 26, **1**). After polymerization the bromine end-group was modified in the presence of sodium azide in DMF, followed by the slow addition (~1 μmol/h) in diluted conditions (~10^{-5} M) of the polymer with alkyne and azide end-groups in a solution of Cu(I)Br and bipyridine in degased DMF [106, 107] affording a folded (cyclic) polymer. The combination of RAFT and azide-alkyne "click" chemistry was also shown to be an efficient method to synthesize such polymers [108] (Figure 26, **2**). An azido group modified 4-cyanopentanoic acid dithiobenzoate was used as the chain transfer agent in the RAFT mediated polymerization of styrene. The thiocarbonylthio end-group was afterwards replaced by an alkyne functional group in the presence of azobis alkyne-modified initiator. The final step – cyclization in the presence of Cu(I)Br and ligand (2,2′-bipyridyl) in DMF – was similar to the one described above. Ring-opening polymerization (ROP) was another polymerization technique used [109]. Linear precursors of *α*,*ω*-functionalized poly(ε-caprolactone) were prepared *via* ROP in the presence of an azido-functionalized initiator, followed by *ω*-end-group modification using 5-hexynoyl chloride to attach a terminal alkyne (Figure 26, **3**). “Click” coupling in the presence of Cu(I)Br and PMDETA in CH_2Cl_2 with a concentration of the polymer of ~10^{-3} M afforded the cyclic polymer. The successful cyclization was proven by MALDI-TOF-MS, NMR, FT-IR and SEC. The molecular weight of the polymer samples remained unchanged after “click” cyclization according to mass spectra. Evidence of the triazole formation was observed in NMR (7.5-7.9 ppm) and FTIR spectra (disappearance of the azide (2090 cm^{-1}) and terminal alkyne (3300 cm^{-1}) peaks). Cyclic polymers exhibit a longer size exclusion retention time than the linear polymer precursors as cyclic polymer structure is more compact.

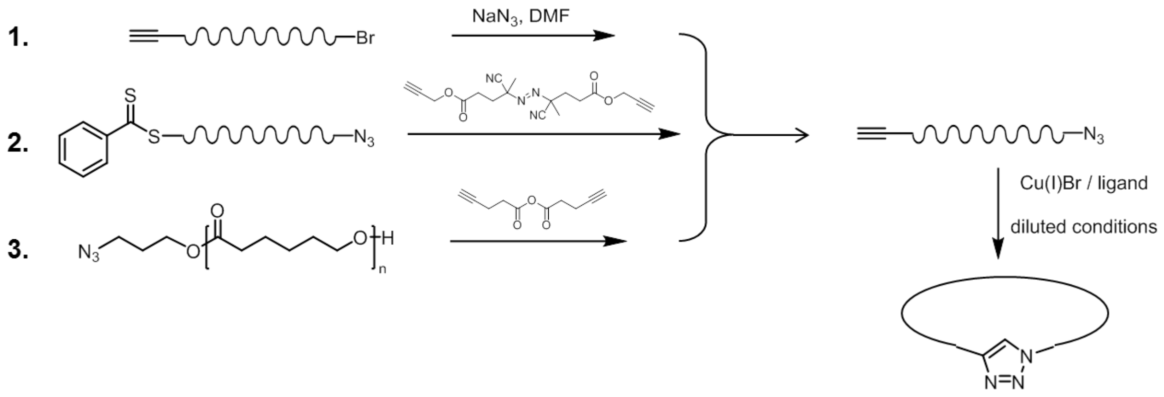

Figure 26 | Synthesis of linear precursors by ATRP, RAFT and ROP, and modification of the chain-ends followed by intramolecular cyclization.

Another example using the reversible coupling of thiol groups/cleavage of disulfide bond was described by Monteiro and coworkers [110]. A linear precursor was synthesized by RAFT polymerization of styrene in the presence of a difunctional RAFT agent (1,3-bis(2-(thiobenzylthio)prop-2-yl)benzene), afterwards conversion of dithioesters into thiol end groups by aminolysis in the presence of hexylamine was performed. Thus, thiol groups were positioned at polymer chain ends, and the transition from linear to cyclic polymer took place by the oxidation of the thiol groups in the presence of $FeCl_3$. The influence of polymer concentration was shown, as in diluted conditions (concentration of polymer below 10^{-3} M) preferentially cyclic polymers were obtained, while at high polymer concentrations linear multiblock polymers were formed. Transformation of cyclic to linear polymer was induced by the reduction of the oxidized polymers with help of zinc powder in acetic acid. Cyclization was confirmed by UV-*vis*, SEC analysis and Ellman’s test.

I.4.1.C.2. Synthesis of Complex Architectures Based on Cyclic Polymers

Complex polymer architectures can be obtained by modification of cyclic macromolecules with functional chain-ends [111-113]. Several examples are described below.

In one of the studies, cyclic polyesters were synthesized using ε-caprolactone with pendant acrylic groups (α-(1-acryloxyethyl)-ε-caprolactone), and the polymerization was initiated by a cyclic tin alkoxide [112]. Thus, after intramolecular cross-linking of the acrylic functions cyclic polyesters were obtained. Successful cyclization was evidenced by ^{1}H NMR spectroscopy and SEC. The ratio of the molecular weights at the maximum of the elution peaks $M_{p,\ cyclic}/M_{p,\ linear}$ was 0.76, and the intrinsic viscosity $[\eta]$ measurements gave a ratio $[\eta]_{cyclic}/[\eta]_{linear}$ equal to 0.69. As the propagating tin oxides remained active, it was possible to prepare a tadpole-shaped morphology by further polymerization of the macrocycle with ε-caprolactone (Figure 27).

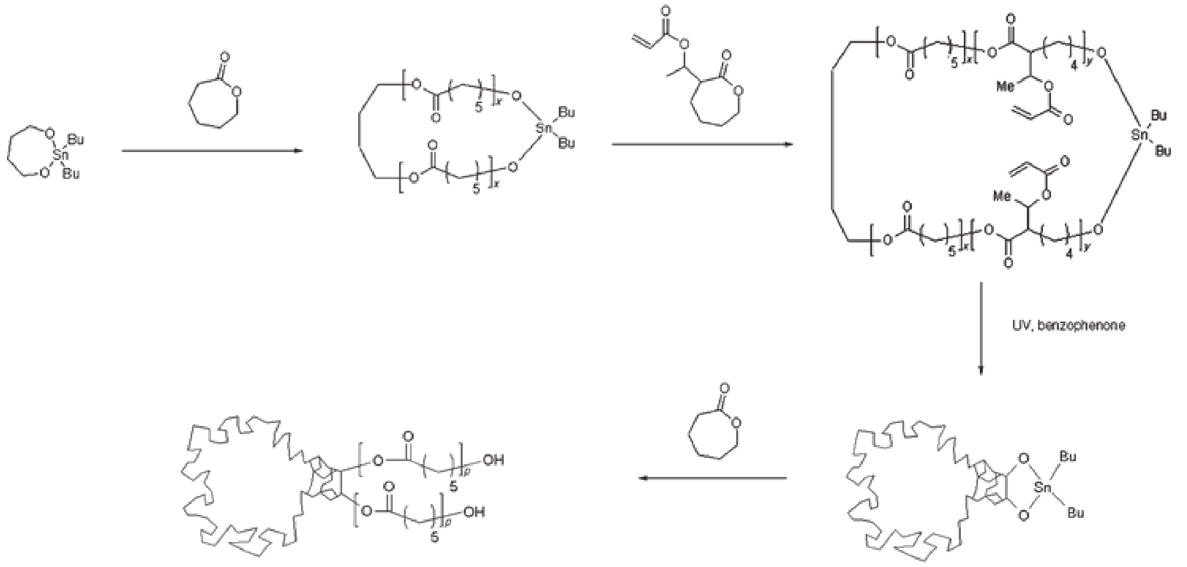

Figure 27 | Synthesis of a tadpole-shaped polymer. Reprinted with permission from [112]. Copyright © 2006 WILEY-VCH Verlag GmbH & Co. KGaA, Weinheim.

In another study [114], complex polymer architectures (tadpole-, 8-shaped, 3-miktoarm) were constructed by combining two building blocks: linear poly(*tert*-butyl acrylate) with block length changing from 21 to 46 units and cyclic polystyrene with constant chain length

(44 units). These building blocks were synthesized by ATRP and "connected" by azide-alkyne cycloaddition reaction. The obtained structures were characterized by DLS and TEM.

Tezuka and coworkers [115] described an approach for a "programmed" folding of the polymers. The first step included the synthesis of cyclic polytetrahydrofuran macromolecules with two oppositely positioned functional groups either allyl and alkyne followed by azide-alkyne cycloaddition with a linear bifunctional azide, or allyl and azide followed by azide-alkyne cycloaddition with a cyclic polytetrahydrofuran containing two alkyne chain-ends. Thus, bridged dicyclic and *spiro* tricyclic polymers were synthesized (Figure 28). The next step consisted in the intramolecular metathesis condensation of these polymers in the presence of Grubbs' catalyst that led to more complex folded objects based on cyclic structures (Figure 28).

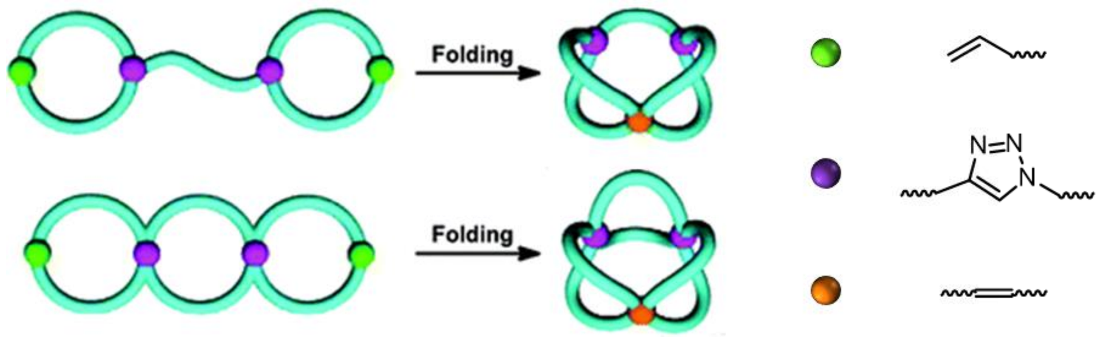

Figure 28 | "Programmed" polymer folding of bridged dicyclic and *spiro* tricyclic polymers. Reprinted with permission from [115]. Copyright © 2011, American Chemical Society.

I.4.1.C.3. Positionable Covalent Bridges

Precise positioning of intramolecular covalent bridges in a polymer chain, and control of single-chain folding remains challenging. A facile and elegant method of intramolecular covalent folding was proposed by Lutz and coworkers [8]. The synthesis of linear precursors – polystyrene chains with narrow length distribution, predictable molecular weight and *N*-functionalized maleimides positioned at specified place of polymer chain – was described above (Chapter I.2.4.). As a consequence of ATRP use, all polymer chains possessed similar terminal groups (*i.e.*, bromine). They were afterwards transformed into azide groups in the presence of sodium azide in DMF. Two alkyne protected monomers were exploited, TMS- and TIPS-protected *N*-propargyl maleimides. Copolymers of styrene were synthesized with *N*-functionalized maleimides positioned once (Figure 29, **P1**-**P3**) or twice (Figure 29, **P4**-**P7**) on the polymer chain, with variable positioning of maleimides (close to the end or in the middle of the polymer chain) and different molecular weights ($2.5\text{-}8\cdot10^3$ $g\cdot mol^{-1}$).

Copper-catalyzed azide-alkyne “click” reaction was used as an effective folding reaction between alkyne group of deprotected *N*-propargyl maleimide and azide terminal group. As a consequence of this reaction in dilute conditions (10^{-4}-10^{-5} M) with slow addition of polymer into the catalyst solution P-shaped (tadpole), Q-shaped and 8-shaped folded polymers were synthesized (Figure 29, **a**, **b**, **c**). Intramolecular Glaser coupling between two alkyne groups within the same chain in diluted conditions (10^{-4} M) led to another shape of folded polymer – α-shaped polymers (Figure 29, **d**).

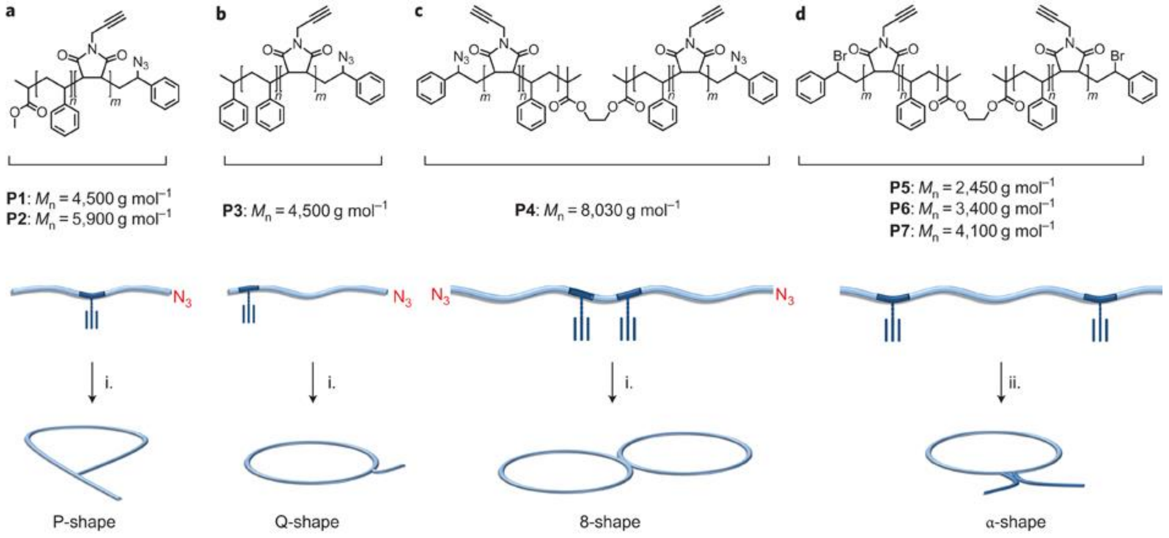

Figure 29 | Covalent folding of linear polymer chains leading to a variety of controlled shapes. Reprinted with permission from [8]. Copyright © 2011, Rights Managed by Nature Publishing Group.

The folded polymers were characterized by SEC, FT-IR and ^{1}H NMR spectroscopies. The increase of elution volume, corresponding to a decrease of apparent molecular weight, of folded compared to linear polymer was observed on the chromatograms (Figure 30). It indicated the decrease of the hydrodynamic volume typical for intramolecular cyclization processes. A compaction parameter <G> was calculated as ratio of molar masses at maximum peak value of the size-exclusion chromatogram of a folded polymer to a linear precursor ($\langle G\rangle = M_{p,f}/M_{p,l}$). Bigger value of <G> for 8-shaped folded polymer confirmed more significant compaction of 8-shaped polymers compared to P- and Q-shaped with comparable molar masses. For α-shaped polymers a significant fraction of intermolecular coupling was observed by SEC. FT-IR spectra confirmed that copper-catalyzed cycloaddition took place as the signals of C-H stretching of the terminal alkyne (3300 cm^{-1}) and asymmetric stretching of the azide (2093 cm^{-1}) vanished after the “click” reaction.

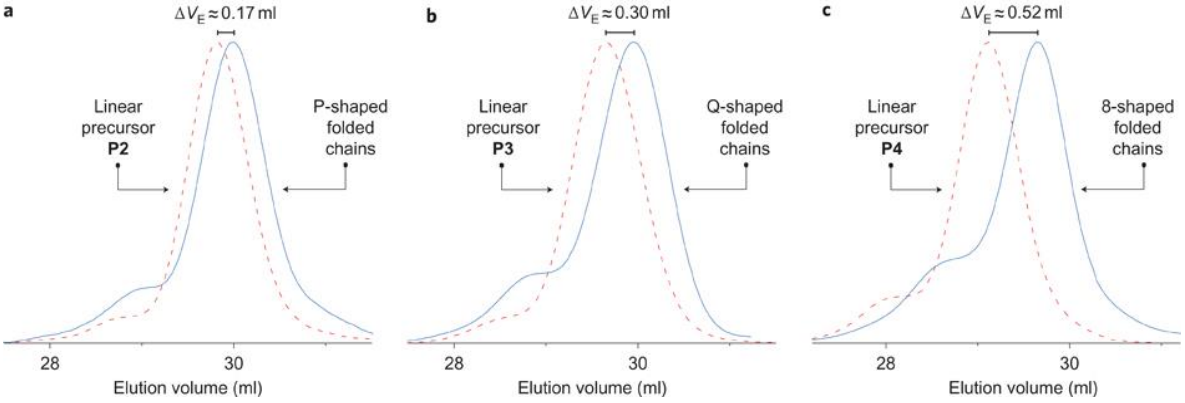

Figure 30 | Chromatograms of linear (dashed line) and folded by covalent link (straight line) polymers. Reprinted with permission from [8]. Copyright © 2011, Rights Managed by Nature Publishing Group.

Another approach for the synthesis of α-shaped polymers with variable sized and loop diameters was investigated [9]. In this study folded polymers were prepared not by a coupling reaction, but by a sequence of chemical steps leading thereby to the formation of intramolecular asymmetric bridges. First, linear polystyrenes with precisely positioned pentafluorophenyl 4-maleidobenzoate (PFP-MI) and TIPS-protected (TIPS-PMI) were obtained by nitroxide mediated polymerization (NMP). Afterwards, pentafluorophenyl activated ester moieties were modified by a primary amine with an azide group (11-azido-3,6,9-trioxaundecan-1-amine), and then alkyne functions were deprotected in the presence of TBAF in THF. The folding of polymer chains was performed by intramolecular azide-alkyne cycloaddition in the presence of CuBr and bipyridine in DMF in diluted conditions (~10^{-4} M) (Figure 31). Successful folding was confirmed by ^{1}H NMR spectroscopy (formation of a triazole function), FT-IR spectroscopy (vanishing of azide and alkyne signals after Huisgen cycloaddition) and SEC (decrease of hydrodynamic volume value for the folded polymer).

Varying the positions of maleimides on the polymer chain and molecular weights (Figure 32) of the polymer allowed, thereby, controlling the sizes of the loop and the linear region. The values of compaction parameter <G> ($\langle G \rangle = M_{p,f}/M_{p,l}$) calculated for the folded polymers were found around 0.9 and were bigger than the one obtained for cyclic polymers of the same molar mass. This increase was caused by the presence of both cyclized and linear regions of the obtained α-shaped polymers. The fraction of cyclized regions in the polymer F_c can be estimated from the average chain lengths of cyclized and linear regions, $DP_{n,c}$ and $DP_{n,l}$, respectively, $F_c = DP_{n,c}/(DP_{n,c} + DP_{n,l})$. The value of the compaction parameter <G> was close to the theoretical value when the values of F_c were taken into consideration [9].

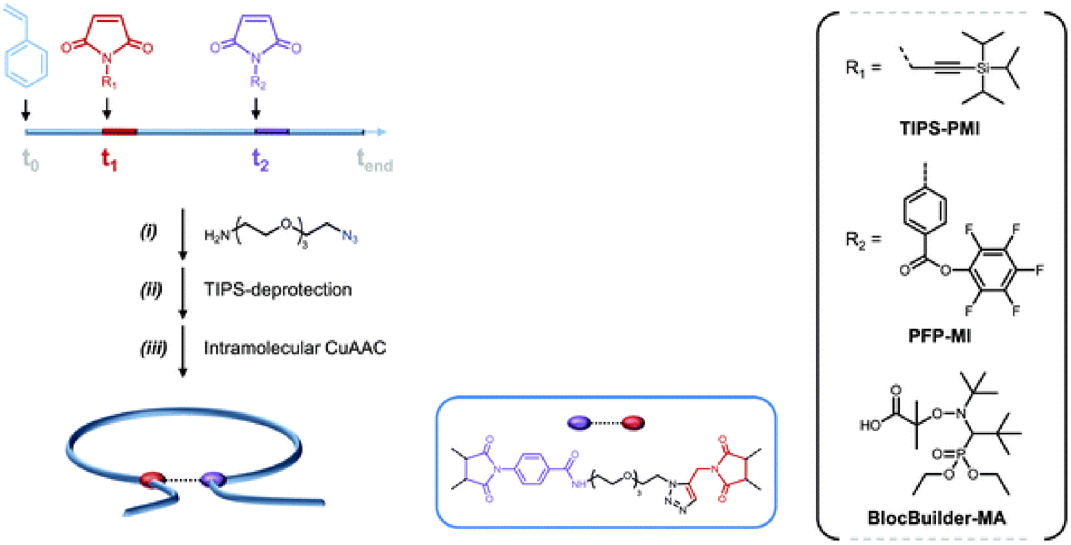
t0
t1
t2
tend
(i)
(ii) TIPS-deprotection
(iii) Intramolecular CuAAC
R1 =
TIPS-PMI
R2 =
PFP-MI
BlocBuilder-MA

Figure 31 | Folding of polystyrene chains using asymmetric covalent bridges in three steps: (*i*) THF, RT, overnight; (*ii*) TBAF, THF, RT, overnight; (*iii*) CuBr/bipy, 80°C, DMF, dilute conditions. Reprinted with permission from [9]. Copyright © 2011, Royal Society of Chemistry.

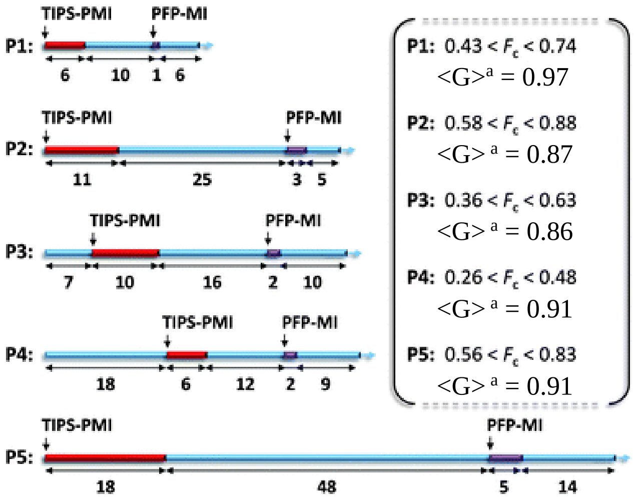
TIPS-PMI
PFP-MI
P1:
6 10 1 6
P2:
11 25 3 5
P3:
7 10 16 2 10
P4:
18 6 12 2 9
P5:
18 48 5 14
P1: 0.43 < Fc < 0.74
<G>a = 0.97
P2: 0.58 < Fc < 0.88
<G>a = 0.87
P3: 0.36 < Fc < 0.63
<G>a = 0.86
P4: 0.26 < Fc < 0.48
<G>a = 0.91
P5: 0.56 < Fc < 0.83
<G>a = 0.91

Figure 32 | Schematic representation of the microstructure of the linear precursors exploited for the synthesis of α-shaped polymers. ᵃCompaction parameter <G> is shown for folded polymers. Reprinted with permission from [9]. Copyright © 2011, Royal Society of Chemistry.

I.4.2. Compaction/Folding of Single Polymer Chains by Non-Covalent Interactions

Non-covalent interactions are weaker than covalent, and their strength generally depends on external influences such as pressure, solvent and temperature. Non-covalent interactions can be roughly classified in three groups according to the bond strength: 1) weak (0-15 kcal·mol^{-1}), for example, hydrophobic interactions and hydrogen bonds; 2) intermediate (15-60 kcal·mol^{-1}), such as weak metal coordination complexes and multiple hydrogen bonds; 3) strong (> 60 kcal·mol^{-1}), such as ionic interactions, host-guest interactions, robust metal coordination, etc.

Introduced by the fascinating work of Lehn [116, 117], non-covalent interactions are highly exploited nowadays in the field of supramolecular chemistry. However, synthesis of single-chain polymers structured by non-covalent interactions is still a developing direction in chemistry. In this subchapter the transformation of a random polymer coil into a single-chain polymer particle driven by non-covalent (hydrogen bonding, metal-ligand, and host-guest) interactions will be presented. Two main approaches will be described, based on isotropic (random) and anisotropic (directional) self-associations.

I.4.2.A. Isotropic Compaction

I.4.2.A.1. Folding of Polymer Chains by Hydrogen Bonding

The interest to this topic is due to the similar processes taking place in nature. One of them is biological self-assembly, and the folding of proteins into two- and three-dimensional structures is the most universal and fundamental example. The hydrogen bonding between the amide and carbonyl groups of the main chain, primarily stabilizes secondary structure, and, consequently appear as an important element in the folding process [118].

Folding is mainly performed by the formation of multiple hydrogen bonds between functional groups belonging to one chain in diluted conditions. Two main types of multiple hydrogen bonds can be distinguished: a) self-complementary if they are formed by dimerization of two identical functionalities [119]; b) hetero-complementary if they are formed by self-recognition of two different functional moieties [120].

The use of self-complementary hydrogen bonds was shown by the group of E.W. Meijer [119]. Poly(methyl methacrylate) with protected 2-ureidopyrimidinone pendant moieties was synthesized by combination of living radical polymerization (SET-LRP) and azide-alkyne cycloaddition “click” chemistry. Further irradiation of the polymer with UV light in diluted conditions led to the collapse of single polymer chains *via* supramolecular interactions (Figure 33). The formation of single chain nanoparticles was proved by the decrease of particle size in atomic force microscopy images and the decrease of the hydrodynamic volume in size exclusion chromatograms after irradiation.

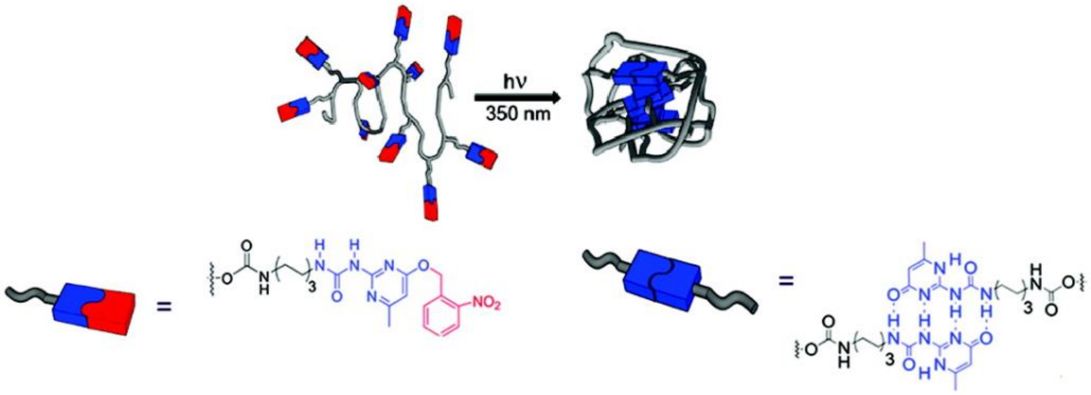

Figure 33 | UV irradiation induced the collapse of a single polymer chain into a nanoparticle *via* supramolecular cross-linking. Reprinted with permission from [119]. Copyright © 2010, American Chemical Society.

I.4.2.A.2. Metal Coordination

The interest to this topic is driven by the mimicking of metalloproteins/ metalloenzymes [121] and investigation of the interactions between biomacromolecules and metal ions [122]. Although synthesis of supramolecular polymers is frequently based on the use of metal-ligand interactions [123, 124], the preparation of unimolecular compaction and single-chain folding by metal coordination is few times mentioned in the literature [6, 7, 33].

Mavila *et al*. described the synthesis of metal-containing single chain nanoparticles [6] (Figure 34). Linear precursors poly(1,5-cyclooctadiene) (poly(COD)) with molecular weight $25 \cdot 10^3$ g·mol^{-3} and polydispersity around 1.3 were prepared by ring-opening metathesis polymerization (ROMP). Intramolecular cross-linking of poly(COD) using a commercially available chlorobis(ethylene)rhodium(I) dimer in THF at diluted conditions and room temperature led to the formation of polymeric nanoparticles. Rhodium(I)-polymer complex formation was evidenced in ^{1}H NMR spectrum by the appearance of a broad resonance corresponding to the olefin protons bound to the rhodium metal center. Decrease in nanoparticles size compared to linear precursor was followed by DLS and SEC. Increase of the amount of added rhodium(I) from 1 to 10 mol. % led to decrease in the hydrodynamic radius from 9.3 nm to 7.3 nm confirming intramolecular complexation. Moreover, removal of the metal by reaction with a phosphine aldehyde derivative regenerated linear precursor. Additionally, nanoparticles were observed by transmission electron microscopy (TEM), and they were about 20 nm in diameter which correlated with the results obtained by DLS.

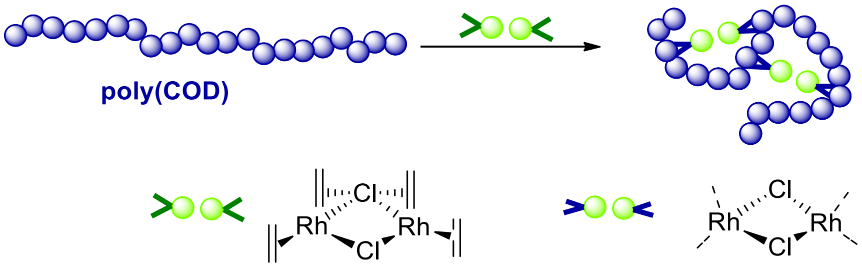

Figure 34 | General idea of metal-containing single chain nanoparticles synthesis [6].

Pomposo and coworkers presented metallo-folded single-chain nanoparticles with catalytic selectivity [7] (Figure 35). Copolymers of methyl methacrylate (MMA) containing 30 mol. % of 2-(acetoacetoxy)ethyl methacrylate (AEMA) were used as linear precursors. Single-chain folded particles were created by interchain complexation of AEMA units with $Cu(OAc)_2$ in highly diluted conditions due to the concurrent folding and binding properties of β-ketoester reactive functions of AEMA with Cu(II). The collapse of linear copolymer precursors was evidenced by SEC (reduction of hydrodynamic size upon the addition of Cu(II)), MALS (decrease of average radius of gyration) and IR (appearance of characteristic stretching C=C vibration band of enol tautomer bonded to Cu(II)).

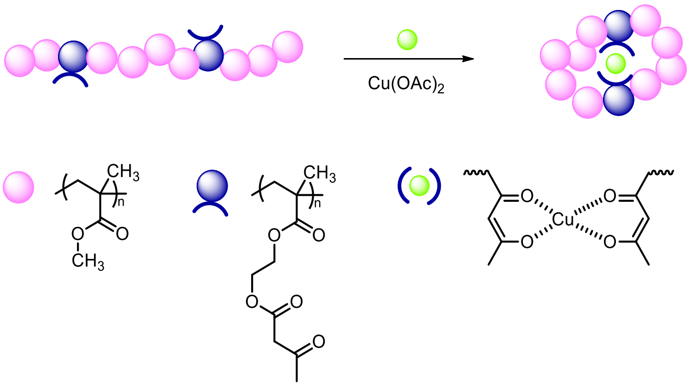

Figure 35 | Idealized picture of metallo-folded single-chain nanoparticle [7].

I.4.2.A.3. Host-Guest Interactions

The Scherman group [125] applied strong host-guest interactions for the synthesis of single chain particles in water. Cucurbit[8]uril (CB[8]) – a macrocyclic host molecule able to bind two aromatic guest molecules simultaneously – was chosen for the preparation of such system. Poly(*N*-hydroxyethylacrylamide) synthesized by ATRP and modified by 5-15% of isocyanates from naphtyl and viologen derivatives was used as a linear precursor (Figure 36). Controlled intermolecular collapse of the precursor took place by addition of CB[8] at concentrations equal or below 0.1 mg·mL^{-1}. The formation of nanoparticles was confirmed by DLS as due to the collapse, the size of polymer decreased after the addition of CB[8]. Nanoparticles were also characterized by atom force microscopy (AFM) that revealed the morphological differences between initial polymers and CB[8]-nanoparticles. The same experiment was performed in the presence of CB[7] instead of CB[8] and did not show formation of the particles neither by DLS, nor by AFM.

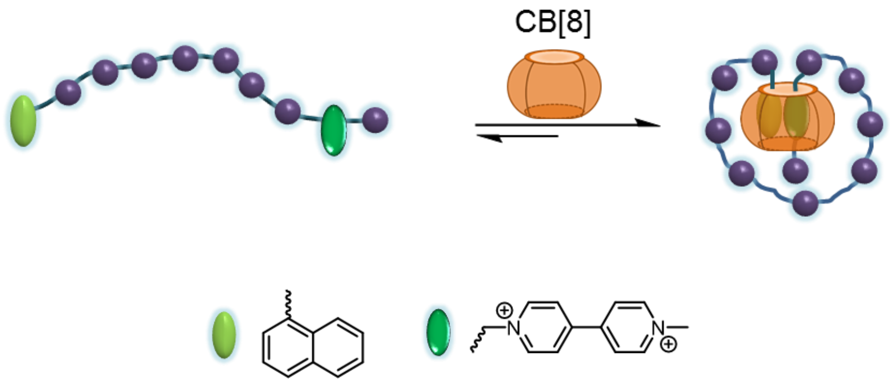

Figure 36 | Folding of polymer chains by host-guest interactions on the example of CB[8] – viologen or naphtyl-modified polyacrylamide.

I.4.2.B. Anisotropic Compaction

Directional interactions to assemble supramolecular architectures were applied for the compaction of polymer chains into structured SCNPs with “secondary structure type” domains. Benzene-1,3,5-tricarboxamide (BTA), a supramolecular motif, was used for its ability to form helical assemblies *via* hydrogen bonding. BTA moieties were either randomly positioned on polymer chains [126], or by formation of a block copolymer [127-129].

The group of Meijer studied extensively the compaction of polymer-chains by self-association of BTA motifs. In one of the first studies BTA functional group were randomly introduced in a polymer chain [126]. Linear precursors were prepared by copolymerization of silyl-protected propargyl methacrylate and isobornyl methacrylate in a ratio of 80:20 using activator regenerated by electron transfer (ARGET) ATRP, followed by deprotection of alkyne groups and partial (around 50%) modification with azide-functionalized BTA containing *o*-nitrobenzyl protecting group. Isobornyl methacrylate was selected to increase the solubility of the final polymer in apolar solvents. Upon irradiation of **1**, the *o*-nitrobenzyl group was cleaved to afford **2**, leading to self-assembly (Figure 37). Circular dichroism (CD) spectroscopy analysis evidenced helical hydrogen bonded BTA aggregates. The influence of temperature changes on the SCPN formation was investigated. It was shown, that at high temperatures BTAs were not aggregated, and the polymer was unfolded. Slow reduction of the temperature induced BTA aggregation. In order to investigate the structure of SCPNs formed by BTA association, two types of polymers containing chiral and achiral BTA moieties were synthesized [127]. Based on various CD data, the authors concluded that SCPN consisted of multiple structured BTA domains (with some mixing of BTA units of different domains), and they adopted an ellipsoidal shape in the solution.

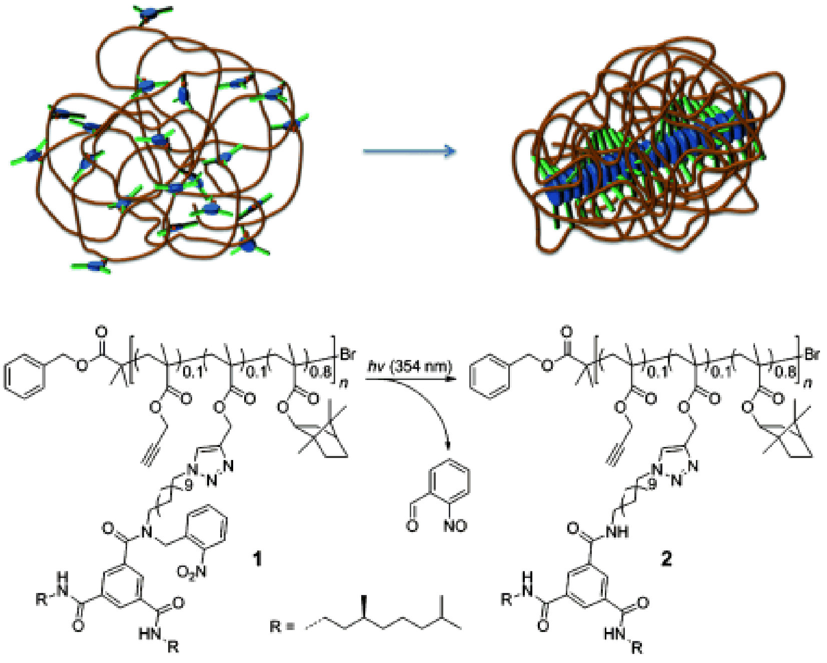

Figure 37 | Compaction of polymer coils due to the self-assembly of BTA moieties upon irradiation and cleavage of *o*-nitrobenzyl groups. Reprinted with permission from [126]. Copyright © 2011 WILEY-VCH Verlag GmbH & Co. KGaA, Weinheim.

Along with random copolymers, ABA-type block copolymers carrying two complementary self-associative motifs, BTA and 2-ureidopyrimidinone (Upy), were synthesized [129]. ABA block copolymers, prepared by ATRP, contained pendant alcohols in the A block and acetylenes in the B block which were postmodified with isocyanate-functionalized *o*-nitrobenzyl protected UPy and azide-substituted BTA, respectively (Figure 38, (**b**)). The double functionalization was performed using orthogonal reactions, and compaction of the prepared block copolymer was also orthogonal, since BTAs self-assembly was induced by the decrease of temperature, and UPys self-assembly was sensitive to irradiation with UV light, in diluted conditions for both processes (Figure 38, (**c**), (**d**)). NMR and CD spectroscopies confirmed the self-assembly of BAB-type block copolymers with inverse order of BTA and UPy functional segments [128]. It was shown that folding behavior of BAB-block copolymer was similar to the one of ABA-block copolymer, however, a slight difference was observed in degree of chain collapse, since ABA-type copolymer adopted more packed structure.

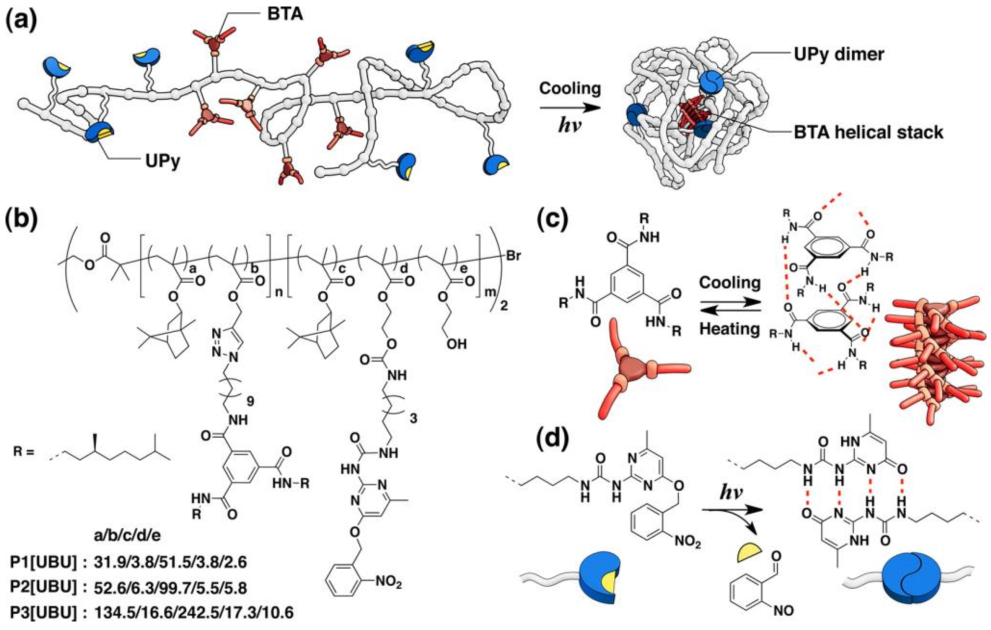
(a)
BTA
UPy
Cooling
hv
UPy dimer
BTA helical stack
(b)
a
b
c
d
e
n
m
2
Br
9
3
R =
a/b/c/d/e
P1[UBU] : 31.9/3.8/51.5/3.8/2.6
P2[UBU] : 52.6/6.3/99.7/5.5/5.8
P3[UBU] : 134.5/16.6/242.5/17.3/10.6
(c)
Cooling
Heating
(d)
hv
NO2
NO

Figure 38 | Orthogonal self-assembly leading to the formation of a SCPN by directional hydrogen bonding. Reprinted with permission from [129]. Copyright © 2013, American Chemical Society.

The group of Meijer reported also SCPNs for catalytic systems in water [130, 131]. A linear precursor was carefully designed in order to a) carry catalytic sites and functional moieties able to self-assemble, b) contain hydrophobic and hydrophilic parts. A diphenylphosphine ligand was chosen as catalytic unit to form a complex with ruthenium ions. BTA substituents were used as supramolecular motifs. Moreover, they formed the hydrophobic part of the linear precursor, whereas the hydrophilic part was formed by introduction of PEG pendant chains. Random linear copolymers were prepared by a one pot-reaction: when ruthenium-catalyzed living radical copolymerization of methacrylate with BTA moieties and poly(ethylene glycol) methyl ether methacrylate reached around 50 % conversion, ruthenium catalyst with diphenylphosphinostyrene (SDP) was added (Figure 39). UV-vis spectroscopy evidenced the successful incorporation of SDP with ruthenium into the copolymers. The formation of compact structures through intramolecular self-assembly of BTA moieties was confirmed by SEC, DLS, diffusion ordered spectroscopy (DOSY) and small-angle X-ray scattering (SAXS). Finally, the prepared single-chain nanoparticle played the role of a catalyst for the hydrogenation of ketone into alcohol with a catalytic activity comparable to previously reported water-soluble ruthenium complexes.

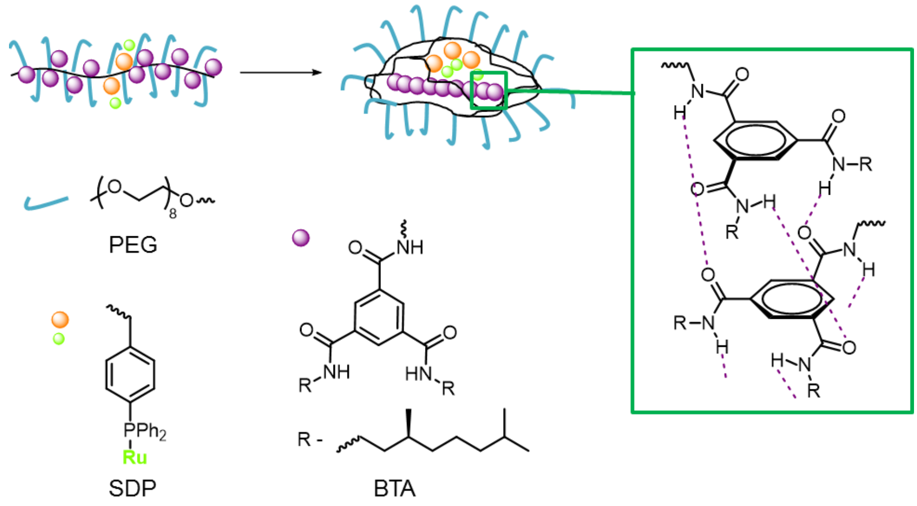

Figure 39 | Single-chain folding caused by self-assembly of BTA groups of a polymer containing catalytic units (SDP with ruthenium), hydrophilic (PEG chains) and hydrophobic parts (BTA substituents) [130].

Cyclized single-chain polymers

Apart SCPNs, some cyclic polymers synthesized by hydrogen-bonding [132] and metal-ligand interactions were reported by the group of Barner-Kowollik [33]. The self-folding of a single polymer chain based on two orthogonal - hetero-complementary - multiple hydrogen bonds was presented [132]. Well-defined polymers bearing two pairs of orthogonal hydrogen bonding recognition moieties were synthesized using ATRP and orthogonal ligation strategy.

Cyanuric acid–Hamilton wedge (CA–HW) and thymine-diaminopyridine (Thy–DAP) were used as orthogonal pairs. Initially full orthogonality of CA–HW and Thy–DAP was shown by ^{1}H NMR spectroscopy in CD_2Cl_2 at ambient temperature. Dynamic and static light scattering analyses of the macromolecular self-assembly systems proved the hydrogen bonding interactions between both the Thy–DAP and CA–HW motifs leading to single chain self-folding. The reversibility of the self-folding action depended on temperature and concentration as confirmed by ^{1}H NMR spectroscopy: the single chain folded structures dominated at low temperature and high dilution.

The application of metal-ligand interactions for cyclization of single polymer chains was also investigated [33]. Linear polymer precursors were synthesized by ARGET ATRP of styrene followed by the “click chemistry” between the azido-end groups of the polymer and triphenylphosphine ligands bearing an alkyne function. Cyclic complexes were obtained by the complexation of the precursors with dichloro(1,5-cyclooctadiene)palladium(II) (Figure 40). The complexation and single-chain folding were proven by ^{1}H and ^{31}P{^{1}H} NMR spectroscopies, SEC and DLS.

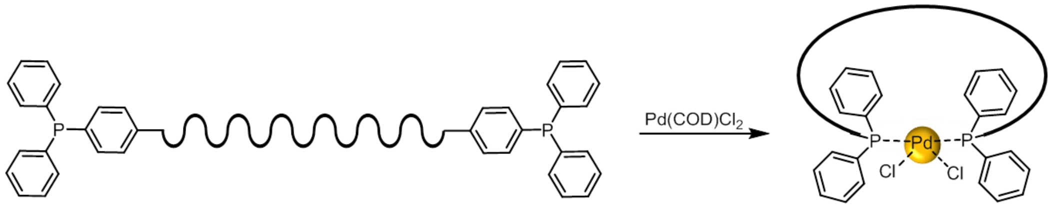

Figure 40 | Cyclization of single polymer chain driven by metal-ligand interactions [33].

In the last paragraph some controlled/living radical polymerization (CLRP) techniques used in this thesis will be briefly presented.

I.5. CONTROLLED/LIVING RADICAL POLYMERIZATION TECHNIQUES

I.5.1. Introduction

The driving force behind the development of CRP was the need of polymers with well-defined molecular weight, polydispersity, chain-end functionalities, composition and chain architecture using easier preparation conditions. Therefore, conventional radical polymerization is highly exploited in the industry due to the broad spectra of suitable monomers and undemanding polymerization conditions. However, it has an important disadvantage: the poor control of the polymerization. Living anionic and cationic polymerizations allow obtaining polymers with high degree of structural and compositional homogeneity, but they have some limitations such as less extensive range of vinylic monomers to be polymerized and demand of ultrapure conditions.

A dynamic equilibrium between dormant species and a low concentration of active growing radicals is established in controlled radical polymerization *via* activation (k_a) and deactivation (k_d) steps, taking into consideration that initiator is consumed at early stage of polymerization and all chains are growing simultaneously. There are some key features of CLRP:

1. **First-order kinetic behavior** that can be illustrated by the following graph (Figure 41, **a**), where the polymerization rate with respect to the logarithm of the monomer concentration is a linear function of time [133]. It is due to the fact that non-reversible termination is negligible, and the concentration of the active propagating species $[P^*]$ is constant. Different deviations from linearity are shown in Figure 41, **a**: increase of $[P^*]$ due to slow initiation results in an upward curvature in the kinetics; decrease of $[P^*]$ due to termination or side reactions results in a downward curvature in the kinetics.
2. **Pre-determinable degree of polymerization** (DP_n) that consists in the linear dependence of molecular weight (M_n) on time (Figure 41, **b**). The ideal growth of molecular weight with conversion is illustrated by a linear line (Figure 41, **b**). The deviations from the linearity and the influence of coupling termination, transfer side reactions and slow initiation are also presented.

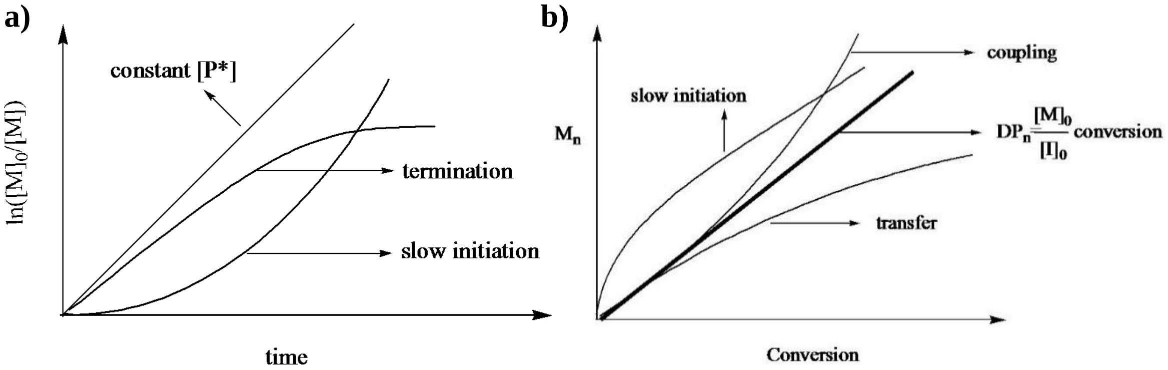

Figure 41 | a) The semilogarithmic plot of the dependence of monomer concentration on time; **b**) the dependence of molecular weight on conversion. Reprinted with permission from [133]. Copyright © 2001, American Chemical Society.

The CLRP techniques can be divided into two main approaches such as reverse termination and degenerative transfer [134]. The first approach including reversible thermal cleavage of weak covalent bonds and transition metal catalyzed processes has been used during this work, therefore it will be discussed in details and the last approach will not be presented in this work.

I.5.2. Reversible Thermal Cleavage of Weak Covalent Bonds

The main idea of this approach is that by reversible thermal cleavage of a covalent bond, a growing radical and a persistent (stable) free radical are formed (Scheme 6). Nitroxide [135], triazolinyl radical [136], trityl , etc. can act as persistent radicals. The use of the most exploited and successful nitroxides for CRP will be shown in the part named "Nitroxide-Mediated Polymerization".

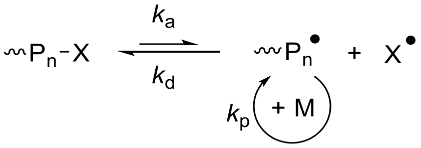

Scheme 6 | Schematic representation of dynamic equilibrium in reversible thermal cleavage of weak covalent bonds.

I.5.2.1. Nitroxide-Mediated Polymerization

NMP which is based on the use of nitroxide as persistent radical, is historically the first approach of CRP [137, 138]. Originally, NMP was initiated by a bicomponent system (Scheme 7, **a**): a conventional thermal radical initiator (AIBN, benzoyl peroxide, etc.) was used in combination with a stable nitroxide, namely, 2,2,6,6-tetramethylpiperidinyl-1-oxy (TEMPO) [135, 139]. Primary radicals are produced by thermal decomposition of the initiator to induce polymerization, then the activation-deactivation equilibrium between propagating radical with control agent (nitroxide) and (macro)alkoxyamine is maintained (Scheme 7, **a**). The initial ratio of nitroxide to initiator is playing an important role as it influences the rate and control of polymerization. The efficiency of the primary radicals produced for the polymerization initiation is difficult to determine precisely, therefore the concept of monocomponent initiating system appeared (Scheme 7, **b**) [140]. The advantage of the use of alkoxyamine initiator (monocomponent initiating system) is the formation of initiating radical and nitroxide in the ratio 1 to 1 after dissociation.

Persistent Radical Effect (PRE)

PRE is a kinetic feature of NMP [141]. Active (transient) radicals and persistent species are formed together in equal amounts and with the same rate after the initiation takes place. The persistent radicals (nitroxides) do not undergo coupling due to their nature, but they reversibly react with the active radicals. The persistent radicals in turn can undergo irreversible self-termination. It leads to a small increase of concentration and slow accumulation of persistent radical species compared to active radicals. This process develops continuously with time. Therefore, the recombination of active growing and persistent radicals becomes more favored compared to self-termination (radical-radical coupling). Although it cannot be avoided, the self-termination is inhibited itself as it proceeds. This self-regulation process causes the PRE and eventual control over the polymerization.

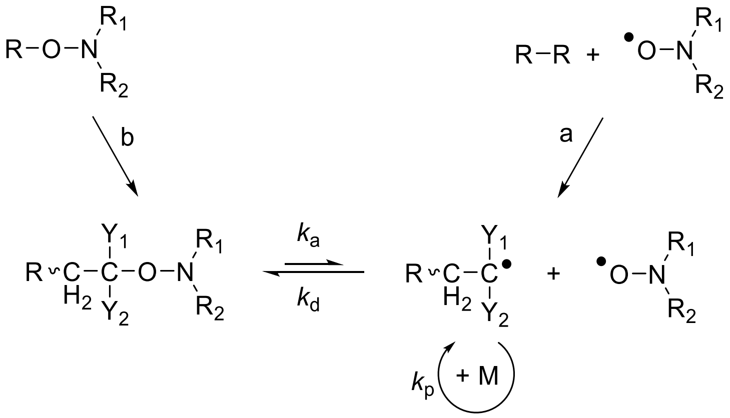

Scheme 7 | Activation-deactivation equilibrium in nitroxide-mediated polymerization: **a**) bicomponent initiating system; **b**) monocomponent initiating system [137].

Nitroxide Radicals and Alkoxyamines

The most used nitroxides in NMP are: 2,2,6,6-tetramethyl-1-piperidinyloxy (TEMPO), 2,2,5-trimethyl-4-phenyl-3-azahexane-N-oxyl (TIPNO), and 4-(diethoxyphosphinyl)-2,2,5,5-tetramethyl-3-azahexane-N-oxyl (SG1 or DEPN). Since SG1-based alkoxyamine BlocBuilder® is commercially available, this initiating system is broadly used in NMP.

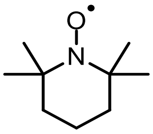

TEMPO

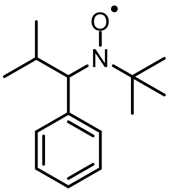

TIPNO

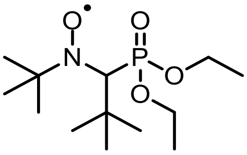

SG1 or DEPN

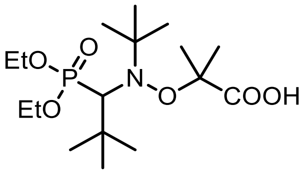

BlocBuilder®

There are some methods for synthesizeing alkoxyamines: (**a**) nucleophilic substitution of the hydroxylaminate anion on the corresponding alkyl halide, (**b**) Meisenheimer rearrangement of allyl or benzyl amine oxides, (**c**) reaction of an oxoammonium salt with olefins or enolates and (**d**) scavenging of an alkyl radical by an aminoxyl radical (Figure 42) [137].

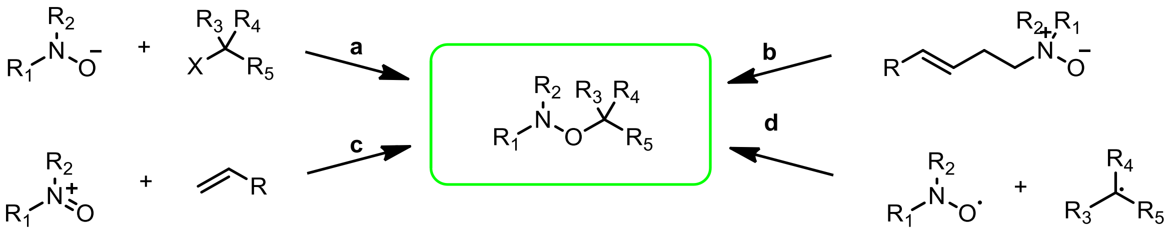

Figure 42 | Synthetic pathways to prepare alkoxyamines [137].

NMP of styrenic monomers

Styrene monomers are probably the most investigated for the NMP from the point of view of kinetics, mechanism and side reactions [142]. Styrene readily undergoes thermal self-initiation to produce a low concentration of propagating radicals, in contrast to acrylates. This fact leads to the rate enhancement without need of additional portion of initiator (and allows keeping reasonable rate under PRE). Well-defined polystyrenes are synthesized in the presence of various nitroxides and alkoxyamines. The polymerization in the presence of most cyclic nitroxides is rather slow but can be improved if acyclic nitroxides are used [143]. The NMP of styrene derivatives (styrene substituted on the aromatic ring) is also successful and leads to well-defined polymers. However, side reactions (*i.e.* chain transfer) can take place if styrene contains interfering reactive groups (*i.e.* chloromethyl).

Chain end degradation

Except termination reactions of propagating radicals, the decomposition of the alkoxyamine chain ends can occur as a side reaction [142]. The mediating nitroxide radical can transform into hydroxylamine **I** by H-transfer that results in a dead polymer chain (Scheme 8). Afterwards, hydroxylamine can potentially react with propagating chain leading to the second dead polymer chain and increase of the polydispersity. The chain end degradation reactions are dependent on the used monomers, solvent and duration of the polymerization. However, the effect of this side reaction is not significant for the NMP of styrene monomers due to thermal initiation, in contrast to methacrylates that do not have thermal initiation.

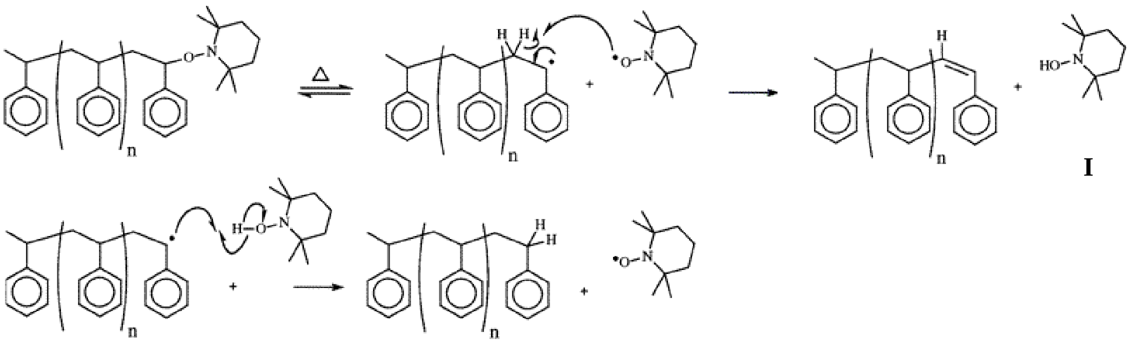

Scheme 8 | Possible chain end degradation during NMP of styrene. Reprinted with permissions from [142]. Copyright © 2001, American Chemical Society.

Along with some significant advantages compared to other CRP techniques:

- The polymerization of styrene with BlocBuilder® is a simple way for the preparation of polystyrenes with a narrow molecular weight distribution (PDI);
- NMP is preferable to ATRP if monomer interacts with the metal catalyst, or if the contamination of polymer is undesirable;
- NMP provides the control of the polymerization of 1,3-dienes, in contrast to ATRP and RAFT;

However, NMP has some limitations:

- Generally slower polymerization kinetics compared to ATRP and RAFT;
- Limited range of monomers to be polymerized with the same initiating system;
- The majority of alkoxyamine initiators are not commercially available that results in sometimes challenging synthesis.

I.5.3. Metal-Catalyzed Living Radical Polymerizations

This approach can be considered as a subset of the above described “Reversible thermal cleavage of weak covalent bonds”. The difference lies in reversible cleavage of a covalent bond *via* a redox process [144, 145]. The equilibrium between a dormant and a growing polymer chain is provided by a transition metal catalyst, and a transfer of an atom between dormant species and the transition metal catalyst in a lower oxidation state leads to the formation of active radicals and transition metal in a higher oxidation state (Scheme 9). The two metal catalyzed processes used for the synthesis of polymers in this work: atom transfer radical polymerization (ATRP) and single electron transfer living radical polymerization (SET-LRP), or supplemental activator and reducing agent atom transfer radical polymerization (SARA ATRP) – are described in details.

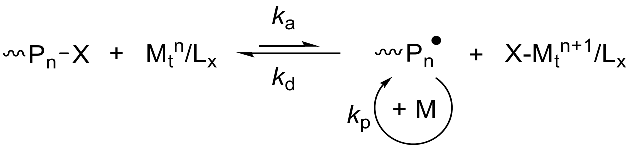

~P$_n$-X + M$_t$^{n}/L$_x$
k_a
k_d
~P$_n$$^•$ + X-M$_t$$^{n+1}$/L$_x$
k_p
+ M

Scheme 9 | Schematic representation of the dynamic equilibrium in transition metal catalyzed processes.

I.5.3.1. Atom Transfer Radical Polymerization

In 1995, a second technique (after NMP) of controlled radical polymerization has emerged [146, 147]. This technique was called “atom transfer radical polymerization in the presence of transition-metal complexes” by Matyjaszewski and coworkers [147] and metal-catalyzed living radical polymerization by Sawamoto and coworkers [146]. An efficient reaction used for carbon-carbon bond formation (atom transfer radical addition) was adapted for this technique. A complex system of styrene (100 Eq.), metal catalyst CuCl with bipyridine as ligand (1 Eq. to 3 Eq.) and 1-phenylethylchloride as initiator (1 Eq.) was applied for this controlled polymerization by Matyjaszewski and coworkers [147]. Since these pioneering works a variety of different monomers, initiators, metal catalysts and ligands were investigated [133, 134].

The general concept of ATRP mechanism is schematically described (Scheme 9), where initiation step is omitted and M_t – metal, L – ligand, X – halogen (usually X = Cl or Br). The polymerization rate is determined by the equilibrium constant ($K_{eq} = k_a/k_d$), in the absence of side reactions. Each monomer has its own radical propagation rate; therefore the concentration of propagating radicals and the rate of radical deactivation should be adjusted for every monomer. This can be performed in ATRP by varying the amount and reactivity of the metal catalyst that should be highly selective for atom transfer, deactivate extremely fast, have easily tunable activation rate constants and should not participate in side reactions. Copper catalysts are the most widely used type due to their versatility and low cost. Various monomers (styrenes, acrylates, methacrylates, etc.) can be successfully polymerized in the presence of copper catalyst.

As catalytic activity and selectivity are strongly dependent on the ligand used, the ligand should be carefully chosen. For example, multidentate aliphatic amines like *N,N,N′,N′,N″*-pentamethyldiethylenetriamine (PMDETA) or tris(2-dimethylaminoethyl)amine (Me6-TREN) increase the rate of the polymerization compared to pyridineimines and phenanthroline multidentate ligands [148], at the same time providing a good control. It is also noticed that if the metal center is sterically hindered or the ligand has strongly electron-withdrawing substituents, the catalytic efficiency is reduced. Cu(I) complex has two main configurations: tetrahedral and square planar – that can be formed either with a tetradentate ligand (*e.g.*, Me6-TREN) or two bidentate ligands (*e.g.*, bipyridine) in the cationic complexes, or with a tetradentate ligand in the neutral complex (*e.g.*, PMDETA). Usually, halides are used as counterions. However, there are other types of copper salts that can be exploited, for example, copper (II) triflate also promotes controlled polymerizations in the presence of PMDETA and Cu(0) [149]. The other roles of the ligand are to control solubility of metal salt in the reaction mixture to ensure stability of the complexes and, in some cases, to facilitate the removal of the catalyst. Only nitrogen ligands were considered, since they work well for copper-mediated ATRP. The choice of the initiator is also important as it should provide fast and quantitative initiation to form well-defined polymers. Generally alkyl halides are used as ATRP initiators.

ATRP of styrenic monomers

ATRP of styrene and its derivatives is carried out in the presence of copper, iron, ruthenium and other catalytic systems, though the copper-based systems are the most commonly used. The most extensively used condition for ATRP is the use of 1Eq. of Cu(I)X to 2 Eq. dinonylbipyridine (DNBP) in the presence of alkyl bromide as initiator at 110°C if X = Br or at 130°C if X = Cl. A more efficient catalyst PMDETA can be used to decrease the temperature to 80-90°C.

Among the advantages of ATRP can be named the following:

- Use of readily accessible and inexpensive catalyst components compared to NMP. Usually they are copper complexes with commercially available pyridine or aliphatic amines based ligands and commercially available or easily to prepare initiators;
- Broad range of monomers are successfully polymerized in diverse media: styrenes, (meth)acrylates, (meth)acrylamides, acrylonitrile;
- The halogen end groups can be displaced with other functionalities;
- Moderately sensitive to oxygen.

Limitations of ATRP:

- It is impossible to control the polymerization of acidic monomers, halogenated alkenes, vinyl esters, monomers containing ligands as functional moieties;
- The catalyst should be removed.

I.5.3.2. SET-LRP, or SARA ATRP

Various additives can influence the rate and control of ATRP. The rate of polymerization R_p can be formulated by the following equation [133]:

$$R_p = k_p \cdot K_{eq} \cdot [M] \cdot [R - X]_0 \cdot [M_t^n]/[X - M_t^{n+1}],$$

where k_p is the propagation constant, K_{eq} the equilibrium constant, [M] the monomer concentration, $[R\text{-}X]_0$ the initial concentration of initiator, $[M_t^n]$ the concentration of the lower oxidation state metal, and $[M_t^{n+1}]$ the concentration of the higher oxidation state metal. As it is can be concluded from the equation, the increased concentration of the higher oxidation state metal (deactivator) results in the decrease of the polymerization rate. The deactivator is necessary to control the polymerization, but its excessive formation slows down the polymerization. It is shown by Grimaldi *et al*. that small amount of Cu(0) added to styrene ATRP system increases the rate of polymerization keeping the control of PDI and molecular weight [150]. Consequently, the polymerization can be carried out with a reduced amount of catalyst. The polymerizations of methyl acrylate and styrene were studied further in the presence of Cu(I) with addition of Cu(0) and Cu(0) with addition of Cu(II) [150]. The addition of small amount of Cu(II) appeared to improve the control of polymerization [150, 151]. It was necessary to use dNbpy or PMDETA as ligand in order to use to solubilize Cu(I) and Cu(II) complexes and to maintain the equilibrium between the two species. The polymerization could be initiated by alkyl halide R-X in the presence of Cu(0) without the addition of Cu(I) or Cu(II), and the process was irreversible. Afterwards, the "nascent" Cu(I) species could start the CRP. Other zerovalent metals were mentioned [150]: for example, the addition of zerovalent iron powder to iron(II) was used to improve the polymerization rate.

Further study of zerovalent metals use in CLRP led to the development of ATRP and appearance of various names for similar reactions utilizing the same components. The polymerization with copper metal as metal catalyst is shortly described below, though the mechanism and name of this kind of polymerization is not well understood and is being debated [152, 153].

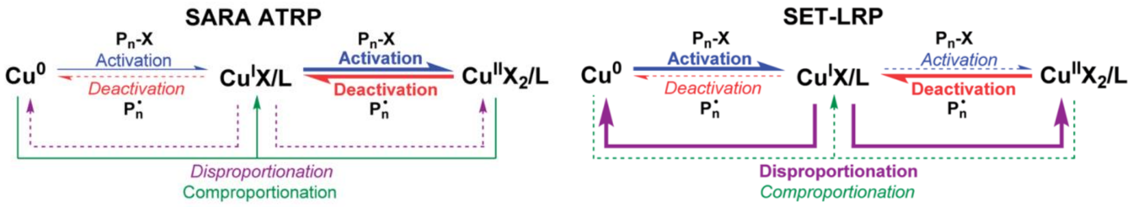
SARA ATRP
P_n-X
Activation
Cu^0
Deactivation
$P_n^\bullet$
Cu^IX/L
P_n-X
Activation
Deactivation
$P_n^\bullet$
$Cu^{II}X_2/L$
Disproportionation
Comproportionation
SET-LRP
P_n-X
Activation
Cu^0
Deactivation
$P_n^\bullet$
Cu^IX/L
P_n-X
Activation
Deactivation
$P_n^\bullet$
$Cu^{II}X_2/L$
Disproportionation
Comproportionation

Figure 43 | SARA ATRP and SET-LRP model mechanisms. Reprinted with permission from [153]. Copyright © 2014, Royal Society of Chemistry.

The key distinction consists in the different contribution of every component and various activation/deactivation steps (Figure 43). SARA ATRP model is based on the traditional ATRP reactions with an activation by Cu(I) and a deactivation by Cu(II) and where Cu(0) has a role of a supplemental activator of alkyl halides R-X and a reducing agent for Cu(II). Disproportionation of Cu(I) has a minimal contribution. In SET-LRP model Cu(0) is the only activator of alkyl halides and Cu(II) plays the role of deactivator, whereas Cu(I) undergoes permanent disproportionation to Cu(0) and Cu(II). Comproportionation of Cu(0) and Cu(II) has a minimal contribution.

Recent progress in the fields of monomer sequence control and compaction/folding of polymer coils into unimolecular structured object was briefly reviewed. Some bases of CRLP techniques were presented, since they are the main “tools” for the preparation of well-defined polymers. The application of the kinetic approach will be shown in Chapter II for the synthesis of sequence-controlled polymers with precisely positioned amino acid moieties. The synthesis of linear precursors with specific functional moieties, and placement of intramolecular bridges leading to the folding/compaction of single-polymer chains will be demonstrated in Chapters III and IV.

CHAPTER II. PRECISE POSITIONING OF AMINO ACID MOIETIES IN POLYMER CHAINS

II.1. INTRODUCTION. ORIGINS AND MAIN IDEA OF THE PROJECT

The purpose of this project consisted in the synthesis of sequence-controlled polymers with precisely positioned amino acid moieties. These polymers were used afterwards as tracks a molecular machine [10, 11] elaborated by Leigh group in Manchester. Our group had previously developed strategies [31] which allowed "writing information on polymer chains" and presented a simple way to position functional groups at any desired position in a macromolecule. Sequence-controlled polymers synthesized by this strategy required two main conditions: 1) the use of controlled/living radical polymerization techniques that provide the simultaneous growth of polymer chains and allow the synthesis of macromolecules with a narrow polydispersity and a predictable molecular weight; 2) donor-acceptor comonomer pairs leading to a fast cross-propagation. The copolymerization of styrene (donor monomer) with *N*-substituted maleimide (acceptor monomer) is investigated in non-stoichiometric conditions when a small amount of acceptor monomer (1 molar equivalent per chain) is added to an excess (40-100 molar equivalents) of donor monomer (Figure 44, **A**). Acceptor monomer is consumed rapidly compared to donor monomer, and the donor-acceptor copolymerization is kinetically favored in comparison with the donor homopolymerization. Consequently, *N*-substituted maleimides (acceptor monomer) is locally incorporated in the polystyrene chain forming functionalized maleimide regions. Thus, this strategy enables the formation of a broad range of polymers containing virtually any functional group. This is due to the diversity of *N*-substituted maleimides (commercially available or synthesized in a few steps [21]); and the possibility to incorporate these maleimides at any position in the polymer chain.

Although this straightforward approach is convenient to introduce functional moieties at any place in a polymer chain (chain-location), it has some drawbacks, since the microstructure from chain to chain is not identical. Two main inherent chain-to-chain deviations exist in this strategy. One of the deviations is connected with the precision of the maleimide placement in the polymer chain (Figure 44, **B I**). While a tiny amount of maleimide (1-3 molar equivalents) is polymerized, a comparatively higher amount of styrene is consumed. Thus, the incorporated maleimides along with styrene form a small region on the polymer chain. The maleimide placement (the probability to position maleimide at a determined place in a polymer chain) is indicated by a red bar on Figure 44, **A**. Another type of deviation is caused by statistical processes and recombination termination reactions leading to the not uniform distribution of maleimides in polymer chains (Figure 44, **B II**). It was demonstrated by MALDI-TOF-MS [21] that when one molar eq. of *N*-benzyl maleimide is added per polystyrene chain, the main type of observed polymers corresponded to one maleimide per polymer chain. However, the distributions corresponding to 0, 2, 3 and 4 incorporated maleimides per chain were also observed in MALDI-TOF spectra.

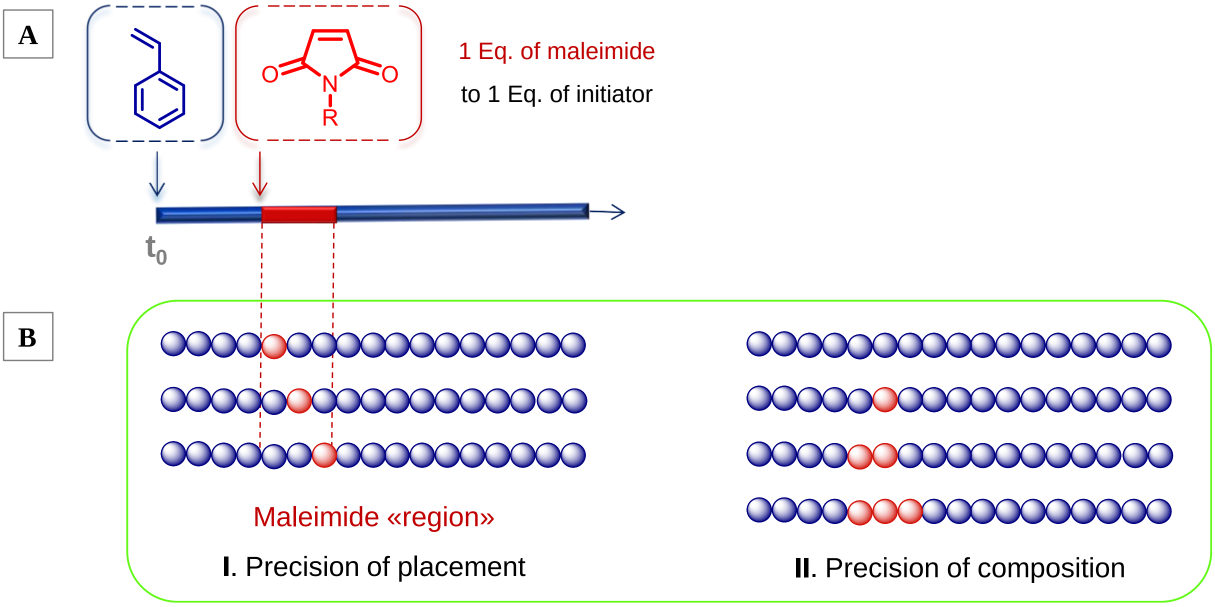

Figure 44 | (**A**) Schematic representation of the precise positioning of a small amount of *N*-functionalized maleimide in a polymer chain. (**B**) Two main types of chain-to-chain deviation.

Polymers with various functional moieties (dendrimers, monosacharides, pyrenyl-groups, and others) prepared with this strategy were mentioned in Chapter I.3.4. The present work consists in synthesizing polymers with precisely positioned amino acid moieties, performed in collaboration with the Leigh group in Manchester. The aim of this collaboration is to broaden this possibilities of the strategy and to demonstrate an alternative method for preparing peptides. Polymers carrying amino acid functional groups were used as a track with amino acid building blocks for sequence-specific peptide synthesis by a molecular machine [10, 11] described in details in Chapter I.3.4. This polymer track has some significant advantages compared to the one previously prepared by Leigh and co-workers [10, 11]. The polymer with amino acid building blocks being prepared in a one-step reaction and isolated by precipitation, the synthesis and purification are simplified and made in a shorter time. Moreover, the artificial small-molecule machine can be used to analyze chain-to-chain distribution of the prepared tracks. However, the analysis of the polymer with more than one positioned maleimide by MALDI-TOF-MS is challenging due to peaks overlapping.

The polymer track was connected with “a preformed rotaxane synthon” [10] that represents a rotaxane based small-molecule machine with a “reactive arm”, blocked on one side with a bulky tertiary group and on the other side by an amino acid building block (Figure 45). The rotaxane synthon contained a terminal azide group. The polymer was synthesized by ATRP in the presence of an alkyne-functionalized initiator, thus allowing further CuAAC “click” chemistry on the polymer chain. Afterwards, the rotaxane synthon and the polymer track were linked together using azide-alkyne Huisgen cycloaddition reaction [154, 155].

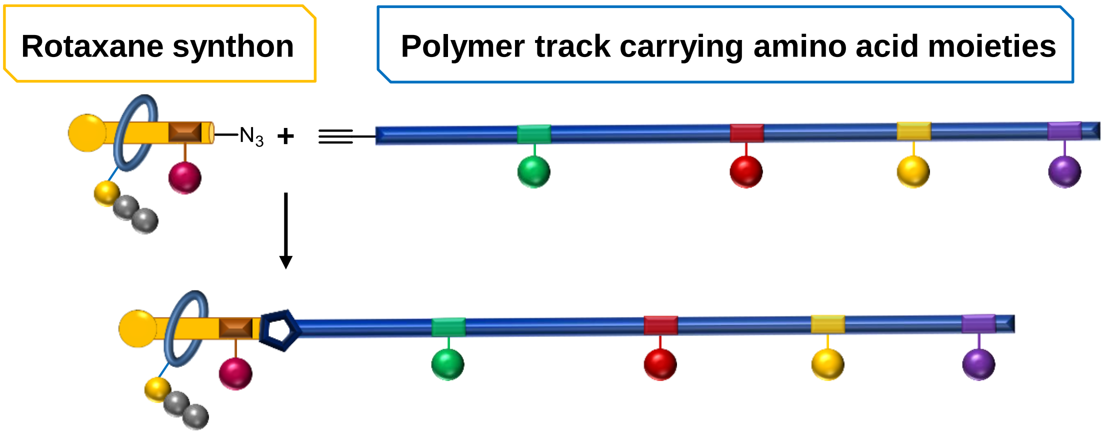

Figure 45 | Assembled molecular machine for a sequence-specific peptide synthesis based on the use of a polymer track connected to a rotaxane synthon.

Another condition that should be fulfilled to obtain an efficient molecular machine is the precise placement of amino acid residues into the polymer chain with a controlled distance between two maleimides containing amino acid moieties. Along with amino acid moieties, a strongly UV-active group was introduced as a terminal unit, allowing the monitoring of the molecular machine operating by UV-spectroscopy. A fluorenyl functional group was chosen as an UV-visible moiety due to the presence of a distinct band (around 310 nm) in the UV spectrum and the compatibility of this group with the polymerization conditions.

The main goal of this chapter is the synthesis and the characterization of sequence-controlled polymers with several precisely positioned amino acids and a terminal fluorenyl building block (Figure 46) by controlled radical polymerization of styrene with *N*-substituted maleimides containing amino acid moieties. First, the design and the synthesis of *N*-

functionalized maleimides possessing amino acid and fluorenyl substituents were performed. Afterwards, copolymers of styrene with *N*-functionalized maleimides were prepared by conventional (Chapter II.3) and recently developed ultra-precise [12] (Chapter II.4) strategies.

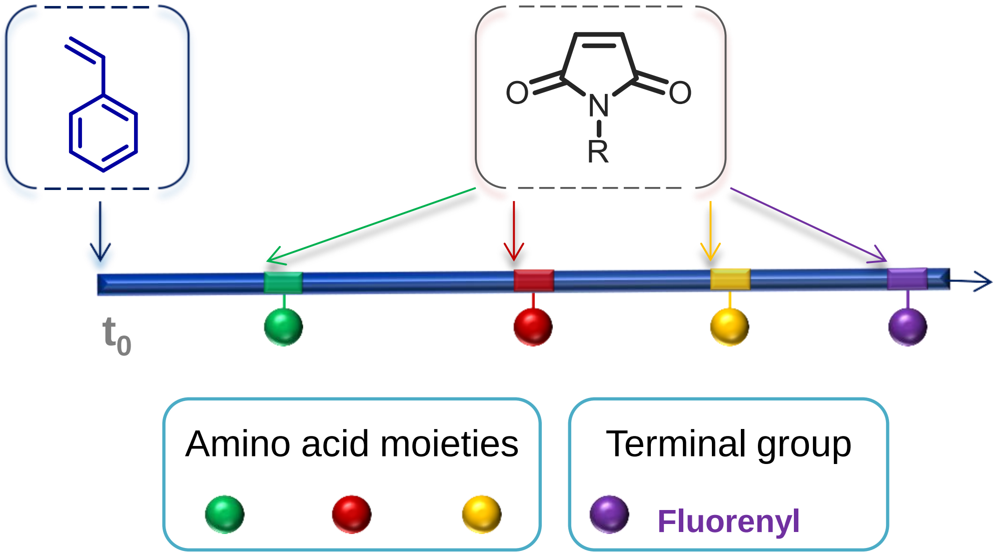

Figure 46 | Schematic representation of the sequence-defined polymer track with several precisely positioned amino acids and a terminal fluorenyl building block prepared by the CRP of styrene with *N*-functionalized maleimides.

II.2. DESIGN AND SYNTHESIS OF MALEIMIDES

Maleimides with amino acid moieties were specially designed in order to be incorporated in a polymer track as a part of the molecular machine of the Leigh group. Some necessary requirements had to be fulfilled concerning the maleimide design:

1. Amino acids should be connected to the maleimide by weak phenolic ester linkages.
2. The unloaded polymer track (polymer with maleimides without amino acid groups) has to go through the macrocycle to allow the molecular machine to operate, whereas the track with amino acid moieties must not go through the rotaxane macrocycle. The molecular machine rotaxane **RM** is presented on Figure 47. Spacers of different length connect the maleimide to the phenyl ester functional groups (Figure 47, **1**, **2** and **3**). If the maleimide is too stiff (Figure 47, **1**) or too large (Figure 47, **2**), the track cannot go through the macrocycle, and the molecular machine cannot “approach” the next amino acid group on the polymer track.

3. Amino acids should be *N*-Boc protected, since the machine starts operating after the deprotection of the amino acid moieties in acidic conditions.

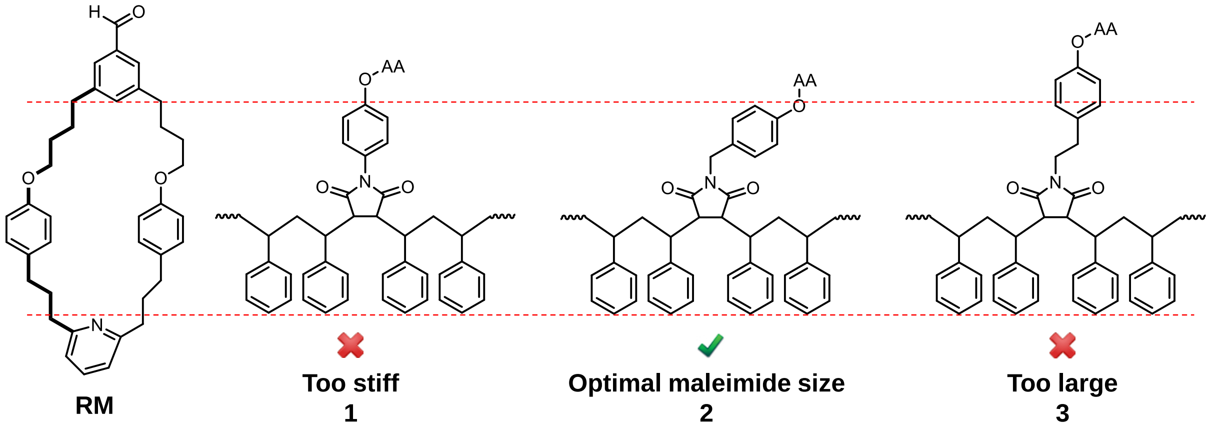

Figure 47 | Possible maleimide designs in comparison with the rotaxane macrocycle of the molecular machine (**RM**). AA – amino acid moiety. Confirmed by three-dimensional molecular models [156] by Leigh group.

N-functionalized maleimides with amino acid moieties were designed according to these requirements (Figure 48). Alanine, leucine, phenylalanine and *O*-methoxytyrosine were chosen as aliphatic and aromatic amino acids to perform the synthesis of sequence-specific peptides using the molecular machine.

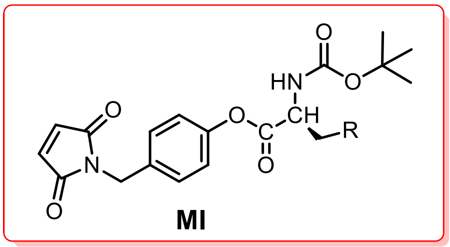

MI	R	Amino acid (AA)
II	-H	Alanine (Ala)
III	-CH(CH$_3$)$_2$	Leucine (Leu)
IV	-C$_6$H$_5$	Phenylalanine (Phe)
V	-C$_6$H$_4$-*p*-OCH$_3$	*O*-methoxytyrosine (*O*-Me Tyr)

Figure 48 | Maleimides (MI) **II-V** structure.

The most common way to prepare maleimide derivatives is the treatment of maleic anhydride with amines followed by a dehydration step [157-161]. The nucleophilic attack of the amine on maleic anhydride leads to the formation of maleanilic acid in mild conditions (Scheme 10, **a**). Then the dehydration of maleanilic acid (Scheme 10, **b**) occurs at high temperature and in the presence of either an excess of sodium acetate in acetic anhydride [157, 158], or hexamethyldisilazane and zinc bromide [159], or a catalytic amount of zinc acetate combined with the use of a Dean-Stark apparatus [160, 161]. As the dehydration of maleanilic acid by the closure of the maleimide cycle demands harsh conditions, it was decided to start with the synthesis of *N*-hydroxybenzyl maleimide **I** (Scheme 11) which was afterwards esterified with *N*-Boc protected amino acids (Scheme 14, Scheme 16).

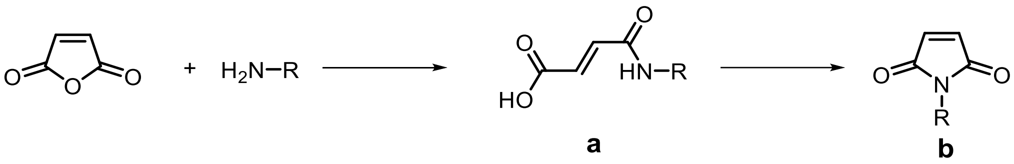

Scheme 10 | General scheme for the synthesis of *N*-substituted maleimide from maleic anhydride and an amine.

II.2.1. Synthesis of *N*-Hydroxybenzyl Maleimide I

N-hydroxybenzyl maleimide **I** was prepared in a two-step reaction (Scheme 11). Maleanilic acid **Ia** was synthesized by the addition of a solution of 4-(aminomethyl)phenol (1 Eq.) in ethyl acetate (AcOEt) to a solution of maleic anhydride (1.2 Eq.) in AcOEt at room temperature. A white precipitate of **Ia** started to form after 1 hour. The reaction was left to stir until the full consumption of 4-hydroxybenzylamine was reached as proved by NMR. The crude product was dissolved in AcOEt, and **Ia** was filtered off (maleic anhydride has a good solubility in AcOEt).

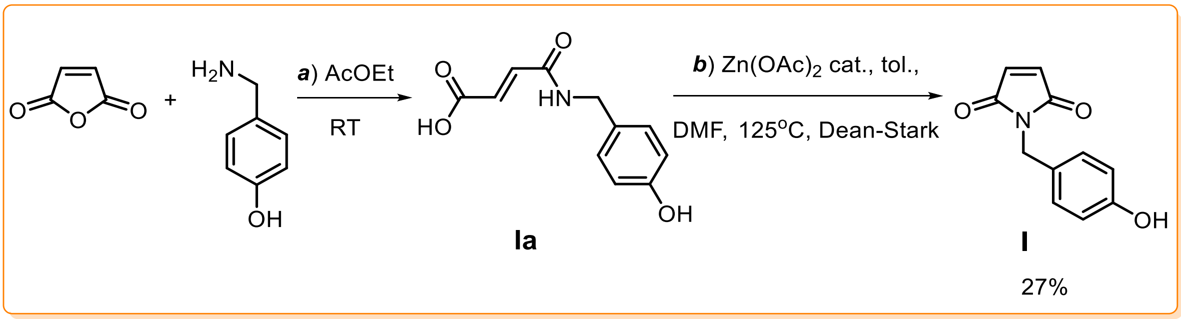

Scheme 11 | Synthesis of *N*-hydroxybenzyl maleimide (**I**). *Reaction conditions*: ***a***) maleic anhydride (1.2 Eq.), 4-hydroxybenzylamine (1 Eq.), AcOEt, RT, 10 hours; quantitative yield; ***b***) **Ia** (1 Eq.), $Zn(OAc)_2$ (0.04 Eq.), toluene/DMF = 10/1, 125°C, 12 hours; 27% yield.

The second step (dehydration of **Ia**) was performed in the presence of a catalytic amount of zinc acetate $Zn(OAc)_2$ in toluene at 125°C. Water was removed from the reaction mixture with a Dean-Stark apparatus. Sodium acetate in acetic anhydride and hexamethyldisilazane were not convenient reagents for this step, since they lead to by-products such as phenyl acetate or trimethylsilyl ether derivatives, respectively (Scheme 11). ESI mass and ^{1}H NMR spectra confirmed the presence of **I** in the reaction mixture after 12 hours (50% conversion). An increase of the reaction time or the temperature to 150ºC (solvent was changed to xylene) did not increase further the conversion. The purification was performed by column chromatography and led to **I** as a white crystalline solid with 27% yield over the two steps. **I** is soluble in methanol, ethyl acetate and chloroform.

The Mitsunobu reaction [162, 163] was also used as an alternative to prepare *N*-hydroxybenzyl maleimide **c** from maleimide **a** and 4-hydroxybenzyl alcohol **b** (Scheme 12). It should be emphasized that the order of the reactants addition was essential, and that the reaction took place with a reasonable conversion only when the procedure described by Walker [164] was followed. An excess of the alcohol **b** (1.5 Eq.) was added to the preformed betaine of Ph_3P (1 Eq.) and diethyl azodicarboxylate DEAD (1 Eq.) at -78ºC followed by the addition of maleimide **a** (1 Eq.). The yield was of 20%, probably due to a competitive reaction of the phenol function of the 4-hydroxybenzyl alcohol **b** with the maleimide.

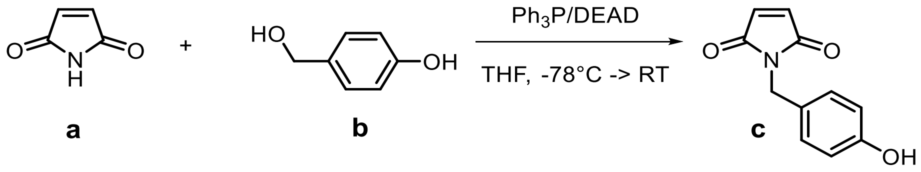

Scheme 12 | Synthesis of *N*-hydroxybenzyl maleimide (**c**) by the Mitsunobu reaction [164]. *Reaction conditions*: maleimide **a** (1 Eq.), 4-hydroxybenzyl alcohol **b** (1.5 Eq.), THF, -78°C → RT, 2 hours.

Consequently, the two methods previously described led to the formation of *N*-hydroxybenzyl maleimide **I** with a moderate yield. The reaction involving maleic anhydride and 4-hydroxybenzylamine (Scheme 11) was chosen for the scale-up, since the reactants were cheaper, and the isolation of the product was easier than for the Mitsunobu reaction.

II.2.2. Synthesis of *N*-Substituted Maleimides II-V

Two main strategies were found for the synthesis of *N*-substituted maleimides **II-V** (Figure 48) including the esterification of *N*-hydroxybenzyl maleimide **I** either with corresponding *N*-

Boc protected amino acids using bromo(tri-1-pyrrolidinyl)phosphonium hexafluorophosphate PyBroP as a coupling agent (Scheme 14), or with a symmetric anhydride of the corresponding *N*-Boc protected amino acids (Scheme 16). The unsuccessful trials will be presented first.

Compound **I** (Scheme 13) consists of a maleimide with strongly electron accepting properties linked to a phenol with weakly acidic properties due to the resonance stabilization of the phenoxide anion by the aromatic ring. Although there is a methylene spacer between the maleimide and the phenol, the presence of an electron acceptor moiety (maleimide) made the esterification of *N*-hydroxybenzyl maleimide (**I**) with amino acids more difficult compared to phenol. Several conditions for the esterification of **I** with *N*-Boc-protected leucine (**AAIII**) to form **III** are presented on Scheme 13. The conditions for the esterification were adapted from literature [165-169]. However, these conditions did not lead to the formation of compound **III**, or the reaction was too low (Scheme 13, conditions ***a.***-***b.***).

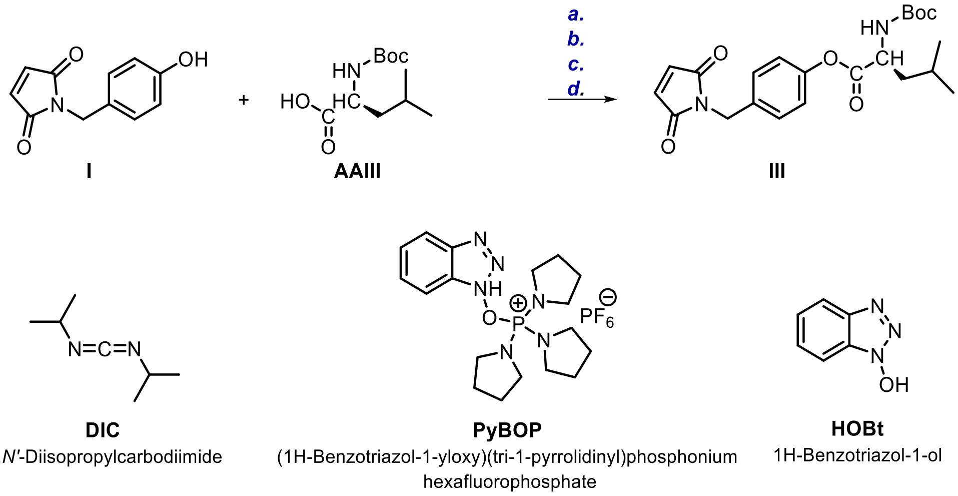
a.
b.
c.
d.
I
AAIII
III
OH
HN
Boc
HO
HC
CH
N
O
DIC
N,N'-Diisopropylcarbodiimide
PyBOP
(1H-Benzotriazol-1-yloxy)(tri-1-pyrrolidinyl)phosphonium hexafluorophosphate
PF6
HOBt
1H-Benzotriazol-1-ol

Scheme 13 | Unsuccessful trials to synthesize maleimide **III** by the esterification of *N*-hydroxybenzyl maleimide **I** with *N*-Boc-protected leucine (**AAIII**). *Reaction conditions*: **I** (1 Eq.), **AAIII** (1.1 Eq.), RT, ***a***). DIC (1.2 Eq.), DMAP (10 % mol.), CH_2Cl_2, DMF, 0°C → RT; ***b***). HOBt (1.1 Eq.), PyBOP (1.1 Eq.), DIPEA (2 Eq.), CH_2Cl_2, DMF, RT; ***c***). PyBOP (1.5 Eq.), DIPEA (3 Eq.), CH_2Cl_2, DMF, RT; ***d***). HOBt (1.1 Eq.), DIC (1.2 Eq.), CH_2Cl_2, DMF, RT.

The use of a phosphonium coupling reagent PyBroP led to the desired maleimide **III** with good yield (Scheme 14). The addition of *N*,*N*-diisopropylethylamine (DIPEA) to the solution of **I** and **AAIII** in CH_2Cl_2/DMF followed by a slow addition of PyBroP led to maleimide **III** with the highest yield among all the tested conditions (37% yield after purification by column chromatography).

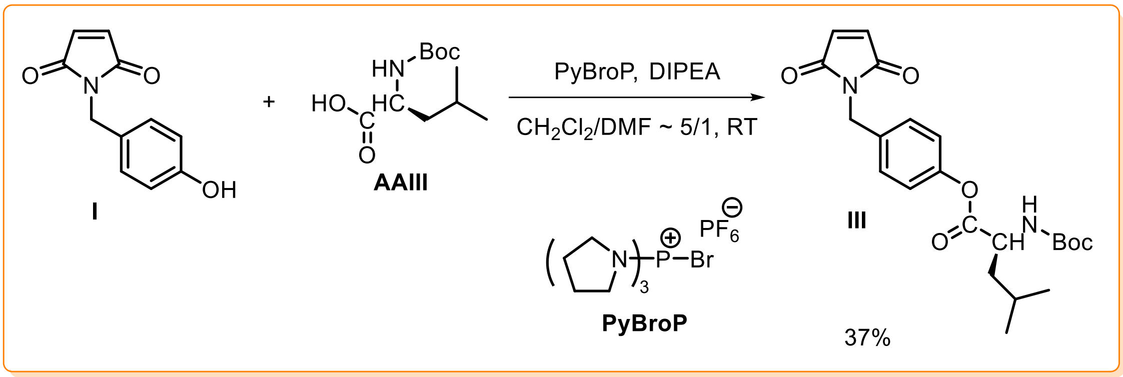

Scheme 14 | Synthesis of the maleimide **III** by esterification of *N*-hydroxybenzyl maleimide **I** with *N*-Boc protected leucine **AAIII**. *Reaction conditions*: **I** (1 Eq.), *N*-Boc-leucine **AAIII** (1.3 Eq.), PyBroP (1.4 Eq.), DIPEA (3 Eq.), CH_2Cl_2/DMF ~ 5/1, RT, 1 day.

PyBroP is usually used for “difficult” couplings of amino acids with weakly nucleophilic and secondary amines [167, 168, 170]. A possible mechanism for the amino acid activation by PyBroP is presented in Scheme 15 [170].

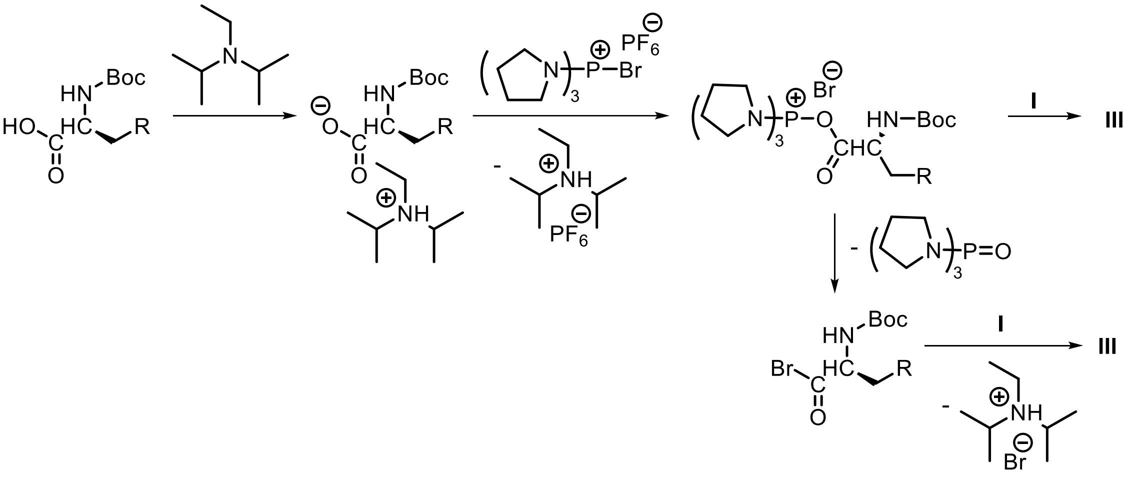

Scheme 15 | A possible mechanism of an amino acid activation by PyBroP [170].

Another way to activate carboxylic acids is to prepare symmetric anhydrides using *N*,*N'*-dicyclohexylcarbodiimide (DCC) [166, 169]. The successful formation of symmetric anhydride **SAIII** (Scheme 16) of amino acid **AAIII** was confirmed by mass spectrometry. **I** was deprotonated by DIPEA and added to the *in situ* formed symmetric anhydride **SAIII** leading to maleimide **III** (Scheme 16). **III** was obtained as a yellowish powder with 48 % yield after purification by column chromatography.

Maleimides **II**, **IV** and **V** were also prepared by the esterification of **I** with the *in situ* formed corresponding symmetric anhydrides **SAII**, **SAIV** and **SAV** (Scheme 16). This method permitted the use of cheaper reagents and slight increase the overall yield, compared to the esterification in the presence of PyBroP.

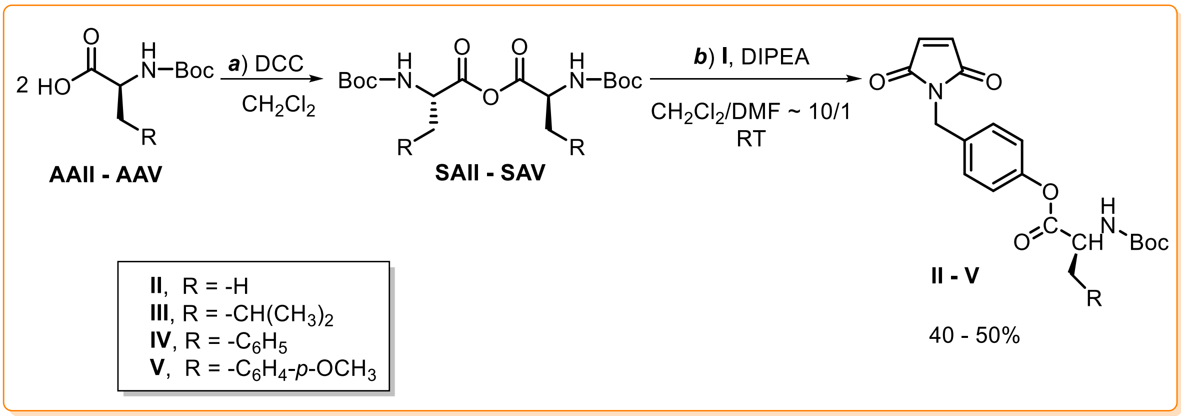

Scheme 16 | Synthesis of maleimides **II** to **V** by esterification of *N*-hydroxybenzyl maleimide **I** with the *in situ* formed corresponding symmetric anhydrides **SA** of amino acids **AA**. *Reaction conditions*: ***a***) **AA** (2.3 Eq.), DCC (1.15 Eq.), CH_2Cl_2, 0ºC → RT, 2 hours; ***b***). **I** (1 Eq.), DIPEA (2 Eq.), CH_2Cl_2/DMF ~ 10/1, RT, 1 day; 40-50% yield over the 2 steps.

II.2.3. Synthesis of the Maleimide with Fluorenyl Moiety VI

Another possibility to esterify a phenol with a carboxylic acid is *via* the nucleophilic acyl substitution (*O*-acylation) of the hydroxyl function of the phenol with an acyl chloride derivative. Acyl chlorides are extremely reactive, and their reaction with phenol is fast and irreversible. Oxalyl chloride [171] was chosen to prepare fluorenyl methyl acyl chloride (Scheme 17). The excess of oxalyl chloride and the side products could easily be removed under vacuum from the reaction mixture. Thus, the maleimide with a fluorenyl moiety **VI** was synthesized by esterification of *N*-hydroxybenzyl maleimide **I** with fluorenyl methyl acyl chloride by a 2 step-procedure, starting from fluorenyl methyl carboxylic acid (Scheme 17). After purification by column chromatography, the maleimide **VI** was obtained with a 80% yield.

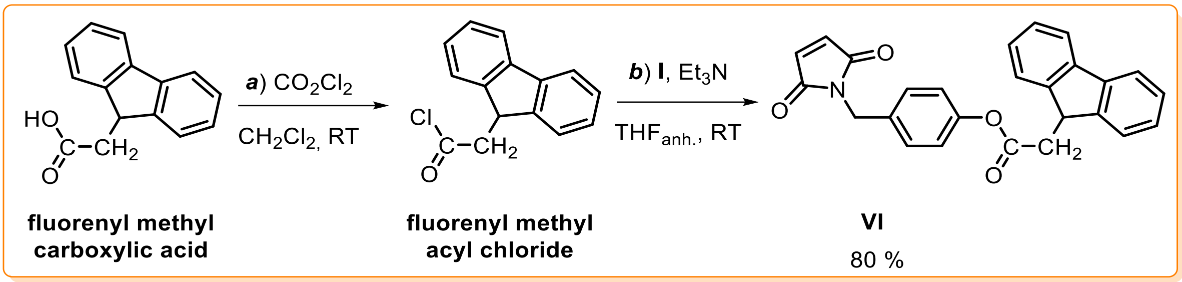

Scheme 17 | Synthesis of maleimide **VI** by esterification of *N*-hydroxybenzyl maleimide **I** with fluorenyl methyl acyl chloride. *Reaction conditions*: ***a***) fluorenyl methyl carboxylic acid (1 Eq.), oxalyl chloride CO_2Cl_2 (5 Eq.), CH_2Cl_2, RT, 3 hours; ***b***) fluorenyl methyl acyl chloride (1.2 Eq.), **I** (1 Eq.), Et_3N (2 Eq.), THF anhydrous, RT, 5 hours.

II.3. SYNTHESIS OF SEQUENCE-CONTROLLED POLYMERS USING A CONVENTIONAL STRATEGY

After the successful synthesis of maleimides with amino acid and fluorenyl moieties **II-VI**, the project was continued with the conventional copolymerization of styrene with the maleimides by ATRP. First, the optimization of the reaction by ATRP was investigated and an alkyne functional initiator was synthesized. Afterwards, the positioning of a single amino acid moiety in the polymer chain was realized. Lastly, polymers with several amino acid sites were synthesized by a conventional strategy (*i.e.*, adding all styrenic monomer at the beginning of polymerization).

II.3.1. Conditions for ATRP

A straightforward and convenient methodology to introduce a terminal alkyne functional group into a polymer chain was reported by Opsteen and Hest [172, 173] *via* ATRP and with an alkyne-functionalized initiator (**VII**, Scheme 18). The alkyne function of this initiator was protected with a trimethylsilyl group to avoid the possible complexation of the alkyne with the copper catalyst during the polymerization reaction.

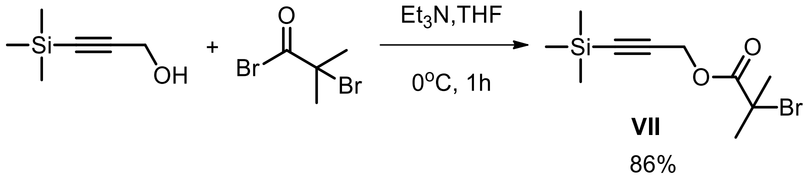

Scheme 18 | Synthesis of the alkyne-functionalized initiator **VII** [173]. *Reaction conditions*: 2-bromoisobutyryl bromide (1.5 Eq.), 3-trimethylsilyl-2-propyn-1-ol (1 Eq.), Et_3N (1.5 Eq.), THF, 0°C → RT, 1 hour; 27% yield.

The ATRP of styrene was performed in the presence of **VII** as initiator and Cu(I)Br / *N*,*N*,*N′*,*N′*,*N″*-pentamethyldiethylenetriamine (PMDETA) as metal catalyst (Scheme 19). As previously described (Chapter I.5.3.1.), Cu(I)Br is a widely used metal salt for the ATRP of styrene [133]. PMDETA is a linear triamine, which has successfully been used as a ligand for ATRP [133, 148, 174] due to several advantages such as a high activity and a low cost. An interesting feature of PMDETA is that it solubilizes only partially Cu(I)Br [175] in contrast to DNBP which solubilizes Cu(I)Br much better. The solubility of Cu(I)Br/PMDETA is much better than $Cu(II)Br_2$/PMDETA since insoluble complex networks are formed in the latter case. Such heterogeneous ATRP allows the easier removal of $CuBr_2$ from the polymers by filtration.

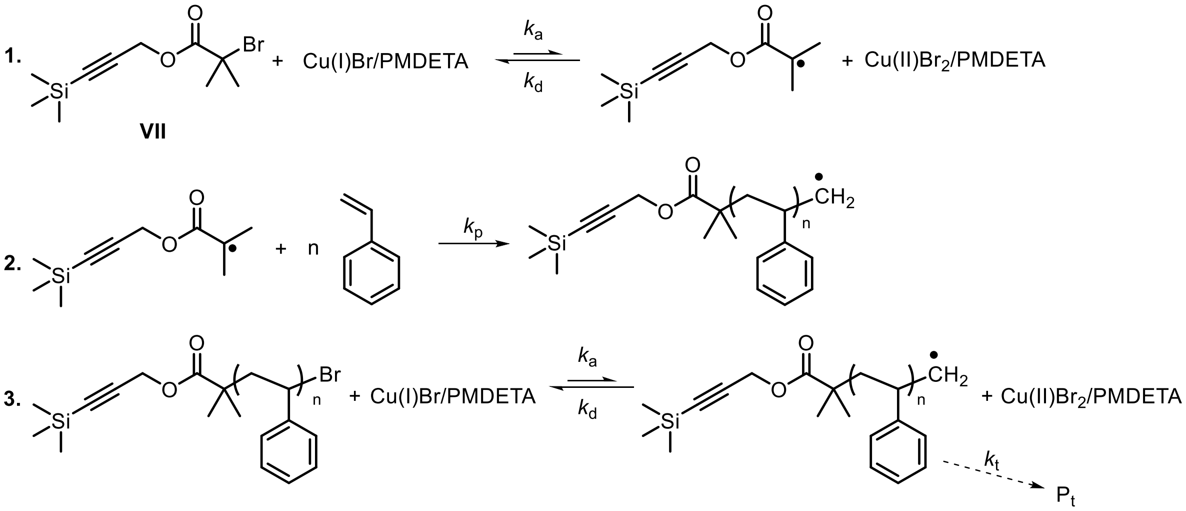

Scheme 19 | ATRP of styrene in the presence of alkyne-functionalized initiator **VII** and Cu(I)Br/PMDETA. **1**. Initiation, **2**. Propagation reaction, **3**. Equilibrium with dormant species and termination reaction; k_a – activation constant, k_d – deactivation constant, k_p – propagation constant, k_t – termination constant; P_t – products of termination reaction.

The conditions for the ATRP of styrene were adapted from the literature [172-174]. After several optimizations (Table 5, **P1** to **P6**), a 1 to 1 molar ratio of metal salt (CuBr) to ligand (PMDETA) was chosen for the polymerization in bulk at 90ºC, leading to the rapid ATRP of styrene (70% of conversion in around two hours) and had a living character according to the narrow molecular weight distribution (M_w/M_n) and the linear dependence of logarithmic monomer concentration as a function of time (Figure 85 - Figure 90).

II.3.2. Positioning of a Single Amino Acid Moiety in Polymer Chains

An amino acid moiety was placed in a polymer chain by copolymerization of a comparatively high amount (40 molar eq.) of styrene with a tiny amount (1 molar eq.) of maleimide **II**, **III** or **IV** (Figure 48), added at a definite reaction time. The kinetics of copolymerization of styrene with **II**, **III** or **IV** positioned once in the polymer chain were investigated, based on ^{1}H NMR spectra (Table 1). The maleimide conversion was calculated by two methods: 1) by integration of the ^{1}H NMR signal of **II**, **III** and **IV** (4.62-4.65 ppm, methylene group –N-CH_2- conjugated with maleimide function); or 2) by the comparison of the integrations of a monomer signal and a malemide signal that was incorporated in the polymer chain (4.38-4.45 ppm, methylene group –N-CH_2-). The polymerizations were stopped at around 70% of styrene conversion leading to polymers **P7** to **P12** with 30 styrene units in average after precipitation and with rather narrow molecular weight distributions (M_w/M_n around 1.2). The results are given in Table 1.

The reactivity ratio of styrene r_s for the copolymers **P7** to **P12** was determined by the simplified equation proposed by Jaacks [176]:

$$\ln[M_S]_t / \ln[M_S]_0 = r_S \cdot \ln[M_{MI}]_t / \ln[M_{MI}]_0,$$

where $[M_S]_0$ and $[M_{MI}]_0$ - initial concentrations of the styrene and of the maleimide; $[M_S]_t$ and $[M_{MI}]_t$ – concentration of the unreacted styrene and maleimide at each moment of polymerization, respectively; r_S – reactivity ratio of styrene (propagation constant of the growing polymer chain containing a terminal styrene unit with styrene divided by propagation constant of the growing polymer chain containing a terminal styrene unit with maleimide).

Consequently, the value of the reactivity ratio of styrene can be found as a slope of the logarithmic plot of styrene monomer conversion *versus* the maleimide monomer conversion. The Jaacks equation is based on two hypotheses: a large excess of a monomer should be used during the copolymerization which should be able to homopolymerize. Both conditions were fulfilled for the copolymerization of styrene with the maleimide **II-IV**. The calculated value of the reactivity ratio for styrene r_S for all the copolymerizations was close to zero (r_S was around 0.01-0.03, Table 6) that indicated that the copolymerization of styrene with maleimide was favored to the homopolymerization of styrene. The obtained r_S is comparable to the reactivity ratio values for similar comonomer pairs found in the literature [177]. For instance, for the system styrene – *N*-benzylmaleimide $r_S = 0.058$ and $r_{MI} = 0.013$.

Table 1 | ATRP copolymerization of styrene with the maleimides **II** to **IV** positioned once in the polymer chain.

P	MI	Conv.$_S$, % (Time, min)^1			DP$_n$^{2}	*MI region*^{3}	M_n^{4}, g·mol^{-1}	M_{theo}^{5}, g·mol^{-1}	M_w/M_n^{4}
		Add.$^{1a)}$	Cons.$^{1b)}$	End$^{1c)}$					
7	**II**	0 (0)	21 (12)	63 (105)	25	8	3600	3280	1.19
8	**II**	57 (100)	66 (122)	69 (135)	28	3	4210	3530	1.28
9	**III**	0 (0)	21 (7)	68 (85)	27	7	3720	3530	1.19
10	**III**	41 (45)	51 (125)	67 (300)	27	4	4280	3420	1.15
11	**IV**	0 (0)	21 (25)	76 (180)	30	8	5000	3890	1.13
12	**IV**	69 (95)	76 (110)	79 (120)	32	2	4020	4020	1.20

Conditions: styrene (S) (40 Eq.), maleimide (MI) **II-IV** (1 Eq.), Cu(I)Br (1 Eq.), PMDETA (1 Eq.), bulk, 90ºC. ^{1}Conversion of styrene (corresponding time) $^{a)}$ when MI was added; $^{b)}$ when MI was consumed; $^{c)}$ at the end of polymerization. The conversions were calculated from ^{1}H NMR spectra. ^{2}DP$_n$ – degree of polymerization. ^{3}The number of styrene units in *Maleimide MI region* was calculated as: (Conv.$_{S\ Cons.}$ – Conv. $_{S\ Add.}$)/100% · Eq. of styrene. ^{4}Estimated from SEC in THF. $^5M_{theo} = M_{VII} + M_S\cdot conv._S\cdot[S]/[\mathbf{VII}] + M_{MI}\cdot[S]/[\mathbf{VII}]$.

Maleimides were added either at the beginning of polymerization (Table 1, **P7**, **P9** and **P11**), or close to the end (Table 1, **P8**, **P10** and **P12**). The maleimide consumption during copolymerization with styrene was investigated based on kinetic data (Figure 91 - Figure 94 in exp. part, Table 1) and was characterized by the number of styrene units positioned along a maleimide unit (Table 1, *Maleimide region*). The number of styrene units in the *Maleimide* *region* was calculated as the difference between conversion of styrene when maleimide was consumed and conversion of styrene when maleimide was added, multiplied by the initial number of mol. eq. of styrene, using the following formula: $(\text{Conv.}_{\text{S Cons.}} - \text{Conv.}_{\text{S add.}})/100\% \cdot 40$. Kinetic monitoring proved that the maleimide was incorporated in the growing chains in a relatively broad region, if the insertion was performed at the beginning of the reaction (Table 1, *Maleimide region* for **P7**, **P9** and **P11**). However, this region became much narrower when maleimide was added at latter stage of polymerization (Table 1, *Maleimide region* for **P8**, **P10** and **P12**). This can be explained by a lower ratio of styrene (donor monomer) to maleimide (acceptor monomer) in the reaction mixture, and therefore, a higher probability of maleimide consumption. Thus, the precision of maleimide positioning is maximized when it is added at high styrene conversion.

The semi-logarithmic plots of comonomer conversions *versus* time and the microstructures of the sequence-controlled polymers obtained by the ATRP of styrene with maleimide IV are presented in Figure 49. Any addition of **IV** at the beginning of the polymerization led to the formation of a broad statistical region of maleimide with styrene (Figure 49, **A**). The maleimide was placed in a narrower region of the polymer chain when it was introduced at high conversion (*i.e.*, 70% of styrene) (Figure 49, **B**). A rapid consumption of maleimide **IV** compared to styrene was observed in both cases.

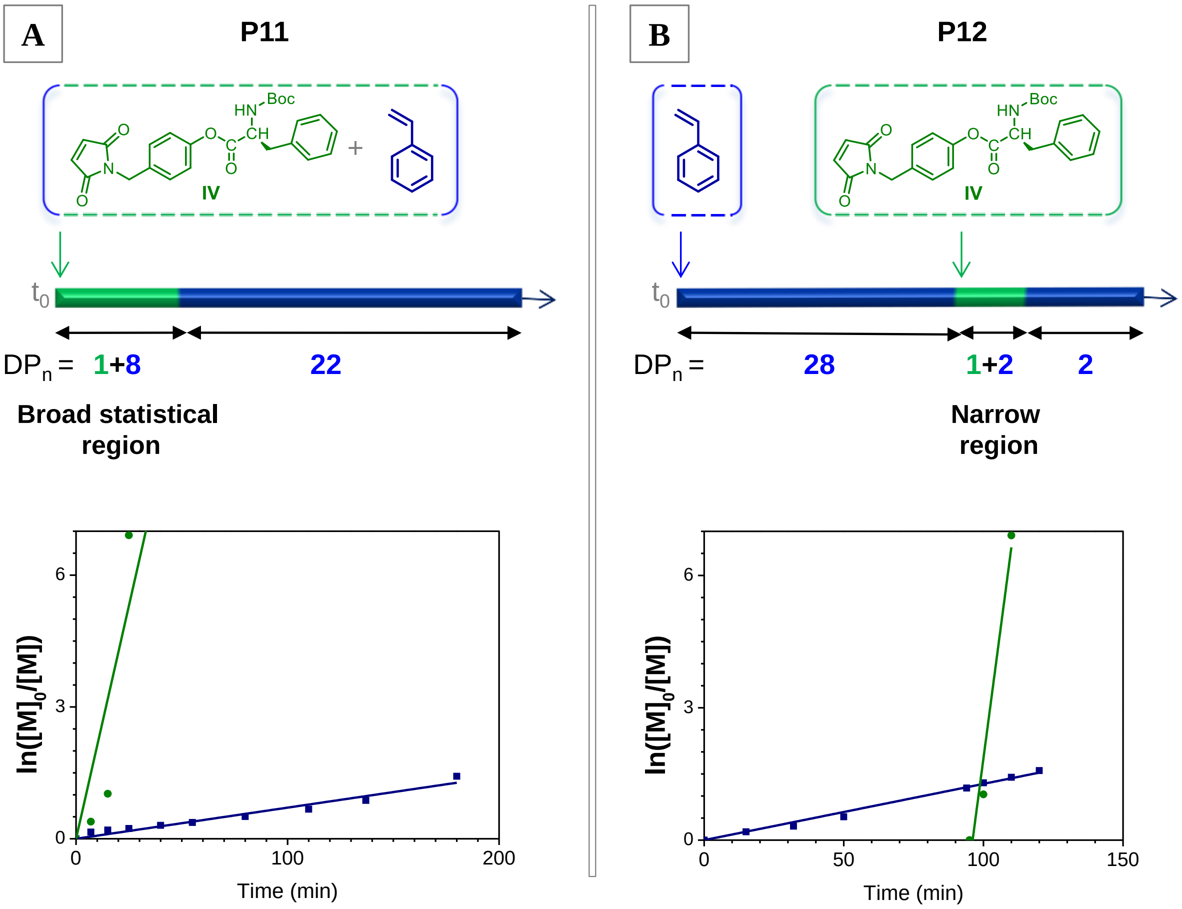

Figure 49 | Probable microstructures and corresponding semi-logarithmic plots of comonomer conversions in function of time recorded for sequence-controlled polymers synthesized by the ATRP of styrene with maleimide **IV** (**A**, **P11**) added at the beginning of the polymer chain and (**B**, **P12**) at the end of polymerization.

The maleimide consumption was monitored by SEC in THF during all polymerization reactions. The evolution of chromatograms (before maleimide addition, after partial incorporation of maleimides into the growing polymer chains and after full maleimide consumption) is presented for **P11** (Figure 50, **A**) and **P12** (Figure 50, **B**). Maleimides were incorporated in the polystyrene chains and did not lead to side growing chains as proved by the monomodal distributions measured by SEC, and the absence of shoulders after maleimide consumption. The conversions of styrene at the indicated times of the polymerization are given in the legends of Figure 50. Polymers isolated by precipitation have monomodal distributions (Figure 50, black line). However, polymer **P12** has a shoulder on the chromatogram that appears most probably due to combination termination reactions at high styrene conversion (around 80 %).

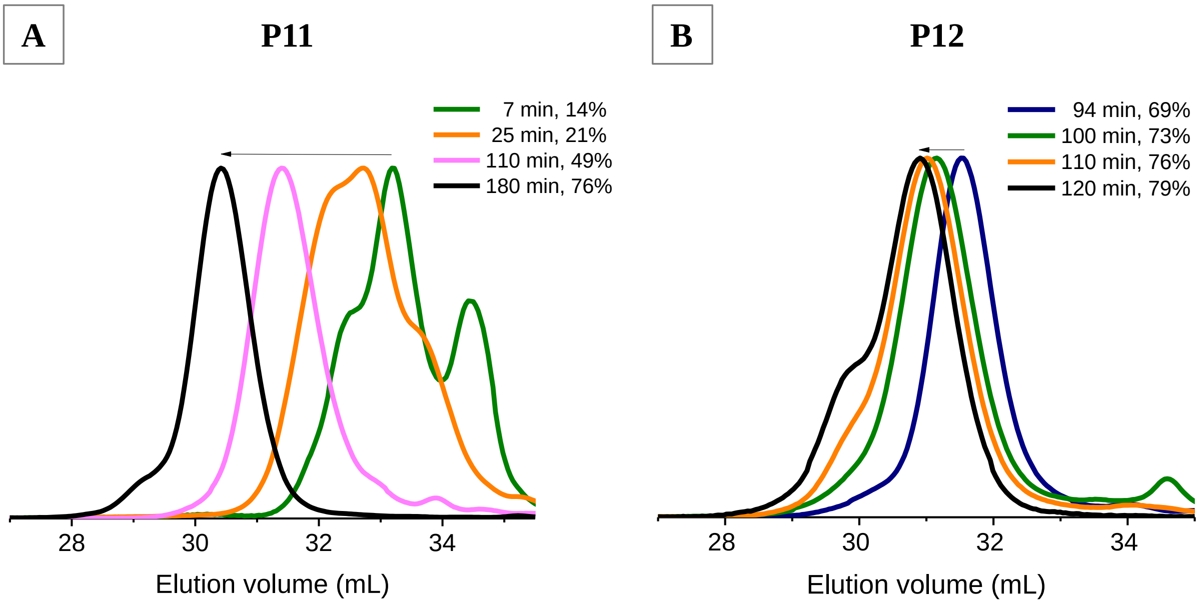

Figure 50 | Evolution of the size exclusion chromatograms of polymers carrying an amino acid moiety, in THF. (**A**) SEC data for **P11** (with phenylalanine precisely positioned at the beginning of polymer chain) before maleimide addition (blue line), after partial incorporation of maleimides (green line), after full maleimide consumption (orange line) and for the purified polymer (black line). (**B**) SEC data for **P12** (with phenylalanine precisely positioned at the end of polymer chain) after partial incorporation of maleimides (green line), after full maleimide consumption (orange line) and for the purified polymer (black line).

Polymers were analyzed by MALDI-TOF spectroscopy. Spectra for **P10** and **P11** are presented in Figure 137, Figure 138 (Annex). The amine group from **P10** was deprotected (*i.e.*, Boc-group removed from leucine moiety), since the maleimide unit **III** (with Boc group) has the same molecular weight as 4 styrene units. The MALDI-TOF results evidenced the presence of polystyrenes containing 1 and 2 maleimide units, although a small amount of polystyrenes without maleimide was also detected. However, the spectrum was too complex to extract more information from it.

The incorporation of maleimides **II-IV** to obtain polymers **P7-P12** was confirmed by ^{1}H NMR spectroscopy. NMR spectrum of **P12** with maleimide **IV** placed at the end of the polymer chain is presented in Figure 51. The characteristic signals of the incorporated maleimide **IV** in **P12** are located at 5.16 ppm (-NH-proton ***a***), 4.88 ppm (methine proton ***b***), 4.48 ppm (methylene protons ***c***), and 3.29 ppm (methylene protons ***d***); the signals of the initiator can be found at 1.04 ppm (***e***) and 0.25 ppm (***f***). An average of one maleimide unit was placed per polymer chain according to NMR spectrum (Figure 125 - Figure 130, Annex).

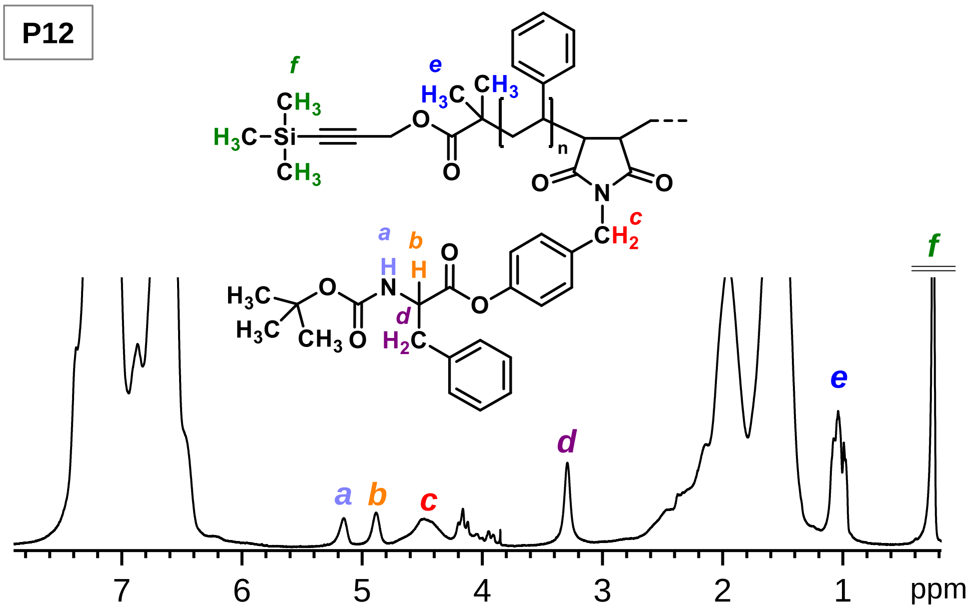

Figure 51 | ^{1}H NMR spectrum of **P12** (similar to **P11**) with phenylalanine moiety, in $CDCl_3$.

II.3.3. Insertion of Several Maleimide Units into a Polymer Chain

The atom transfer radical copolymerization of styrene with a model monomer *N*-benzyl maleimide was first examined to determine the main kinetic parameters and the influence of the maleimide additions on kinetics. Several copolymers with two MI-Bz positioned per polymer chain were synthesized (**P13** to **P15**, Figure 95 - Figure 97 in exp. part), and had quite narrow polydispersity (PDI 1.22) and monomodal chromatograms. The addition of maleimide slowed down the polymerization, due to addition of the maleimide in an anisole solution that led to a dilution of the system, and decreased the concentration of propagating species.

Two and three maleimides with amino acid moieties were introduced at higher styrene conversion. These results are illustrated on two examples: 1) **P16** was prepared by the ATRP of styrene with maleimides **III** and **IV** that were positioned close to the polymer chain end (⅔ of the polymer chain length) and in the end of the polymer chain (Figure 52, **A**); 2) **P17** was prepared by the ATRP of styrene with maleimide **III** introduced three times (Figure 52, **B**).

The kinetic monitoring of the maleimide incorporation confirmed the more precise placement of maleimides at high styrene conversions. Polymerizations were stopped at around 60% of styrene conversion to minimize the side termination reactions. Isolated polymers had controlled molecular weights in agreement with the theoretical predictions (M_n 4160 g·mol^{-1} for **P16** and M_n 3800 g·mol^{-1} for **P17**), and monomodal chromatograms were obtained without shoulders (Figure 98, in exp. part).

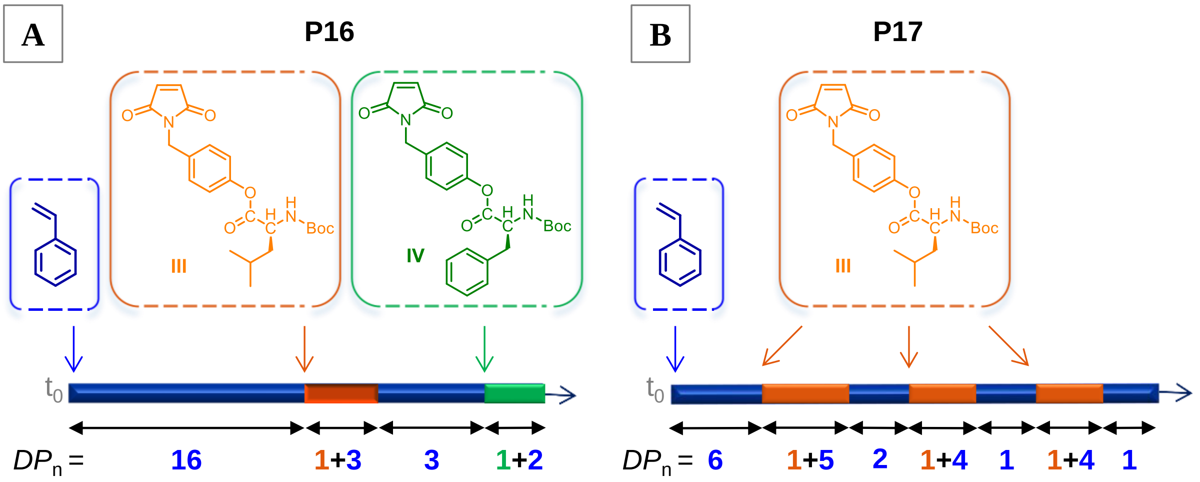

Figure 52 | Synthesis of sequence-controlled polymers **P16** and **P17**. Semi-logarithmic plots of comonomer conversions *versus* time and probable microstructures for (**A**) **P16** and (**B**) **P17**.

The possibility to introduce four maleimide units at different positions in a polymer chain is illustrated on **P18** (Figure 53). The ATRP of styrene (40 Eq.) with MI-Bz (4 additions of 1 Eq.) was stopped at 80% of styrene conversion corresponding to an average of 32 units of styrene per polymer chain. Although 3 insertions performed at higher conversion of styrene led to a more precise insertion of maleimides, the maleimide added at the beginning of polymerization formed as expected a broad statistical region (they were accompanied by 8 styrene units) (Figure 53, **B**). Moreover, the last three maleimides were separated only by 3 and 2 styrene units. As it was mentioned before, amino acid moieties (and therefore maleimides) should be positioned at some distance from each other. Consequently, maleimides should be inserted at the end of the polymer chain in order to obtain a placement as precise as possible. However, this is impossible without intersecting the maleimide zones and positioning maleimides close to each other. Therefore, a strategy leading to more precise placement of maleimides in a polymer chain was developed that will be described in the next subchapter. This strategy was named "Ultra-precise insertion of functional monomers in chain-growth polymerizations" [12].

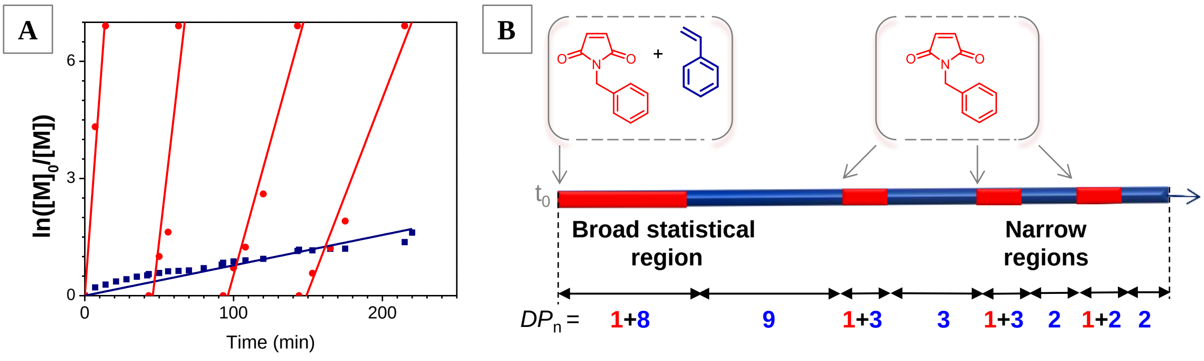

Figure 53 | (**A**) Semi-logarithmic plot of comonomer conversions *versus* time and (**B**) probable microstructure for **P18**.

II.4. SYNTHESIS OF SEQUENCE-CONTROLLED POLYMERS USING ULTRA-PRECISE METHODOLOGY

II.4.1. Origins and Main Features of the Ultra-Precise Methodology

It was demonstrated on several examples that the introduction of maleimide in a polystyrene chain at the latter stage of polymerization led to a narrow sequence distribution in the maleimide region (styrene conversion higher than 60%). Since the polymerization has a living character, styrene can be added to the growing polymer chains after the consumption of the first maleimide. When styrene reaches high conversion (> 60%), the second maleimide is inserted in the polymerization media. This can be repeated at least several times in a single polymerization. Thereby, instead of adding the whole amount of styrene at the beginning of polymerization like in the conventional approach, polymerization is started with a small amount of styrene followed by the insertion of small feeds of maleimide and styrene (Figure 54). Since each addition of acceptor monomer is performed at high conversion of donor monomer with a low donor/acceptor ratio in the polymerization medium and since the acceptor is consumed more rapidly compared to the donor monomer, a narrow sequence distribution containing in average 1-2 styrene (S) units for 1 unit of maleimide (MI) is formed. Taking into consideration the uncertainty of the maleimide (MI) positioning, several short sequences are formed in a polystyrene chain: S-S-MI, S-MI-S and MI-S-S. By combining the characteristic features and advantages of controlled radical polymerization (simultaneous growth of polymer chains and minimization of termination reactions), kinetic control (use of donor and acceptor comonomer pair) and the ultra-precise method, a precise placement of functional groups can be realized at any position in the polymer chain.

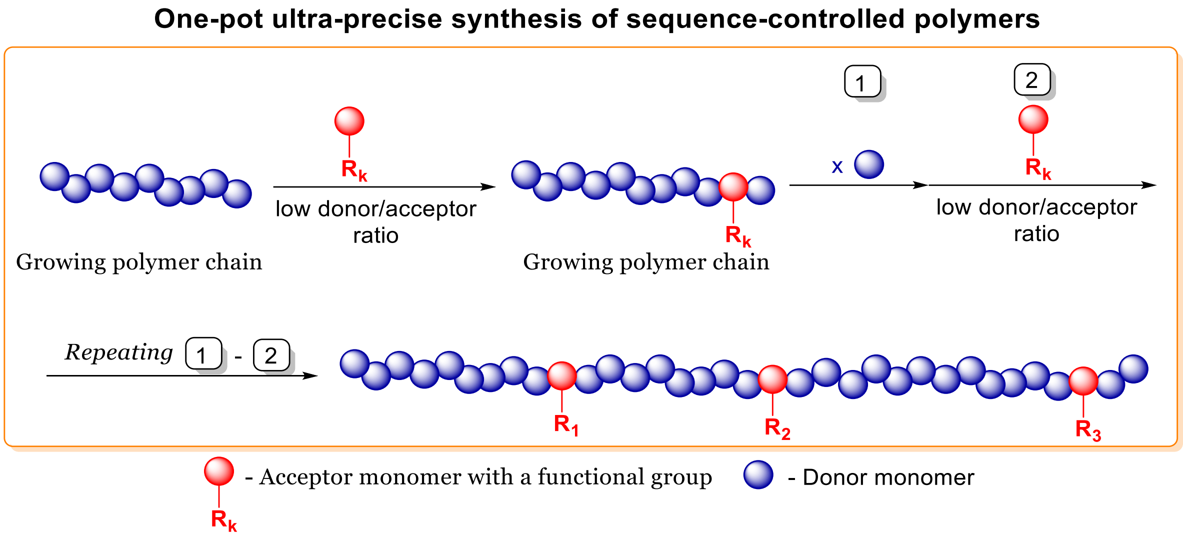
One-pot ultra-precise synthesis of sequence-controlled polymers

Growing polymer chain
R_k
low donor/acceptor ratio
Growing polymer chain
R_k
1
x
2
R_k
low donor/acceptor ratio
Repeating 1 - 2
R_1
R_2
R_3
R_k
- Acceptor monomer with a functional group
- Donor monomer

Figure 54 | General concept of the ultra-precise synthesis of sequence-controlled polymers.

Various CRP techniques, such as NMP, ARGET ATRP and SARA ATRP, or SET-LRP can be used for the synthesis of polystyrene containing two and three precisely positioned *N*-substituted maleimides [12]. The best control over macromolecular structure and minimal loss of active chain ends were reached when ARGET ATRP and SET-LRP were used. The finest control was obtained with SET-LRP leading to polymers with a narrow molecular weight distribution (M_w/M_n = 1.27 for the polymer with 3 precisely positioned maleimides). Therefore, SET-LRP (SARA ATRP) technique was used in the present work for the synthesis of polymers by ultra-precise method (Figure 55).

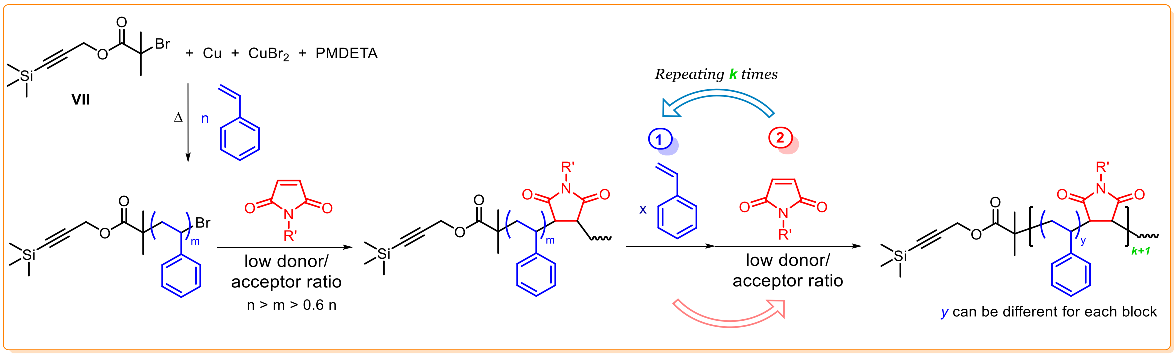
VII
+ Cu + CuBr2 + PMDETA
Δ
n
Br
m
R'
low donor/ acceptor ratio
n > m > 0.6 n
Repeating k times
1
2
x
low donor/ acceptor ratio
y
k+1
y can be different for each block

Figure 55 | Ultra-precise synthesis of sequence-controlled polymers using controlled radical copolymerization (SET-LRP) of styrene with *N*-substituted maleimides.

Two possibilities can be envisaged for the calculation of the styrene conversion using this strategy, leading to the same results (Equations 1-2, exp. part). Only the *Overall styrene conversion* will be calculated, when the total amount of polystyrene and styrene present at a given time in the copolymerization medium were taken into consideration.

II.4.2. Model Polymers

Before applying the ultra-precise method for the synthesis of polymers with precisely positioned amino acid moieties, the polymerization conditions with SET-LRP were tested on several model monomers: MI-Bz, MI-Pr and MI-PFP (Scheme 20). Copper (Cu(0), 0.25 Eq.), copper(II) bromide ($CuBr_2$, 0.1 Eq.), the ligand PMDETA (0.35 Eq.) and initiator **VII** were used for the copolymerization of styrene with maleimide at 90ºC in toluene leading to polymers with a good control over molecular weight and polydispersity [151].

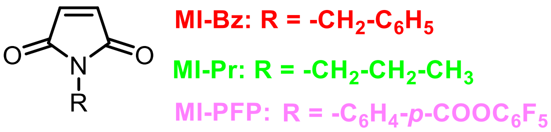
O
N
O
R
MI-Bz: R = $-CH_2-C_6H_5$
MI-Pr: R = $-CH_2-CH_2-CH_3$
MI-PFP: R = $-C_6H_4$-*p*-$COOC_6F_5$

Scheme 20 | Structures of MI-Bz, MI-Pr and MI-PFP.

Both maleimides MI-Bz and MI-Pr were positioned in the polystyrene chain (Figure 56). The polymerization was started with a small amount of styrene (25 Eq. and 1 Eq. of initiator) followed by the addition of MI-Bz (1 Eq.) when the conversion of styrene reached 65% (DP_n was around 16 styrene units). The maleimide was fully consumed after 50 minutes of polymerization corresponding to an increase of styrene conversion of only 9% (around 2 units of styrene). The size-exclusion chromotagram (Figure 56, **C** , red curve) after the consumption of MI-Bz was monomodal with a narrow distribution. Afterwards, a new feed of styrene (20 Eq.) was added in the reaction medium followed by the insertion of MI-Pr (1 Eq.) at high styrene conversion (*overall conversion* 69%). The conversion of MI-Pr was above 99% after 2.5 hours, whereas the conversion of styrene increased of only 5%. Polymerization kinetic was monitored by ^1H NMR spectroscopy by considering the disappearance of signals at 4.67 ppm for MI-Bz and at 3.48 ppm for MI-Pr. Although the polymerization was stopped at high conversion of styrene, the synthesized polymer **P19** had a narrow polydispersity (PDI 1.1) and a molecular weight close to the theoretical one according to SEC data (Figure 56, **C**).

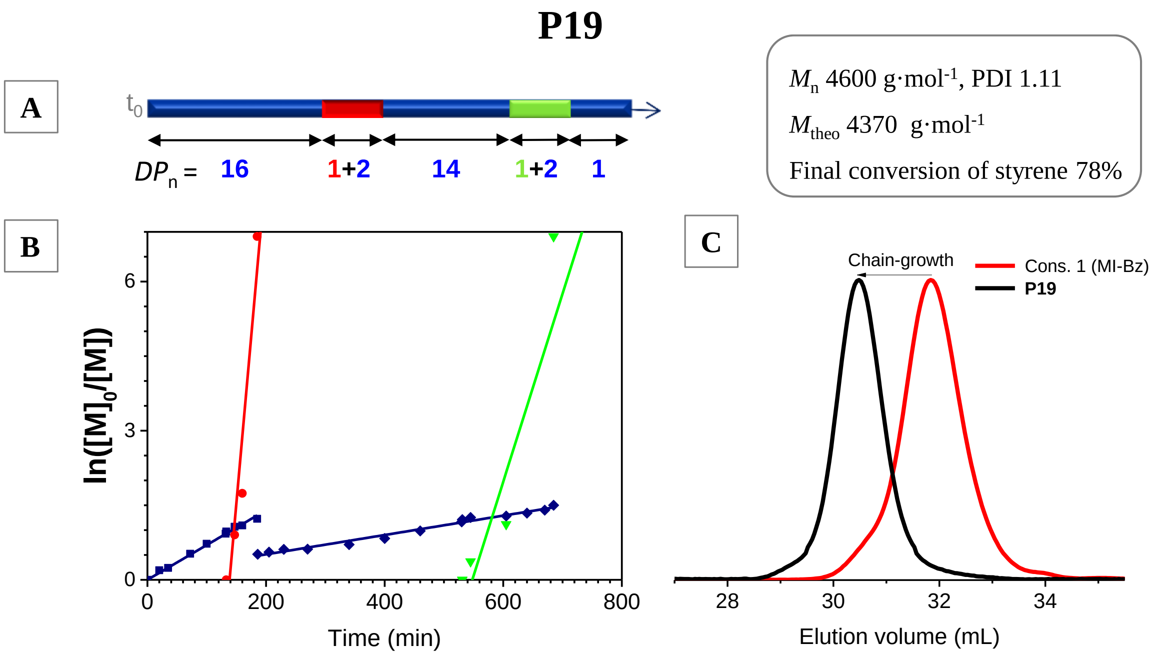

Figure 56 | Ultra-precise synthesis of a sequence-controlled polymer **P19** with two maleimides MI-Bz and MI-Pr. (**A**) Probable microstructure of **P19**. (**B**) Semi-logarithmic plot of comonomer conversions *versus* time (calculated from ^{1}H NMR spectra). (**C**) Size-exclusion chromatograms after consumption of MI-Bz (red curve) and of the purified polymer (black curve), in THF.

The ultra-precise strategy was extended to polymers with three precisely positioned maleimide units: MI-Pr, MI-Bz and MI-PFP, 1 Eq. each. In contrast to the conventional polymerization where three additions of acceptor monomers led to statistical insertions of the monomers in the polymer chain (Figure 57, **B**), the use of the ultra-precise strategy led to the well-defined polymer **P20** containing three precisely positioned *N*-functionalized maleimides (Figure 57 , **A**). The kinetics of MI-PFP consumption was monitored by the disappearance of the signal at 8.30 ppm in ^{1}H NMR spectrum. After the successful placement of the last maleimide, the polymerization was continued to add a styrene unit at the end of the polymer chain. SEC analyses of the polymer after each maleimide insertion (Figure 57, **C**) showed the formation of well-defined structures with a narrow polydispersity. However, the final polymer had a broader molecular distribution with a PDI of 1.33, probably due to side termination reactions that took place at the last stage of the polymerization.

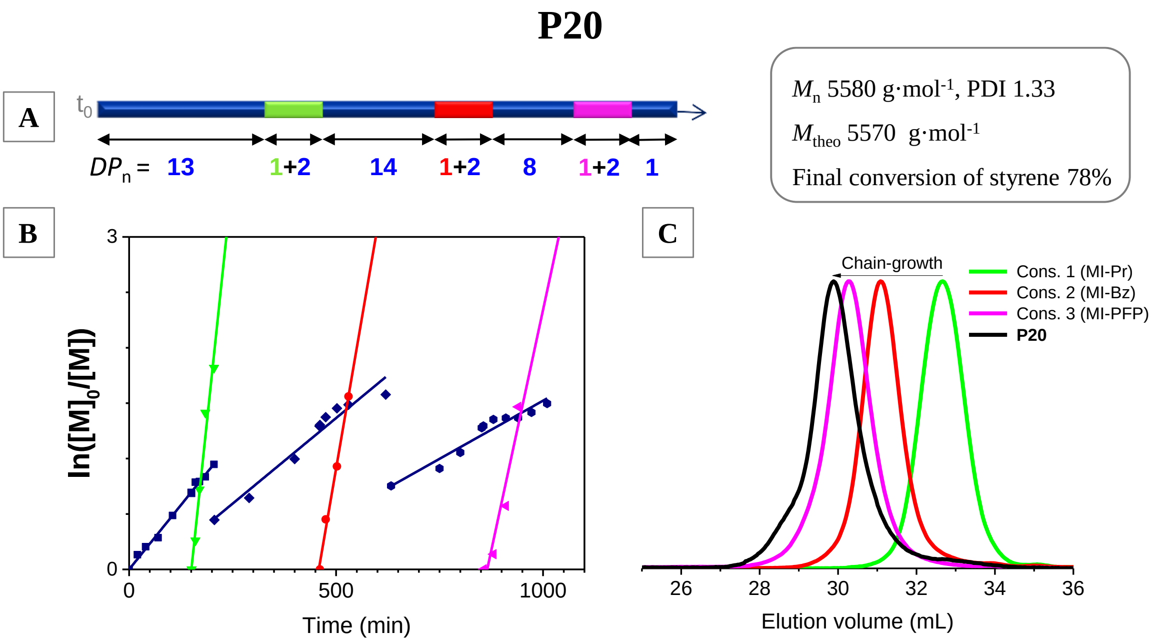

Figure 57 | Ultra-precise synthesis of the sequence-controlled polymer **P20** with three positioned model maleimides MI-Pr, MI-Bz and MI-PPF. (**A**) Probable microstructure of **P20**. (**B**) Semi-logarithmic plot of comonomer conversions *versus* time (calculated from ^{1}H NMR spectra). (**C**) Size-exclusion chromatograms after consumption of MI-Pr (green curve), MI-Bz (red curve), MI-PFP (pink curve) and of the purified polymer (black).

The polymerization slowed down after the addition of each monomer due to the dilution of the polymerization mixture by the solution of maleimide in toluene and styrene. Therefore, for the precise insertion of four maleimides and in order to decrease the number of feeds, the first two maleimides (MI-Bz and MI-Pr) were positioned using the ultra-precise strategy, and the last two (MI-Pr and MI-PFP) were inserted by combing conventional and ultra-precise methods (Figure 58, **B**). The first and second maleimides were inserted at high styrene conversions (*overall conversions* 64% and 77%, respectively) followed each time by the addition of styrene. The other two maleimides (MI-Pr and MI-PFP) were successively added at 52% of and 74% of styrene conversions, and they were accompanied by 3 and 1 styrene units, respectively (Figure 58, **A**). Therefore, combination of "ultra-precise" and conventional methodologies was successful. The analysis by SEC showed a partial loss of the living character of polymerization and appearance of a shoulder in the chromatogram of the isolated polymer (Figure 58, **C**).

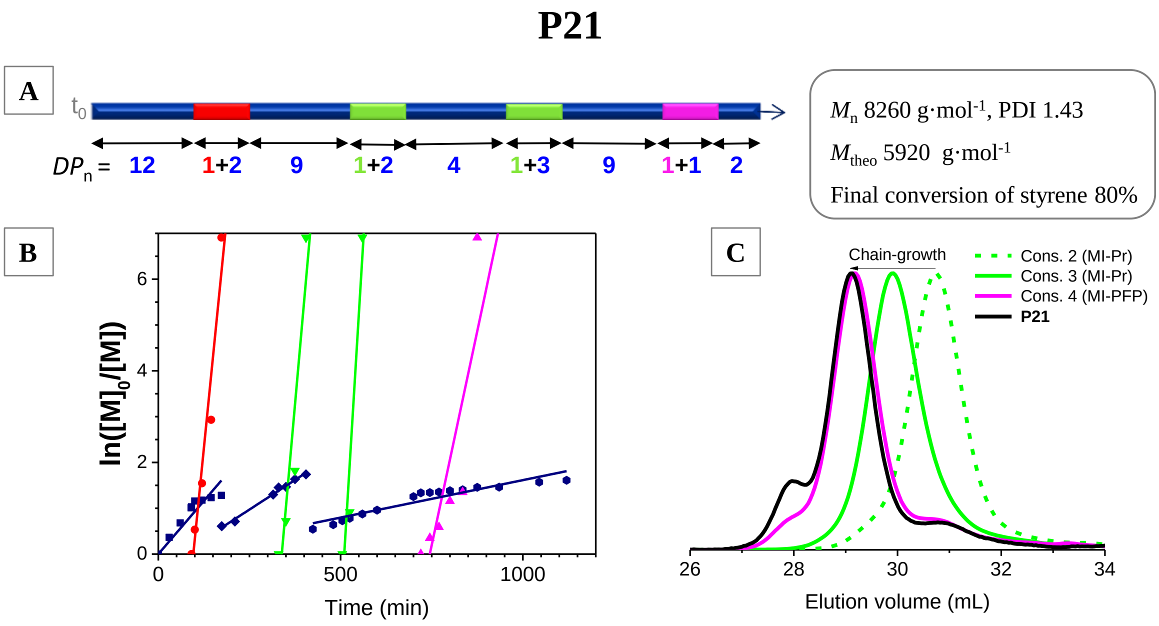

Figure 58 | Synthesis of a sequence-controlled polymer **P21** with four positioned model maleimides MI-Bz, MI-Pr added twice and MI-PPF by combination of ultra-precise and conventional methods. (**A**) Probable microstructure of **P21**. (**B**) Semi-logarithmic plot of comonomer conversions *versus* time (calculated from ^{1}H NMR spectra). (**C**) Size-exclusion chromatograms after consumption of the first added MI-Pr (solid green curve), the second added MI-Pr (dash green curve), MI-PFP (pink curve) and of the purified polymer (black).

II.4.3. Ultra-Precise Insertion of Amino Acid Moieties in Polymer Chains

The polymer tracks with amino acid (leucine, phenylalanine, and *O*-CH_3-tyrosine) residues and fluorenyl group were synthesized by the ultra-precise insertion of the maleimides **III-VI** in the polystyrene chain. Only three polymers carrying precisely positioned amino acid functions will be demonstrated (Figure 59 - Figure 61). The polymerization conditions were those used for the model polymers (Chapter II.4.2). The total amount of styrene (40-55 Eq.) was divided into several parts depending on the number of positioned maleimides. The fluorenyl group was introduced at the end of the polymer chain in order to monitor by UV-spectroscopy the last functional moiety “picked up” by the molecular machine.

A sequence-controlled polymer with tyrosine and fluorenyl moieties **P22** was prepared by time-controlled additions of the maleimides **V** and **VI** (1 Eq., each). The polymerization was started with a small amount of styrene (25 Eq. and 1 Eq. of initiator). The first maleimide (**V**) was added in the polymerization mixture at 58% of styrene conversion (*DP*$_n$ was around 15 styrene units, Figure 59, **A**). The styrene conversion increased only of 8%, when maleimide was incorporated in the polymer chains. Afterwards, a new feed of styrene (20 Eq.) was added in the reaction medium followed by the insertion of **VI** (1 Eq.) at high conversion of styrene (*overall conversion* 78%). The maleimide was consumed at 82% of styrene conversion. The addition of maleimides at high conversion of styrene led to a microstructure with precisely positioned maleimides in the polymer chain, with at least ten styrene units between *N*-Boc-*O*-methoxytyrosine and fluorenyl moieties (Figure 59 , **A**). SEC analysis of the polymerization mixture after the insertion of the first maleimide (Figure 59 , **C**, red curve) and of the final purified polymer (Figure 59, **C**, black curve) revealed the formation of a well-defined structure with a narrow molecular weight distribution (PDI 1.18) and molecular weight (M_n = 5410 g·mol^{-1}) only slightly higher than the theoretical one (M_{theo} = 5230 g·mol^{-1}). P22 was characterized by ^{1}H NMR spectroscopy (Figure 134, Annex) which confirmed the insertion of one equivalent of each maleimide per polystyrene chain.

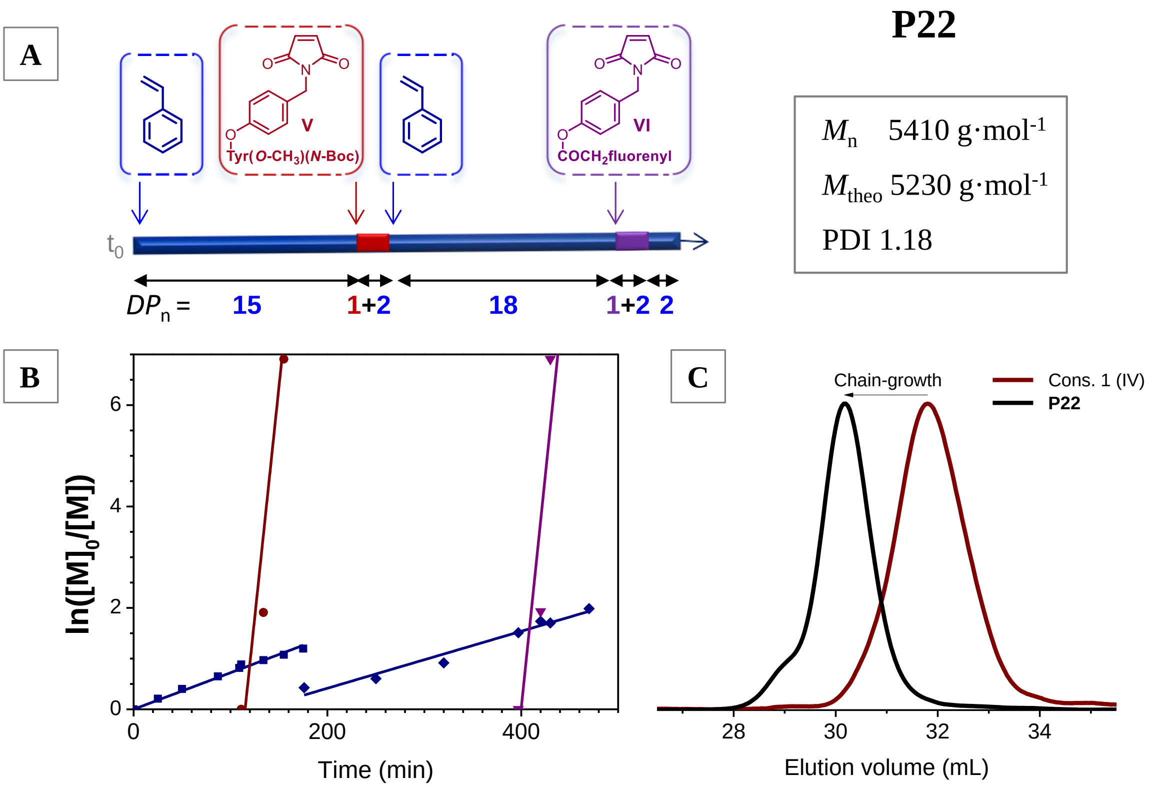

Figure 59 | Ultra-precise synthesis of a sequence-controlled polymer **P22** with two positioned maleimides **V** and **VI**. (**A**) Probable microstructure of **P22**. (**B**) Semi-logarithmic plot of comonomer conversions *versus* time (calculated from ^{1}H NMR spectra). (**C**) Size-exclusion chromatograms after consumption of **V** (red curve) and of the purified polymer (black curve).

In analogy with the polymer **P22**, a sequence-controlled polymer **P23** with three positioned functional moieties (*N*-Boc-phenylalanine, *N*-Boc-leucine and fluorenyl) was synthesized. Each maleimide insertion was performed at high styrene conversion (*overall conversions* corresponding to each stage were 72%, 82% and 66%, respectively) leading to the precise positioning of functional moieties in the polymer chain (Figure 60 , **A**). The chromatogram was monomodal with a quite narrow polydispersity (PDI = 1.26) and without shoulders (Figure 60 , **C**) after the maleimide additions and the purification. However, the measured molecular weight (M_n = 7390 g·mol^{-1}) was higher than the calculated one (M_{theo} = 5330 g·mol^{-1}), probably due to too long polymerization times resulting in a partial loss of the living character of growing chains. The integration of the ^{1}H NMR spectrum (Figure 135, Annex) corresponds to the insertion of one equivalent of each maleimide per polystyrene chain. The presence of a fluorenyl group in the polymer chain was also evidenced by UV-spectroscopy (characteristic band at 302 nm).

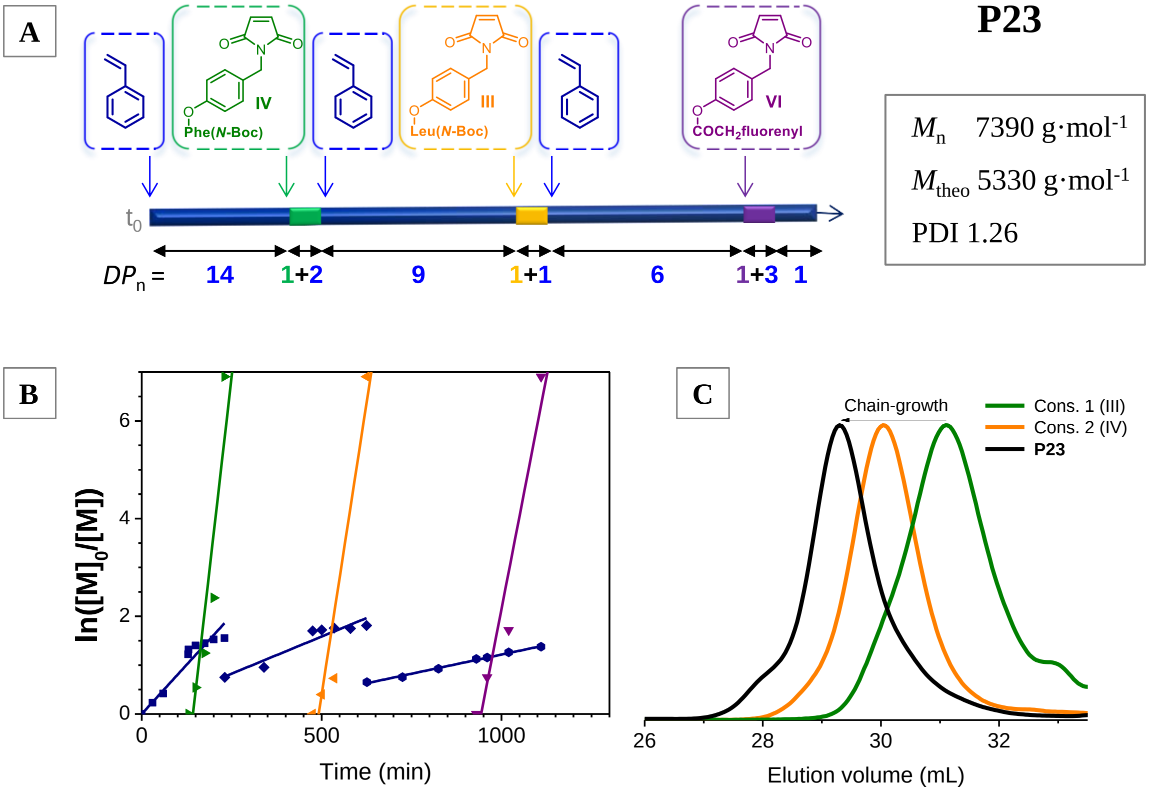

Figure 60 | Ultra-precise synthesis of the sequence-controlled polymer **P23** with three positioned maleimides **IV**, **III** and **VI**. (**A**) Probable microstructure of **P23**. (**B**) Semi-logarithmic plot of comonomer conversions *versus* time (calculated from ^{1}H NMR spectra). (**C**) Size-exclusion chromatograms after consumption of **IV** (green curve), **III** (orange curve) and of the purified polymer (black curve).

Inspired by the successful synthesis of the well-defined and controlled polymer with three positioned moieties, a sequence-controlled polymer with four precisely introduced functional moieties was prepared using the ultra-precise strategy, although the living character of the polymerization can be lost when the polymerization time increases. The polymerization was started with the homopolymerization of styrene (20 Eq.) until 68% of conversion and followed by the placement of maleimide **III** (1 Eq.) in a narrow region in the polymer chain (Figure 61, **A**). Afterwards, the kinetic conditions were repeated three more times, including the addition of styrene (10 Eq. for each feed) and a maleimide (1 Eq.). Three maleimides **IV**, **V** and **VI** were also introduced at high styrene conversions (*overall conversions* were around 70% - 80%) resulting in the formation of narrow sequence-controlled distributions of a maleimide unit accompanied by one to two styrene units (Figure 61, **A**).

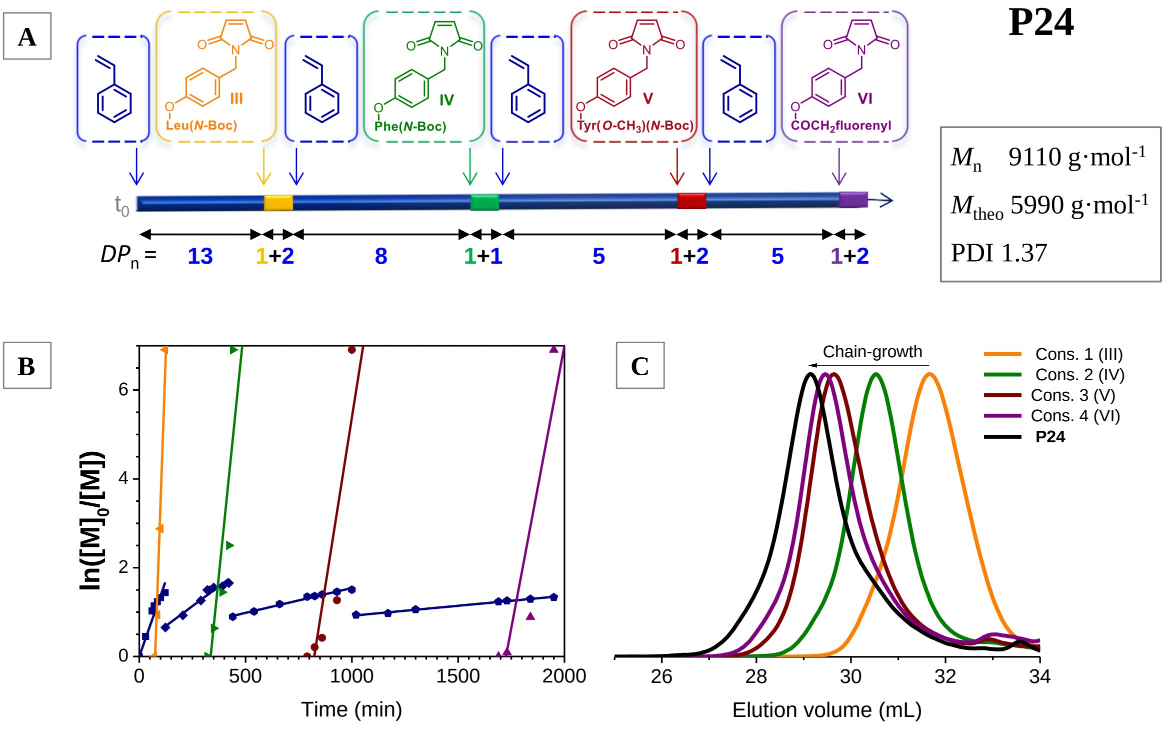

Figure 61 | Ultra-precise synthesis of a sequence-controlled polymer **P24** with four positioned maleimides **III**, **IV**, **V** and **VI**. (**A**) Probable microstructure of **P24**. (**B**) Semi-logarithmic plot of comonomer conversions *versus* time (calculated from ^{1}H NMR spectra). (**C**) Size-exclusion chromatograms after consumption of **III** (orange), **IV** (green), **V** (red), **VI** (purple) and of the purified polymer (black).

Although the structure was well-defined according to the kinetic data, and the molecular weight distribution was monomodal (Figure 61, **C**), the value of the molecular weight exceeded significantly the theoretical value and the polydispersity (PDI 1.37) was higher than for the polymers with two and three ultra-precisely inserted maleimides. This result can be explained by the presence of terminal reactions and a partial loss of the living character of the polymer chains. Additionally, the alkyne group was deprotected during polymerization that could lead to side reactions (Glaser coupling).

The presence of all maleimides in the polymer chain was confirmed by the ^{1}H NMR signals at 1.01 ppm for **III**, at 3.22 ppm for **IV**, at 3.18 and 3.77 ppm for **V** and at 7.56 and 7.77 ppm for **VI** (Figure 62). The integration corresponds to the incorporation of one unit of each maleimide per polymer chain (Figure 136 in Annex). The presence of a fluorenyl group in **P24** was confirmed by UV-spectroscopy (Figure 99).

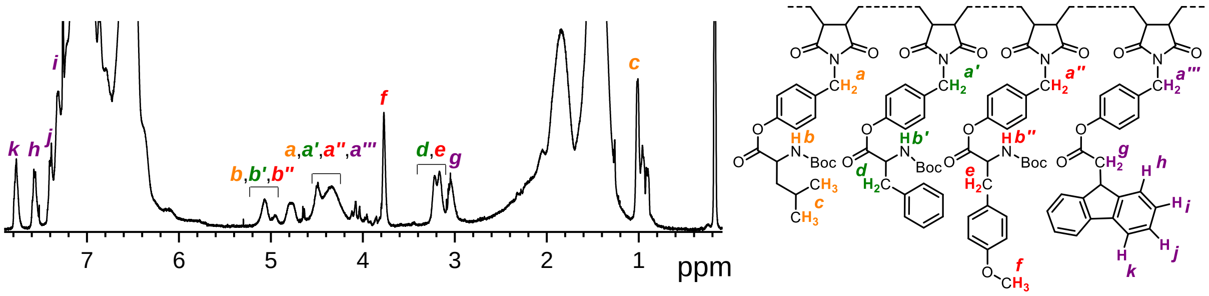

Figure 62 | ^{1}H NMR spectrum of the polymer **P24**, in $CDCl_3$.

II.5. REMOVAL OF THE TRIMETHYLSILYL GROUP

According to NMR data, trimethylsilyl (TMS) group is partially removed during ATRP. For example, after 2 hours of polymerization reaction (1 Eq. of CuBr, 1 Eq. of PMDETA, 90ºC) around 20% of the alkyne function was deprotected. The deprotection during ATRP was also described in the literature for the direct use of TMS-alkynes as cycloaddition partner in azide-alkyne "click" reaction [178]. However, the remaining TMS-protecting group was removed, in order to have all the chains with free alkyne-group and to simplify the understanding of MALDI spectra.

Removal of TMS-protecting group is well described in the literature [172, 179-182]. A mild base such as tetra-*n*-butylammonium fluoride (TBAF) in THF solution is sufficient reagent for the efficient deprotection of alkyne group. 0.01 M solution of TBAF (10 Eq.) in THF to one equivalent of TMS-group at room temperature were used as conditions for the deprotection of polystyrene **P1** (Figure 63, **A**). According to ^{1}H NMR spectrum (Figure 63,

B), TMS-group was removed (disappearance of TMS-signal, ***c***, at 0.17 ppm and appearance of an alkyne terminal proton, ***f***, at 2.34 ppm), at the same time chain end signal (***a***) at 4.36 to 4.60 ppm vanished, and new signals at 6.03-6.23 ppm (***d***) and at 3.09 ppm (***e***) appeared after the TBAF treatment. These signals most probably correspond to a polystyrene terminal vinyl protons [183] and a methine proton located in the α-position of terminal bromine atom [184], thus indicating a dehydrobromination of the polymer chain end.

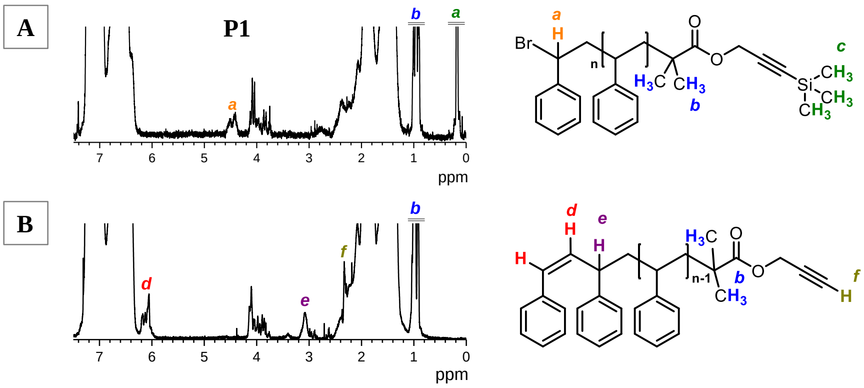

Figure 63 | ^{1}H NMR spectra of **P1** before and after deprotection: (**A**) after synthesis by ATRP and purification; (**B**) after TBAF treatment. *Reaction conditions*: 0.01 M solution of TBAF (10 Eq.) in THF to 1 Eq. of TMS-group (**P1**), RT, 12 hours.

Under milder conditions (0.01 M solution of TBAF (2 Eq.) in THF to 1 Eq. of TMS-group, RT, 1 hour) no dehydrobromination of the polymer chain end was observed, and the TMS-group was successfully removed. However when these conditions were applied to the deprotection of polymers with *N*-Boc-protected amino acid moieties, an alkyne signal appeared (***g***), the signal of TMS-protected group disappeared (***f***), the signals belonging to maleimide **III** (***b***, ***c***, ***e***) at 4.95, 4.53 and 1.48 ppm, partially from ^{1}H NMR spectrum (Figure 64, **B**).

After optimization, suitable conditions for the alkyne function deprotection were found. Addition of a 0.01 M solution of TBAF (1 Eq.) in THF to the TMS-protected polymer (1 Eq.) followed after several minutes by the precipitation of the polymer in a methanol/water (95/5 v/v) solution led to the complete removal of TMS without influencing the other functional groups. It was found that some drops of water added to MeOH accelerated the deprotection as evidenced by the ^{1}H NMR of initiator **VII** and **P9**.

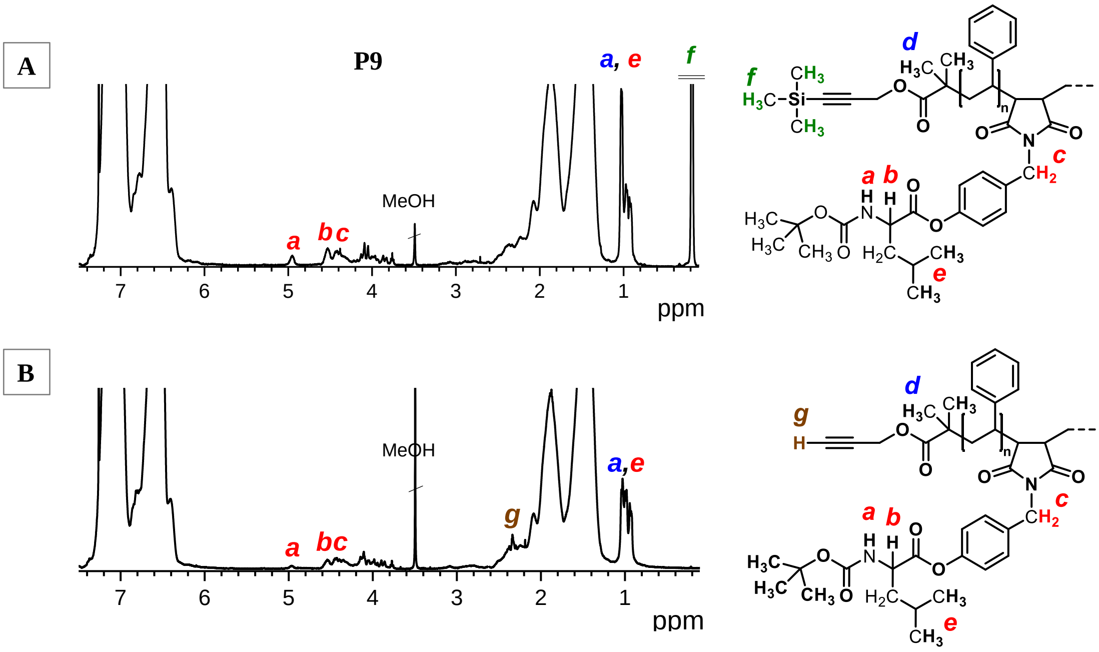

Figure 64 | ^{1}H NMR spectra for a α-alkyne functional polymer **P9** with *N*-Boc-protected leucine moieties: (**A**) after synthesis by ATRP and purification and (**B**) after TBAF treatment. *Reaction conditions*: 0.01 M solution of TBAF (2 Eq.) in THF to 1 Eq. of TMS-group (**P9**), RT, 1 hour.

II.6. CONCLUSIONS

Sequence-controlled copolymers containing amino acid and fluorenyl moieties were synthesized for a collaboration with the group of Leigh in Manchester which will integrate these polymer tracks into a complex peptide synthesizing molecular machine. First, especially designed maleimides with amino acid and fluorenyl moieties were prepared in two steps using commercially available reactants. An alkyne functionalized initiator has also been synthesized and used to connect the polymer track to the rest of the molecular machine by Huisgen cycloaddition. Subsequently, the positioning of one to several amino acid moieties was performed using a conventional methodology. However, maleimide insertion in the polymer chain using this method was not precise enough for its incorporation in the molecular machine that requires a finely controlled placement of the amino acid moiety. Therefore, the recently developed ultra-precise strategy was used for the synthesis of the polymer tracks containing two, three and four precisely positioned functional moieties (several *N*-Boc-protected amino acid and a terminal fluorenyl). Although the polymerization conditions can still be further optimized and termination side reactions could not be completely avoided, this strategy successfully allowed the precise placement of the amino acids at any desired position in the polymer chains by the means of straightforward chain-growth polymerization. The polymer tracks carrying amino acid and fluorenyl moieties were then sent to Manchester for further investigation and the sequence-specific peptide syntheses by the molecular machine using our polymer tracks are currently performed by Leigh group.

CHAPTER III. SINGLE-CHAIN TOPOLOGIES FORMED BY POSITIONABLE DISULFIDE BRIDGES

III.1. INTRODUCTION. GENERAL IDEA

The strategies for the design and synthesis of single-chain objects folded or compacted by covalent interactions were highlighted in Chapter I.4. It was shown that, apart from the folding of synthetic oligomers and polymers into helical or sheet conformations [46, 86, 185], polymer chains with a random-coil conformation in dilute solution can also be transformed into compact objects using intramolecular chemistry. Three main routes were described: 1) single-chain polymer (nano)particles (SCPN) based on randomly positioned and intramolecularly cross-linked functional groups [3-5]; 2) polymers with several compacted domains synthesized by the precise placement of orthogonal moieties into the polymer chains followed by intramolecular post-modifications [95]; and 3) various topologies originating from cyclic architectures [8, 9, 115]. The third route will be described in this chapter for the synthesis of single-chain topologies by intramolecular covalent bonds (positionable disulfide bridges).

The precise placement of intramolecular bridges by covalent interactions leading to complex topologies was demonstrated by our group to be a convenient and simple route toward synthetic folded macromolecules [8, 9]. The synthesis of these complex topologies consisted of several steps. First, linear precursors with precisely introduced reactive groups were synthesized by sequence-controlled copolymerization of styrene or styrene derivatives with *N*-substituted maleimides that were incorporated in short regions (discrete patches) in polystyrene chains (Chapters I.2 and II). Afterwards, the functional maleimide moieties were post-modified and reacted intramolecularly leading to the compaction of single polymer chains. The chemical reactions used for the formation of covalent bridges included azide-alkyne Huisgen cycloaddition, alkyne-alkyne Glaser coupling and amidation of activated esters. These strategies allowed the synthesis of folded macromolecules with knotted, pseudocyclic and bicyclic as well as tadpole shapes. Although the intramolecular bridges described in the literature were only obtained by permanent covalent links, compaction and folding of biomacromolecules in nature is often dynamic and responsive to environmental changes. For example, the intramolecular dynamic disulfide bridges obtained by the coupling between two cysteine residues are positioned precisely in natural proteins; and the subsequent stabilization of their tertiary structure (due to the oxidation of the thiols) leads to the precise folding of the macromolecules.

It was recently shown by Gauthier and coworkers that the amino-acid sequence cysteine-*any amino acid*-cysteine (CXC) led to much more specific and efficient disulfide bridge formation compared to the sequence containing only a single cysteine residue [13]. Although oxidized CXC sequences are uncommon in nature [186], they revealed some interesting properties: oxidation of thiol groups of CXC fragments leads to the orthogonal pairing of cysteine residues while forming cyclic dimers with a negligible amount of oxidized unique CXC unit or oligomers [13, 187]. This avoids orthogonal protecting/deprotecting thiol group strategies to form disulfide bonds. The dimers of oxidized CXC-motifs represent a 22-units macrocycle stabilized by two disulfide bridges (Figure 65).

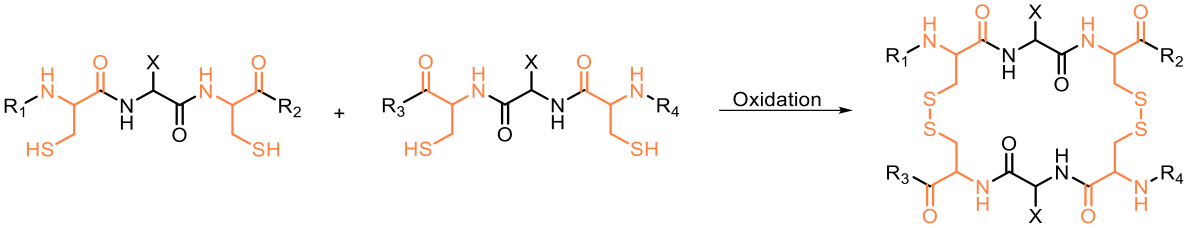

Figure 65 | Oxidation of two CXC motifs into a 22-units macrocycle containing two disulfide bonds. Only one of the two possible cycles is shown.

It was demonstrated that the central X amino acid residue (Figure 65) influenced the dimerization properties of CXC sequences [13]. For instance, arginine residue strongly directed the equilibrium toward the formation of the dimer (Figure 65, X = $-(CH_2)_3-NH-C(=NH_2)-NH_2$) due to the presence of positively charged guanidinium moiety that changed the stability of the thiolate group [188]. Therefore, a CRC sequence with a central arginine (R) amino acid was used in this study.

Cyclic peptides have some advantages over linear peptides such as possible improved stability, biological activity and size reduction [189-191]. Some promising applications were reported in the field of peptidic drugs [187, 189, 192, 193]. For instance, dynamic cyclic peptides containing disulfide bonds are promising for the identification of biomimetic carbohydrate receptors [187, 189, 192, 193]. Furthermore, CGC (G – glycine) were investigated as components of redox buffers for protein folding [186].

Thus, inspired by the folding of natural biomacromolecules, the synthesis of polymer conjugates with peptides containing CRC fragments will be described in this chapter, as well as their transformation into single-chain polymers compacted by positionable disulfide bridges. This project was realized in the collaboration with two scientific groups. Gauthier, Leroux and coworkers presented an extensive study of the orthogonal pairing of CXC-motifs [13] that inspired the present work. The group of Börner kindly provided an oligopeptide containing the CRC sequence (Scheme 21, **IX**).

III.2. DESIGN OF LINEAR POLYMER CONJUGATES. GENERAL SCHEME

Oligopeptides with cysteine-arginine-cysteine (CRC) sequences were precisely placed at two different positions in a polystyrene chain by the controlled radical copolymerization of styrene with a small amount of *N*-substituted maleimide (2 molar eq. per chain). CRC fragments could be introduced in the polymer chains either by post-modifications of a polystyrene chain with reactive sites (“grafting to”), or by the direct polymerization of styrene with a maleimide containing CRC sequence (“grafting through”). The first route was chosen, since it leads to an easier synthesis of the oligomers containing the CRC sequence by solid phase synthesis and a facile purification of the modified polymer by precipitation. The synthesis of linear sequence-controlled polymer conjugates consisted of two steps:

1. Synthesis of a sequence-controlled polystyrene with reactive groups.
2. A post-modification to introduce the CRC motifs.

The second step demands the use of chemical reactions leading to a quantitative modification of the reacting groups. The chemistry based on a nucleophilic substitution reaction between activated ester (pentafluorophenyl ester) and amines was chosen, since the amidation of pentafluorophenyl activated ester with primary amines is a simple, efficient and quantitative reaction [194-196]. Moreover, it can be monitored by ^{19}F NMR and FT-IR spectroscopies.

Sequence-controlled polymer conjugates with CRC motifs were prepared by copolymerization of styrene with pentafluorophenyl 4-maleimidobenzoate (MI-PFP), which was introduced twice at specific positions in the growing chains (Figure 66, **A**), followed by post-polymerization modifications with a derivative of CRC containing an amine terminal group (Figure 66, **B**). The guanidinium of arginine residues were protected with 2,2,4,6,7-pentamethyl dihydrobenzofuran-5-sulfonamide (Pbf). The thiols of cysteine residues had to be protected with trityl (Trt) groups, in order to prevent the unwanted oxidation of the thiol groups during the modification (compounds were commercially available). Moreover, the protection of the reactive groups of the CRC motifs was necessary to avoid a nucleophilic substitution of the thiol with the pentafluorophenyl activated ester [197, 198]. The last step consisted of orthogonal pairing of CRC motifs by oxidation of thiol groups in dilute conditions. It led to the compaction of the polymer chains by two intramolecular disulfide bridges and the formation of a small "inner" 22-units ring due to the dimerization of CRC sequences (Figure 66, **C**).

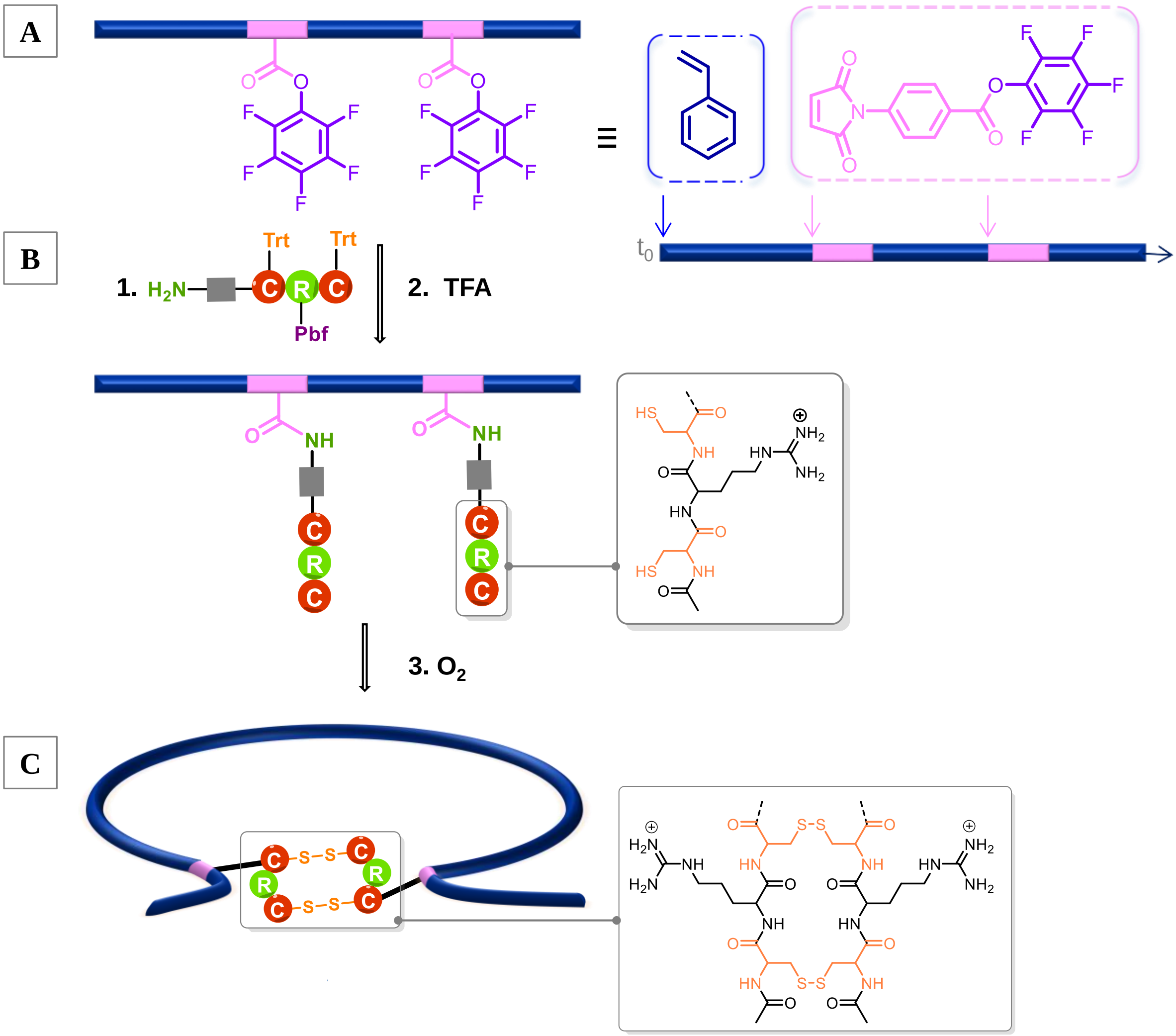

Figure 66 | General scheme of the project. (**A**) The synthesis of sequence-controlled precursors by copolymerization of styrene with pentafluorophenyl 4-maleimidobenzoate. (**B**) Synthesis of polymer conjugates by *1*) attachment of cysteine-arginine-cysteine fragments (CRC) with protected amino acid groups by activated ester/amine chemistry followed by *2*) the removal of the protecting groups. (**C**) *3*) Intramolecular oxidation of the cysteine residues leading to a single-polymer chain folded by precisely positioned orthogonal disulfide bridges.

III.3. SYNTHESIS OF LINEAR POLYMER CONJUGATES

III.3.1. Synthesis of Polymers with Positioned Pentafluorophenyl Ester Groups

Sequence-controlled polymers with reactive pentafluorophenyl (PFP) ester groups were synthesized by the nitroxide-mediated polymerization (NMP) of styrene with pentafluorophenyl 4-maleimidobenzoate (MI-PFP). The synthesis of the MI-PFP was performed in three steps: i) reaction between maleic anhydride and 4-amino benzoic acid, ii) closure of the maleimide with sodium acetate at 60°C, and iii) modification of 4-maleimidobenzoic acid with pentafluorophenyl trifluoroacetate [199].

Two approaches were used for the synthesis of polymers with two positioned PFP ester moieties due to the controlled/living character of the polymerization: 1) NMP was performed in the presence of a monofunctional alkoxyamine that demanded two additions of 1 mol. eq. MI-PFP and led to the "asymmetric" placement of functional moieties in the polymer chains; and 2) NMP was performed in the presence of a bifunctional alkoxyamine that demanded only one addition of 2 mol. eq. MI-PFP and led to the "symmetric" placement of functional moieties in the polymer chains. Therefore, two types of functionalized precursors were synthesized:

1. "Asymmetric" well-defined polymers (**P25** to **P28** in Table 2) were obtained by the nitroxide-mediated copolymerization of styrene with maleimide MI-PFP added at the beginning of the polymer chain and close to the chain end in the presence of BlocBuilder® (BB).

BlocBuilder® is a commercially available monofunctional alkoxyamine. It contains a nitroxide and an initiating motif and allows a simple preparation of well-defined polystyrenes with a narrow molecular weight distribution. The polymerizations of **P25** to **P28** were stopped at around 70% styrene conversion leading to an average of 70 styrene and 2 maleimide units per chain. The maleimide conversion was calculated from ^{1}H NMR spectra by the disappearance of the signal of MI-PFP benzene ring at 8.34 ppm. The microstructure and kinetic plot are presented for **P25** in Figure 67, **A**. According to the SEC data all the polymers had a M_w/M_n close to 1 (around 1.13-1.6) and all molecular weights were in agreement with the theoretical predictions (Table 2).

Table 2 | A. Kinetic data recorded for the nitroxide-mediated polymerization (NMP) of styrene with pentafluorophenyl 4-maleimidobenzoate (MI-PFP) using BlocBuilder®.

	1st insertion of MI-PFP				2nd insertion of MI-PFP				End of polymerization	
	$t_{add\ 1}{}^{a}$, [min]	Conv.$_S$ at $t_{add\ 1}{}^{b}$	$t_1{}^{c}$, [min]	Conv.$_S$ at $t_1{}^{b}$	$t_{add\ 2}{}^{a}$, [min]	Conv.$_S$ at $t_{add\ 2}{}^{b}$	$t_2{}^{c}$, [min]	Conv.$_S$ at $t_2{}^{b}$	$t_{end}{}^{d}$, [min]	Conv.$_S$ at $t_{end}{}^{b}$
P25	0	0	6	0.12	46	0.51	52	0.54	100	0.70
P26	0	0	8	0.17	75	0.63	84	0.68	115	0.71
P27	0	0	14	0.09	163	0.63	175	0.64	185	0.69
P28	21	0.23	30	0.32	71	0.55	80	0.59	124	0.72

Table 2 | B. SEC data for the polymers **P25** to **P28**.

	$M_n{}^{e}$, [g·mol^{-1}]	$M_{theo}{}^{f}$, [g·mol^{-1}]	$M_w/M_n{}^{e}$
P25	9070	8440	1.16
P26	9930	8540	1.14
P27	8640	8330	1.13
P28	9250	8650	1.16

Polymerization conditions: styrene (100 Eq.), MI-PFP (1 Eq. for each addition), BlocBuilder® (1 Eq.) in styrene/anisole 2/1 v/v, 120°C (at 115°C for Entry 3). [a]Time at which the 1st and 2nd additions of MI-PFP were performed. [b]Styrene conversion calculated from ^{1}H NMR spectra. [c]Time at which full conversion of MI-PFP was observed. [d]Final polymerization time. [e]Measured by SEC in THF. [f]$M_{theo} = M_{BB} + M_S \cdot conv._S \cdot [S]/[BB] + M_{MI\text{-}PFP} \cdot [MI\text{-}PFP]/[BB]$, S – styrene, BB – BlocBuilder®.

2. „Symmetric” well-defined polymers (**P29** to **P31** in Table 3) were obtained by the nitroxide-mediated copolymerization of styrene (100 Eq.) with MI-PFP (2 Eq.) added once at the end of polymerization using a bifunctional alkoxyamine **VIII** (Figure 67, **C**).

Alkoxyamine **VIII** is constituted of two initiating active sites connected to nitroxide groups (SG1) that enables the growth of the polymer chain in two directions. **VIII** was synthesized by the coupling of 1,2-bis(bromopropionyloxy)ethane with *N*-*tert*-Butyl-*N*-[1-diethylphosphono(2,2-dimethylpropyl)]nitroxide.

For "symmetric" polymers, MI-PFP was introduced once at high styrene conversion in order to reach precise placement of the maleimides into the polymer chains. The microstructure and kinetic plot of a polymer with MI-PFP placed symmetrically close to the chain ends are presented for **P29** in Figure 67, **B**. The maleimide conversion was calculated from ^{1}H NMR spectra by the disappearance of the signal of MI-PFP benzene ring at 8.34 ppm. SEC analysis of **P29** to **P31** evidenced a narrow molecular weight distributions (PDI of 1.18-1.23), but the theoretical molecular weights (M_{theo}) were higher than the molecular weights (M_n) obtained by SEC for **P30** and **P31**. This can be explained by the influence of termination side reactions that became more pronounced at latter stage of the polymerization (above 60% of styrene conversion) due to the presence of two growing chain-ends.

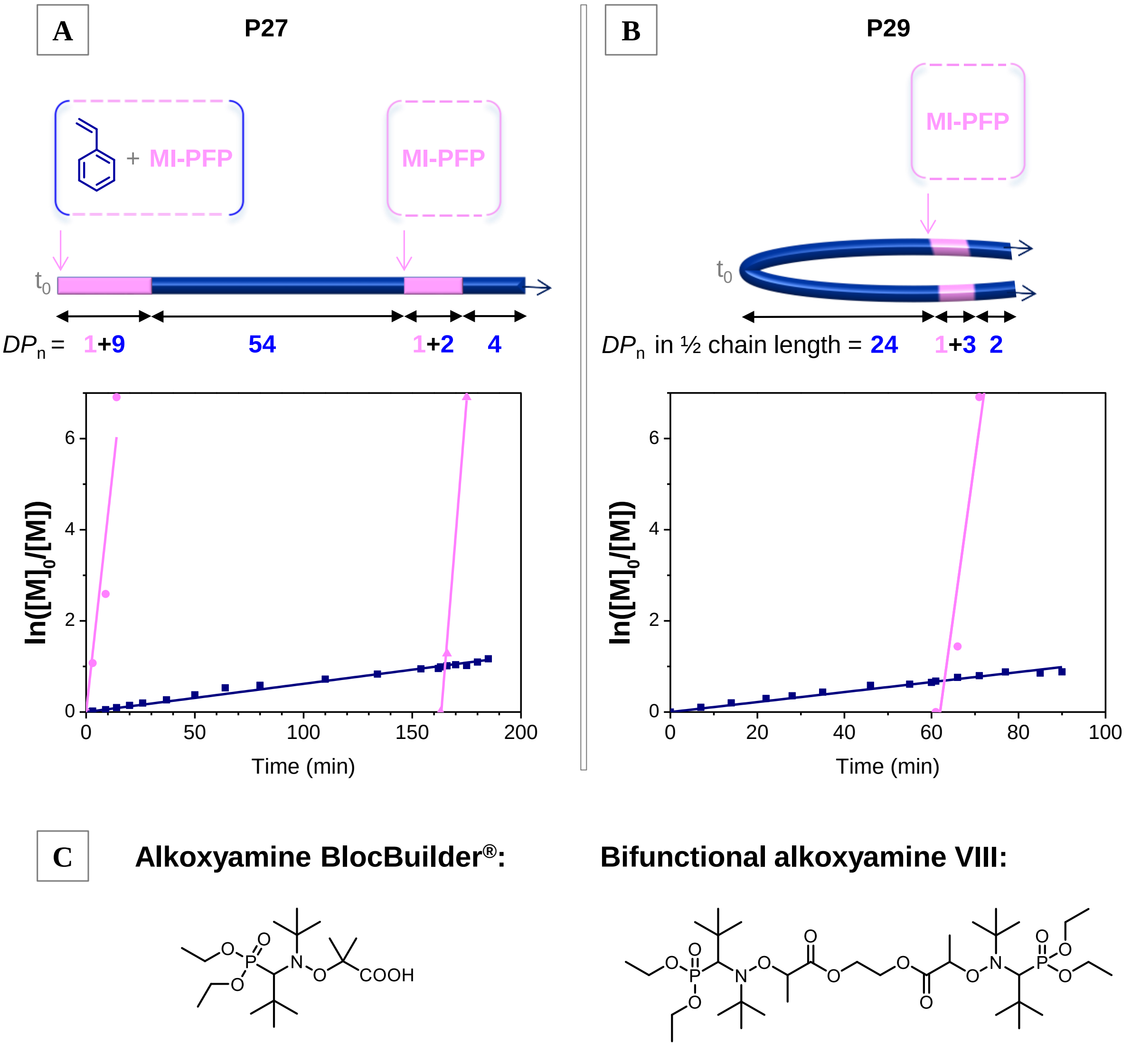
A
P27
+ MI-PFP
MI-PFP
t0
DPn = 1+9
54
1+2
4
ln([M]0/[M])
0
2
4
6
0
50
100
150
200
Time (min)
B
P29
MI-PFP
t0
DPn in ½ chain length = 24
1+3
2
ln([M]0/[M])
0
2
4
6
0
20
40
60
80
100
Time (min)
C
Alkoxyamine BlocBuilder®:
Bifunctional alkoxyamine VIII:
O
P
N
COOH

Figure 67 | (A) Synthesis of "asymmetric" sequence-controlled precursor by the NMP of styrene with MI-PFP in the presence of BlocBuilder®. **(B)** Synthesis of "symmetric" sequence-controlled precursor by NMP of styrene with MI-PFP in the presence **VIII**. **(C)** The structures of BlocBuilder® and bifunctional alkoxyamine **VIII**.

Table 3 | Kinetic data recorded for the nitroxide-mediated polymerization of styrene with pentafluorophenyl 4-maleimidobenzoate (MI-PFP) using **VIII**.

	Insertion of MI-PFP				End of polymerization		SEC data		
	t_{add} [a], [min]	Conv.$_S$ at t_{add} [b]	t_1 [c], [min]	Conv.$_S$ at t_1 [b]	t_{end} [d], [min]	Conv.$_S$ at t_{end} [b]	M_n [e], [g·mol^{-1}]	M_{theo}, [g·mol^{-1}]	M_w/M_n [e]
P29	60	0.48	71	0.55	90	0.60	8520	7780	1.18
P30	71	0.70	85	0.75	91	0.78	12180	9650	1.23
P31	50	0.57	59	0.63	75	0.69	11550	8710	1.23

Conditions of polymerization: styrene (100 Eq.), MI-PFP (2 Eq.) added in 0.4 mL of anisole, **VIII** (1 Eq.) styrene/anisole 2/1 v/v, 116°C. [a]Time at which the addition of MI-PFP was performed. [b]Styrene conversion calculated from ^{1}H NMR spectra. [c]Time at which full conversion of MI-PFP was observed. [d]Final polymerization time. [e]Measured by SEC in THF. [f]$M_{theo} = M_{\mathbf{VIII}} + M_S \cdot conv._S \cdot [S]/[\mathbf{VIII}] + M_{MI\text{-}PFP} \cdot [MI\text{-}PFP]/[\mathbf{VIII}]$.

All the polymers were analyzed by ^{1}H NMR and ^{19}F NMR spectroscopies (Figure 68).

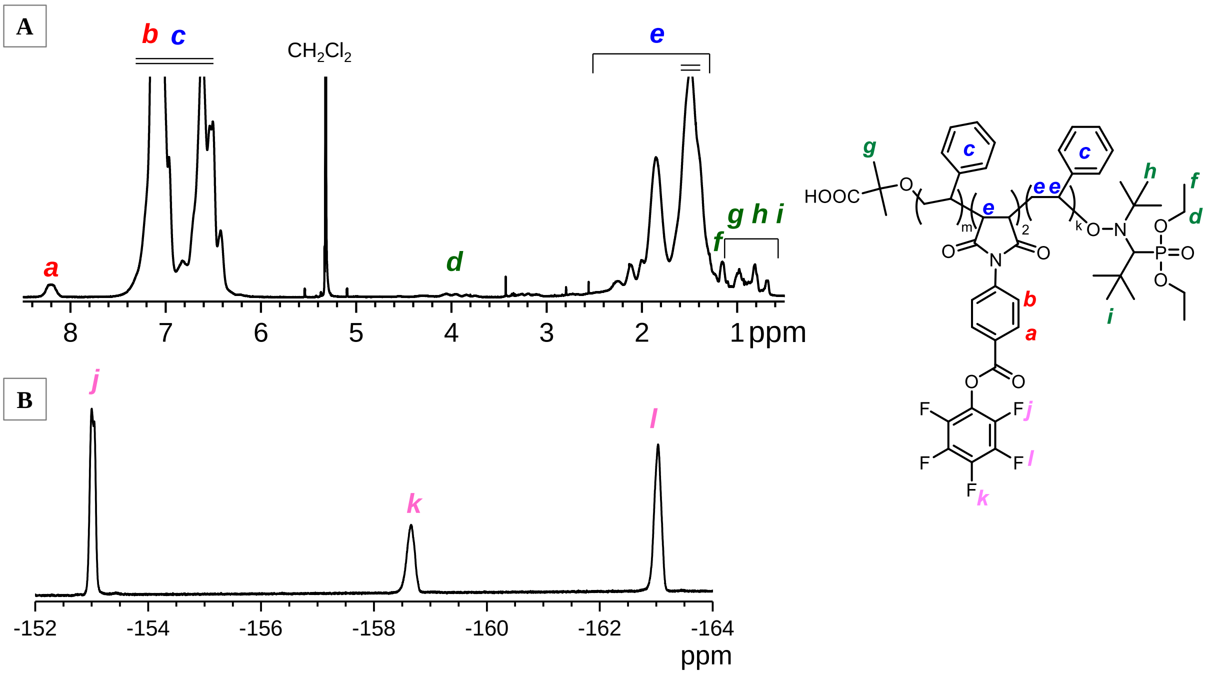

Figure 68 | (**A**) ^{1}H NMR spectrum of the polymer with PFP ester moieties **P27** and (**B**) ^{19}F NMR spectrum of **P27**, in CD_2Cl_2.

In the ^{1}H NMR spectrum of **P27** a broad signal in 8.2 to 8.4 ppm range was assigned to two protons of the benzene ring of MI-PFP (Figure 68, **A**). The ^{19}F NMR spectrum showed three broad signals at -153, -158.7 and -163 ppm with a 2:1:2 integral ratio, corresponding to the three different fluorine signals expected for pentafluorophenyl ester (Figure 68, **B**, on the example of **P27**), showing that PFP moieties remained intact under the NMP conditions.

III.3.2. Synthesis of Polymer Conjugates with Protected Cysteine-Arginine-Cysteine Motifs

The sequence-controlled polymers with PFP ester moieties reacted with the primary amine moiety of the oligomer **IX** containing cysteine-arginine-cysteine (CRC) fragment (Scheme 21). The thiol moieties of cysteine residues were protected with trityl (Trt) groups, and the guanidinium moiety of arginine was protected with a 2,2,4,6,7-pentamethyl dihydrobenzofuran-5-sulfonamide (Pbf).

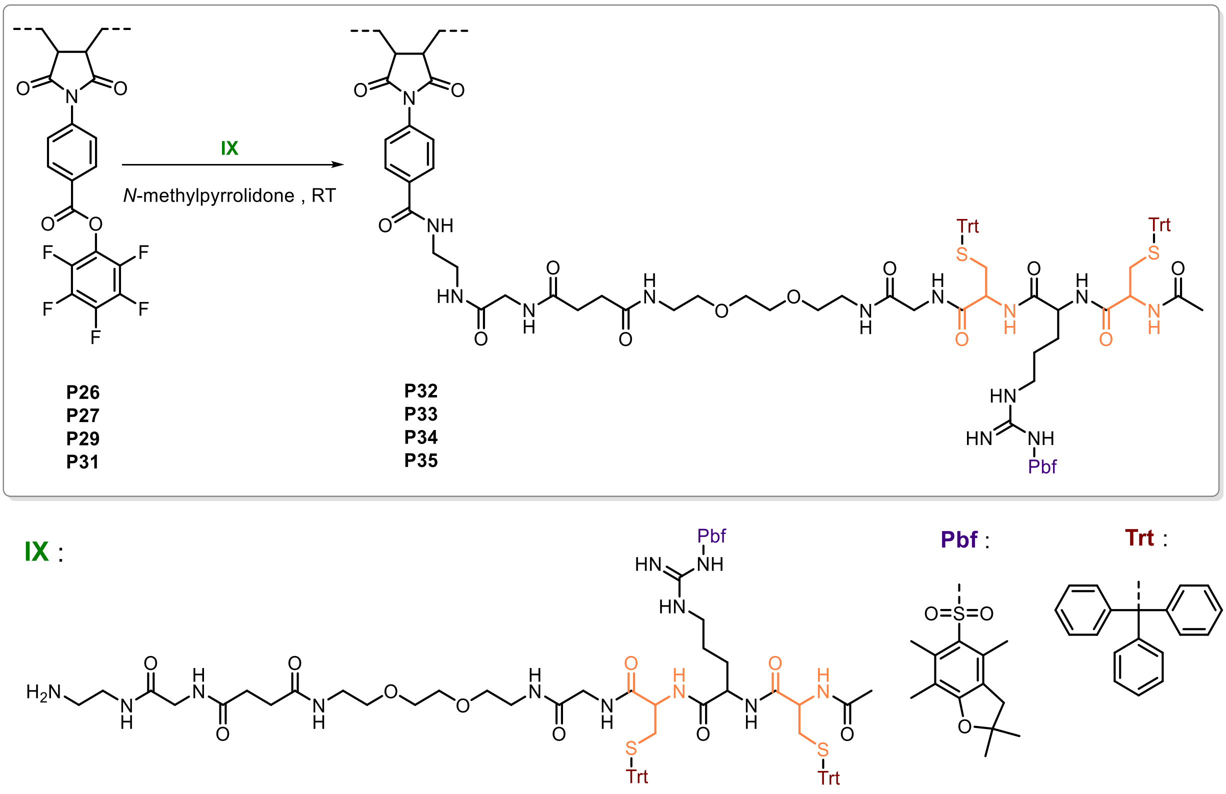

Scheme 21 | Synthesis of polymer conjugates with a cysteine-arginine-cysteine motif (**P32** to **P35**) by modification of polymers with PFP ester moieties (**P26**, **P27**, **P29** and **P30**) with **IX**. *Reaction conditions*: polymer with PFP moieties (1 Eq.), **IX** (1.2 Eq.), *N*-methylpyrrolidone, RT, 10 hours, 70% yield.

The conditions for the modification of PFP ester moieties by a primary amine are well described in the literature [9, 194, 195]. These reactions are usually performed using an excess of the amine (2-5 Eq.) and THF as solvent at room temperature. Polymers **P25** to **P31** were well-soluble in the solvents used for polystyrene: THF, $CHCl_3$ and CH_2Cl_2, and were not soluble in CH_3OH and H_2O. In contrast, **IX** was soluble in both MeOH and H_2O, poorly in THF and only moderately in CH_2Cl_2. When the polymers reacted with **IX** in CH_2Cl_2, 2 days and an excess (3 Eq.) of **IX** were necessary to quantitatively convert the activated ester moieties into an amide. Only when the reaction was performed in *N*-methylpyrrolidone the quantitative conversion of PFP ester moieties was reached using shorter times (around 10 hours) and a small excess of **IX** (1.2 Eq.). The polymers were purified by precipitation of the reaction mixture in cold MeOH followed by centrifugation. The successful modification of the precursors and formation of the conjugates was proven by ^1H NMR and ^{19}F NMR spectroscopies (Figure 69).

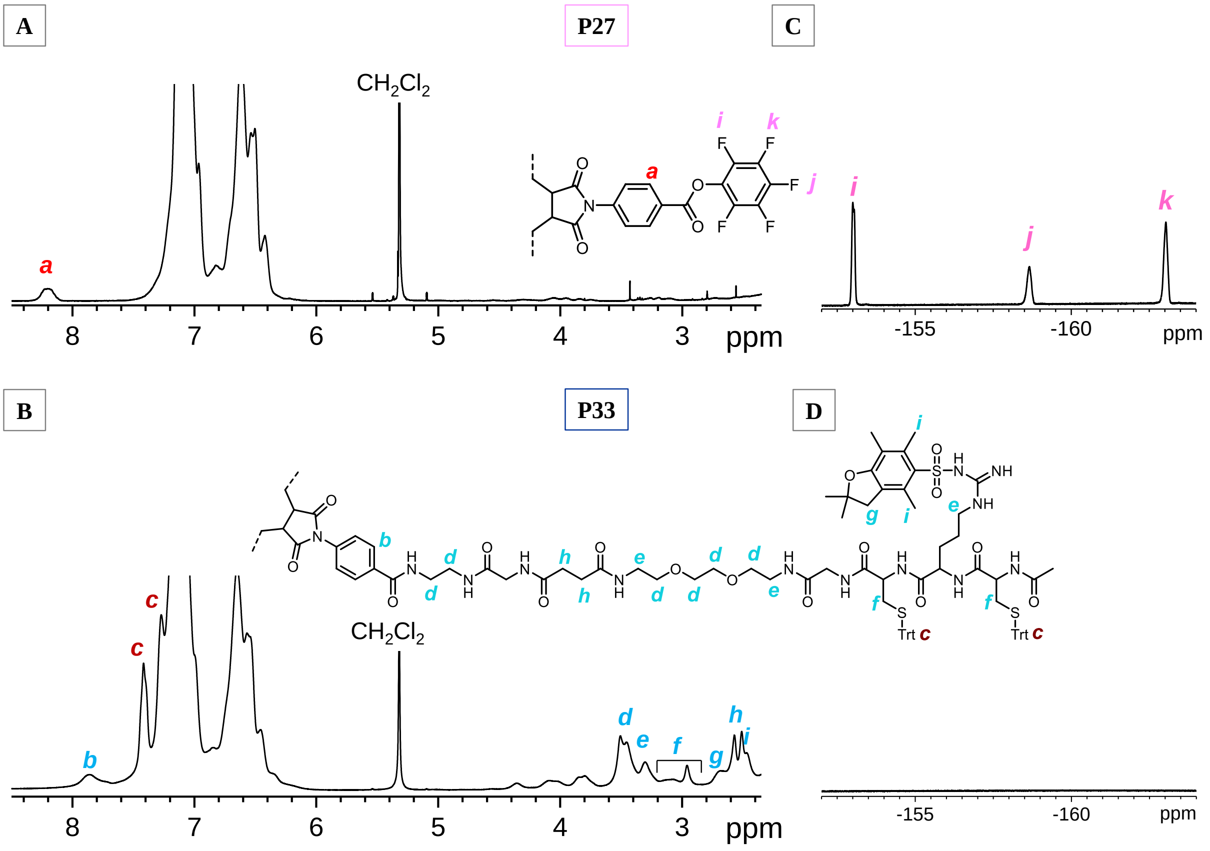

Figure 69 | (A) ^1H NMR spectrum of **P27** containing pentafluorophenyl ester moieties, **(B)** the resulting polymer **P33** after the reaction with **IX** and (**C**, **D**) the corresponding ^{19}F NMR spectra for **P27** and **P33**, in CD_2Cl_2.

The signal of the aromatic protons of pentafluorophenyl 4-succinimidobenzoate at 8.2 ppm were shifted to 7.8 ppm after the successful amidation as proved by ^{1}H NMR spectra of all polymers with CRC fragments. Moreover, the signals corresponding to the trityl group from 7.46 to 7.21 ppm and some characteristic signals of CRC fragment appeared in the spectrum (Figure 69, **B**). The spectra for the “symmetric polymer” **P29** are presented in Figure 104. The signals of pentafluorophenyl moieties vanished from all ^{19}F NMR spectra after modification, thus proving the complete transformation of PFP ester moieties.

The analysis by FT-IR spectroscopy was an additional proof that the PFP ester moieties were successfully transformed into amides. A broad activated ester carbonyl C=O stretch band at 1764 cm^{-1} and a sharp band at 1521 cm^{-1} due to the pentafluorophenyl aromatic ring for **P27** (Figure 70, **A**) vanished from the FT-IR spectrum after modification with **IX** for **P33** (Figure 70, **B**). A carbonyl C=O stretch band of a newly formed amide group band at 1660 cm^{-1} and a distinct amide bending band at 1544 cm^{-1} were observed in the FT-IR spectrum of **P33**. Moreover, a N-H band at around 3300 cm^{-1} appeared after the amidation (Figure 70, **B**).

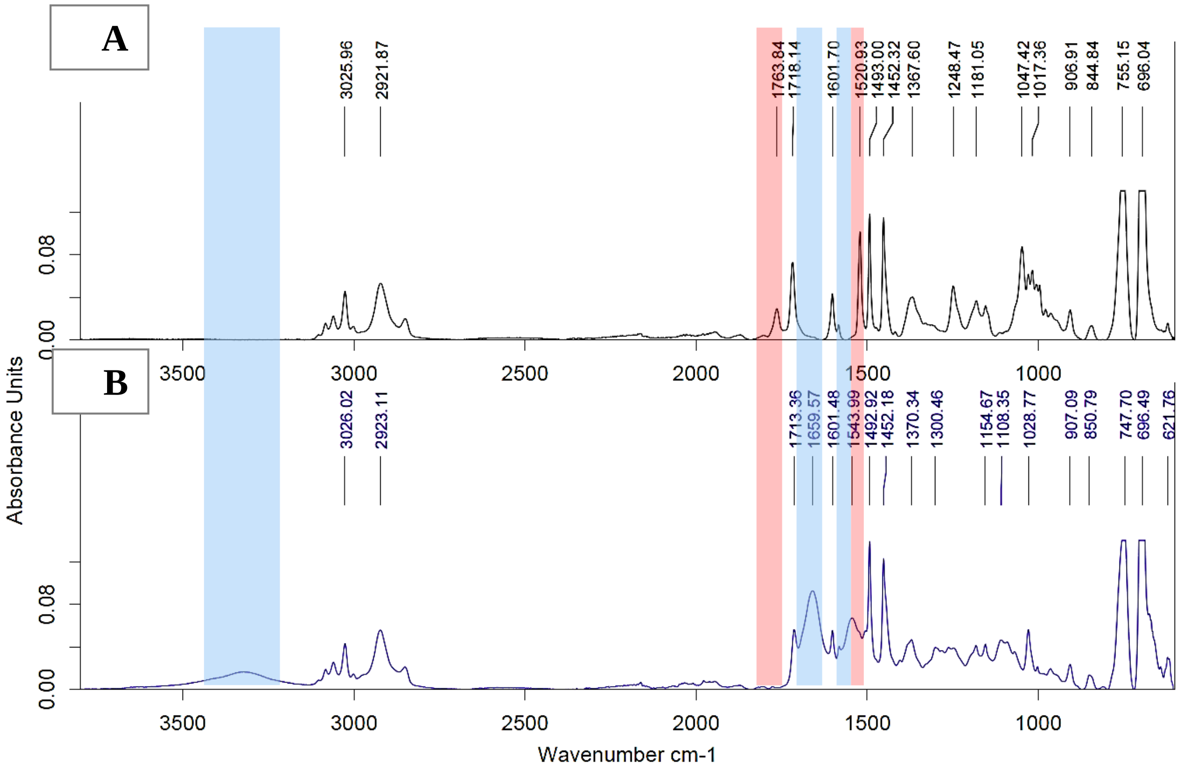

Figure 70 | (**A**) FT-IR spectrum of **P27** with PFP ester moieties and (**B**) FT-IR spectrum of the resulting polymer with CRC fragment **P33**.

An apparent decrease of the elution volume connected with the increase of molecular weight was observed by SEC after the reaction of the polymers with PFP activated ester moieties with **IX**. This result is presented for **P27** in Figure 71 (for **P29** in Figure 108). Theoretically, the difference of molecular weights after modification with 2 Eq. of **IX** should be 2724 g·mol^{-1}. The difference of molecular weights measured by SEC (ΔM_p of 2840 g·mol^{-1} for **P27** and 3540 g·mol^{-1} for **P29**) roughly corresponded to the attachment of two CRC fragments per copolymer chain. The polydispersities of the polymers with ester moieties and the modified polymers with amide moieties were similar.

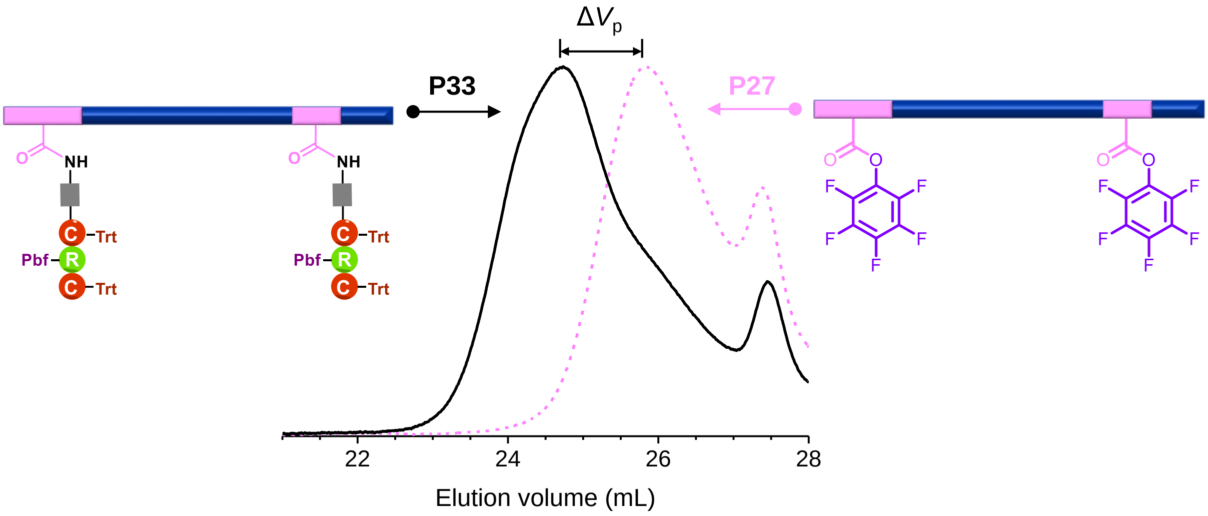

Figure 71 | Size-exclusion chromatograms of **P27** with PFP ester moieties (dashed line) and the resulting polymer after reaction with the oligomer **IX** (solid line), in DMF with 0.1 M LiBr.

III.3.3. Polymer Conjugates with CRC Fragments. Removal of Protecting Groups

After the successful insertion of CRC fragments with protected amino acid groups in the polymer chain, the Trt- and Pbf-protecting groups were removed according to a protocol adapted from the literature [200-204] (Scheme 22).

Since the trityl protecting group is stable under basic conditions and labile under acidic conditions, TFA was used for the deprotection of the thiols of the cysteine residues. Trityl cations are formed during deprotection, therefore the use of scavengers is mandatory. Silanes (such as triethylsilane (TES) and triisopropylsilane (TIS)) and water are the most efficient trityl cations scavengers and were used in the reaction since silanes can reduce them to inert triphenylmethane [202]. The solution of polymer in THF was flushed with argon to remove oxygen and avoid unwanted oxidation of the newly formed thiol groups. Moreover, a TFA/THF solution was used instead of pure TFA to avoid the degradation of the CRC motifs as proved by ^{1}H NMR.

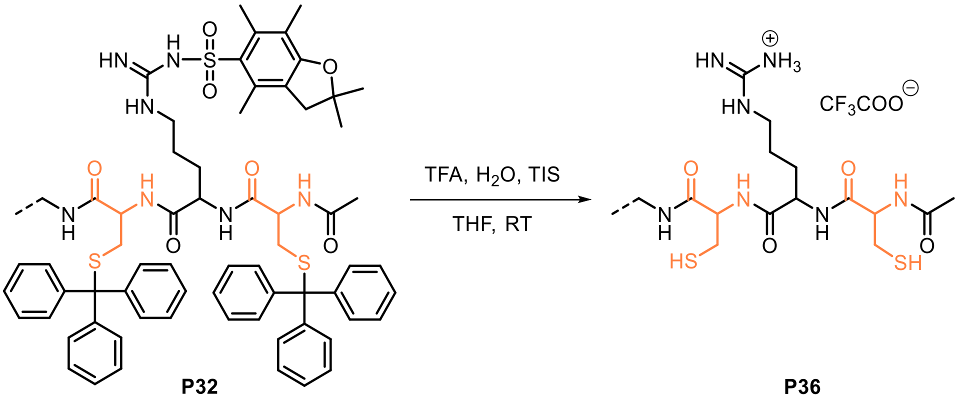

P32
P33
P34
P35

P36
P37
P38
P39

Scheme 22 | Removal of Trt- and Pbf-protecting groups from the polymers **P32** to **P36**. *Reaction conditions*: a polymer with CRC protected moieties (10^{-2} mmol), 2.5 mL of TFA / THF / H_2O / TIS = 60/45/4/1 (v/v) mixture, RT, 0.5 hour (2 hours for **P38**, **P39**), 70% yield.

In order to check if some thiol groups remain after the deprotection, the Ellman's test was used [205, 206]. Ellman's reagent (5,5'-dithiobis-(2-nitrobenzoic acid, or DTNB) reacts with thiol groups (of cysteine residues) leading to the cleavage of the disulfide bond of DTNB and the formation of 2-nitro-5-thiobenzoate, giving a yellow color due to the ionization of 2-nitro-5-thiobenzoate in the presence of a base (at neutral or alkaline pH in aqueous solution). Practically, the polymers to analyze were dissolved in a MeOH /THF 1/1 (v/v) mixture with DIPEA (0.3% vol.) followed by the addition of the Ellman's reagent in solution. A change from transparent to yellow color indicated the presence of thiol groups. This result was also confirmed by UV-spectroscopy by the appearance of the band at 425 nm (Figure 72). The successful removal of thiol groups was also evidenced by ^{1}H NMR (Figure 73), as the characteristic signals of the trityl group ranging from 7.46 to 7.21 ppm vanished after the deprotection.

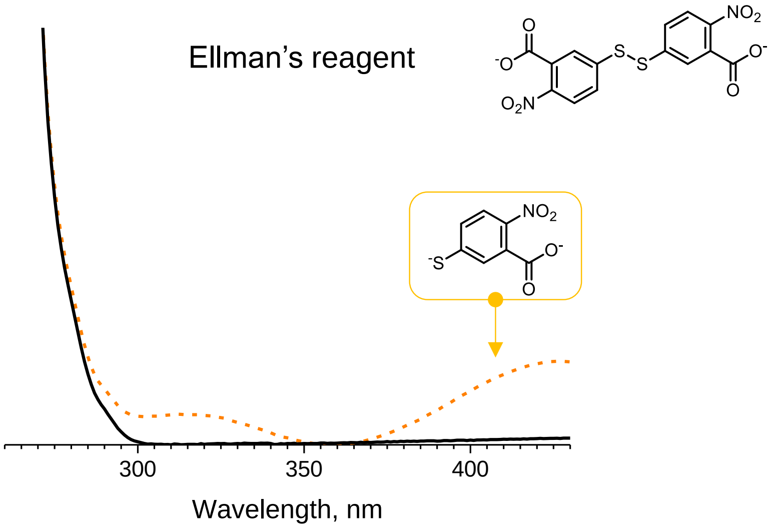

Figure 72 | Normalized UV spectra of polymers with CRC motifs, on the example of **P33** (solid line) and in the presence of the Ellman's reagent (dashed line), MeOH (UV) / THF (UV) and a drop of DIPEA.

Typical conditions for the removal of the Pbf protecting group from the guanidinium moiety of arginine include the use of an aqueous TFA solution with water as scavenger. Using the same conditions as for the deprotection of cysteine residues (Scheme 22), arginine was also deprotected as evidenced by ^{1}H NMR spectroscopy with the disappearance of the signals of Pbf-group at 2.67 and 2.43 ppm (Figure 73).

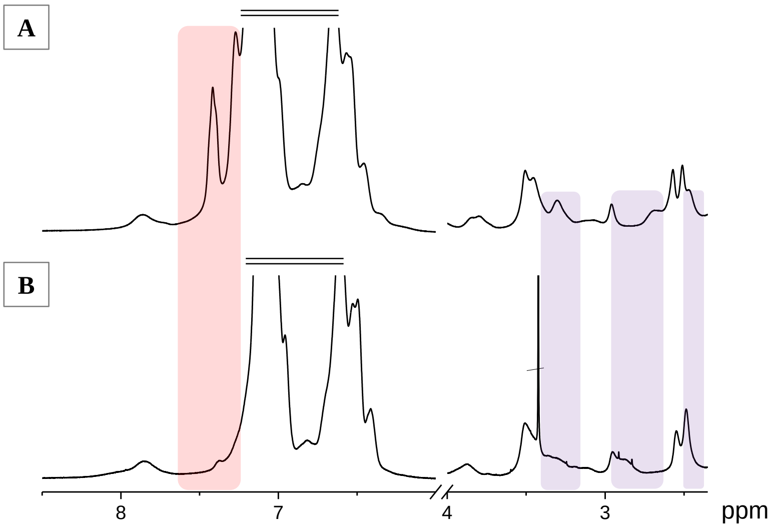

Figure 73 | (**A**) ^{1}H NMR spectrum of **P33** containing CRC motifs with Trt-cysteine and Pbf-arginine protected residues and (**B**) the resulting polymer **P37** after the removal of protecting groups, in CD_2Cl_2.

The deprotected polymers were analyzed by SEC in DMF (Figure 110) and in CH_2Cl_2 (Figure 74). A tailing was observed in the chromatograms, probably due to the interactions of the amino acid residues with the SEC column. The elution volume did not change significantly before and after deprotection.

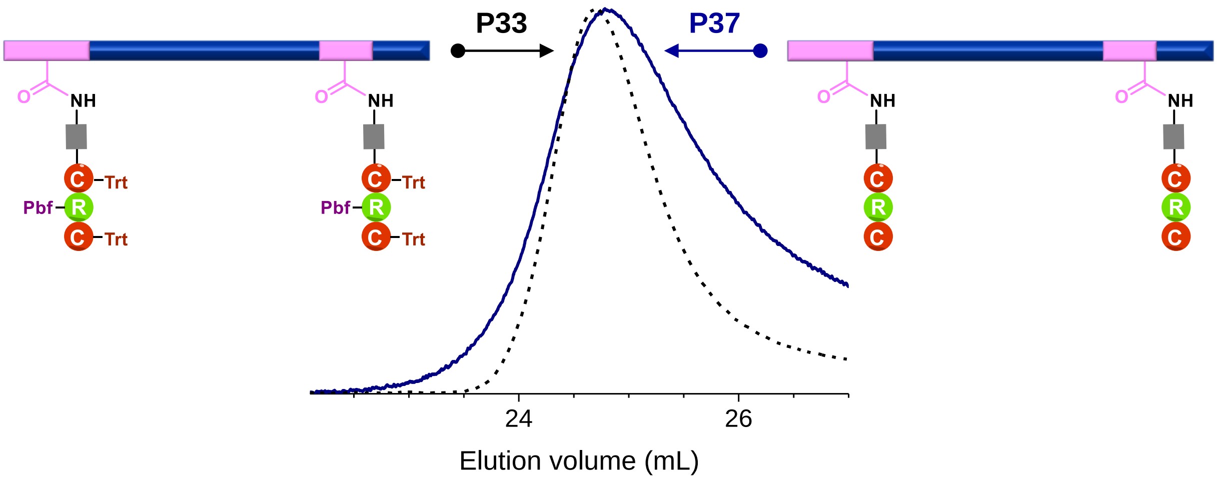

Figure 74 | Size-exclusion chromatograms of **P33** with cysteine (Trt)-arginine (Pbf)-cysteine (Trt) motifs (dashed line) and the resulting polymer after the deprotection of amino acid residues **P37** (solid line), in CH_2Cl_2.

III.4. INTRAMOLECULAR FORMATION OF DISULFIDE BRIDGES

After the successful deprotection of the thiol moieties from cysteines, intramolecular disulfide bridges could be formed by oxidation of the thiol groups from the polymers with CRC motifs in dilute conditions and in the presence of atmospheric oxygen (Scheme 23). The polymers were dissolved at a concentration of 10^{-4} M in a solution of *N*-methylpyrrolidone with 0.1-0.5% of DIPEA. Afterwards, air was bubbled into the solution for 1.5 days and 1-5% of DMSO was added to accelerate the reaction. The reaction was stopped when no thiol function was detected by Ellman's test and when the molecular weight was constant for two consecutive measurements by SEC.

During the optimization of the oxidation conditions, (Scheme 23), it was noticed that the use of both THF and DMF as solvent did not lead to the desired intramolecular reaction as proved by SEC chromatograms (Figure 111, **A**). Moreover, the addition of a base such as DIPEA was necessary for the reaction to occur and the introduction of DMSO, although not mandatory, decreased significantly the reaction time. The compaction was evidenced in the

SEC chromatogram by the increase of elution volume of the oxidized polymer compared to that with free thiols, after the addition of DIPEA (Figure 111, **B**).

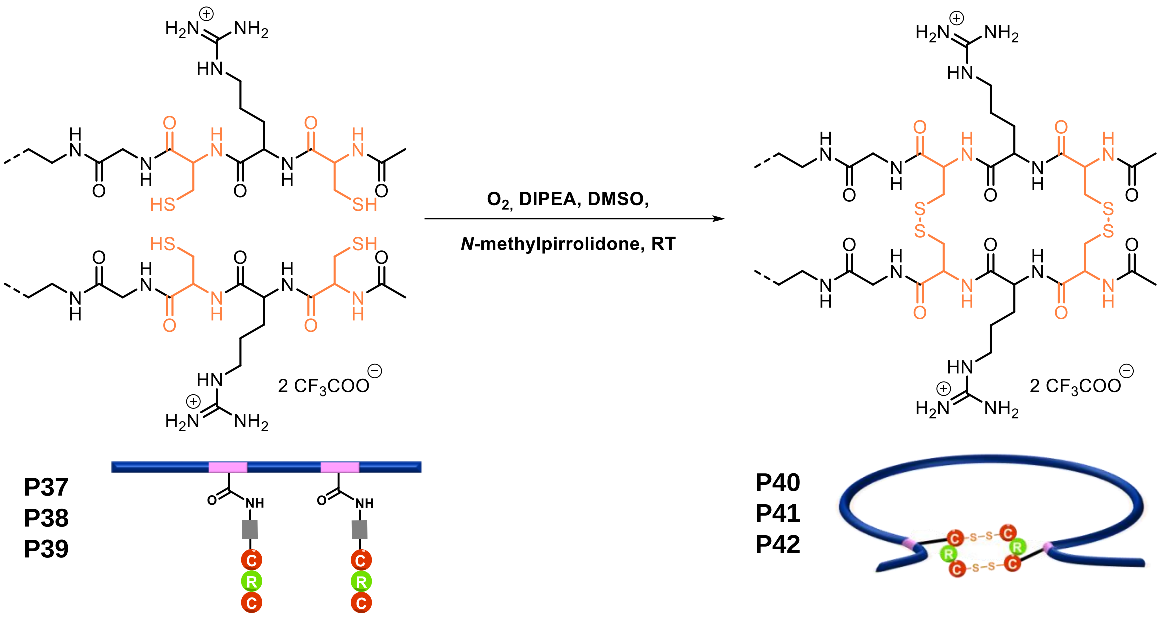

Scheme 23 | Oxidation of the polymers with CRC fragments. *Reaction conditions*: a polymer with a CRC motif (C = 10^{-4} M in *N*-methylpyrrolidone), O_2 (atmospheric), DIPEA (0.1-0.5% v/v), DMSO (1-5% v/v), RT, 1.5 days.

Indeed, disulfide bond formation depends on major factors such as the thiolate anions concentration and the accessibility of thiol groups [204].Although thiol group (protonated form) is unreactive, thiolates are able to generate disulfide bond [204]. Therefore, the pH of the reaction media plays an important role in the formation of disulfide bonds, and the oxidation of thiol group occurred preferentially when an organic base is added. Furthemore, reactive thiolate groups should be accessible, that was possible in *N*-methylpyrrolidone: a good solvent for oligomer solvation.

Optimized conditions (*i.e.*, the use of *N*-methylpyrrolidone with 0.3% DIPEA and 3% DMSO, v/v) were applied for the positioning of intramolecular disulfide bridges (Figure 75) in “asymmetric” (**P37**) and “symmetric” (**P38**) polymers with CRC motifs. Negative results of Ellman’s test confirmed the disappearance of the thiols due to the formation of the disulfide bonds. The successful compaction of the polymers was evidenced by the increase of the elution volume (ΔV_p around 0.25 mL) in SEC. This augmentation was linked to the decrease of the hydrodynamic volume (Figure 75). The difference of elution volume is similar for both **P37** and **P38**.

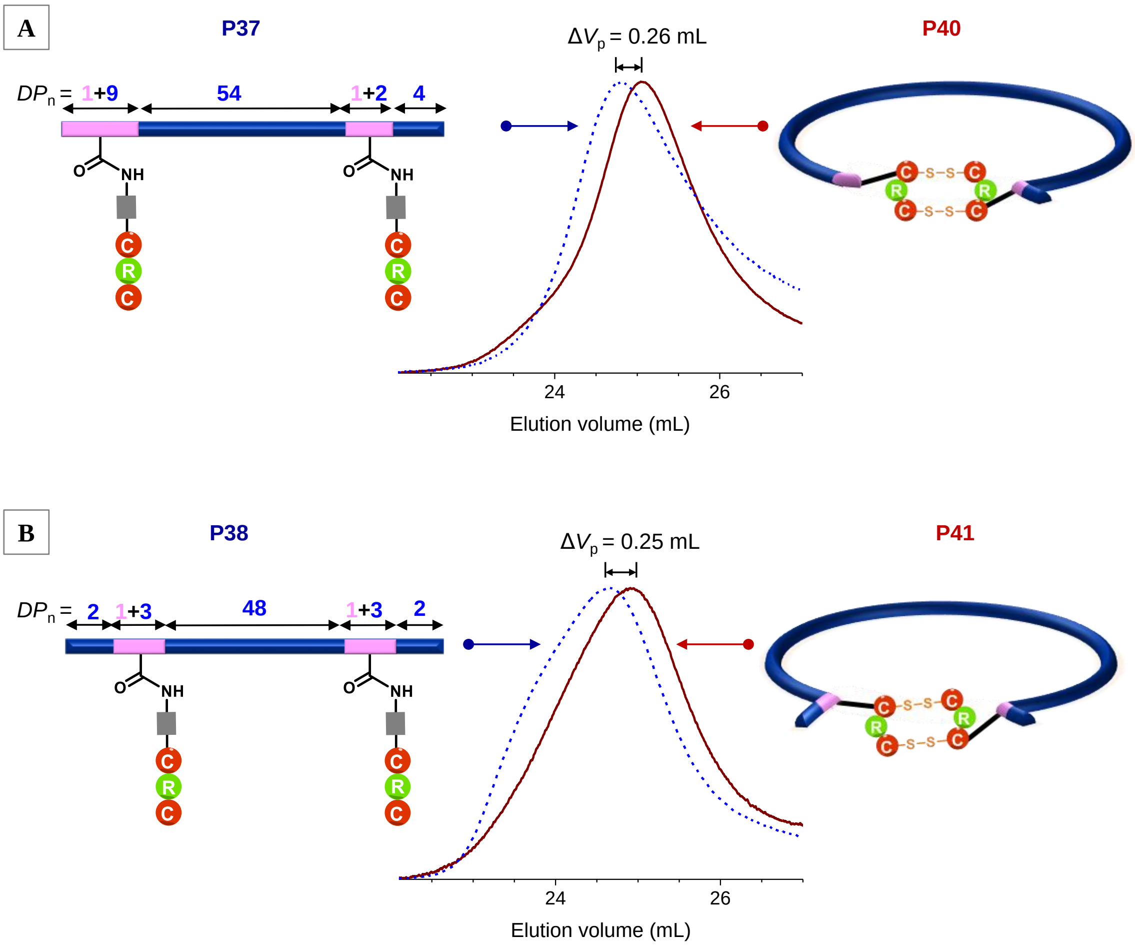

Figure 75 | SEC chromatograms for two polymers before and after oxidation. (**A**) Size-exclusion chromatograms of the polymers with CRC motifs (dashed line) **P37** and the resulting polymers after oxidation of the thiol group (solid line) **P40** in CH_2Cl_2. (**B**) Size-exclusion chromatograms of the polymers with CRC motifs **P38** and the resulting polymers after oxidation of the thiol group (solid line) **P41**, in CH_2Cl_2.

Tadpole (Figure 75, **A**) and knotted (Figure 75, **B**) single-chain topologies formed by the disulfide bonds consisted of two cycles and external “styrene arms”. The orthogonal oxidation of the CRC tripeptide thiol groups led to a “small” 22-units ring. The “big” cycle of polystyrene and oligomer fragments had similar sizes for both polymers, explaining the close changes of elution volume ΔV_p.

III.5. CONCLUSIONS

Single-chain objects with positionable twin disulfide bridges were synthesized in three steps starting from sequence-controlled precursors with precisely positioned pentafluorophenyl ester moieties. Interestingly, the sizes of the polymer ring and the external “arms”, and therefore the shape of the compacted single-chain objects could be controlled by varying the placement of reactive functions in the polymer chains. Cysteine-arginine-cysteine (CRC) motifs were successfully incorporated into the polymer chains by activated ester/amine chemistry on these reactive functions. Moreover, intramolecular cyclization was favored compared to intermolecular reactions. Although this study presented model single-chain objects with self-associating CRC motifs, it is possible to envision the design of new water-soluble multi-cyclic bio-hybrids polymer for applications in aqueous medium, by the combination of the polymers and peptides properties [207-209].

CHAPTER IV. SINGLE-CHAIN POLYMER METAL COMPLEXES

IV.1. METAL-LIGAND INTERACTIONS DRIVING POLYMER COMPACTION

IV.1.1. Introduction

In the previous chapter, single polymer chain folding using dynamic covalent bonds was studied. This chapter focuses on the compaction of polymer chains by non-covalent metal-ligand interactions. Although this type of interactions has been widely investigated in the field of supramolecular chemistry and for supramolecular polymers [123, 210-215], the use of metal complexation for single polymer chain folding/compaction has been rarely described in the literature [6, 7, 33]. Taking into consideration the originality of the study and the wide range of available metal complexes, the possibility to synthesize and characterize single chain polymer metal complexes was investigated. An interesting feature of the metal/ligand coordination is the possibility to tune the bond strength by changing the metal ion, ligand and reaction conditions; thus, polymer complexes range from stable to dynamic.

In the last years some progress in the synthesis of metal-containing single chain polymers was reported by Lemcoff, Pomposo and Barner-Kowollik [6, 7, 33] as discussed in Chapter I.4.2.A.2. Their studies were connected with the synthesis and characterization of either a cyclic polymer containing intramolecular metal-coordination bond, or SCNPs with multiple metal-ligand self-associations. The ligands were positioned either at polymer chain ends, or randomly in the polymer chains. In this thesis, a precise placement of ligands in the polymer chain followed by the formation of metal-ligand self-associations of the single polymer chains was studied. The linear polymers were designed to contain two ligands at two different positions in the polymer chain in order to complex a chosen metal ion with two parts of the same polymer chain. The formation of coordination bonds is based on donation of a lone electron pair of the ligand (Lewis base) to the metal ion (Lewis acid) [123]. In addition to the binding strength, each metal/ligand couple is characterized by an exchange rate leading to different stabilities of metal polymer complexes and influencing the dynamic nature of the bonding. Chelating properties of the ligand also determine the stability of the formed metal complex. Furthermore, different complex geometries can be obtained depending on the metal coordination, such as linear, tetrahedral, octahedral, trigonal-planar, *etc*.

IV.1.2. Selection of Metals and Ligands

Ruthenium(II) was used in the present work, since it is a transition metal resulting in thermally, chemically and photo-chemically stable structures [123, 216]. A versatile Ru(II) precursor in inorganic synthesis, dichlorotetrakis(dimethyl sulfoxide) ruthenium(II) (Scheme 24, [Ru(II)Cl_2(DMSO)$_4$]), was chosen as metal complex, since it is easy to prepare, handle, and it is soluble in a wide range of solvents [216]. Moreover, it has a versatile reactivity: neutral ligands preferentially replace the sulfoxide groups (from one to four depending on the reaction conditions) and anionic ligands or weak organic acids replace both DMSO and halide ligands.

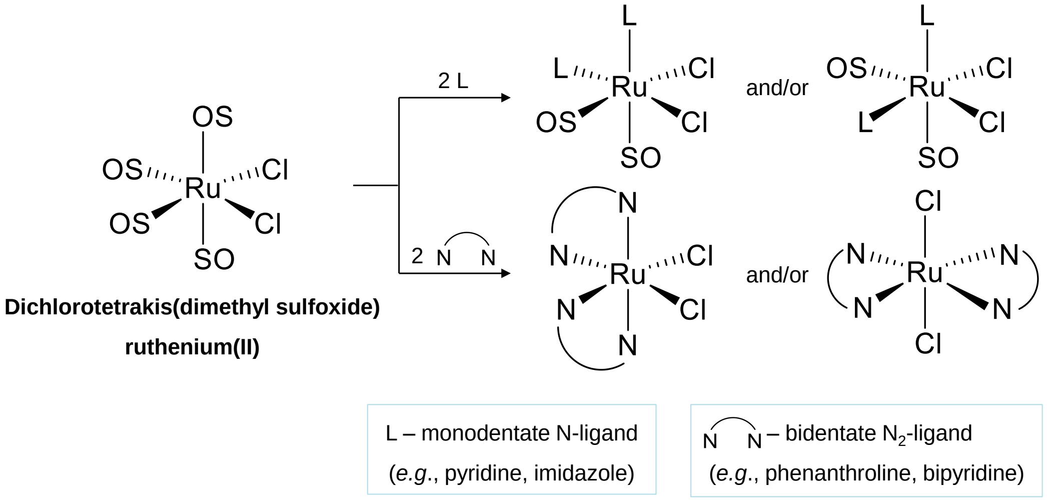
OS
OS
Ru
Cl
OS
Cl
SO
Dichlorotetrakis(dimethyl sulfoxide) ruthenium(II)
2 L
2 N N
L
L
Ru
Cl
OS
Cl
SO
and/or
L
OS
Ru
Cl
L
Cl
SO
N
N
Ru
Cl
N
Cl
N
and/or
Cl
N
Ru
N
N
N
Cl
L – monodentate N-ligand
(e.g., pyridine, imidazole)
N N – bidentate N2-ligand
(e.g., phenanthroline, bipyridine)

Scheme 24 | Modification of dichlorotetrakis(dimethyl sulfoxide) ruthenium(II) [Ru(II)Cl_2(DMSO)$_4$] complex with monodentate N-donor (L) and bidentate N_2 ligands [216].

Since DMSO ligands could be selectively replaced by neutral ligands and since each polymer chain should contain two ligand units, it was decided to choose monodentate N-donor (L) or bidentate N_2 ligands (Scheme 24) for the intramolecular folding by complexation with Ru(II). The O-bonded DMSO is the most labile, therefore it is the first to be replaced by stronger donors under mild conditions (room temperature) [216]. Two DMSO ligands can be substituted quite easily by two monodentate ligands or a bidentate ligand in refluxing organic solvents (*e.g.*, ethanol, toluene, $CHCl_3$). The use of two equivalents of a bidentate chelating ligand for one equivalent of Ru(II) complex results in the replacement of the four DMSO ligands, although in some cases [217] refluxing in DMF was necessary.

The synthesis of polymer metal complexes with palladium(II) was also investigated. The complexes formed by Pd(II) have a different geometry compared to those formed by Ru(II); a stable electronic configuration is achieved at 18 electrons for Ru(II) complexes with a favored octahedral geometry, whereas a stable electronic configuration is achieved at 16 electrons for Pd(II), leading to the formation of square planar complexes [218]. A commercially available reagent, tetrakis(acetonitrile)palladium(II) tetrafluoroborate (Scheme 25), was used as Pd(II) precursor [219]. The replacement of two acetonitrile groups by two equivalents of stronger monodentate ligands (*e.g.*, pyridine) usually leads to a mixture of cis- and trans-complexes, although trans-complexes are thermodynamically more stable. The substitution of all acetonitrile groups by two equivalents of bidentate N_2-ligands was described in the literature [218, 220], and it was noticed that the square-planar geometry of palladium atom is distorted due to the intramolecular steric interactions of the bidentate ligands [221]. For instance, the planes of the two ligand molecules of bipyridine and phenanthroline are tetrahedrally twisted (with an angle around 20º) [218].

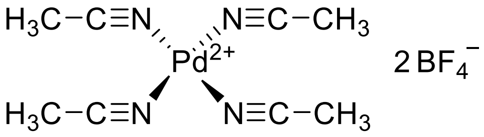

Tetrakis(acetonitrile)palladium(II) tetrafluoroborate

Scheme 25 | Tetrakis(acetonitrile)palladium(II) tetrafluoroborate $[Pd(CH_3CN)_4(BF_4)_2]$.

1,10-Phenantroline was chosen as chelating ligand for the synthesis of polymer metal complexes with Ru(II) and Pd(II). Compared to aliphatic diamines the nitrogen atoms of 1,10-phenantroline (phen) are less nucleophilic [222]. Nevertheless, phen usually displays strong coordination with most transition metal cations [222-224]. Coordination ability of phen is determined by distinct features such as a rigid planar structure with two nitrogen atoms held in juxtaposition. In contrast to bipyridine, the free rotation around the linking bond is absent.

IV.1.3. General Strategy

The synthesis of the polymer metal complexes was divided into two parts (Figure 76). First, sequence-controlled polymers with phenanthroline moieties were synthesized with two phenanthroline ligands positioned in the polymer chain. The second part consisted in the intramolecular complexation of these polymers with Ru(II) and Pd(II) metal ions.

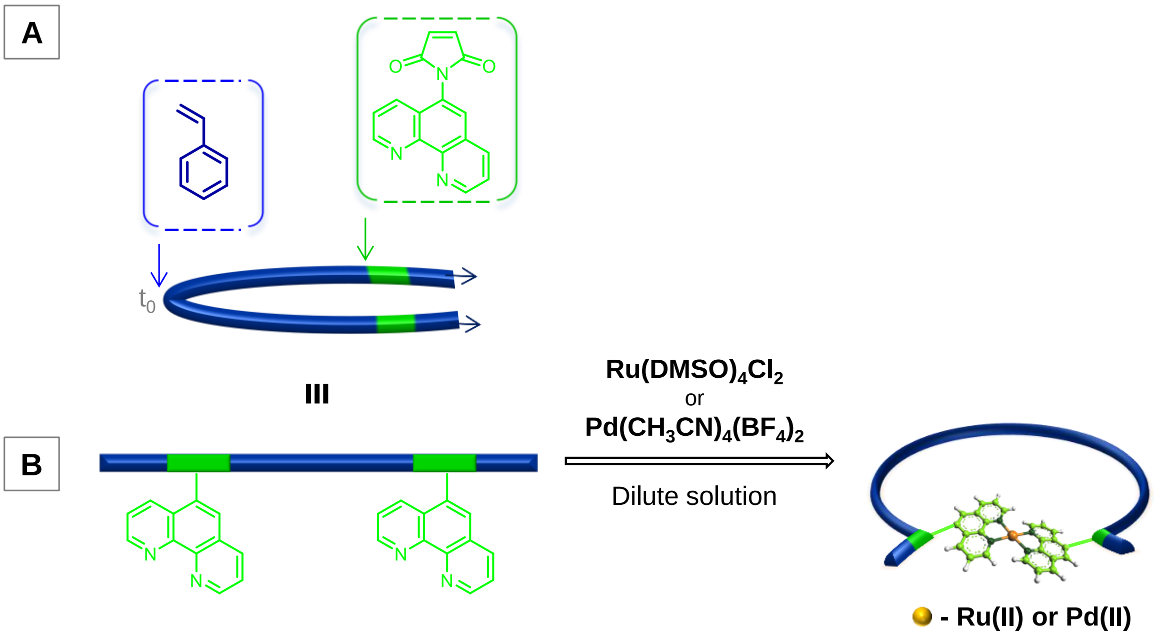

Figure 76 | General strategy of the project. (**A**) Synthesis of sequence-controlled precursors by copolymerization of styrene with 1,10-phenanthrolin-5-maleimide (MI-phen). (**B**) Intramolecular complexation leading to a single-polymer chain folded by metal-ligand interactions.

Two synthetic routes were considered for the synthesis of the polymers with precisely positioned phenanthroline ligands:

1) The controlled/living radical copolymerization of styrene with maleimides containing a phenanthroline moiety;
2) The controlled living radical copolymerization of styrene with maleimides containing reactive groups (*i.e.*, PFP ester or anhydride) followed by a substitution of these groups by a compound containing a phenanthroline moiety (1,10-phenanthrolin-5-amine).

The first method being straightforward, it has been initially examined.

IV.2. SEQUENCE-CONTROLLED POLYMERS CONTAINING PHENANTHROLINE MOIETIES

IV.2.1. Direct Synthesis of Sequence-controlled Polymers Containing Phenanthroline

IV.2.1. Synthesis of 1,10-Phenanthrolin-5-maleimide X

1,10-phenanthrolin-5-maleimide **X** (Scheme 26) was synthesized in two steps[225]. Maleic anhydride reacted with 1,10-phenanthrolin-5-amine in CH_2Cl_2 followed by the closure of the maleimide cycle in the presence of a big excess of sodium acetate in acetic anhydride. The crude was dissolved in CH_2Cl_2, washed with water and then precipitated in pentane. Compound **X** was obtained as an orange powder after filtration and drying. The product was characterized by ^{1}H (Figure 124), ^{13}C and DEPT-135 NMR spectroscopies confirming the formation of the targeted compound **X**. The presence of a small amount of impurities was detected, but they did not interfere with the polymerization.

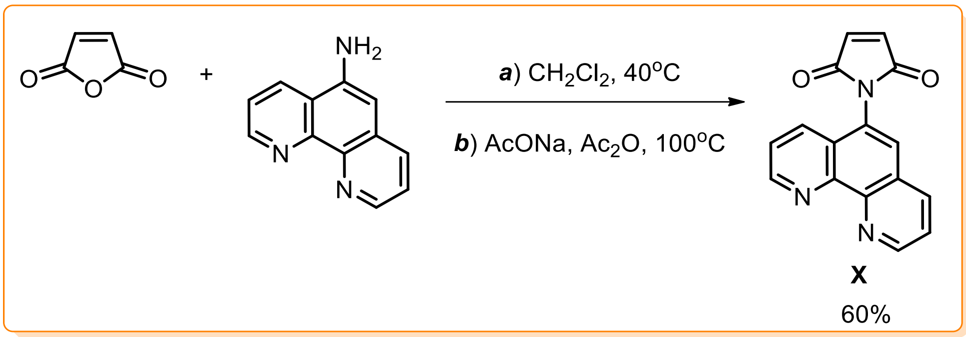

Scheme 26 | Synthesis of 1,10-phenanthrolin-5-maleimide **X**. *Reaction conditions*: ***a***) maleic anhydride (3 Eq.), 1,10-phenanthrolin-5-amine (1 Eq.), CH_2Cl_2, 40ºC, 10 hours; ***b***) AcONa (12 Eq.), Ac_2O, 100ºC, 3 hours; total yield 60%.

IV.2.2. Sequence-controlled Polymers Containing Phenanthroline Groups

Among all CRP techniques that could have been used for the copolymerization of the phenanthroline maleimides with styrene, NMP was chosen for its simplicity and the absence of metal salts which could complex the phenanthroline moiety [210]. Sequence-controlled polystyrenes with precisely positioned phenanthroline functional groups were prepared by the NMP of styrene with maleimide **X** in the presence of the bifunctional alkoxyamine **VIII**

(Figure 67). The results will be illustrated by a few examples as shown in Table 4 (Not all synthetized polymers are displayed).

Table 4 | Kinetic data recorded for the NMP of styrene with MI-phen **X** using **VIII**.

	Insertion of MI-phen **X**					End of polymerization		SEC data		
	Eq. **X**	$t_{add.}$[a], [min]	Conv.$_S$ at t_{add}[b]	t_1[c], [min]	Conv.$_S$ at t_1[b]	t_{end}[d], [min]	Conv.$_S$ at t_{end}[b]	M_n[e], [$g \cdot mol^{-1}$]	M_{theo}[f], [$g \cdot mol^{-1}$]	M_w/M_n[e]
P43	1	60	0.60	95	0.75	95	0.75	8210[g]	7290	1.12[g]
P44	2	49	0.62	70	0.72	90	0.80	10260	9640	1.60
P45	2	98	0.55	112	0.62	126	0.66	5690	8190	1.72
P46	6	52	0.60	85	0.78	85	0.78	-	-	-

Polymerization conditions: styrene (100 Eq.), **X** (1 – 6, see table), **VIII** (1 Eq.) styrene/anisole 1/1 (2/1 for **P44**, **P46**) v/v, 116°C. [a]Time at which the addition of **X** was performed. [b]Styrene conversion calculated from ^{1}H NMR spectra. [c]Time at which full conversion of **X** was observed. [d]Time at which the polymerization was ended. [e]Measured by SEC in *N*-methylpyrrolidone with 0.1 M LiBr. [f]$M_{theo} = M_{\mathbf{VIII}} + M_S \cdot conv._S \cdot [S]/[\mathbf{VIII}] + M_X \cdot [\mathbf{X}]/[\mathbf{VIII}]$. [g]Measured by SEC in CH_2Cl_2.

VIII provided the growth of polymer chains in two directions during the polymerization (Figure 77, **A**). MI-phen was added at the end of the reaction, since the introduction of maleimides close to the polymer chain ends should have led to a more precise placement of **X**. However, the regions of the incorporation of acceptor monomer were quite broad for **P43-P46**. For example, each maleimide unit was accompanied by 5 styrene units for **P44** (Figure 77, **B**). This result can be explained by the moderate solubility of **X** in the polymerization medium, although the maleimide was added in a solution of DMF. Moreover, the nature of **X** played an important role that will be further discussed with the calculation of the styrene reactivity ratio r_S.

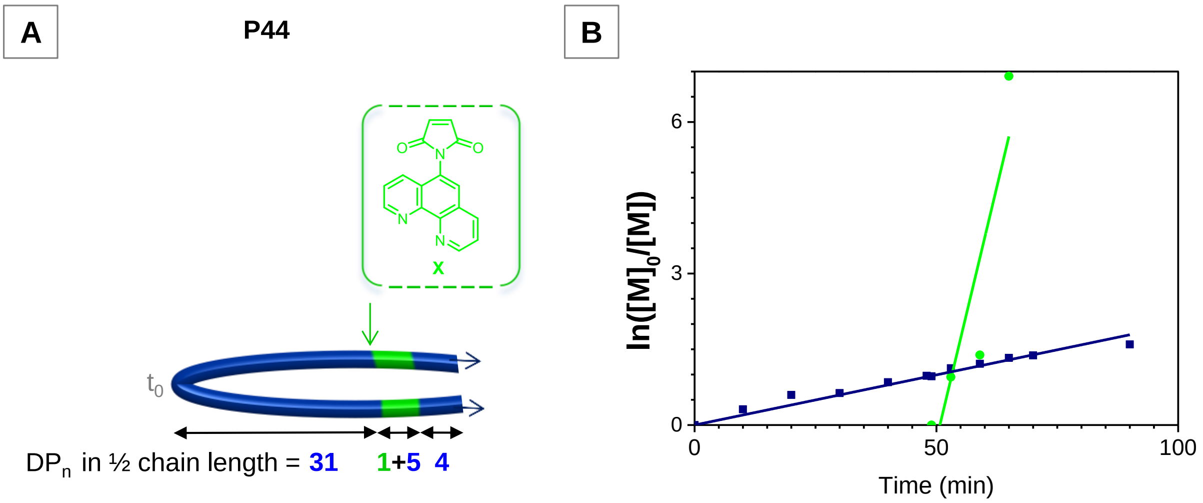

Figure 77 | Synthesis of sequence-controlled polymer by NMP of styrene with 1,10-phenanthrolin-5-maleimide **X** added at the end of the polymerization in the presence of the bifunctional alkoxyamine **VIII**. (**A**) Estimated microstructure of **P44**. (**B**) Corresponding semi-logarithmic plot of comonomer conversions *versus* time for **P44**.

The styrene reactivity ratio was calculated by the Jaacks equation [176]:

$$\ln[M_S]_t / \ln[M_S]_0 = r_S \cdot \ln[M_X]_t / \ln[M_X]_0,$$

where $[M_S]_0$ and $[M_X]_0$ - initial concentrations of the styrene and MI-phen **X**; $[M_S]_t$ and $[M_X]_t$ – concentration of the unreacted styrene and **X**, respectively; r_S – reactivity ratio of styrene.

This equation can be applied for this copolymerization, since styrene is a homopolymerizable monomer that was taken in a big excess compared to the maleimide. The styrene reactivity ratio r_S was obtained as a slope of the logarithmic plot of styrene monomer conversion *versus* the maleimide monomer conversion (Figure 78). For all the copolymerizations that have been performed in this chapter, the measured styrene reactivity ratio r_s was around 0.2-0.3 (*e.g.*, r_s = 0.18±0.01 for **P44** and r_s = 0.29 ±0.04 for **P46**). Consequently, the copolymerization of styrene with maleimide was still more favorable than the homopolymerization of styrene. However, this reactivity ratio indicated a smaller tendency to alternation compared to the reactivity ratios presented in Chapter 2 and 3 for similar systems (with r_s closer to zero). These results can be easily explained, since the electron-rich phenanthroline group decreases the acceptor properties of maleimide **X** comparatively to the maleimides previously used (MI-PFP or maleimides **II-V** (Figure 48)), leading to a less precise placement of **X** in the polymer chain.

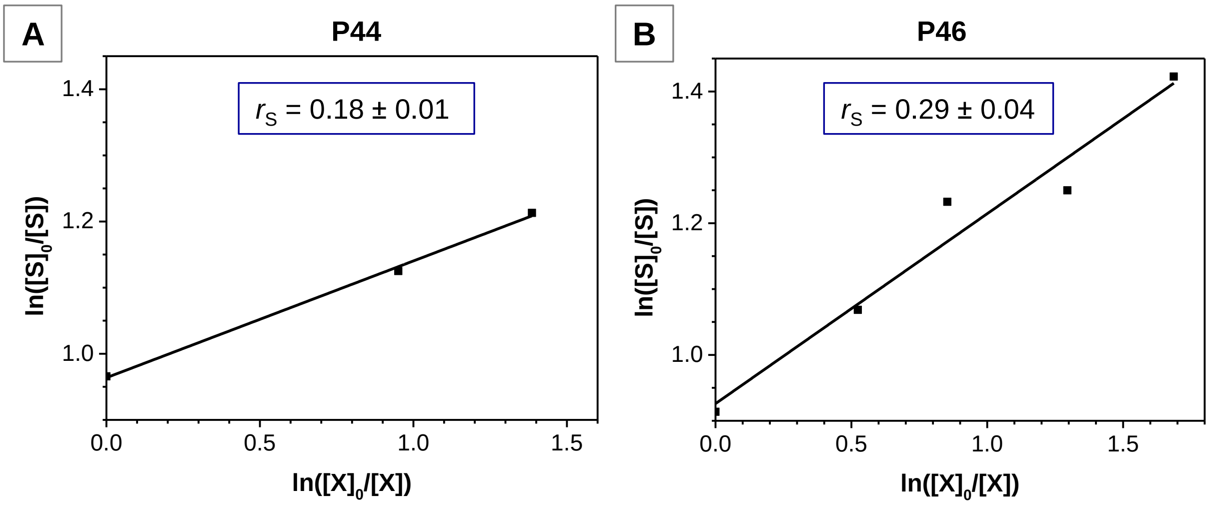

Figure 78 | Calculation of styrene reactivity ratio r_S (Jaacks plots). (**A**) Logarithmic plot of styrene **S** monomer conversion *versus* maleimide **X** monomer conversion for **P44**. (**B**) Logarithmic plot of styrene **S** monomer conversion *versus* maleimide **X** monomer conversion for **P46**.

Polystyrenes with phenanthroline ligands **P43** to **P46** were characterized by SEC. The choice of the conditions (solvent, temperature and additives) was important due to the interactions of the polar phenanthroline with the active sites of the SEC column. Moreover, the number of phenanthrolines per polymer chain strongly influenced the results obtained by SEC. The standard protocol for the SEC analysis of these polymers in THF at room temperature was difficult due to peak overlapping caused by a partial absorption of the polymers on the column. As a result, the measured molecular weight distributions were broad, and the chromatograms had a low molecular weight tailing. In addition, no signal on the chromatogram could be obtained for the polymer with six phenanthroline moieties (**P46**). As an example, the analysis of **P43** by SEC in THF at 30°C is presented in Figure 79, **A**. **P43** was analyzed by SEC of in CH_2Cl_2 that gave a better result (Figure 79, **B**). The molecular weight of **P43** in CH_2Cl_2 (M_n = 8210 g·mol^{-1}) was close to the theoretical one (M_{theo} = 7290 g·mol^{-1}) and the molecular weight distribution was narrow with a M_w/M_n = 1.12 (Table 4).

The characterization of **P44-P45** (with two phenanthroline groups in the polymer chains) by SEC in CH_2Cl_2 did not succeed. However, the change of the solvent from CH_2Cl_2 to *N*-methylpyrrolidone, the addition of a salt (0.1M LiBr) and the increase of the temperature to 60ºC allowed the analysis of these polymers by SEC (Figure 80). However, the molecular weight distributions were still broad due to the remaining presence of interactions of the phenanthroline groups with the SEC column (Table 4). The SEC analysis of **P46** (with six phenanthroline moieties) using 0.1M LiBr in *N*-methylpyrrolidone at 60ºC did not succeed. Consequently, a better separation system (eluent with additive) should be found.

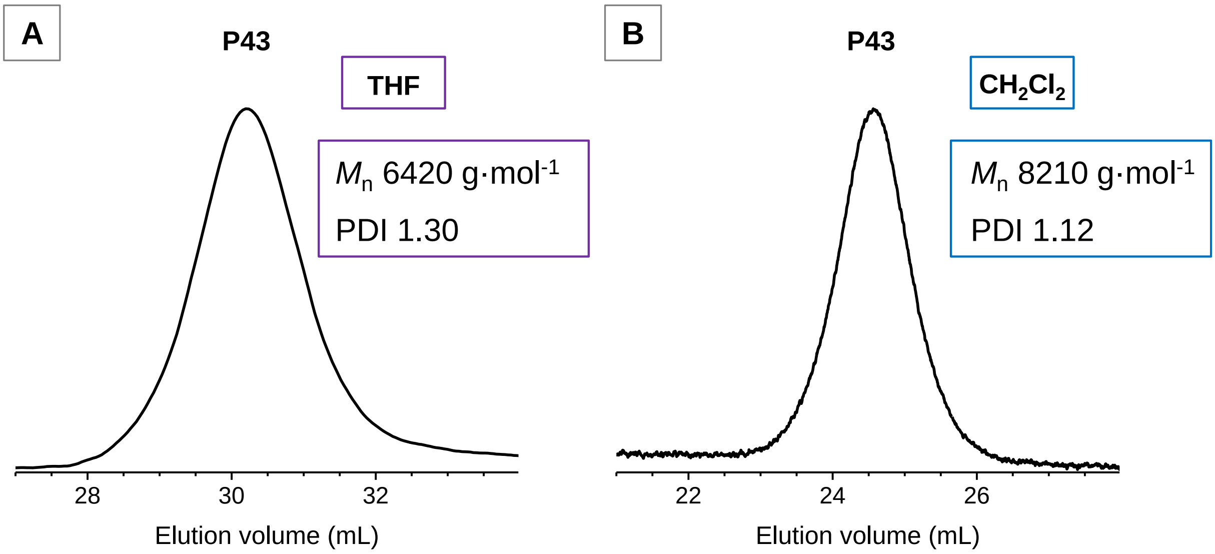

Figure 79 | SEC analysis of **P43** with one phenanthroline moiety. (**A**) Chromatogram in THF. (**B**) Chromatogram in CH_2Cl_2.

The difficulties to analyze similar polymer complexes carrying terpyridine units have been already described by Trouillet *et al*. [211], Peter *et al*. [212] and Meier *et al*. [226]. The SEC analysis was unsuccessful when eluents such as THF, $CHCl_3$ or dimethylacetamide, without and with additives (salts, Et_3N or *i*-PrOH), were used. However, the non-specific interactions of the supramolecular complexes containing metal-ligand (ruthenium(II) bis-terpyridine) moieties were overcome when a specific chromatographic system with $5 \cdot 10^{-3}$ M NH_4PF_6 in DMF at 50ºC was chosen [226]. These conditions could not be examined in the present work, since the SEC service provides only a narrow range of solvents, with 0.1 M LiBr as additive and 60ºC column temperature for *N*-methylpyrrolidone. In perspective, more elaborated systems could be tested in order to determine more precisely the molecular weight distributions of the polymers with phenanthroline units.

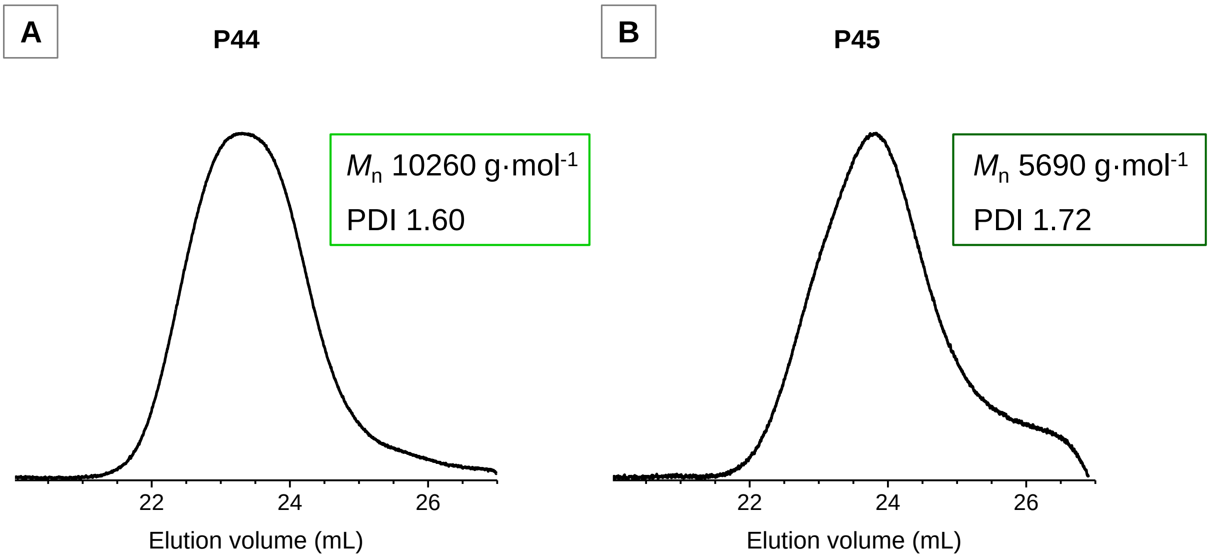

Figure 80 | SEC analysis of the polymers with two phenanthroline moieties, in *N*-methylpyrrolidone with 0.1 M LiBr. (**A**) Chromatogram of **P44**. (**B**) Chromatogram of **P45**.

The presence of phenanthroline moieties in the polymers was confirmed by ^{1}H NMR spectroscopy (Figure 81). The characteristic signals of phenanthroline were observed at 9.06-9.33 ppm, 8.22 ppm and 7.67 ppm. ^{1}H NMR spectroscopy was also used to calculate monomer conversions by the disappearance of the MI-phen (2,9-phen protons) at 9.30 ppm and the appearance of a broad signal of the MI-phen incorporated in the polystyrene from 9.06 to 9.33 ppm (Figure 81, **a**, **a'**).

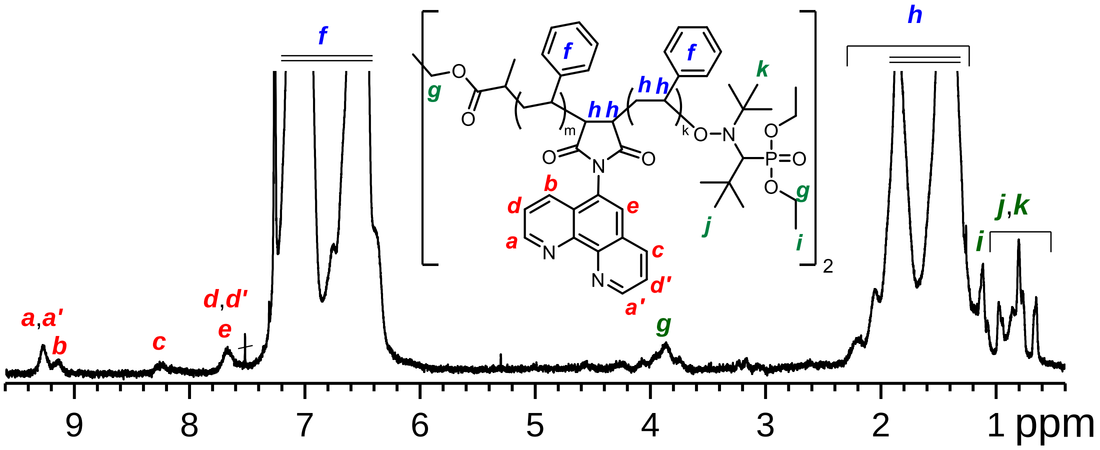

Figure 81 | ^{1}H NMR spectrum of **P44**, in $CDCl_3$.

Maleimide **X** carrying a phenanthroline unit was positioned in a broad region of the polystyrene chain (Figure 77). In order to reduce the size of this region (*i.e.*, insert more precisely the maleimide), the maleimide could be chemically modified by the addition of an alkyl spacer between the phenanthroline and the maleimide moieties or by post-polymerization modifications with a reactant carrying a phenanthroline functional group.

IV.2.2. Post-Polymerization Modification using 1,10-Phenanthrolin-5-amine

Another method was investigated for the precise insertion of phenanthroline moieties in a polystyrene chain *via* the chemical modification of sequence-controlled polystyrene/maleimide-activated acid copolymers. The strategy consisted in the nucleophile substitution of the activated acid moiety with the amine function of 1,10 phenanthrolin-5-amine after the polymerization. Two polymers reactive toward amidation were chosen such as polystyrene with PFP ester groups (**P29**) and a polymer containing succinic anhydride units (**P47**). Nevertheless, the modification using 1,10-phenanthrolin-5-amine did not work (Scheme 27), as confirmed by ^{1}H NMR and IR spectra, under various conditions: polymer (1 Eq. of reactive groups), 1,10 phenanthrolin-5-amine (3 Eq.) *a*) in CH_2Cl_2 anhydrous at 40ºC for 2 days; *b*) in THF anhydrous at 60°C for 5 days; *c*) in DMF at 70°C for 1 day; *d*) using DMAP (1 Eq.) in DMF at 70°C for 1 day. The use of DMAP in DMF at 70ºC led to the removal of the PFP-group.

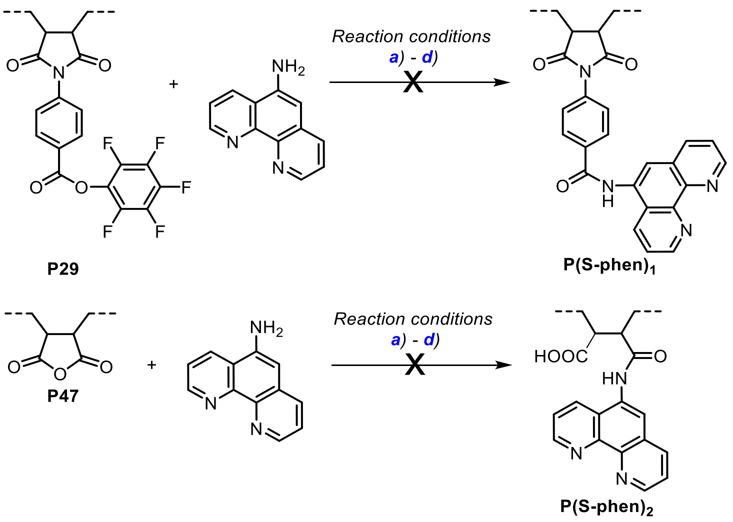

Scheme 27 | Trials to synthesize the polymers with phenanthroline ligand **P(S-phen)** by modification of **P47** or **P29** with 1,10-phenantrolin-5-amine. *Reaction conditions*: **P29** or **P47** (1 Eq. of PFP ester groups or succinic anhydride), 1,10-phenantrolin-5-amine (3 Eq.) ***a***). THF, 1 day, RT; ***b***). THF anhydrous, 5 days, 60°C; ***c***). DMF, 1 day, 70°C; ***d***). DMAP (1 Eq.), DMF, 1 day, 70°C.

Theato and coworkers reported that poly(pentafluorophenyl 4-vinylbenzoate) reacts with primary aromatic amines yielding the corresponding amide with a 100% conversion [195], though the modification under the same conditions of poly(pentafluorophenylmethacrylate) does not occur [227]. However, the transformation of both polymers with primary and secondary aliphatic amines proceeded with a close to 100% conversion rate [195, 227], proving that the nature of the activated ester and the amine are crucial for the reaction success. Therefore, another type of activated acid should be found, or the use of a phenanthroline derivative containing a primary aliphatic amine moiety. However, these aspects were not investigated, since the first methodology (*i.e.*, direct copolymerization of styrene with phenanthroline-bearing maleimide) was straightforward and allowed a simple methodology for the insertion of phenanthroline moieties in polymer chains. Afterwards, the synthesis of polymer metal complexes based on **P43** to **P45** (Table 4) was examined using $[Ru(II)Cl_2(DMSO)_4]$ or $[Pd(CH_3CN)_4(BF_4)_2]$.

IV.3. POLYMER METAL COMPLEXES

IV.3.1. Polymer Ruthenium(II) Complexes

The conditions for the synthesis of the polymer complexes using $[Ru(II)Cl_2(DMSO)_4]$ were first examined for **P43** (containing only one phenanthroline moiety). The complexation was performed in $CHCl_3$ with DMF at 60ºC in diluted conditions (10^{-4} – 10^{-3} M) using various Ru(II) complex to polymer molar ratio (from 1/1 to 1/3). Solvents such as EtOH, $CHCl_3$ and DMF are usually used to replace the four DMSO molecules by two bidentate neutral ligands [216]. One day after the addition of the metal in the diluted polymer solution, the solvent was partially evaporated followed by the precipitation of the complexes in cold MeOH. Centrifugation yielded the metal polymer complexes as violet powders, and then they were characterized by ^1H NMR spectroscopy and SEC. The complexation of **P43** with Ru(II) broadened the signals of phenanthroline and eventually made them vanish (Figure 82, **B**). The ratio of phenanthroline group to metal complex (1/1) resulted in the formation of mono- and bi-polymer complexes (or a mixture of them).

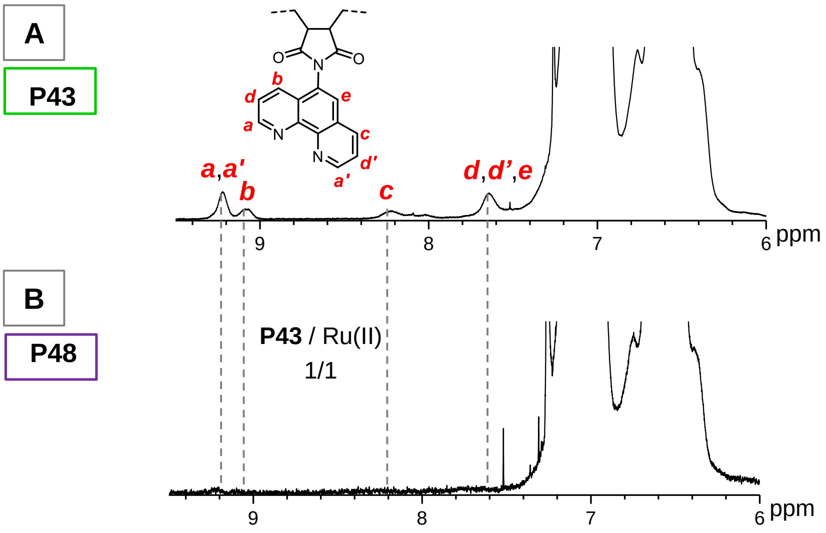

Figure 82 | ^{1}H NMR spectra of **P43** and its complexes with Ru(II). (**A**) ^{1}H NMR spectrum of **P43**; (**B**) ^{1}H NMR spectrum of Ru(II) polymer complex **P48**, (**P43**/Ru(II) = 1/1 molar ratio), in $CDCl_3$.

The metal polymer complexes were also investigated by SEC in CH_2Cl_2 (Figure 83, **A**). A decrease of the elution volume (corresponding to an increase of molecular weight) and the broadening of the molecular weight distribution were evidenced. The molecular weight of Ru(II) polymer complexes was almost two times bigger than that of **P43** (M_n of **P48** = 12040 g·mol^{-1}). The reaction was performed in dilute solution, therefore most polymers were connected to either a [Ru(II)(phen)$(DMSO)_2Cl_2$], or two polymer chains were connected by a [Ru(II)$(phen)_2Cl_2$] complex. Similar increase of the average molecular weight and polydispersity were also observed by SEC in THF (Figure 113).

The same conditions were applied for the synthesis of single chain polymer complexes from **P44** (containing two phenanthroline moieties) and Ru(II) metal ion. The ruthenium complex [Ru(II)$Cl_2(DMSO)_4$] (1 Eq.) was dissolved in a DMF/$CHCl_3$ mixture and then slowly added into a dilute solution of the polymer in $CHCl_3$ (1 Eq. of **P44**; C = 10^{-6} M) at 60°C using a syringe pump (with a speed of 10^{-6} mol/h). The speed of addition was important for the formation of intramolecular coordination bond between the polymer chain ends. When the experiments were repeated in dilute solution, but with a faster ruthenium complex addition (with the speed around 10^{-4} mol/h), a decrease of the elution volume was observed corresponding to the unwanted formation of intermolecular polymer links. The complexes were characterized by ^{1}H NMR spectroscopy, SEC and DLS. Several polymer complexes were prepared; however, only the results obtained with one polymer (**P49**) are displayed, since the other complexes were very similar to it. ^{1}H NMR of the polymer complex **P49** revealed a broadening and vanishing of the signals of phenanthroline (Figure 114).

The analysis of **P49** by SEC in *N*-methylpyrrolidone with 0.1 M LiBr confirmed the absence of high-molecular weight shoulders. A small increase of the elution volume (ΔV_p = 0.2 mL) after the complexation compared to the initial polymer (**P44**) was observed (Figure 83, **B**). This deviation in elution volume indicates a reduction of the hydrodynamic volume of **P49** compared to **P44**.

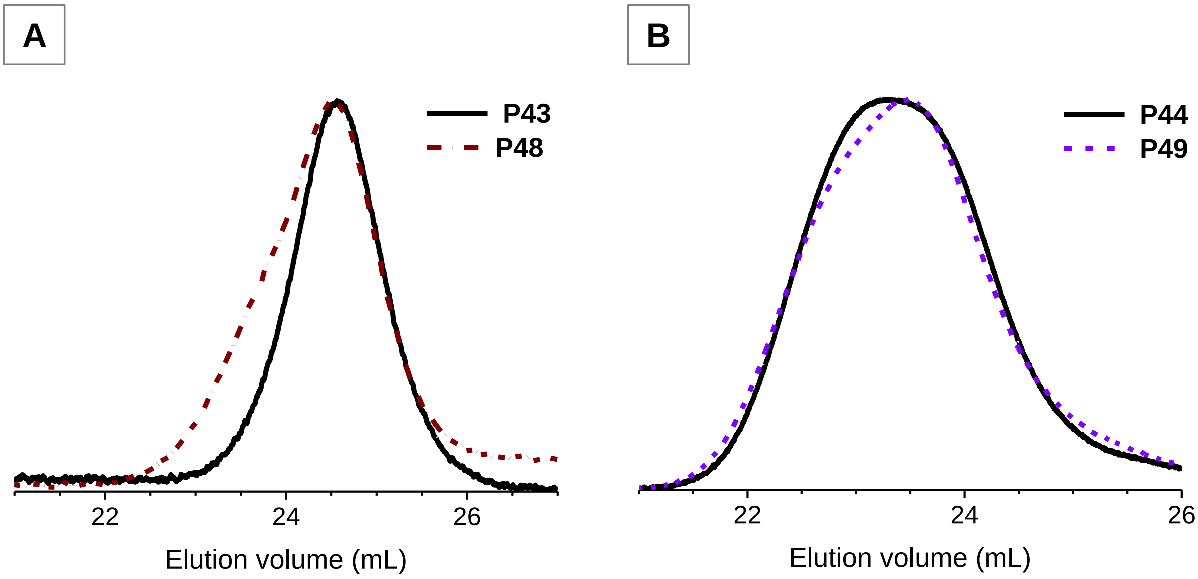

Figure 83 | SEC analysis of Ru(II) polymer complexes. (**A**) Chromatograms of **P43** (solid black line) and **P48** (dash-dot red line), in CH_2Cl_2. (**B**) Chromatograms of **P44** (solid black line) and **P49** (dash violet line), in *N*-methylpyrrolidone with 0.1 M LiBr.

Two main factors influenced the changes of hydrodynamic volume of the polymer complexes such as the compaction and complexation with a metal ion. Intramolecular placement of metal-ligand bonds in the polymer chains (compaction) led to the decrease of the hydrodynamic volume. Simultaneously, the coordination of phenanthroline with ruthenium complex resulted in a small increase of molecular weight and hydrodynamic volume. These two factors probably compensated each other, leading to an insignificant change of elution volume. Although the compaction and formation of folded single polymer chains was not confirmed by SEC, the presence of intermolecular products was not detected either. The polymers were analyzed in CH_2Cl_2 (C= 10^{-3} M) by DLS. The hydrodynamic radius of **P44** was 7.32±0.07 nm, and the hydrodynamic radius of the polymer complex **P49** was close to this value (7.25±0.05 nm). Although the hydrodynamic radius for the polymer metal complex is slightly smaller, we cannot rely on the DLS data, since the standard deviation was too big to observe such a small difference in polymer size.

IV.3.2. Polymer Palladium(II) Complexes

By analogy with the ruthenium polymer complexes, palladium polymer complexes were prepared using $[Pd(CH_3CN)_4(BF_4)_2]$. The conditions for the synthesis of the polymer complexes were first examined for **P43** and repeated afterwards for **P44**. A solution of $[Pd(CH_3CN)_4(BF_4)_2]$ in CH_3CN and CH_2Cl_2 was slowly added to the dilute solution of polymer (**P43** or **P44**) in CH_2Cl_2 (concentration 10^{-5} – 10^{-4} M) at room temperature. After one day the solutions were concentrated followed by their precipitation in cold diethyl ether and centrifugation yielding the metal polymer complexes as yellowish powders. The complexes were characterized by ^{1}H NMR spectroscopy, SEC and DLS. The broadening of phen signals was observed in ^{1}H NMR spectra after complexation with Pd(II) (Figure 116 in exp. part).

The SEC data are presented for two polymer complexes synthesized from **P43** and **P44** (1 Eq. of polymer) with one equivalent of $[Pd(CH_3CN)_4(BF_4)_2]$. For both polymer complexes a tailing effect was observed in the chromatograms due to the interactions of the complexes with SEC column. The SEC analysis confirmed the increase of the hydrodynamic volume of Pd(II) polymer complexes synthesized from **P43** (with one phen moiety in the polymer chain) compared to **P43** (Figure 84, **A**), indicating the formation of mono- and bi-polymer complexes (or a mixture of them). The analysis of **P50** by SEC confirmed the absence of high-molecular shoulders. A small increase of the elution volume (ΔV_p = 0.15 mL) after the complexation compared to the initial polymer (**P44**) was observed (Figure 84, **B**), indicating a possible compaction. However, DLS analysis of **P50** did not confirm this result. The size of **P50** was obtained as 9.4±0.5 nm (the size of **P44** was 7.32±0.07 nm).

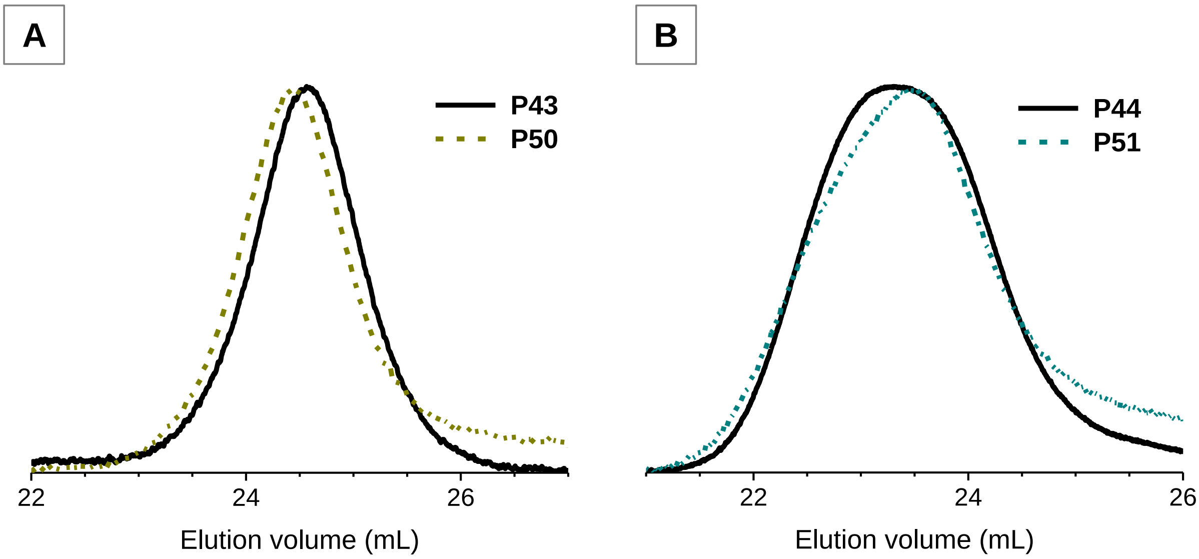

Figure 84 | SEC analysis of Pd(II) polymer complexes. (**A**) Chromatograms of **P43** (solid) and **P50** (dash), in CH_2Cl_2. (**B**) Chromatograms of **P44** (solid) and **P51** (dash), in *N*-methylpyrrolidone with 0.1 M LiBr.

IV.4. CONCLUSIONS AND PERSPECTIVES

Two approaches were investigated to synthetize sequence-controlled polymers containing phenanthroline moieties. The first one consisted in the copolymerization of styrene with 1,10-phenanthrolin-5-maleimide (MI-phen) *via* the NMP in the presence of a bifunctional alkoxyamine. This strategy, although straightforward, led to the incorporation of the acceptor monomer (*i.e.*, MI-phen) in a broad zone of the polymer chains. This result was explained by a less favorable cross-propagation of styrene with maleimide compared to the previously studied styrene-maleimide pairs in this thesis. A solution to this problem could be the addition of an alkyl spacer between the phenanthroline and the maleimide moieties to influence the acceptor properties of the maleimide. Another investigated approach consisted of the synthesis of copolymers containing precisely placed reactive moieties followed by post-polymerization modifications with a reactant carrying a phenanthroline functional group. However, the reaction between the succinic anhydride and PFP ester moieties on the polymer chain and a commercially available 1,10-phenantrolin-5-amine was not successful. In perspective, polymers with more reactive groups should be investigated, or more nucleophilic phenanthroline derivative should be synthesized. Other ligands than phenanthroline could also be investigated.

The synthesis of single polymer chain metal complexes using copolymers carrying phenanthroline moieties and metals (Ru(II) and Pd(II)) was also examined in this work. First, complexes of polystyrenes carrying one phenanthroline moiety with metals were prepared in dilute solutions. The formation of the polymer metal complexes (with mostly one or two polymer chains per metal atom) was evidenced by NMR and SEC. Afterwards, the formation of complexes of the polystyrene carrying two phenanthrolines (per polymer chain) with the metals was performed in dilute solution to form single polymer chain complexes. Although the characterization by SEC and DLS did not strongly support their presence, the formation of complexes with several polymers attached to the metal was not either detected. In order to improve the characterization of these systems, other eluent systems (*e.g.*, $5 \cdot 10^{-3}$ M NH_4PF_6 in DMF at 50ºC) should be examined for the SEC analysis of the synthesized polymers.

GENERAL CONCLUSIONS AND PERSPECTIVES

In the thesis, design of new macromolecular systems for single-chain technology was realized. In first study, tracks containing precisely positioned functional groups for single-chain rotaxane-based molecular machines were designed and successfully synthesized. In the second study, folded macromolecular origami were investigated, and specifically single-chain complex topologies such as pseudocyclic (Q-shaped) and knotted (α-shaped) using positionable disulfide bridges and intramolecular metal-ligand self-associations. The placement of functional moieties and intramolecular bridges in polymer chains was possible due to the control of monomer sequence, by relying on the kinetics of copolymerization of donor styrenic monomer with acceptor *N*-substituted maleimide monomers. Indeed, time-controlled monomer additions of *N*-substituted maleimides into growing polystyrene chains by means of controlled/living radical polymerization techniques proved to be a convenient, rapid and scalable strategy for sequence regulation. Furthermore, any other architectures such as tadpole or bicyclic could also be realized by varying the placement of functionalized maleimides.

The first project (described in **Chapter II**) was dedicated to the synthesis of sequence-controlled copolymers containing precisely placed amino acid and fluorenyl moieties by copolymerization of styrene with *N*-functionalized maleimides. Firstly, maleimide derivatives were designed and synthesized in two steps starting from maleic anhydride and 4-(aminomethyl)phenol. The subsequent modification of the *N*-hydroxybenzyl maleimide yielded maleimides carrying amino acid moieties, either by the reaction of *N*-Boc protected amino acid in the presence of PyBroP, or with a symmetric anhydride constituted of *N*-Boc protected amino acid. The maleimide with a fluorenyl moiety was obtained by the reaction of *N*-hydroxybenzyl maleimide with fluorenyl methyl acyl chloride. Afterwards, the atom transfer radical copolymerization of styrene with maleimides was investigated by means of conventional and ultra-precise methodologies. Both strategies proved to be successful for the insertion of functional moieties in polymer chains at any targeted position. However, the application of the ultra-precise methodology allowed the incorporation of acceptor monomers (*N*-substituted maleimides) more precisely in the polymer chains forming shorter patches, containing in average one maleimide and two styrene units. The ultra-precise insertion of up to four functional moieties (amino acid and a terminal fluorenyl) was performed. However, a broadening of the molecular weight distribution was observed by SEC on the last stages of polymerization for the polymer with four maleimide units, and thus the conditions of polymerization for the ultra-precise methodology still need to be optimized. Besides that, chain-to-chain sequence defects were formed due to the statistical nature of the chain-growth polymerization process. Nevertheless, the precise chain-positioning of four functional groups was realized for the first time using chain-growth polymerization. These copolymers are currently being used as polymer tracks carrying amino acid and fluorenyl moieties for the molecular machine by Leigh group. Furthermore, the molecular machine will be used for the analysis of chain-to-chain distribution of the synthesized polymer tracks (with amino acid moieties).

Afterwards, the synthesis of macromolecules with controlled molecular architectures was investigated in **Chapter III**. The placement of intramolecular dynamic covalent bridges leading to the formation of single-chain polymer objects was demonstrated. Recently investigated cysteine-arginine-cysteine (CRC) sequences were employed for the formation of intramolecular twin disulfide bonds. Linear sequence-controlled polymer conjugates containing CRC motifs were synthesized by a three-step strategy. Sequence-controlled copolymers containing precisely positioned pentafluorophenyl (PFP) ester moieties were first prepared by the nitroxide mediated copolymerization of styrene with PFP ester functionalized maleimide in the presence of a monofunctional alkoxyamine (*i.e.*, BlocBuilder® MA). The use of a bifunctional alkoxyamine instead of BlocBuilder® MA in the copolymerization led to macromolecules with symmetrically positioned functional groups (*i.e.*, PFP ester). The second step consisted in the attachment of CRC fragments with protected amino acid moieties by activated ester/amine chemistry followed by the removal of the protecting groups. The intramolecular cyclization was performed by the oxidation of the thiol groups of CRC motifs in dilute solution, and the successful compaction of polymer chains was evidenced by SEC. Moreover, the absence of free residual thiol groups was confirmed by Ellman's test. This study presented a simple strategy for the formation of single-chain cyclic topologies with positionable dynamic bridges. In perspective, disulfide bonds can be reduced and oxidized again leading to dynamic single-chain objects. Additionally, the properties of the polymer conjugates could be tuned, for example by the use of water-soluble styrene derivatives leading to possible applications in aqueous medium.

Lastly, the single-chain polymer folding using metal-ligand interactions was investigated (**Chapter IV**). The nitroxide-mediated copolymerization of styrene with 1,10-phenanthrolin-5-maleimide (MI-phen) in the presence of a bifunctional alkoxyamine was used to obtain linear polymers containing phenanthroline moieties. Afterwards, the synthesis of single polymer chain metal complexes using copolymers carrying two phenanthroline moieties and different metals (*i.e.*, Ru(II) and Pd(II)) was examined in dilute solutions. A slight increase of elution volume (connected with the decrease of hydrodynamic volume) was evidenced by SEC. However, these data did not completely prove the polymer compaction after complexation. The characterization of the polymers should be performed in other eluent systems that overcome the non-specific interactions of the phenanthroline ligands and the supramolecular complexes with the SEC material. Other solution could be the synthesis of *N*-substituted maleimides containing an alkyl spacer between the phenanthroline and the maleimide moieties. Furthermore, ligands other than phenanthroline could also be investigated.

The present thesis demonstrated the extension of kinetic control strategies to other functional copolymers. Although some defects are present in the microstructure, sequence regulation was performed by means of convenient chain-growth polymerizations (*i.e.*, NMP and ATRP). Moreover, the application of the ultra-precise methodology allowed an extremely precise insertion of functional units (groups) at any targeted chain-position. It was demonstrated that control of monomer sequence allowed the synthesis of single-chain complex topologies.

EXPERIMENTAL PART

1. CHEMICALS

Pentafluorophenyl 4-maleimidobenzoate (MI-PFP) [199], 1,2-bis(bromopropionyloxy)ethane, diethyl 2,2-dimethyl-1-(1,1-dimethylethylamino)propylphosphonate and *N*-*tert*-Butyl-*N*-[1-diethylphosphono(2,2-dimethylpropyl)]nitroxide were synthesized according to literature procedures [228-230]. Styrene (S, Sigma-Aldrich, 99 %) was distilled over CaH_2 (90-95%) under reduced pressure and stored under argon atmosphere at -15 ºC. Copper (I) bromide (CuBr, Sigma-Aldrich, 98%) was washed with glacial acetic acid in order to remove any soluble oxidized species, filtered, washed with ethanol, and dried. Triethylamine (Et_3N, Merck, >97%) was stored over molecular sieves or KOH. Dry toluene was distilled over sodium with deep red 1,1-diphenylethylene /*sec*-butyllithium.

The *N*,*N*'-Dicyclohexylcarbodiimide (DCC, Alfa Aesar 99%), maleic anhydride (Fluka, >99%), 4-hydroxybenzylamine (Fluorochem (ChemPur)), zinc acetate anhydrous (Alfa Aesar, 99.9+%), Boc-L-alanine (Boc-Ala-OH, Sigma-Aldrich, ≥99.0% (TLC)), Boc-L-leucine (Boc-Leu-OH, Fluka, ≥99.0% (HPLC)), Boc-L-phenylalanine (Boc-Phe-OH, Sigma-Aldrich, ≥99.0% (TLC)), N-alpha-t-butyloxycarbonyl-O-methyl-L-tyrosine (Boc-L-Tyr(Me)-OH, Iris Biotech), bromotripyrrolidinophosphonium hexafluorophosphate (PyBrOP, TCI, >98.0%), (PyBOP, Novabiochem/Merck, 99%), fluorene-9-acetic acid (Alfa Aesar, 99.5+%), oxalyl chloride (CO_2Cl_2, Sigma-Aldrich, 98%), 2-bromoisobutyryl bromide (Alfa Aesar, 97%), 3-(trimethylsilyl)propargyl alcohol (Alfa Aesar, 98+%), *N*,*N*,*N*′,*N*″,*N*″-pentamethyldiethylenetriamine (PMDETA, Sigma-Aldrich , 99%), copper(II) bromide ($CuBr_2$, Alfa Aesar, 99%), copper powder (Cu, Alfa Aesar, 99.5%), *N,N,N′,N″,N″*-pentamethyldiethylenetriamine (Sigma-Aldrich, 99%), 5,5'-dithiobis(2-nitrobenzoic acid) (Ellman’s reagent, Alfa Aesar, 99%), *N*-(*tert*-butyl)-*N*-(1-diethylphosphono-2,2-dimethylpropyl)-*O*-(2-carboxylprop-2-yl)-hydroxylamine (BlocBuilder MA® **2**, Arkema, 97 %), *N*-(n-propyl)maleimide (MI-Pr, Alfa Aesar, 94%), *N*-benzylmaleimide (MI-Bz, Alfa Aesar, 99%), 1,10-phenanthrolin-5-amine (Sigma-Aldrich, 97%), acetic anhydride (Ac_2O, Sigma-Aldrich, >99%), anhydrous sodium acetate (AcONa, Sigma-Aldrich, ≥99.0%), tetra-n-butylammonium fluoride, 1 M solution in THF (TBAF, 1 M, Alfa Aesar), tetrakis(acetonitrile)palladium(II) tetrafluoroborate ($[Pd(CH_3CN)_4(BF_4)_2]$, Alfa Aesar, Pd 23.9%), acetonitrile (CH_3CN, Sigma-Aldrich, ≥99.9%), anisole (Sigma-Aldrich, 99%), trifluoroacetic acid (TFA, Sigma-Aldrich, 99%), triisopropylsilane (TIS, Sigma-Aldrich, 99%), *N*-diisopropylethylamine (DIPEA, Alfa Aesar, 99%), 1-methyl-2-pyrrolidinone

(Sigma-Aldrich, 99%), dimethyl sulfoxide (DMSO, Sigma-Aldrich, >99.6%), ethyl acetate (AcOEt, Sigma-Aldrich, ≥99.5% puriss.), *N*,*N*-dimethylformamide (DMF, ≥99.0%, Sigma-Aldrich), anhydrous dichloromethane (CH_2Cl_2, Sigma-Aldrich, ≥99.8%, contains 50-150 ppm amylene) were used as received.

Chemicals for peptide synthesis: N-α-Fmoc protected amino acids (Fmoc-Gly-OH, Fmoc-L-Arg(Pbf)-OH, Fmoc-L-Cys(Trt)-OH), 2-(1H-benzotriazole-1-yl)-1,1,3,3-tetramethyl-uronoium hexafluorophosphate (HBTU) were used as received from IRIS Biotech GmbH (Marktredwitz, Germany). 2-Chlortrityl chloride resin preloaded with 1,2-diaminoethane, 0,79mmol/g-1 loading, have been used as described. 1,1,1,3,3,3-Hexafluoro-2-propanol (HFIP, Acros, 99+%,pure), acetic anhydride (Roth,≥99%, for synthesis), 1-hydroxybenzotriazole hydrate (HOBt, Sigma-Aldrich,purum) have been used as received. Piperidine (Alfa Aesar, 99%) and *N,N,N*-diisopropylethylamine (DIPEA; IRIS Biotech, 99,96%) were distilled from KOH prior to use. *N*-methyl-2-pyrrolidone (99.9+ %, peptide synthesis grade, IRIS Biotech) was purified by filtration through a column (10×60 cm filled with aluminum oxide and silica gel) at a rate of 1 $mL\cdot min^{-1}$. Dichloromethane (CH_2Cl_2, IRIS Biotech, peptide grade) was distilled from CaH_2 prior to use. Fmoc-4-(2-(2-(2-aminoethoxy)ethoxy)ethylamino)-4-oxobutanoicacid) was prepared as described previously [231].

2. CHARACTERIZATION METHODS

- **Nuclear magnetic resonance (NMR) spectroscopy**

The ^{1}H NMR and ^{19}F NMR spectra were recorded using a 400 MHz Bruker Avance spectrometer equipped with Ultrashield magnet, at 25 °C. ^{1}H NMR spectra were calibrated with respect to the solvent signal. The measurements were performed in deuterated chloroform ($CDCl_3$), dichloromethane (CD_2Cl_2), methanol (CD_3OD), dimethylsulfoxide (DMSO-d6) that is indicated for each spectrum. Styrene conversion ($Conv._S$) and the consumption of maleimides ($Conv._{MI}$) were calculated from the ^{1}H NMR spectra of the crude reaction samples by comparing the integration of unreacted monomers peaks to the integration of proton signals of the formed copolymer. The chemical shifts are reported in ppm (δ).

- **Size exclusion chromatography (SEC)**

Characterizations of the sequence-controlled copolymers (if it is not mentioned otherwise) were performed at 30°C in HPLC quality THF at a flow rate of 1 mL·min^{-1} using a Shimadzu LC20AD pump. The number average molecular weight, or number average molar mass (M_n) and the polydispersity index (M_w/M_n = PDI) were estimated using a calibration based on 16 linear polystyrene standards from Polymer Laboratories. The SEC (THF) set-up was equipped with four PLgel mixed C columns (particle size 5 μm, separation range 10^3-10^6 g/mol). The detection was performed with a refractometer (Optilab T-rEX), viscometer (Viscostar-II), light scattering detector (TREOS) and a diode array UV detector (Shimadzu SPD M20A). Toluene was used as internal reference.

Characterizations of the CRC-polymer conjugates and some sequence-controlled copolymers (**P26**, **P27**, **P29**, **P31** – **P37**) were performed at 60°C in HPLC quality DMF, 0.1M LiBr, characterizations of the CRC-polymer conjugates, some sequence-controlled copolymers and folded polymers (**P32** – **P43**, **P48**, **P50**) – at 28°C in HPLC quality CH_2Cl_2 and characterizations of **P44, P44**, **P49** and **P51** – at 60°C in HPLC quality *N*-methylpyrrolidone, 0.1M LiBr, at a flow rate of 1 mL·min^{-1} using a Shimadzu LC20AD pump. The SEC (DMF, *N*-methylpyrrolidone and CH_2Cl_2) set-up was equipped with three PLgel mixed B columns (particle size 10 μm, separation range 10^3-10^7 g/mol). The detection was performed with a Viscotek TDA 302 (Light scattering and refractometer).

- **Fourier transform infrared spectroscopy (FT-IR)**

Infrared spectra (IR) were recorded on a Bruker Vertex 70 spectrophotometer in ATR mode in a range of 700-4000 cm^{-1}. Samples were measured in solid form at room temperature.

- **Matrix-assisted laser desorption/ionization time-of-flight (MALDI-TOF) mass spectrometry**

Mass measurements were carried out on an Ultraflex^{TM} MALDI-TOF/TOF mass spectrometer (Bruker Daltonics GmbH, Bremen, Germany). This instrument was used at a maximum accelerating potential of 25 kV in positive mode and was operated in mode reflector at 25 kV. The delay extraction was fixed at 110 ns and the frequency of the laser (nitrogen 337 nm) was set at 20 Hz. The acquisition mass range was set to 400-4000 m/z with a matrix suppression deflection (cut off) set to 500 m/z. The equipment was externally calibrated with a standard peptide calibration mixture that contained 7 peptides (Bruker Peptide Calibration Standard #206196, Bruker Daltonics GmbH, Bremen, Germany) covering the 1000-3200 m/z. Each raw spectrum was opened with flexAnalysis 3.3 build 65 (Bruker Daltonics GmbH, Bremen, Germany) software and processed using the following parameters: signal-to-noise threshold of 1, Savitzky-Golay algorithm for smoothing, median algorithm for baseline substraction, and SNAP algorithm for monoisotopic peak detection and labelling. In all cases, resolution was higher than 9000. Sample preparation was performed with the dried droplet method using a mixture of 0.5 µl of sample with 0.5 µl of matrix solution dry at room temperature. The matrix solution was prepared from a solution of 1, 8, 9-trihydroxyanthracen (dithranol) 10mg/ml in CH_2Cl_2.

- **Ellman's test**

The test is used to detect the presence of thiol groups. Ellman's reagent solution was prepared: 3 mg of 5,5'-dithiobis(2-nitrobenzoic acid) was dissolved in 5mL of the mixture of solvents MeOH (UV) / THF (UV) 1/1, then 15 µL of DIPEA was added. 1-2 mg of polymer was dissolved in 1 mL of the mixture of solvents MeOH (UV) / THF (UV) 1/1, 3-4 drops of Ellman's reagent solution were added. The change of color to yellow in some minutes indicated the presence of thiol groups.

3.

3. SYNTHESIS OF COMPOUNDS I - X

N-Hydroxybenzyl Maleimide I

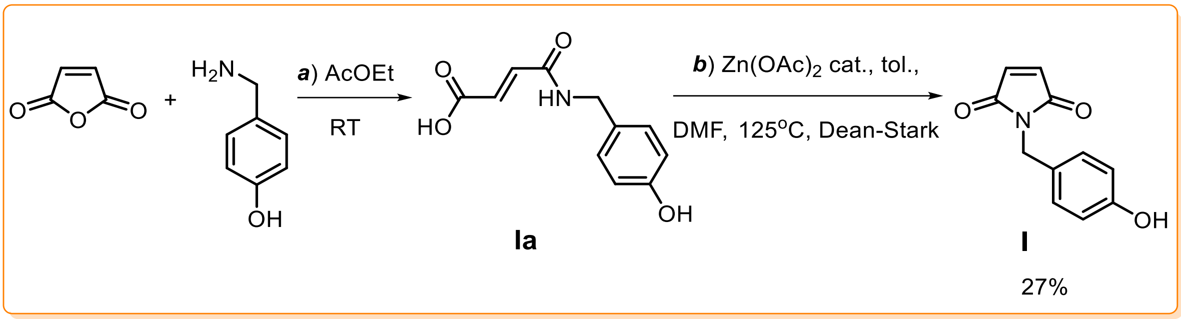

Ia

I

27%

Ia (Scheme 11). A round bottom flask was charged with maleic anhydride (4.35 g, 44.36 mmol, 1.2 Eq.) and AcOEt (70 mL). Dry 4-hydroxybenzylamine (4.5 g, 37 mmol, 1 Eq.) was added. The reaction was left for 10 hours at room temperature. The formed solid was filtered off, washed with a small amount of AcOEt, dried and used for the second step (7.9 g, 35.7 mmol, quantitative yield). ^1H NMR (400 MHz, CD_3OD) δ *(ppm):* 7.16 (d, J = 8.5 Hz, $2H_d$), 6.76 (d, J = 8.5 Hz, $2H_e$), 6.46 (d, J = 12.6 Hz, $1H_b$), 6.25 (d, J = 12.6 Hz, $1H_a$), 4.37 (s, $1H_c$); ^{13}C NMR (100 MHz, CD_3OD), δ *(ppm):* 165.6 (C_d), 165.1 (C_a), 156.7 (C_i), 132.9 (C_b), 131.5 (C_c), 129.1 (C_g), 127.8 (C_f), 115.2 (C_h), 42.4 (C_e).

^1H NMR

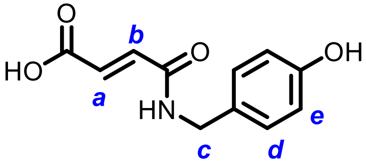

^{13}C NMR

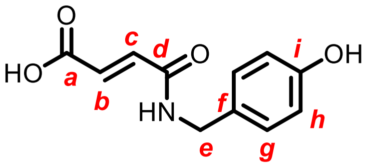

I (Scheme 11). **Ia** was placed in a two-neck round bottom flask, fitted with a Dean-Stark apparatus. DMF (10 mL) and toluene (100 mL) were added, and the reaction mixture was heated to 80°C. Afterwards, zinc acetate (0.26 g, 1.43 mmol, 0.04 eq.) was added as a catalyst and the temperature of the mixture was raised to reflux for 12 hours. The toluene/DMF solution was separated and concentrated under reduced pressure. The crude product was dried under vacuum for 1 day. Column chromatography (SiO_2, CH_2Cl_2/MeOH, *v/v*, 98/2) of the residue afforded **I** as a white solid (1 g, 27%). ^1H NMR (400 MHz, CD_3OD), δ *(ppm):* 7.03 (d, J = 8.5 Hz, $2H_c$), 6.66 (d, J = 8.5 Hz, $2H_d$), 6.55 (s, $2H_a$), 4.78 (s, $1H_e$), 4.43 (s, $2H_b$); ^{13}C NMR (100 MHz, CD_3OD), δ *(ppm):* 172.35 (C_b), 158.07 (C_g), 135.45 (C_a), 130.63 (C_e), 129.13 (C_d), 116.38 (C_f), 41.69 (C_c); ESI-MS: calc. for $C_{11}H_9LiNO_3^+$ 210.07 $[M+Li]^+$; found 210.07.

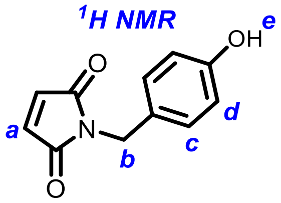
^{1}H NMR
OH
e
O
a
N
b
c
d
O

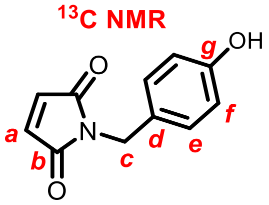
^{13}C NMR
g
OH
O
a
N
b
c
d
e
f
O

N-Substituted Maleimides II-V

Esterification of I using a symmetric anhydride

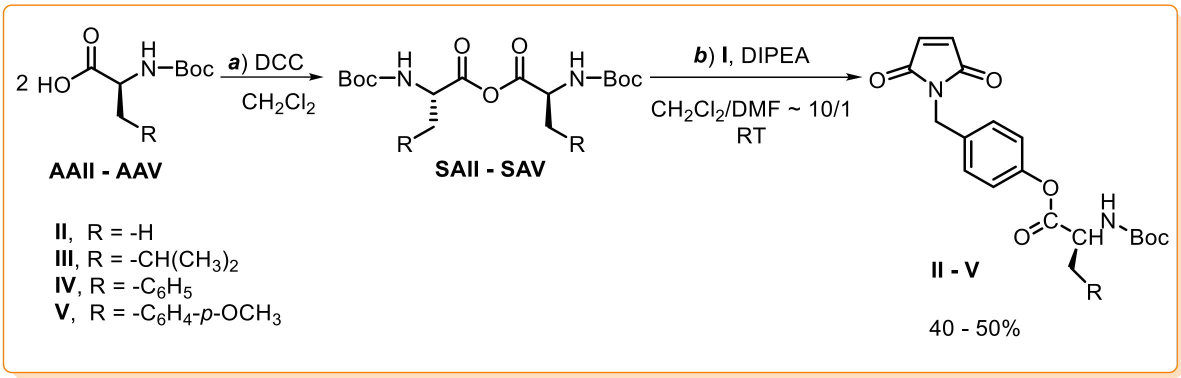
2 HO
O
H
N–Boc
R
AAII - AAV
a) DCC
CH_2Cl_2
Boc–N
H
O
O
O
H
N–Boc
R
R
SAII - SAV
b) **I**, DIPEA
CH_2Cl_2/DMF ~ 10/1
RT
O
N
O
O
O=C
CH
H
N
Boc
R
II - V
40 - 50%
II, R = -H
III, R = -$CH(CH_3)_2$
IV, R = -C_6H_5
V, R = -C_6H_4-*p*-OCH_3

II (Scheme 16). *N*-Boc-Ala-OH (**AAII**) (2.2 g, 11.4 mmol, 2.3 Eq.) was dissolved in anhydrous CH_2Cl_2 under argon atmosphere. Then the solution of DCC (1.2 g, 5.7 mmol, 1.15 Eq.) in CH_2Cl_2 was added at 0°C using an ice bath. The reaction was left at room temperature for 2 hours. The solution of **I** (1 g, 5 mmol, 1 Eq.) in CH_2Cl_2 (with some drops of DMF for better solubilisation) and DIPEA (1.7 mL, 9.9 mmol, 2 Eq.) were added to the reaction mixture. The reaction was left at room temperature for 1 day (the consumption of **I** was checked by NMR). The urea was filtrated off, and the solvents were removed under reduced pressure. Column chromatography (SiO_2, CH_2Cl_2/AcOEt, *v/v*, 100/0 to 98/2) of the residue afforded **II** as white solid (0.77 g, 41% yield). ^{1}H NMR (400 MHz, $CDCl_3$), δ *(ppm):* 7.33 (d, J = 8.5 Hz, $2H_d$), 7.01 (d, J = 8.5 Hz, $2H_c$), 6.67 (s, $2H_a$), 5.24-5.13 (broad, $1H_f$), 4.62 (s, $2H_b$), 4.53-4.42 (m, $1H_e$), 1.50 (d, J = 7.2 Hz, $3H_h$), 1.42 (s, $9H_g$); ^{13}C NMR (100 MHz, $CDCl_3$), δ *(ppm):* 172.1 (C_h), 170.4 (C_b), 155.3 (C_g), 150.2 (C_j), 134.3 (C_a), 134.2 (C_d), 129.9 (C_e), 121.7 (C_f), 80.2 (C_k), 49.6 (C_i), 40.9 (C_c), 28.4 (C_l), 18.4 (C_m); ESI-MS: calc. for $C_{19}H_{23}N_2O_6^+$ 375.16 $[M+H]^+$; found 375.20.

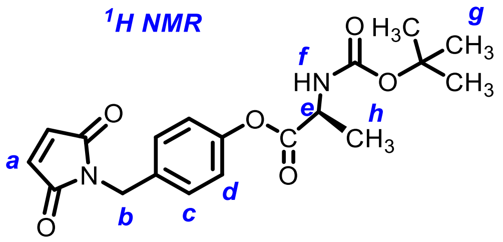

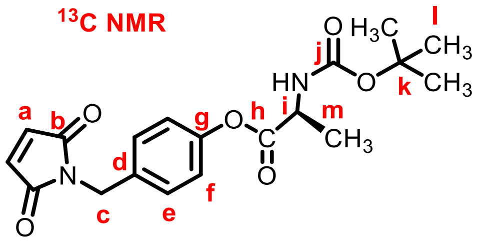

III (Scheme 16). *N*-Boc-Leu-OH (**AAIII**) (1.32 g, 5.66 mmol, 2.3 Eq.) was dissolved in anhydrous CH_2Cl_2 under argon atmosphere. Then the solution of DCC (0.58 g, 2.83 mmol, 1.15 Eq.) in CH_2Cl_2 was added at 0°C using an ice bath. The reaction was left at room temperature for 2 hours. The solution of **I** (0.5 g, 2.46 mmol, 1 Eq.) in CH_2Cl_2 (with some drops of DMF for better solubilisation) and DIPEA (0.85 mL, 4.9 mmol, 2 Eq.) were added to the reaction mixture. The reaction was left at room temperature for 1 day. The urea was filtrated off, and the solvents were removed under reduced pressure. Column chromatography (SiO_2, CH_2Cl_2/AcOEt, *v/v*, 100/0 to 98/2) of the residue afforded **III** as transparent (yellowish) solid (0.49 g, 48% yield). ^{1}H NMR (400 MHz, $CDCl_3$), *δ (ppm):* 7.33 (d, *J* = 8.5 Hz, 2H_d), 7.00 (d, *J* = 8.5 Hz, 2H_c), 6.67 (s, 2H_a), 5.10-5.0 (broad, 1H_f), 4.61 (s, 2H_b), 4.53-4.41 (m, 1H_e), 1.82-1.66 (m, 2$H_{h,i}$), 1.65-1.57 (m, 1$H_{h'}$), 1.42 (s, 9H_g), 0.97 (d, *J* = 6.3 Hz, 6H_j); ^{13}C NMR (100 MHz, $CDCl_3$), *δ (ppm):* 172.1 (C_h), 170.3 (C_b), 155.5 (C_g), 150.2 (C_j), 134.2 (C_a), 134.0 (C_d), 129.8 (C_e), 121.6 (C_f), 80.2 (C_k), 52.4 (C_i), 41.5 (C_c), 40.8 (C_m), 28.3 (C_l), 24.9 (C_o), 22.9 (C_n); ESI-MS: calc. for $C_{22}H_{28}LiN_2O_6^+$ 423.21 $[M+Li]^+$; found 423.21.

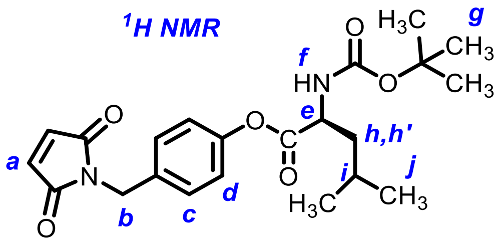

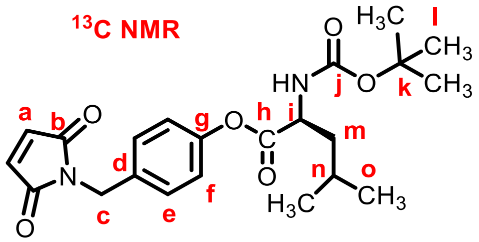

IV (Scheme 16). *N*-Boc-Phe-OH (**AAIV**) (3.04 g, 11.3 mmol, 2.3 Eq.) was dissolved in anhydrous CH_2Cl_2 under argon atmosphere. Then the solution of DCC (1.2 g, 5.7 mmol, 1.15 Eq.) in CH_2Cl_2 was added at 0°C using an ice bath. The reaction was left at room temperature for 2 hours. The solution of **I** (1 g, 4.9 mmol, 1 Eq.) in CH_2Cl_2 (with some drops of DMF for better solubilisation) and DIPEA (1.6 mL, 9.6 mmol, 2 Eq.) were added to the reaction mixture. The reaction was left at room temperature for 1 day (the consumption of **I** was checked by NMR). The urea was filtered off, and the solvents were removed under reduced pressure. Column chromatography (SiO_2, CH_2Cl_2/AcOEt, *v/v*, 100/0 to 98/2) of the residue

afforded **IV** as white solid (1.1 g, 50 %). ^{1}H NMR (400 MHz, $CDCl_3$), *δ (ppm):* 7.38-7.21 (m, 7$H_{d, j, k, i}$), 6.94 (d, *J* = 8.5 Hz, 2H_c), 6.69 (s, 2H_a), 5.25-5.06 (s broad, 1H_f), 4.89-4.72 (m, 1H_e), 4.64 (s, 2H_b), 3.23 (d, *J* = 5.6 Hz, 2H_h), 1.45 (s, 9H_g); ^{13}C NMR (100 MHz, $CDCl_3$), *δ (ppm):* 170.6 (C_h), 170.4 (C_b), 155.2 (C_j), 150.0 (C_g), 135.9 (C_n), 134.3 (C_a), 134.2 (C_d), 129.8 (C_e), 129.5 (C_p), 128.8 (C_o), 127.3 (C_q), 121.6 (C_f), 80.2 (C_k), 54.8 (C_i), 40.8 (C_c), 38.4 (C_m), 28.4 (C_l); ESI-MS: calc. for $C_{25}H_{27}N_2O_6^+$ 451.19 [M+H]$^+$; found 451.23.

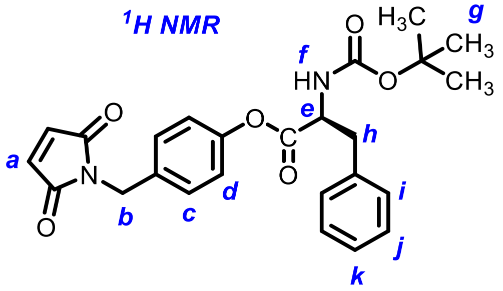

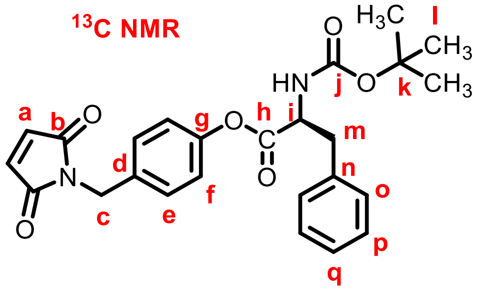

V (Scheme 16). *N*-Boc-Tyr(*O*-CH_3)-OH (**AAV**) (1.56 g, 5.3 mmol, 2.3 Eq.) was dissolved in anhydrous CH_2Cl_2 under argon atmosphere. Then the solution of DCC (0.55 g, 2.65 mmol, 1.15 Eq.) in CH_2Cl_2 was added at at 0°C using an ice bath. The reaction was left at room temperature for 2 hours. The solution of **I** (0.47 g, 2.3 mmol, 1 Eq.) in CH_2Cl_2 (with some drops of DMF for better solubilisation) and DIPEA (0.8 mL, 4.6 mmol, 2 Eq.) were added to the reaction mixture. The reaction was left at room temperature for 1 day. The urea was filtered off, and the solvents were removed under reduced pressure. Column chromatography (SiO_2, CH_2Cl_2) of the residue afforded **V** as white solid (0.52 g, 47 %). ^{1}H NMR (400 MHz, $CDCl_3$), *δ (ppm):* 7.34 (d, *J* = 8.5 Hz, 2H_d), 7.12 (d, *J* = 8.5 Hz, 2H_i),6.94 (d, *J* = 8.5 Hz, 2H_c), 6.85 (d, *J* = 8.5 Hz, 2H_j), 6.68 (s, 2H_a), 5.15-5.03 (s broad, 1H_f), 4.79-4.68 (m, 1H_e), 4.63 (s, 2H_b), 3.77 (s, 3H_k), 3.14 (d, *J* = 5.6 Hz, 2H_h), 1.44 (s, 9H_g); ^{13}C NMR (100 MHz, $CDCl_3$), *δ (ppm):* 170.7 (C_h), 170.4 (C_b), 159.0 (C_j), 150.0 (C_g), 134.3 (C_a), 134.2 (C_d), 130.6 (C_e), 129.9 (C_o), 127.7 (C_n), 121.7 (C_f), 115.2 (C_p), 80.2 (C_k), 55.4 (C_i), 54.9 (C_r), 40.9 (C_c), 37.5 (C_m), 28.4 (C_l); ESI-MS: calc. for $C_{26}H_{28}LiN_2O_7^+$ 487.21 [M+Li]$^+$; found 487.21.

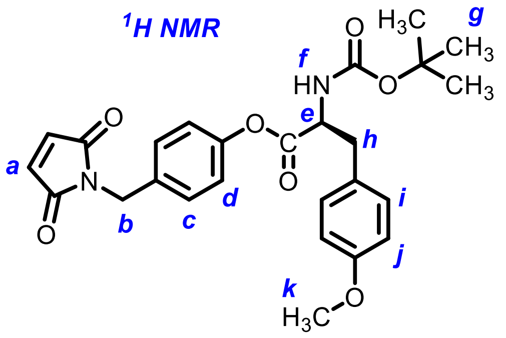
^{1}H NMR
a
b
c
d
e
f
g
h
i
j
k

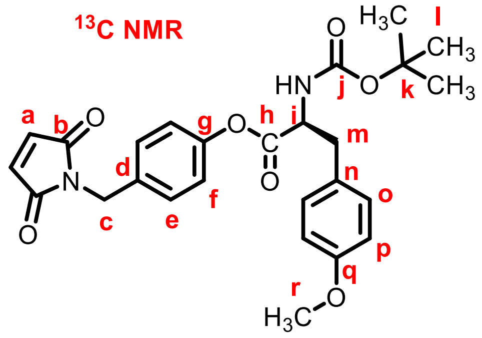
^{13}C NMR
a
b
c
d
e
f
g
h
i
j
k
l
m
n
o
p
q
r

Esterification of I in the presence of PyBroP

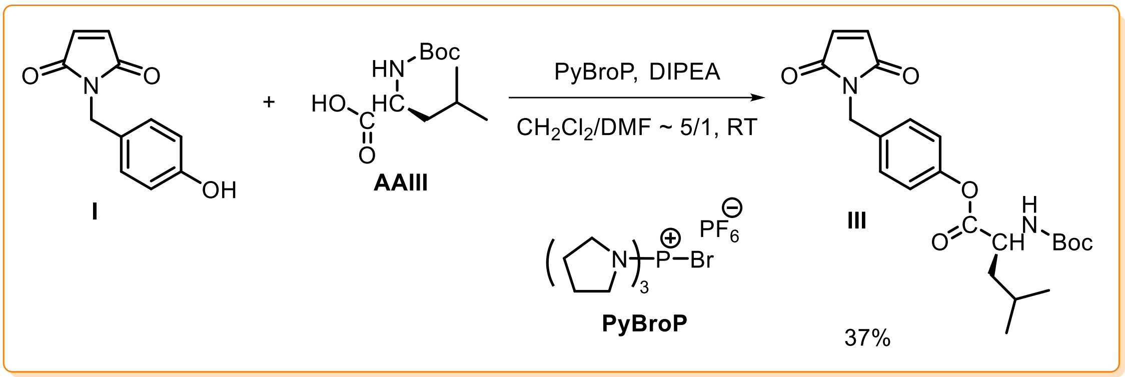
I
AAIII
PyBroP, DIPEA
CH2Cl2/DMF ~ 5/1, RT
PyBroP
III
37%

III (Scheme 14). **I** (0.5 g, 2.46 mmol, 1 Eq.) and *N*-Boc-Leu-OH (**AAIII**) (0.74 g, 3.2 mmol, 1.3 Eq.) were dissolved in DMF (1 mL), then CH_2Cl_2 (5 mL) was added. Subsequently PyBrOP (1.61 g, 3.4 mmol, 1.4 Eq.) and DIPEA (1.3 mL, 7.4 mmol, 3 Eq.) were added. The mixture was stirred at room temperature for 1 day and then extracted in a mixture of EtOAc (20 mL) and H_2O (15 mL). The aqueous phase was extracted with EtOAc (2 x 10 mL). The combined organic extracts were washed with brine (2 x 20 mL), dried over $MgSO_4$ and the solvent removed under reduced pressure. Column chromatography (SiO_2, petrol ether/EtOAc, *v/v*, 85/15 to 40/60) of the residue afforded **III** (0.38 g, 37%) as yellowish solid.

Maleimide VI (Scheme 17)

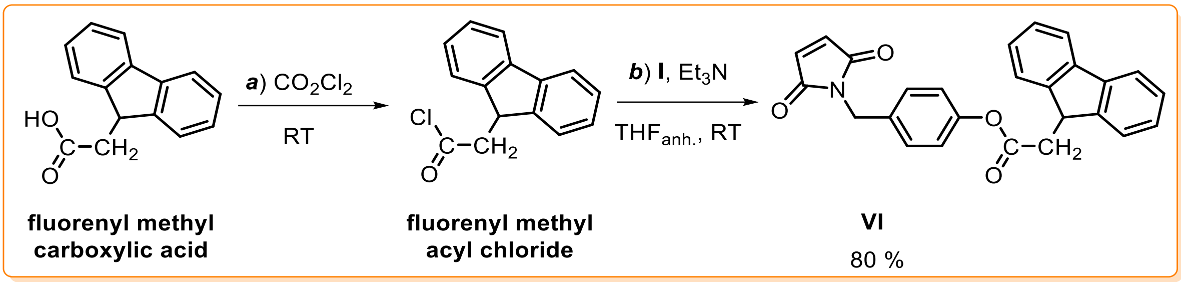

fluorenyl methyl carboxylic acid

fluorenyl methyl acyl chloride

VI

80 %

Fluorenyl methyl acyl chloride. The fluorenyl methyl carboxylic acid (0.7 g, 3.1 mmol, 1 Eq.) was dissolved in CH_2Cl_2 (4 mL). Oxalyl chloride (0.9 mL, 10.5 mmol, 3.4 Eq.) was added into the solution. The mixture was stirred 3 hours at room temperature. The resulting mixture was concentrated and dried in *vacuo*. The residue was used without further purification.

VI. **I** (0.42 g, 2.07 mmol, 1 Eq.) was dissolved in anhydrous THF (2 mL). Then Et_3N previously dried over molecular sieves (0.6 mL, 4.15 mmol, 2 Eq.) was added into the solution followed by a slow addition of the solution of fluorenyl methyl acyl chloride (0.57 g, 2.35 mmol, 1.1 Eq.) in anhydrous THF (3 mL). The resulting mixture was concentrated and dried in *vacuo*. Column chromatography (SiO_2, CH_2Cl_2, 100%) of the residue afforded **VI** as yellowish solid (0.67 g, 80%). ^{1}H NMR (400 MHz, $CDCl_3$), δ *(ppm):* 7.78 (d, J = 7.5 Hz, $2H_j$), 7.58 (d, J = 7.5 Hz, $2H_g$), (m, $6H_{d,\ h,\ i}$), 7.01 (d, J = 8.5 Hz, $2H_c$), 6.72 (s, $2H_a$), 4.67 (s, $2H_b$), 4.50 (t, $1H_f$), 3.07 (d, J = 7.1 Hz, $2H_e$); ^{13}C NMR (100 MHz, $CDCl_3$), δ *(ppm):* 170.9 (C_h), 170.4 (C_b), 150.3 (C_g), 146.0 (C_k), 141.0 (C_p), 134.3 (C_a), 134.2 (C_d), 130.0 (C_e), 127.8 (C_n), 127.4 (C_o), 124.6 (C_m), 121.9 (C_f), 120.2 (C_l), 43.6 (C_c), 40.9 (C_j), 38.7 (C_i); ESI-MS: calc. for $C_{26}H_{19}LiNO_4^+$ 416.15 $[M+Li]^+$; found 416.15.

^{1}H NMR

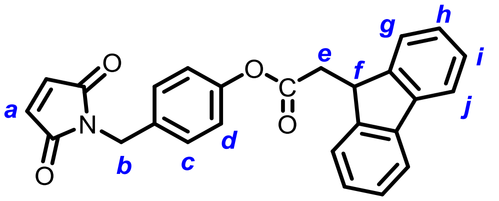

^{13}C NMR

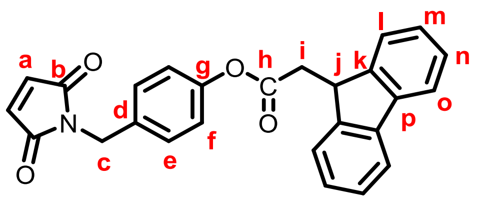

Iniator VII

VII. A solution of 2-bromoisobutyryl bromide (4.2 mL, 32 mmol, 1.5 Eq.) in anhydrous THF was added dropwise to a solution of 3-(trimethylsilyl)propargyl alcohol (3.2 mL, 21.4 mmol, 1 Eq.) and triethylamine (kept over KOH; 4.6 mL, 32 mmol, 1.5 Eq.) in anhydrous THF at ~0°C. After complete addition, the reaction mixture was left to stir for 1 hour at room temperature, then 15 mL of methanol were added. The formed triethylammonium bromide was filtered off and the solvent was removed *in vacuo*. The crude product was dissolved in dichloromethane and washed three times with a saturated ammonium chloride solution and three times with distilled water. The organic layer was dried with magnesium sulfate overnight and the solvent was removed *in vacuo*, yielding a yellow oil which was purified using column chromatography (SiO_2, heptane/EtOAc 19:1). The product was isolated as a colorless oil which was dried under vacuum (5.07 g, 86%). ^1H NMR (400 MHz, $CDCl_3$), δ *(ppm):* 4.75 (s, $2H_b$), 1.94 (s, $6H_c$), 0.17 (s, $9H_a$). ^{13}C NMR (100 MHz, $CDCl_3$), δ *(ppm):* 171 (C_e), 98.4(C_c), 93.0 (C_b), 55.3 (C_d), 54.4 (C_f), 30.9 (C_g), -0.1 (C_a).

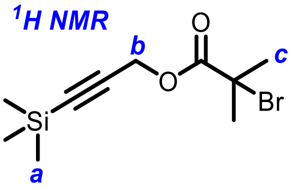

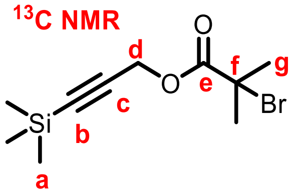

Bifunctional Alkoxyamine VIII

This synthesis was performed by Laurence OSWALD (Institut Charles Sadron).

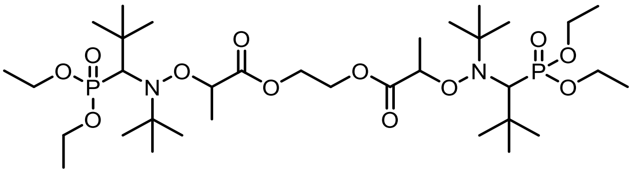

The synthesis of bifunctional initiator **VIII** was adapted from a literature procedure [229] using 1,2-bis(bromopropionyloxy)ethane as a precursor. To Cu(0) (0.81 g, 0.0127 mol., 2 Eq.) and CuBr (1.82 g, 0.0127 mol., 2 Eq.) mixed in 44 mL dry toluene under argon atmosphere was added degazed *N,N,N′,N″,N″*-pentamethyldiethylenetriamine (5.30 mL, 0.0254 mol., 4 Eq.). In a second flask, *N*-*tert*-Butyl-*N*-[1-diethylphosphono(2,2-dimethylpropyl)]nitroxide (4.40 g, 0.0127 mol., 2 Eq.), 1,2-bis(bromopropionyloxy)ethane (2.11 g, 0.0063 mol., 1 Eq.) were dissolved in 8 mL dry toluene under argon atmosphere. This solution was added dropwise to the first mixture. The dark green mixture was stirred 3 hours at RT. The crude product was filtered through celite to remove the copper salts. The celite was well washed with 500 mL toluene. The filtrate was washed with 3 x 250 mL water until the aqueous phase was no more colored. The organic phase was dried over Na_2SO_4 and the solvent was evaporated. The crude compound was purified by chromatography on silica gel (eluent: diethyl ether/pentane 1/1 to diethyl ether/methanol 95/5, v/v) to give the **4** as a pale yellow oil (3.86 g, 80 %). ^{1}H NMR ($CDCl_3$), δ (ppm): 4.59 (m, $2H_f$), 4.37 - 3.87 (m, $12H_{b, h}$), 3.40 - 3.19 (m, $2H_c$),1.48 - 1.42 (dd, $6H_g$), 1.24 (m, $12H_a$), 1.12 - 1.05 (m, 36 $H_{d, e}$). ^{13}C NMR ($CDCl_3$), δ (ppm): 173.59, 172.21 (C_j), 88.18, 77.24 (C_h), 69.89, 68.50 (d, C_c), 62.07,61.93, 61.78, 61.44 (C_b), 61.60, 61.41 (C_f), 58.88, 58.71(C_k), 35.49, 35.16 (C_d), 30.13, 29.53 (C_e), 27.96, 27.88 (C_g), 19.16, 17.91 (C_i), 16.45, 16.12 (C_a); ESI-MS: calc. for $C_{34}H_{71}N_2O_{12}P_2^+$ 761.45 [M+H]$^+$; found 761.77.

^{1}H NMR

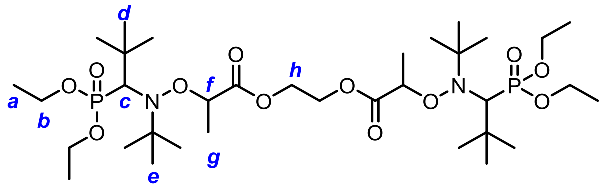

^{13}C NMR

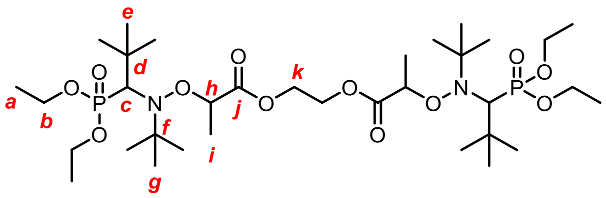

Oligomer IX

This synthesis was performed by Katharina LINKERT (Humboldt-Universität zu Berlin).

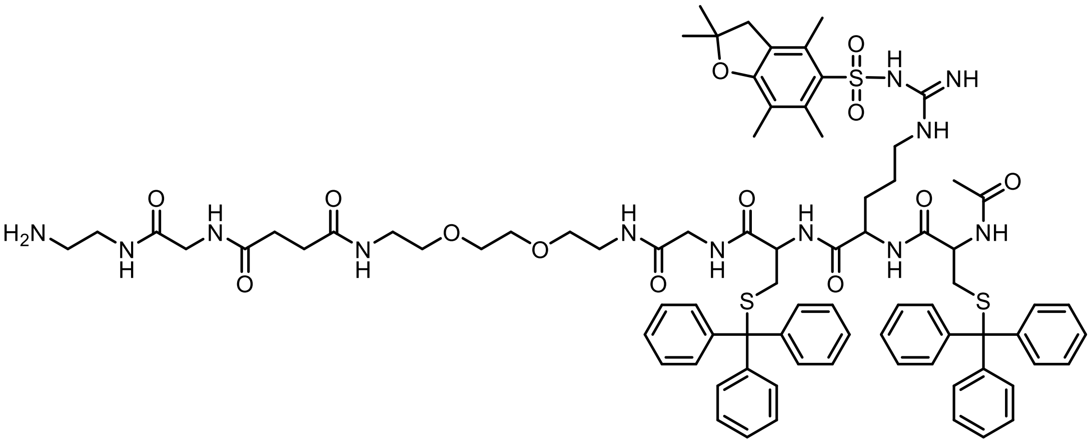

Peptide synthesis was performed on an Applied Biosystems 433a peptide synthesizer in a 0.25 mmol scale, using a 2-chlorotrityl chloride solid support that has been preloaded with 1,2-diaminoethane (0.35 mmol/g). Fmoc-amino acid derivatives were coupled following standard ABI-Fastmoc protocols (no capping, with single coupling except first glycine and Fmoc-4-(2-(2-(2-aminoethoxy)ethoxy)ethylamino)-4-oxobutanoic acid which were coupled via double coupling). Coupling was performed in *N*-methylpyrrolidone facilitated by HBTU/DIPEA. After final Fmoc removal the N-terminus was acetylated with a solution of acetic anhydride, DIPEA, HOBt in *N*-methylpyrrolidone. The support was washed finally with CH_2Cl_2 and dried overnight under vacuum at 25°C. The peptide was liberated from the resin by treatment with 1,1,1,3,3,3-Hexafluoro-2-propanol in CH_2Cl_2 (20/80 v/v%) for 0.5 h to obtain the fully protected peptide. The peptide was isolated by diethyl ether precipitation, washed once with diethyl ether, centrifugation and lyophilization from acetonitrile/water. The chemical identity of the product was confirmed by MALDI-TOF-MS. MALDI-TOF-MS: Theoretical mass 1546.9 Da; exp. m/z 1548.1 assignable to $[M+H]^+$. Further ion adducts can be observed with m/z 1569.7 and 1585.7 assignable to $[M+Na]^+$ and $[M+K]^+$ respectively. Additionally mass signals could be found with low intensity that correspond to removed protective groups (-Trt, -Pbf). These are probably caused by in source fragmentation as occasionally observable due to high laser intensity required to desorb fully protected peptides.

Maleimide X

The synthesis was performed according to the modified procedure [225]. Maleic anhydride (1.51 g, 15.36 mmol, 3 Eq.) was added to the solution of 1,10-phenanthrolin-5-amine (1 g, 5.12 mmol, 1 Eq.) in 100 mL CH_2Cl_2. The reaction was stirred at 40°C for 10 hours. A yellow precipitate (1.2 g, 4.1 mmol; 80% yield) was collected by vacuum filtration, washed with 3 × 100 mL of CH_2Cl_2, and air-dried. The product was then added to 50 mL of acetic anhydride containing 5 g of sodium acetate. The solution was stirred and heated to 100°C for 3 hours. After the solution cooled to room temperature, 200 mL of ice−water was added and the solution was stirred until all of the acetic anhydride was consumed. The product was extracted with 3 × 150 mL CH_2Cl_2, washed with 3 × 100 mL of water, and dried over $MgSO_4$. The $MgSO_4$ was filtered off and the CH_2Cl_2 removed under reduced pressure. The product was dissolved in 20 mL of CH_2Cl_2, precipitated in 100 mL of pentane, collected by vacuum filtration, and air-dried. This procedure was repeated one more time. The final product presented an orange-brownish powder (0.61 g, 43% overall yield). ^1H NMR (400 MHz, $CDCl_3$), δ (*ppm*): 9.21-9.29 (m, $2H_{d,\ e}$), 8.26 (d, J = 3 Hz, $1H_g$), 7.95 (dd, J = 3 Hz, $1H_b$), 7.75 (s, $1H_h$), 7.20-7.62 (m, $2H_{c,\ f}$), 7.03 (s, $2H_a$); ^{13}C NMR (100 MHz, $CDCl_3$), δ (*ppm*): 170.2 (C_b), 151.7 (C_j), 151.1 (C_g), 147.1 (C_c), 146.5 (C_h), 136.5 (C_l), 135.0 (C_a), 131.4 (C_e), 130.7 (C_m), 127.8 (C_n), 126.4 (C_i), 126.2 (C_d), 123.8 (C_k), 123.5 (C_f).

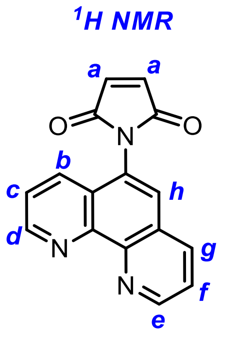

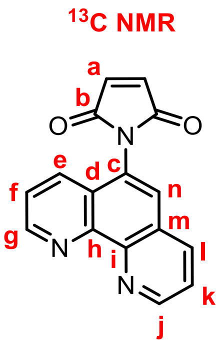

4. SYNTHESIS OF POLYMERS

Atom transfer radical polymerization of styrene

The following example corresponds to polymer **P1** in Table 5. 47 mg of CuBr (0.33 mmol, 1 Eq.) were weighted in a round-bottom flask. The flask was sealed with a rubber septum and subsequently degassed with argon. Then, 90.7 mg of **VII** (0.33 mmol, 1 Eq.), 1.5 mL of degassed styrene (13.1 mmol, 40 Eq.) and lastly 68 μL of degassed PMDETA (0.33 mmol, 1 Eq.) were added into the flask. The mixture was heated at 90 °C in an oil bath. Samples were taken regularly from the polymerization mixture and were analyzed by ^{1}H NMR to determine styrene conversion. After 110 minutes of polymerization, the reaction mixture was exposed to air, dissolved in THF and the polymer precipitated in cold methanol. The precipitate was collected by filtration, washed with methanol and dried in a vacuum oven at room temperature, overnight (white powder, 0.88 g, 85 % yield). The purified polymer was characterized by ^{1}H NMR (400 MHz, $CDCl_3$), *δ (ppm):* 7.44-6.28 (m, 138H, aromatic *H*), 4.22-3.70 (m, 2H, $-CH_2-O-$), 2.63-1.09 (m, 84H, alkyl *H*), 1.08-0.81 (m, 6H, $-CH-(CH_3)_2$), 0.18 (s, 9H, $-C-(CH_3)_3$); and SEC in THF: M_n = 5425 g mol^{-1}, M_w/M_n = 1.15.

Table 5 | ATRP of styrene with varied concentration of metal catalyst Cu(I)Br/PMDETA and temperature of polymerization.

	CuBr/PMDETA	T, °C	Conv.^{a}, %	t^b, min	$M_n{}^c$	$M_{theo}{}^d$	$M_w/M_n{}^c$
P1	1/1	90	0.69	110	5425	3150	1.15
P2	1/1	100	0.70	110	2950	3190	1.19
P3*	0.5/0.5	100	0.71	240	3860	3235	1.12
P4	0.5/0.5	100	0.58	180	1940	2690	1.07
P5	0.5/0.5	110	0.86	110	3000	3860	1.15
P6	0.2/0.2	110	0.68	140	2640	3110	1.12

Conditions: styrene (40 Eq.), Cu(I)Br, PMDETA, bulk. *Styrene/anisole 2/1, v/v. ^{a}Final conversion of styrene that was calculated from ^{1}H NMR spectra. ^{b}Final polymerization time. ^{c}Measured by SEC in THF. $^d M_{theo} = M_{VII} + M_S \cdot conv._S \cdot [S]/[\mathbf{VII}]$.

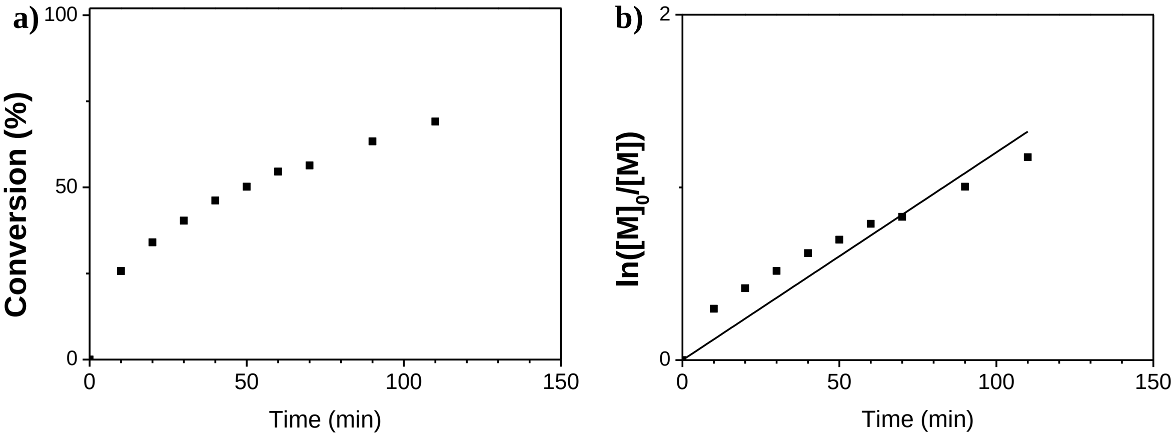

Figure 85 | Monomer conversion (**a**) and semi-logarithmic plot of monomer conversion *versus* time (**b**) for **P1**.

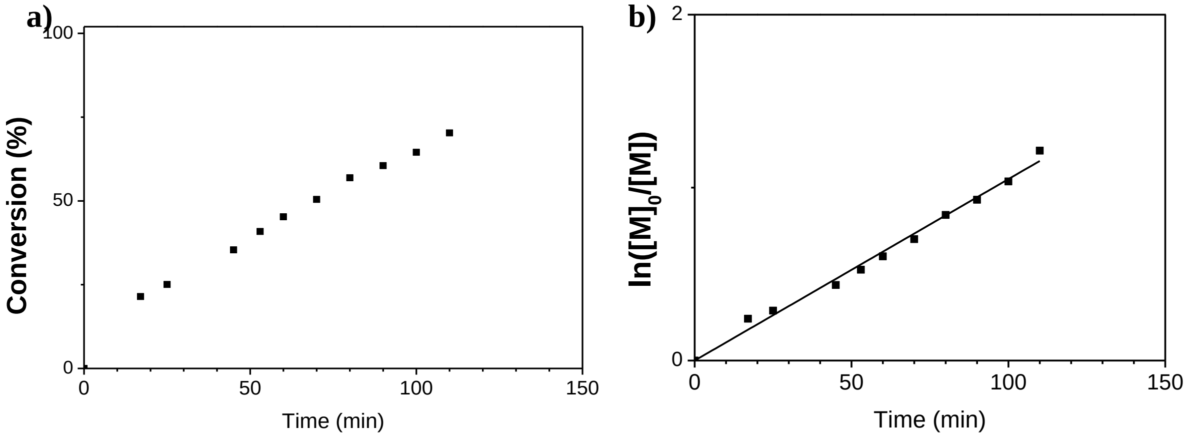

Figure 86 | Monomer conversion (**a**) and semi-logarithmic plot of monomer conversion *versus* time (**b**) for **P2**.

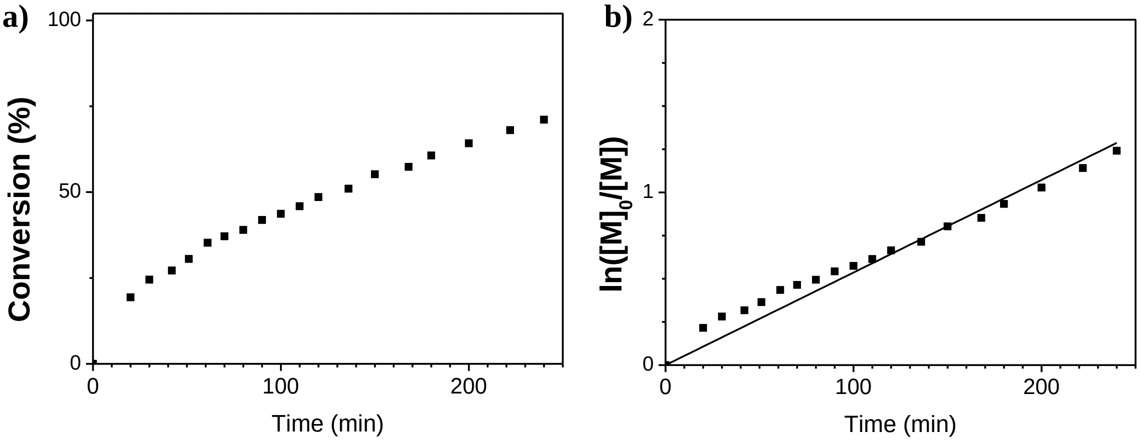

Figure 87 | Monomer conversion (**a**) and semi-logarithmic plot of monomer conversion *versus* time (**b**) for **P3**.

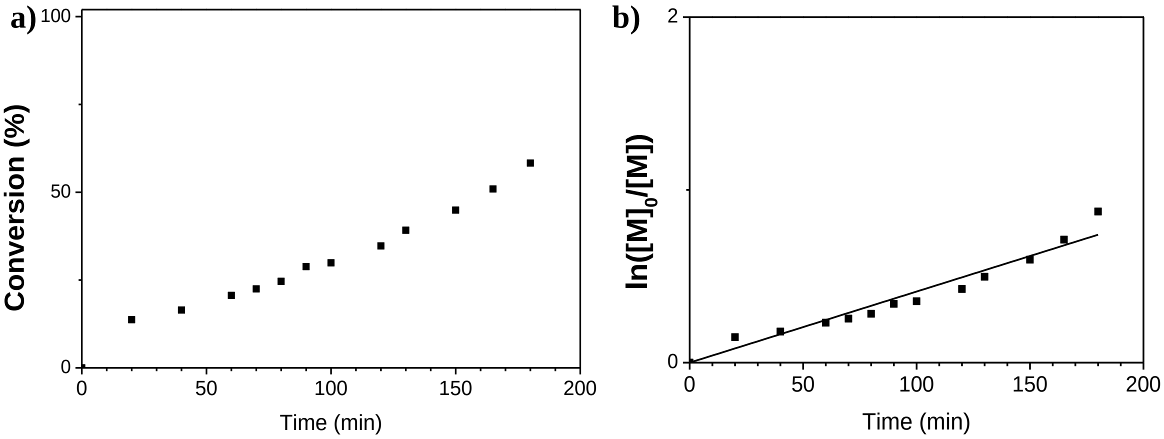

Figure 88 | Monomer conversion (**a**) and semi-logarithmic plot of monomer conversion *versus* time (**b**) for **P4**.

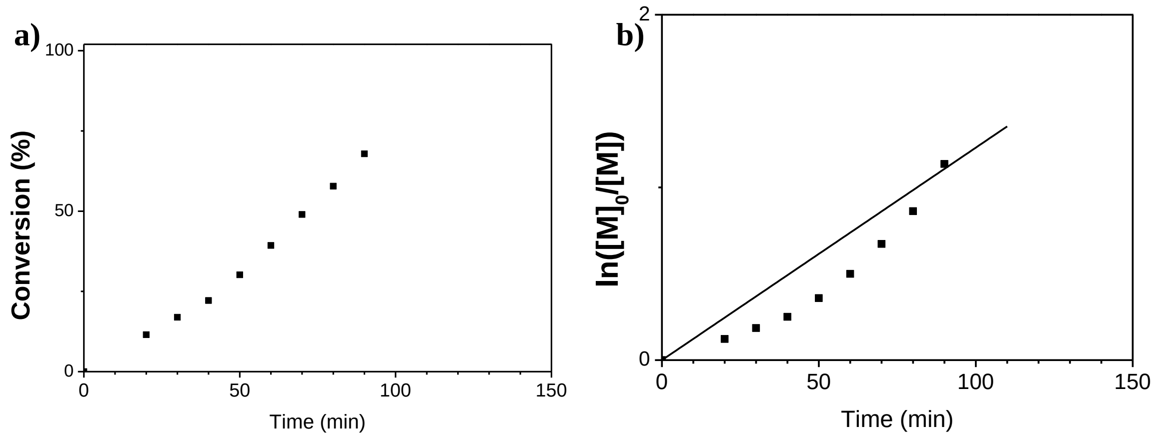

Figure 89 | Monomer conversion (**a**) and semi-logarithmic plot of monomer conversion *versus* time (**b**) for **P5**.

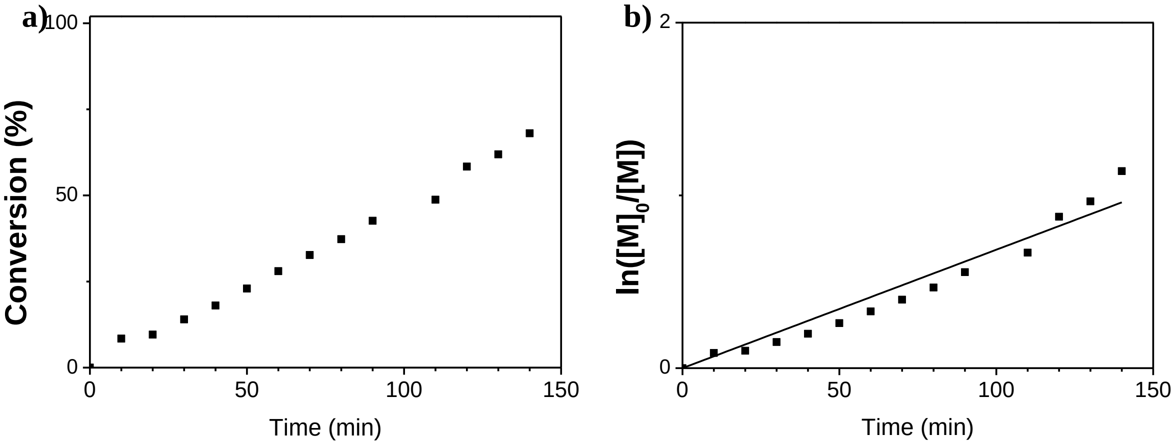

Figure 90 | Monomer conversion (**a**) and semi-logarithmic plot of monomer conversion *versus* time (**b**) for **P6**.

Positioning of a single amino acid moiety at the beginning of the polymer chain

The following example corresponds to polymer **P11** in Table 1. 31.3 mg of CuBr (0.22 mmol, 1 Eq.) and 98 mg of maleimide **IV** (0.22 mmol, 1 Eq.) were weighted in a round-bottom flask. The flask was sealed with a rubber septum and subsequently degassed with argon. Then, 60.5 mg of **VII** (0.22 mmol, 1 Eq.), 1 mL of degassed styrene (8.7 mmol, 40 Eq.) and lastly 46 μL of degassed PMDETA (0.22 mmol, 1 Eq.) were added into the flask. The mixture was heated at 90 °C in an oil bath. Samples were withdrawn periodically and analyzed by SEC and ^{1}H NMR to determine the styrene conversion and the incorporation of

IV in the growing polymer chains. After 180 minutes of polymerization, the reaction mixture was exposed to air, dissolved in THF and the polymer precipitated in cold methanol. The precipitate was collected by filtration, washed with methanol and dried in a vacuum oven at room temperature, overnight (white powder, 0.63 g, 74 % yield). The purified polymer was characterized by ^{1}H NMR (400 MHz, $CDCl_3$), *δ (ppm):* 7.63-5.97 (m, 159H, aromatic *H*), 5.17-5.02 (broad, 1H, -N*H*-), 4.90-4.72 (broad, 1H, -C*H*-NH-), 4.70-4.28 (m, 2H, -N-CH_2-C-), 4.25-3.83 (m, 2H, -CH_2-O-), 3.35-3.15 (broad, 2H, -CH_2-C_6H_5), 2.63-1.09 (m, 99H, alkyl *H* in PS, -C-(CH_3)$_3$)), 1.10-0.82 (m, 6H, -CH-(CH_3)$_2$); and SEC in THF: M_n = 5000 g mol^{-1}, M_w/M_n = 1.13.

Positioning of a single amino acid moiety at the end of the polymer chain

The following example corresponds to polymer **P12** in Table 1. 31.3 mg of CuBr (0.22 mmol, 1 Eq.) were weighted in a round-bottom flask. The flask was sealed with a rubber septum and subsequently degassed with argon. Then, 60.5 mg of **VII** (0.22 mmol, 1 Eq.), 1 mL of degassed styrene (8.7 mmol, 40 Eq.) and lastly 46 µL of degassed PMDETA (0.22 mmol, 1 Eq.) were added into the flask. The mixture was heated at 90 °C in an oil bath. After 95 minutes of reaction (69% of styrene conversion) a degassed solution of 98 mg of maleimide **IV** (0.22 mmol, 1 Eq.) in 0.5 mL anisole was added with a degassed syringe. Samples were withdrawn periodically and analyzed by SEC and ^{1}H NMR to determine the styrene conversion and the incorporation of **IV** in the growing polymer chains. After 120 minutes, the reaction mixture was exposed to air, dissolved in THF and the polymer precipitated in cold methanol. The precipitate was collected by filtration, washed with methanol and dried in a vacuum oven at room temperature, overnight (white powder, 0.64 g, 73 % yield). The purified polymer was characterized by ^{1}H NMR (400 MHz, $CDCl_3$), *δ (ppm):* 7.63-6.0 (m, 161H, aromatic *H*), 5.27-5.02 (broad, 1H, -N*H*-), 5.0-4.72 (broad, 1H, -C*H*-NH-), 4.72-4.28 (m, 2H, -N-CH_2-C-), 4.25-3.83 (m, 2H, -CH_2-O-), 3.39-3.19 (broad, 2H, -CH_2-C_6H_5), 2.73-1.23 (m, 99H, alkyl *H* in PS, -C-(CH_3)$_3$)), 1.18-0.91 (m, 6H, -CH-(CH_3)$_2$), 0.25 (s, 9H, -Si-(CH_3)$_3$) and SEC in THF: M_n = 4020 g mol^{-1}, M_w/M_n = 1.20.

Table 6 | Reactivity ratios r_s for **P7** to **P12**.

Copolymer	**P7**	**P8**	**P9**	**P10**	**P11**	**P12**
r_S*	0.027±0.012	0.027±0.012	0.034	0.024±0.009	0.010±0.006	0.030±0.012

*Determined by the Jaacks equation. Calculated based on logaritmic dependence of styrene monomer conversion *versus* maleimide conversion.

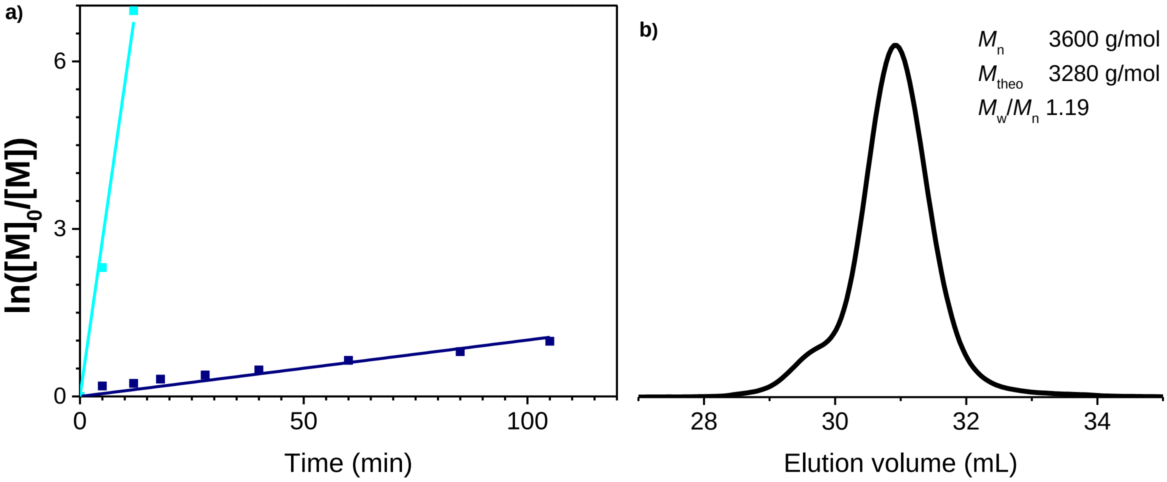

Figure 91 | Characterization of **P7**: **a**) Semi-logarithmic plot of monomer conversion versus time for ATRP of styrene (squares) with **II** (dots) added at the beginning of the polymerization; **b**) Size exclusion chromatogram of the copolymer, in THF.

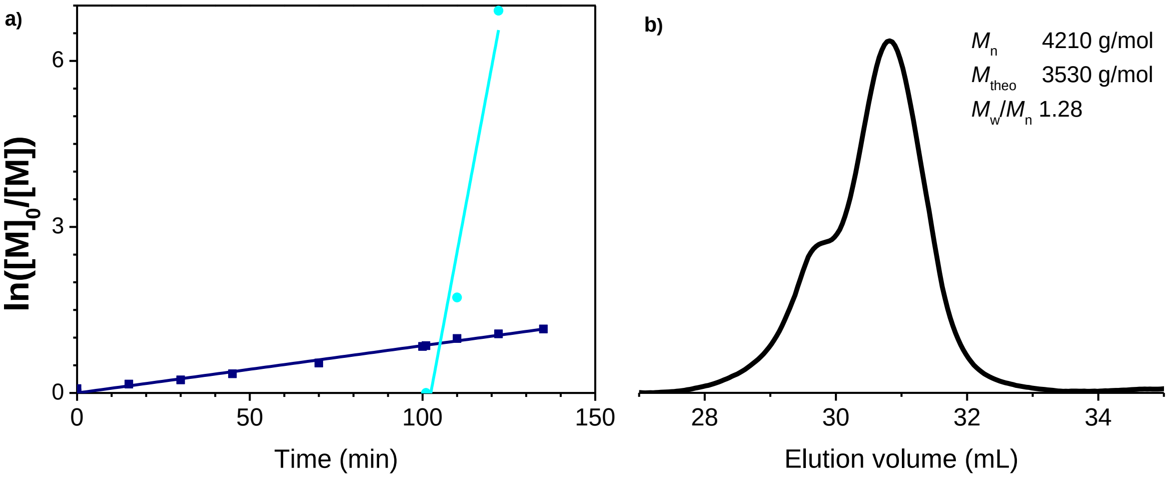

Figure 92 | Characterization of **P8**: **a**) Semi-logarithmic plot of monomer conversion versus time for ATRP of styrene (squares) with **II** (dots) added at the end of the polymerization; **b**) Size exclusion chromatogram of the copolymer, in THF.

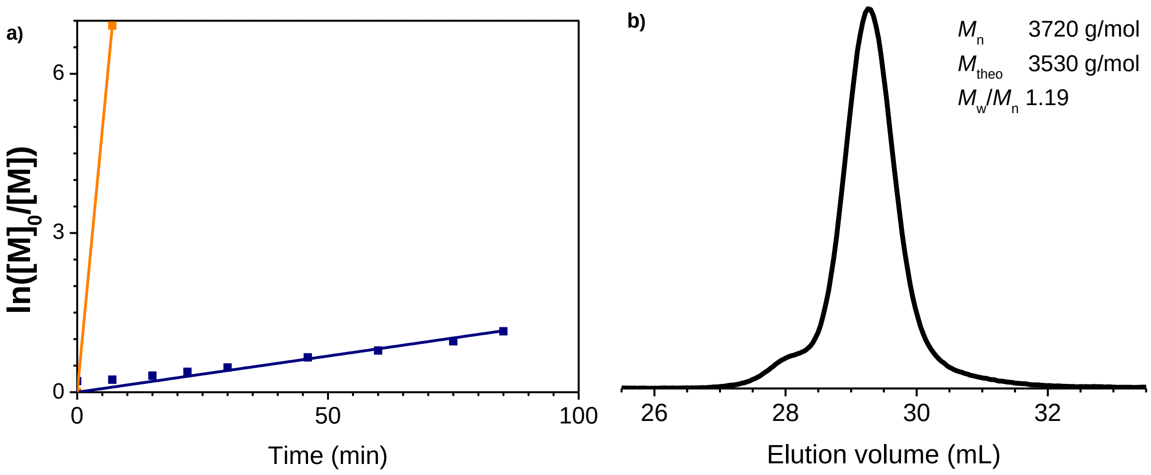

Figure 93 | Characterization of P9: **a**) Semi-logarithmic plot of monomer conversion versus time for ATRP of styrene (squares) with III (dots) added at the beginning of the polymerization; **b**) Size exclusion chromatogram of the copolymer, in THF.

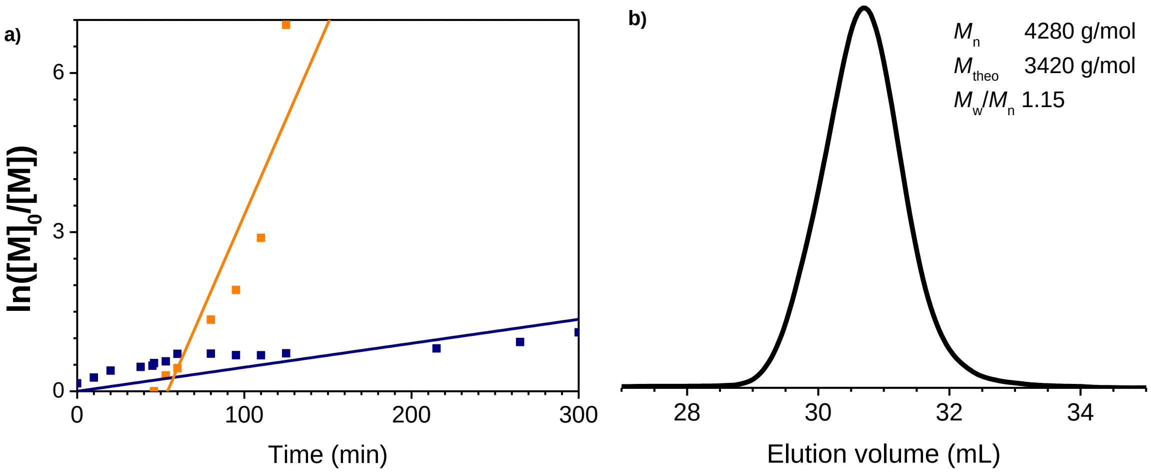

Figure 94 | Characterization of P10: **a**) Semi-logarithmic plot of monomer conversion versus time for ATRP of styrene (squares) with III (dots) added at the end of the polymerization; **b**) Size exclusion chromatogram of the copolymer, in THF.

ATRP of styrene with 2 conventional insertions of maleimide

The following example corresponds to polymer **P16**. 41.7 mg of CuBr (0.29 mmol, 1 Eq.) were weighted in a round-bottom flask. The flask was sealed with a rubber septum and subsequently degassed with argon. Then, 80.6 mg of **VII** (0.29 mmol, 1 Eq.), 1.5 mL of degassed styrene (13.1 mmol, 45 Eq.) and lastly 61 μL of degassed PMDETA (0.29 mmol, 1 Eq.) were added into the flask The mixture was heated at 90 °C in an oil bath. After 90 minutes (37% of styrene conversion) a degassed solution of 121 mg **III** (0.29 mmol, 1 Eq.) in 0.3 mL anisole was added with a degassed syringe. After the conversion of **III** reached >99%, a degassed solution of 131 mg **IV** (0.29 mmol, 1 Eq.) in 0.4 mL anisole was added with a degassed syringe (153 minutes of polymerization, 54% of styrene conversion). Samples were withdrawn periodically and analyzed by SEC and ^{1}H NMR to determine the styrene conversion and the incorporation of **III** and **IV** in the growing polymer chains. After 220 minutes, the reaction mixture was exposed to air, dissolved in THF and the polymer precipitated in cold methanol. The precipitate was collected by filtration, washed with methanol and dried in a vacuum oven at room temperature, overnight (white powder, 0.78 g, 0.69 % yield). The purified polymer was characterized by ^{1}H NMR (400 MHz, $CDCl_3$), *δ (ppm):* 7.51-6.0 (m, 133H, aromatic *H*), 5.19-5.03 (broad, 1H, -N*H*- of **IV**), 5.03-4.91 (broad, 1H, -N*H*- of **III**), 4.90-4.73 (broad, 1H, -C*H*-NH- of **IV**), 4.62-4.18 (m, 5H, -N-CH_2-C-, -C*H*-NH- of **III**), 4.17-3.77 (m, 2H, -CH_2-O-), 3.29-3.15 (broad, 2H, -CH_2-C_6H_5), 2.58-1.20 (m, 97H, alkyl *H* in PS, -C-(CH_3)$_3$), -CH_2-C*H*-(CH_3)$_2$), 1.09-0.83 (m, 12H, -CH-(CH_3)$_2$), 0.17 (s, 9H, -Si-(CH_3)$_3$); and SEC in THF: M_n = 4160 g mol^{-1}, M_w/M_n = 1.16.

Table 7 | ATRP of styrene with *N*-benzyl maleimide (MI-Bz) added at certain conversion of styrene, with varied concentration of metal catalyst Cu(I)Br/PMDETA.

	$t_{add\,1}$[a], min	Conv.$_S$ at $t_{add\,1}$[b]	t_1[c], min	Conv.$_S$ at t_1[b]	$t_{add\,2}$[a], min	Conv.$_S$ at $t_{add\,2}$[b]	t_2[c], min	Conv.$_S$ at t_2[b]	t_{end}[d], min	Conv.$_S$ at t_{end}[b]
P13	95	0.50	124	0.65	130	0.69	150	0.76	170	0.81
P14	70	0.47	120	0.56	146	0.59	210	0.64	210	0.64
P15	43	0.47	75	0.55	90	0.58	210	0.64	210	0.64

Conditions of polymerization: styrene (40 Eq.), *N*-benzyl maleimide for each addition (1 Eq.), CuBr(I) (1 Eq.), PMDETA (1 Eq.), bulk, 90ºC. [a]Time at which the addition of MI-Bz was performed. [b]Styrene conversion calculated from ^{1}H NMR spectra. [c]Time at which full conversion of MI-Bz was observed. [d]Final polymerization time.

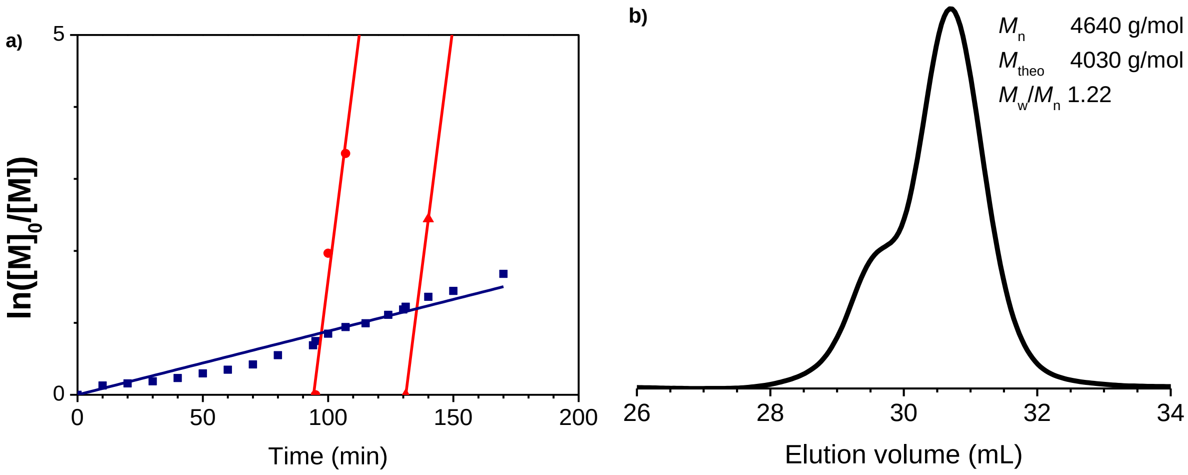

Figure 95 | Characterization of **P13**: **a**) Semi-logarithmic plot of monomer conversion versus time for ATRP of styrene (squares) with MI-Bz added in the middle (dots) and at the end (triangles) of the polymerization; **b**) Size exclusion chromatogram of the copolymer, in THF.

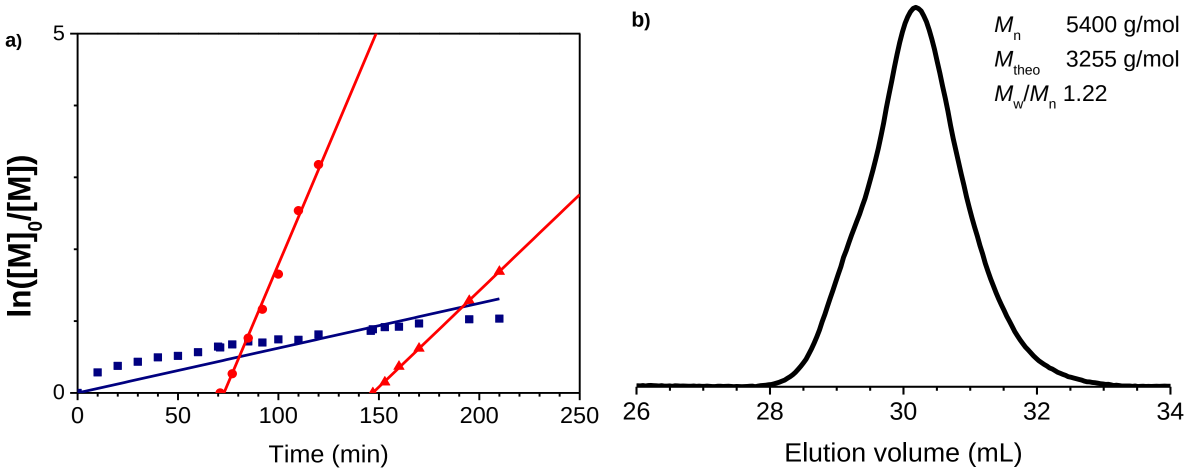

Figure 96 | Characterization of **P14**: **a**) Semi-logarithmic plot of monomer conversion versus time for ATRP of styrene (squares) with MI-Bz added in the middle (dots) and at the end (triangles) of the polymerization; **b**) Size exclusion chromatogram of the copolymer, in THF.

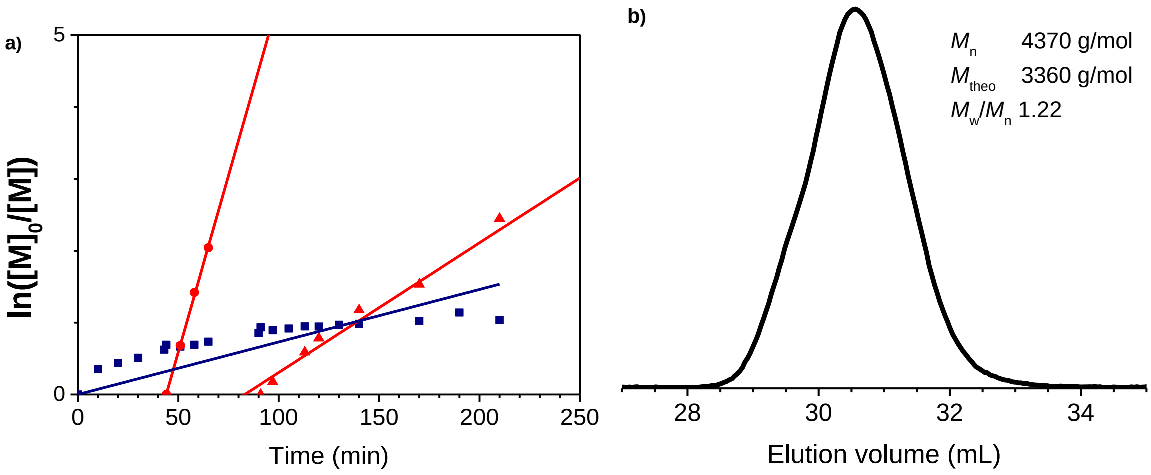

Figure 97 | Characterization of **P15**: **a**) Semi-logarithmic plot of monomer conversion versus time for ATRP of styrene (squares) with MI-Bz added in the middle (dots) and at the end (triangles) of the polymerization; **b**) Size exclusion chromatogram of the copolymer, in THF.

ATRP of styrene with 3 conventional insertions of maleimide

The following example corresponds to polymer **P17**. 31.3 mg of CuBr (0.22 mmol, 1 Eq.) were weighted in a round-bottom flask. The flask was sealed with a rubber septum and subsequently degassed with argon. Then, 60.5 mg of **VII** (0.22 mmol, 1 Eq.), 1 mL of degassed styrene (8.7 mmol, 40 Eq.) and lastly 46 µL of degassed PMDETA (0.22 mmol, 1 Eq.) were added into the flask. The mixture was heated at 90 °C in an oil bath. After 10 minutes of reaction (17% of styrene conversion) a degassed solution of 91 mg **III** (0.22 mmol, 1 Eq.) in 0.3 mL anisole was added with a degassed syringe. The conversion of **III** (first addition) was above 99% at 30 minutes of polymerization (27% of styrene conversion). After 42 minutes of reaction (32% of styrene conversion) a second degassed solution of 91 mg **III** (0.22 mmol, 1 Eq.) in 0.3 mL anisole was added again with a degassed syringe. The conversion of **III** was above 99% at 92 minutes of polymerization (43% of styrene conversion). After 110 minutes of reaction (47% of styrene conversion) a third degassed solution of 91 mg **III** (0.22 mmol, 1 Eq.) in 0.3 mL anisole was added. The conversion of **III** was above 99% at 215 minutes of polymerization (57% of styrene conversion). Samples were withdrawn periodically and analyzed by SEC and ^{1}H NMR to determine the styrene conversion and the incorporation of **III** in the growing polymer chains. After 230 minutes of polymerization, the reaction mixture was exposed to air, dissolved in THF and the polymer precipitated in cold methanol. The precipitate was collected by filtration, washed with methanol and dried in a vacuum oven at room temperature, overnight (white powder, 0.49 g, 72% yield). The purified polymer was characterized by ^{1}H NMR (400 MHz, $CDCl_3$), *δ (ppm):* 7.54-5.9 (m, 127H, aromatic *H*), 5.15-4.90 (broad, 3H, -N*H*-), 4.63-4.46 (broad, 3H, -C*H*-NH-), 4.46-4.18 (broad, 6H, -N-CH_2-C-), 4.17-3.91 (m, 2H, -CH_2-O-), 2.48-1.26 (m, 114H, alkyl *H* in PS, -C-(CH_3)$_3$), -CH_2-C*H*-(CH$_3$)$_2$), 1.10-0.83 (m, 24H, -CH-(CH_3)$_2$), 0.17 (s, 9H, -Si-(CH_3)$_3$); and SEC in THF: M_n = 3800 g mol^{-1}, M_w/M_n = 1.30.

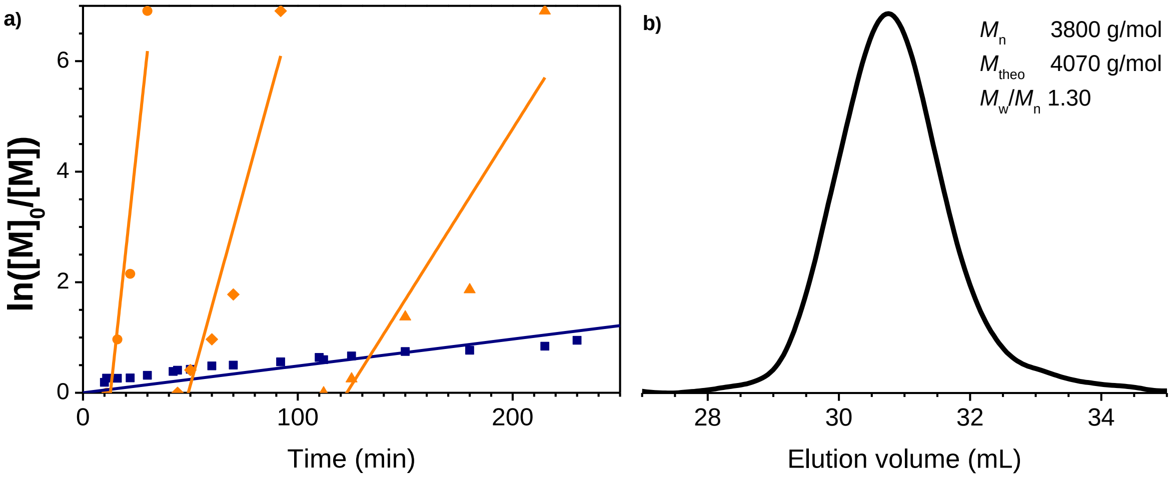

Figure 98 | Characterization of **P17**: **a**) Semi-logarithmic plot of monomer conversion versus time for ATRP of styrene (squares) with **III** added at the beginning (dots), in the middle (rhomb) and at the end (triangles) of the polymerization; **b**) Size exclusion chromatogram of the copolymer, in THF.

Calculation of styrene conversion in ultra-precise methodology

Two ways to calculate styrene conversion leading to the same result were used in the “ultra-precise” experiments:

(1) Overall conversion (*Conv*$_S$). The total amount of polystyrene and styrene present at a given time (t) in the copolymerization medium are taken into consideration (equation 1).

$$Conv_S = [\text{Polystyrene}]_t/([\text{Polystyrene}]_t + [\text{Styrene}]_t) \quad (1)$$

The instantaneous concentrations of polymer and monomer (polystyrene and styrene) were based on direct measurement by ^{1}H NMR spectroscopy. According to (1) the overall styrene conversion diminishes after addition of styrene in the copolymerization medium, but it does not drop down to zero, since styrene is already present in the copolymerization medium.

(2) Feed conversion ($Conv_{S\text{-}fx}$). The amount of polymer formed in previous styrene feeds x (before new styrene addition) is not taken into account. The correlation with the instantaneous concentration of polymer and of monomer measured by NMR results in equation 2. The concentration of polymer formed in previous feeds can also be estimated from the NMR monitoring.

$$Conv_{S\text{-}fx} = ([\text{Polymer}]_t - [\text{Polymer formed in previous feeds}]) / ([\text{Polymer}]_t - [\text{Polymer formed in previous feeds}] + [\text{Monomer}]_t) \quad (2)$$

Ultra-precise insertion of two functional groups in the polymer chains

The following example corresponds to polymer **P22**.

Preparation of initial reaction. 4 mg copper powder (0.061 mmol, 0.25 Eq.) and 5.5 mg $CuBr_2$ (0.024 mmol, 0.1 Eq.) were weighted in a round-bottom flask. The flask was sealed with a rubber septum and subsequently degassed with dry argon. Then, 68 mg of initiator **VII** (0.24 mmol, 1 Eq.), 0.7 mL of degassed styrene (6.1 mmol, 25 Eq.), 0.35 mL of degassed toluene (1:2 volume ratio with respect to S) and lastly 18 µL of degassed PMDETA (0.086 mmol, 0.35 Eq.) were added into the flask. The mixture was heated at 90 °C in an oil bath for several hours.

Controlled addition of the first maleimide (**V**). After 110 minutes of reaction (58% conversion of S at this stage), a degassed solution of 118 mg **V** (0.24 mmol, 1 Eq.) in 0.25 mL toluene was added with a degassed syringe. Samples were withdrawn periodically and analyzed by SEC and ^{1}H NMR to determine molecular weight and the incorporation of **V** in the growing polymer chains, respectively.

Controlled addition of S. After 175 minutes of reaction (70% conversion of S at this stage), 0.56 mL of degassed styrene (4.9 mmol, 20 Eq.) was added in the reaction mixture using a degassed syringe. Samples were taken with a degassed syringe and analyzed by ^{1}H NMR.

Controlled addition of the second maleimide (**VI**). After 400 minutes of reaction (78% conversion of total S at this stage), a degassed solution of 107 mg **VI** (0.24 mmol, 1 Eq.) in 0.25 mL toluene was added with a degassed syringe. Samples were taken regularly from the polymerization mixture and were analyzed by ^{1}H NMR to determine the incorporation of **VI** in the growing polymer chains.

Purification. After 470 min of polymerization, the reaction mixture was exposed to air, dissolved in THF and the polymer precipitated in cold methanol. The precipitate was collected by filtration, washed with methanol and dried in a vacuum oven at room temperature, overnight (white powder, 0.87 g, 69 % yield). The purified polymer was characterized by ^{1}H NMR (400 MHz, $CDCl_3$), *δ (ppm):* 7.88-7.75 (m, 2H, –C-C-C*H*- of **VI**), 7.67-7.51 (m, 2H, -CH_2-CH-C-C*H*- of **VI**), 7.50-6.0 (m, 211H, aromatic *H*), 5.15-4.97 (broad, 1H, -N*H*-), 4.91-4.71 (broad, 1H, -C*H*-NH-), 4.63-4.23 (broad, 5H, -N-CH_2-C-, -CH_2-C*H*-C-), 4.24-3.88 (m, 2H, -CH_2-O-), 3.88-3.67 (s, 3H, -OCH_3), 3.32-3.11 (m, 2H, -CH_2-C_6H_5), 3.10-2.96 (m, 2H, -CH_2-CH-C- of **VI**), 2.56-1.14 (m, 130H, alkyl *H* in PS, -C-$(CH_3)_3$), 1.12-0.85 (m, 6H, -CH-$(CH_3)_2$), 0.20 (s, 9H, -Si-$(CH_3)_3$); and SEC in THF: M_n = 5410 g mol^{-1}, M_w/M_n= 1.18.

Ultra-precise insertion of three amino acid moieties in the polymer chains

The following example corresponds to polymer **P23**.

Preparation of initial reaction. 4.6 mg copper powder (0.07 mmol, 0.25 Eq.) and 6.4 mg $CuBr_2$ (0.03 mmol, 0.1 Eq.) were weighted in a round-bottom flask. The flask was sealed with a rubber septum and subsequently degassed with dry argon. Then, 80 mg of initiator **VII** (0.29 mmol, 1 Eq.), 0.66 mL of degassed styrene (5.76 mmol, 20 Eq.), 0.35 mL of degassed toluene (1:2 volume ratio with respect to S) and lastly 21 µL of degassed PMDETA (0.10 mmol, 0.35 Eq.) were added into the flask. The mixture was heated at 90 °C in an oil bath for several hours.

Controlled addition of the first maleimide (**IV**). After 130 minutes of reaction (73% conversion of S at this stage), a degassed solution of 130 mg **IV** (0.29 mmol, 1 Eq.) in 0.25 mL toluene was added with a degassed syringe. Samples were withdrawn periodically and analyzed by SEC and ^{1}H NMR to determine molecular weight and the incorporation of **IV** in the growing polymer chains, respectively.

Controlled addition of S (1). After 230 minutes of reaction (79% conversion of S at this stage), 0.33 mL of degassed styrene (29 mmol, 10 Eq.) was added in the reaction mixture using a degassed syringe. Samples were taken with a degassed syringe and analyzed by ^{1}H NMR.

Controlled addition of the second maleimide (**III**). After 475 minutes of reaction (82% conversion of total S at this stage), a degassed solution of 120 mg **III** (0.29 mmol, 1 Eq.) in 0.25 mL toluene was added with a degassed syringe. Samples were taken regularly from the polymerization mixture and were analyzed by ^{1}H NMR to determine the incorporation of **III** in the growing polymer chains.

Controlled addition of S (2). After 625 minutes of reaction (84% conversion of S at this stage), 0.33 mL of degassed styrene (29 mmol, 10 Eq.) was added in the reaction mixture using a degassed syringe. Samples were taken with a degassed syringe and analyzed by ^{1}H NMR.

Controlled addition of the third maleimide (**VI**). After 930 minutes of reaction (68% conversion of total S at this stage), a degassed solution of 118 mg **VI** (0.29 mmol, 1 Eq.) in 0.25 mL toluene was added with a degassed syringe. Samples were taken regularly from the polymerization mixture and were analyzed by ^{1}H NMR to determine the incorporation of **VI** in the growing polymer chains.

Purification. After 1110 min of polymerization, the reaction mixture was exposed to air, dissolved in THF and the polymer precipitated in cold methanol. The precipitate was collected by filtration, washed with methanol and dried in a vacuum oven at room temperature, overnight (white powder, 1.23 g, 77 % yield). The purified polymer was characterized by ^{1}H NMR (400 MHz, $CDCl_3$), δ *(ppm):* 7.88-7.69 (m, 2H, –C-C-C*H*- of **VI**), 7.67-7.48 (m, 2H, -CH_2-CH-C-C*H*- of **VI**), 7.50-6.0 (m, 205H, aromatic *H*), 5.18-4.88 (broad, 2H, -N*H*-), 4.90-4.73 (broad, 1H, -C*H*-NH-), 4.61-4.17 (m broad, 7H, -N-CH_2-C-, -

CH_2-C*H*-C-), 4.15-3.78 (m, 2H, -CH_2-O-), 3.32-3.14 (m, 2H, -CH_2-C_6H_5), 3.10-2.96 (m, 2H, -CH_2-CH-C- of **VI**), 2.45-1.13 (m, 135H, alkyl *H* in PS, -C-(CH_3)$_3$, -CH_2-C*H*-(CH_3)$_2$), 1.07-0.80 (m, 12H, -CH-(CH_3)$_2$), 0.18 (s, 9H, -Si-(CH_3)$_3$); and SEC in THF: M_n = 7390 g mol^{-1}, M_w/M_n= 1.26.

Ultra-precise insertion of four amino acid moieties in the polymer chains

The following example corresponds to polymer **P24**.

Preparation of initial reaction. 4.6 mg copper powder (0.07 mmol, 0.25 Eq.) and 6.4 mg $CuBr_2$ (0.03 mmol, 0.1 Eq.) were weighted in a round-bottom flask. The flask was sealed with a rubber septum and subsequently degassed with dry argon. Then, 80 mg of initiator **VII** (0.29 mmol, 1 Eq.), 0.66 mL of degassed styrene (5.76 mmol, 20 Eq.), 0.35 mL of degassed toluene (1:2 volume ratio with respect to S) and lastly 21 μL of degassed PMDETA (0.10 mmol, 0.35 Eq.) were added into the flask. The mixture was heated at 90 °C in an oil bath for several hours.

Controlled addition of the first maleimide (**III**). After 70 minutes of reaction (68% conversion of S at this stage), a degassed solution of 120 mg **III** (0.29 mmol, 1 Eq.) in 0.25 mL toluene was added with a degassed syringe. Samples were withdrawn periodically and analyzed by SEC and ^{1}H NMR to determine the molecular weight and the incorporation of **III** in the growing polymer chains, respectively.

Controlled addition of S (1). After 122 minutes of reaction (76% conversion of S at this stage), 0.33 mL of degassed styrene (29 mmol, 10 Eq.) was added in the reaction mixture using a degassed syringe. Samples were taken with a degassed syringe and analyzed by ^{1}H NMR.

Controlled addition of the second maleimide (**IV**). After 320 minutes of reaction (78% conversion of total S at this stage), a degassed solution of 130 mg **IV** (0.29 mmol, 1 Eq.) in 0.25 mL toluene was added with a degassed syringe. Samples were taken regularly from the polymerization mixture and were analyzed by ^{1}H NMR to determine the incorporation of **IV** in the growing polymer chains.

Controlled addition of S (2). After 440 minutes of reaction (81% conversion of S at this stage), 0.33 mL of degassed styrene (29 mmol, 10 Eq.) was added in the reaction mixture using a degassed syringe. Samples were taken with a degassed syringe and analyzed by ^{1}H NMR.

Controlled addition of the third maleimide (**V**). After 790 minutes of reaction (74% conversion of total S at this stage), a degassed solution of 139 mg **V** (0.29 mmol, 1 Eq.) in 0.25 mL toluene was added with a degassed syringe. Samples were taken regularly from the polymerization mixture and were analyzed by ^{1}H NMR to determine the incorporation of **V** in the growing polymer chains.

Controlled addition of S (3). After 1000 minutes of reaction (78% conversion of S at this stage), 0.33 mL of degassed styrene (29 mmol, 10 Eq.) was added in the reaction mixture using a degassed syringe. Samples were taken with a degassed syringe and analyzed by ^{1}H NMR.

Controlled addition of the fourth maleimide (**VI**). After 1690 minutes of reaction (71% conversion of total S at this stage), a degassed solution of 118 mg **VI** (0.29 mmol, 1 Eq.) in 0.25 mL toluene was added with a degassed syringe. Samples were taken regularly from the polymerization mixture and were analyzed by ^{1}H NMR to determine the incorporation of **VI** in the growing polymer chains.

Purification. After 1950 min of polymerization, the reaction mixture was exposed to air, dissolved in THF and the polymer precipitated in cold methanol. The precipitate was collected by filtration, washed with methanol and dried in a vacuum oven at room temperature, overnight (white powder, 1.23 g, 77 % yield). The purified polymer was characterized by ^{1}H NMR (400 MHz, $CDCl_3$), *δ (ppm):* 7.81-7.74 (m, 2H, –C-C-C*H*- of **VI**), 7.61-7.52 (m, 2H, -CH_2-CH-C-C*H*- of **VI**), 7.48-6.0 (m, 223H, aromatic *H*), 5.15-4.88 (m broad, 3H, -N*H*-), 4.88-4.72 (broad, 2H, -C*H*-NH- of **IV**, **V**), 4.60-4.16 (m broad, 10H, -N-CH_2-C-, -C*H*-NH- of **III**, -CH_2-C*H*-C-), 4.15-3.91 (m, 2H, -CH_2-O-), 3.77 (s, 3H, -OCH_3), 3.27-3.11 (m, 4H, -CH_2-C_6H_5, -CH_2-C_6H_4-), 3.10-2.96 (m, 2H, -CH_2-CH-C- of **VI**), 2.40-1.11 (m, H, alkyl *H* in PS, -C-$(CH_3)_3$, -CH_2-C*H*-$(CH_3)_2$), 1.11-0.84 (m, 12H, -CH-$(CH_3)_2$), 0.18 (s, 9H, -Si-$(CH_3)_3$); and SEC in THF: M_n = 9110 g mol^{-1}, M_w/M_n= 1.37.

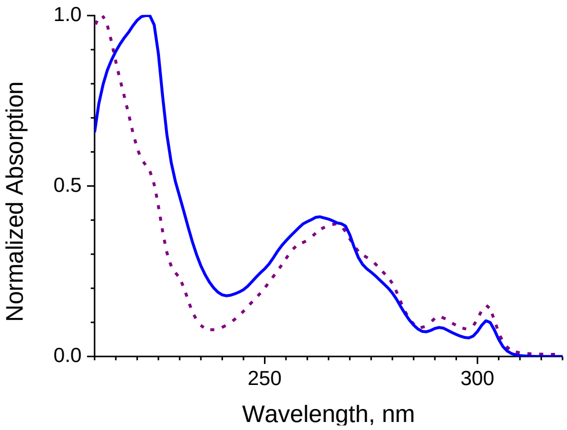

Figure 99 | Normalized UV spectra of **P24** (solid line) and **VI** (dashed line), in THF (UV).

Removal of TMS-protecting groups

Polymers containing TMS-protected alkyne groups (1 Eq. of TMS-group) was dissolved in THF (C = 10^{-2} M). TBAF solution in THF (C = 1 M, 1 Eq.) was added. After several minutes the reaction mixture was precipitated in cold methanol/H_2O (95/5 v/v). The precipitate was filtered and dried *in vacuo* at RT (75-90 % yield). The deprotected polymers were characterized by ^{1}H NMR spectroscopy and SEC.

"Asymmetric" sequence-controlled polymers containing PFP-ester groups

Copolymers of styrene with successive additions of MI-PFP were synthesized by nitroxide mediated polymerization. The following example corresponds to polymer **P25** in Table 2. 103 mg of BlocBuilder MA® (0.26 mmol, 1 Eq.) and 102 mg of MI-PFP (0.27 mmol, 1 Eq.) were dissolved in 1.5 mL of anisole, the flask was sealed with a septum and purged with dry argon for 30 minutes. Then 3 mL of degassed styrene (26 mmol, 100 Eq.) was added with a degassed syringe. Afterwards, the mixture was immersed in a preheated oil bath at 120°C. During the copolymerization, aliquots were taken from the mixture with a degassed syringe in order to monitor the incorporation of MI-PFP in the growing copolymer chains. After the conversion of styrene reached approximately 50% (i.e. 46 minutes of reaction), a degassed solution of 106 mg of MI-PFP (0.29 mmol, 1 Eq.) in degassed anisole was added with a degassed syringe. Due to the poor solubility of MI-PFP in anisole at RT, the solution was preheated at 60-80 °C using an electronic heat gun. The reaction mixture was exposed to air after the conversion of styrene reached 70% (100 minutes of reaction). ~3 mL of THF were added, and the polymer was precipitated in cold methanol. The precipitate was filtered and dried *in vacuo* at RT (1.75 g, 81 % yield). The purified polymer was characterized by FT-IR, ^{19}F NMR (400 MHz, CD_2Cl_2), δ (ppm): -153 (b, 2F, -COO-C-C*F*-), -158.7 (b, 1F, -C*F*-), -163 (b, 2F, -CF-C*F*-CF-); ^{1}H NMR (400 MHz, CD_2Cl_2), δ (ppm): 8.4-8.2 (m, 4H, -C*H*-C-COO-), 7.44-6.20 (m, 354H, aromatic *H*), 4.20-3.75 (m, 4H, -CH_2-O-), 3.28-3.12 (m, 1H, -C*H*-(CH_3)$_3$), 2.30-1.23 (m, 230H, -CH_2-C*H*-, -C*H*-C*H*-, -O-C-(CH_3)$_2$), 1.23-1.05 (m, 6H, -CH_2-CH_3), 1.05-0.60 (m, 18H, -C-(CH_3)$_3$, -CH-C-(CH_3)$_3$); and SEC in THF: M_n = 9070 g mol^{-1}, M_w/M_n 1.16.

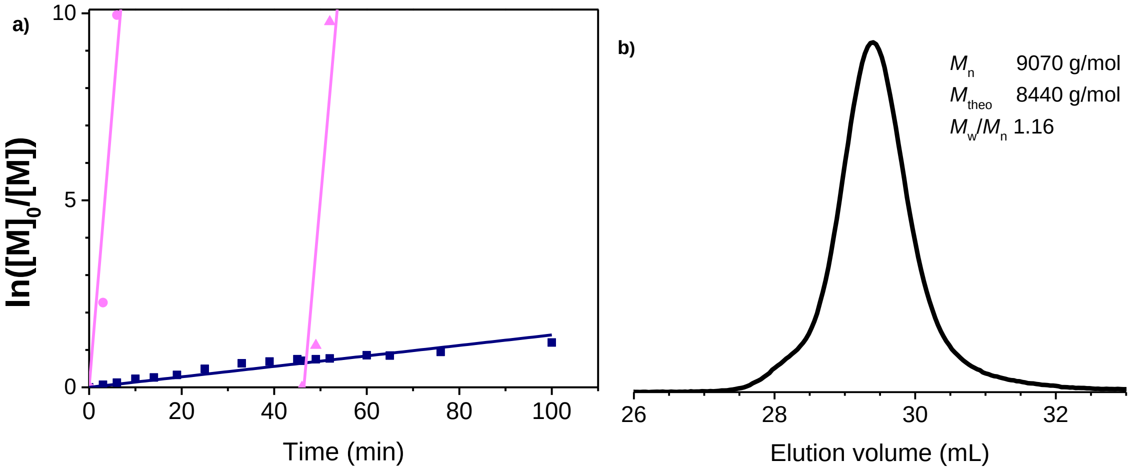

Figure 100 | Characterization of P25: a) Semi-logarithmic plot of monomer conversion versus time for NMP of styrene (squares) with MI-PFP added at the beginning of the polymerization (dots) and at 3/4 of the chain (triangles); **b**) Size exclusion chromatogram of the copolymer, in THF.

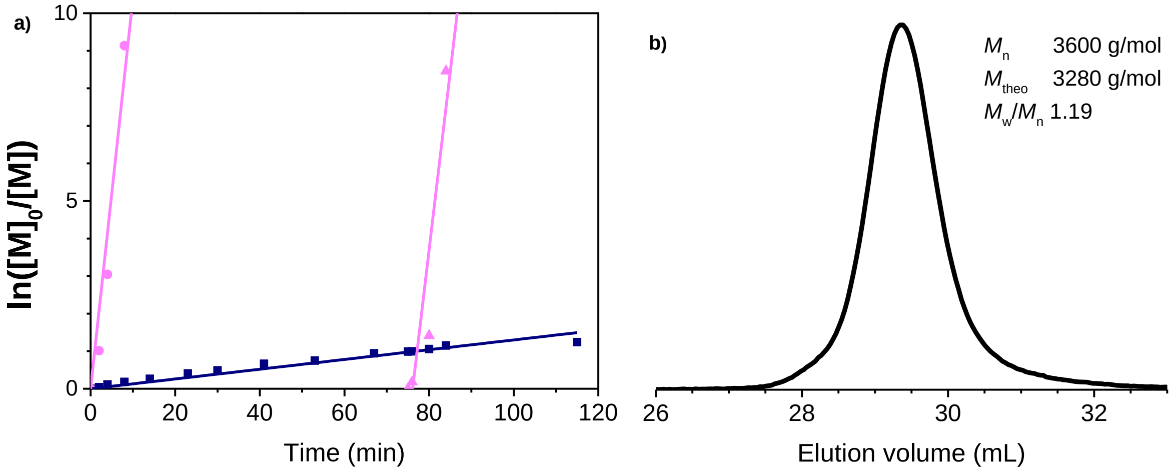

Figure 101 | Characterization of P26: **a**) Semi-logarithmic plot of monomer conversion versus time for NMP of styrene (squares) with MI-PFP added at the beginning of the polymerization (dots) and at the end of polymer chain (triangles); **b**) Size exclusion chromatogram of the copolymer, in THF.

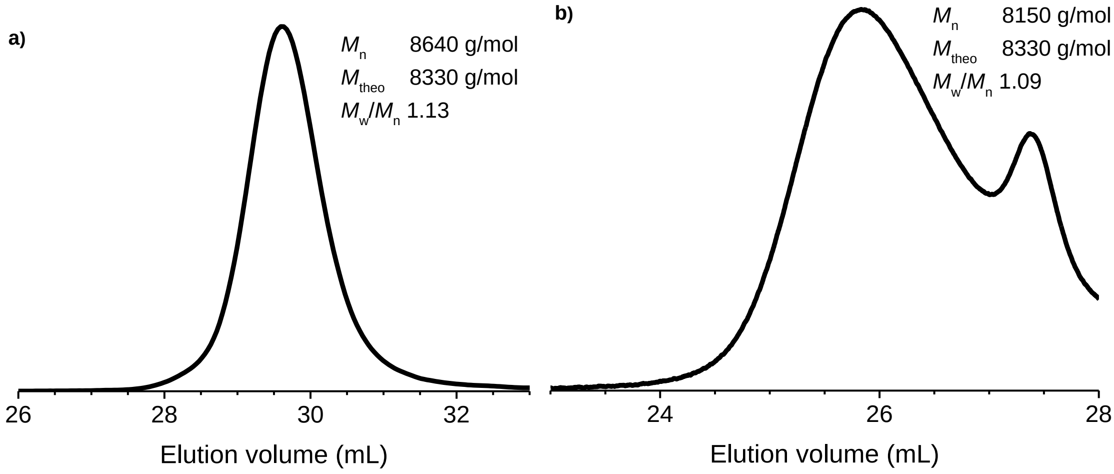

Figure 102 | Size exclusion chromatograms of **P27**: **a**) in THF; **b**) in DMF with 0.1M LiBr.

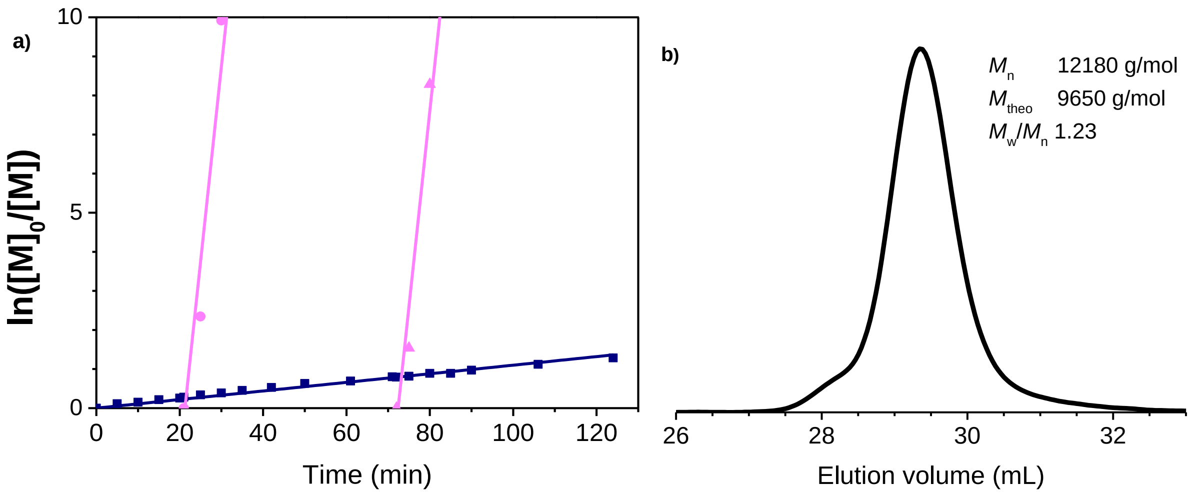

Figure 103 | Characterization of **P28**: **a**) Semi-logarithmic plot of monomer conversion versus time for the NMP of styrene (squares) with MI-PFP added at ~ 1/4 (dots) and ~3/4 of the polymer chain (triangles); **b**) Size exclusion chromatogram of the copolymer, in THF.

“Symmetric” sequence-controlled polymers containing PFP-ester groups

Copolymers of styrene with symmetrically inserted MI-PFP were synthesized by NMP in the presence of **VIII**. The following example corresponds to polymer **P29** in Table 3. 200 mg of **VIII** (0.26 mmol, 1 Eq.) were put in a flask, dissolved in 1.5 mL of anisole. The flask was sealed with a septum and purged with dry argon for 30 minutes. 3 mL of degassed styrene (26 mmol, 100 Eq.) were added with a degassed syringe. The mixture was then immersed in a preheated oil bath at 116°C. During the copolymerization, aliquots were taken from the mixture with a degassed syringe in order to monitor the incorporation of MI-PFP in the growing copolymer chains. After the conversion of styrene reached approximately 50% (i.e. 60 minutes of reaction), a degassed solution containing 218 mg of MI-PFP (0.57 mmol, 2 Eq.) in degassed anisole was added with a degassed syringe. Due to the poor solubility of MI-PFP in anisole at RT, the solution was preheated at 60-80 °C using an electronic heat gun. The reaction mixture was exposed to air after the conversion of styrene reached 60% (90 minutes of the reaction). ~3 mL of THF were added, and the polymer was precipitated in cold methanol. The precipitate was filtered and dried *in vacuo* at RT (1.60 g, 78 % yield). The purified polymer was characterized by FT-IR, ^{19}F NMR (400 MHz, CD_2Cl_2), δ (ppm): -153 (m, 2F, -COO-C-C*F*-), -158.7 (s, 1F, -C*F*-), -163 (s, 2F, -CF-C*F*-CF-); ^{1}H NMR (400 MHz,

CD_2Cl_2), δ (ppm): 8.4-8.2 (m, 4H, -C*H*-C-COO-), 7.50-6.20 (m, 304H, aromatic *H*), 4.67-3.67 (m, 14H, -C*H*-CH_3, -C*H*$_2$-CH_3, -C*H*$_2$-C*H*$_2$-), 3.44 - 3.01 (m, 2H, -C-C*H*-(CH_3)$_3$), 2.40-1.23 (m, 190H, -C*H*$_2$-C*H*-, -C*H*-C*H*-, -CH-C*H*$_3$), 1.23-1.05 (m, 12H, -CH_2-C*H*$_3$), 1.05-0.60 (m, 36H, -C-(C*H*$_3$)$_3$, -CH-C-(C*H*$_3$)$_3$); and SEC in THF: M_n 8520 g·mol^{-1}, M_w/M_n 1.18.

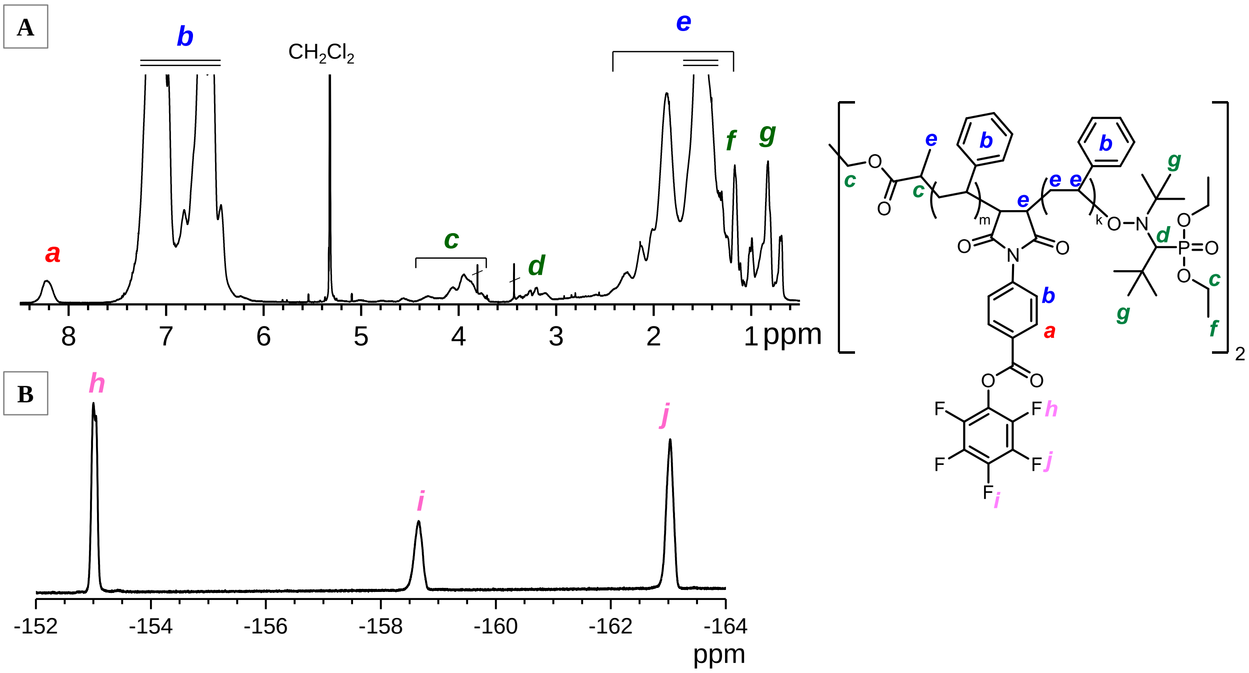

Figure 104 | (A) ^{1}H NMR spectrum of **P29**, in CD_2Cl_2. (**B**) ^{19}F NMR spectrum of **P29**, in CD_2Cl_2.

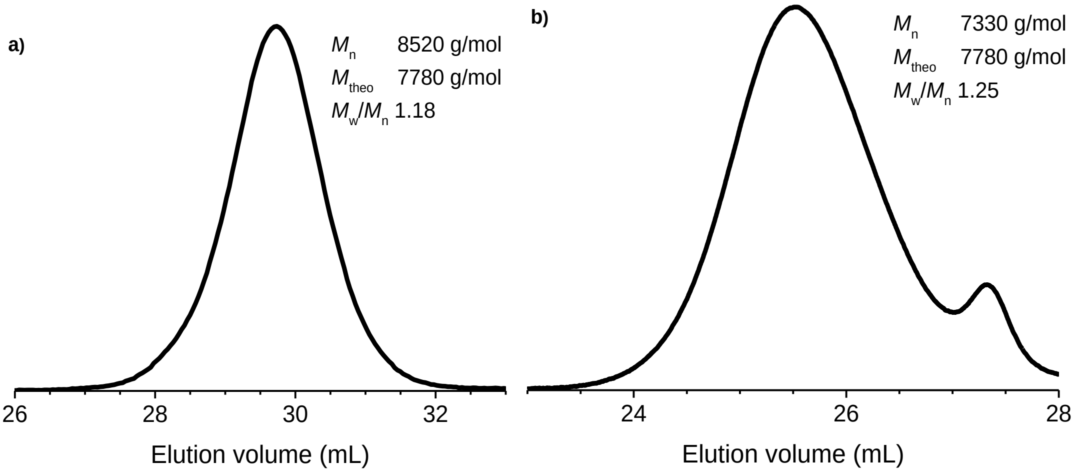

Figure 105 | a) Size exclusion chromatogram of **P29**, in THF; **b**) Size exclusion chromatogram of **P29**, in DMF with 0.1M LiBr.

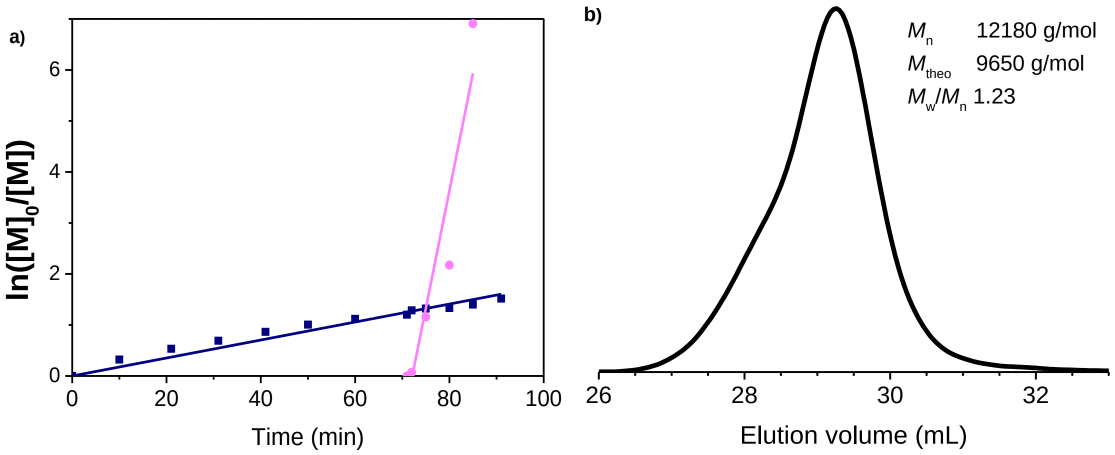

Figure 106 | Characterization of **P30**: **a**) Semi-logarithmic plot of monomer conversion versus time for NMP of styrene (squares) with MI-PFP added close to the ends of the polymer chain (dots); **b**) Size exclusion chromatogram of the copolymer, in THF.

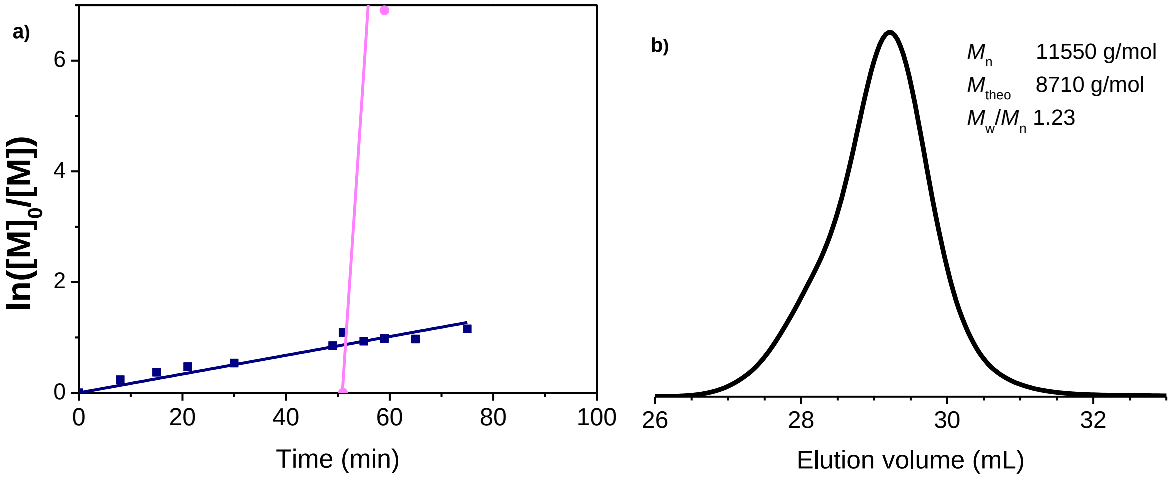

Figure 107 | Characterization of **P31**: **a**) Semi-logarithmic plot of monomer conversion versus time for NMP of styrene (squares) with MI-PFP added close to the ends of the polymer chain (dots); **b**) Size exclusion chromatogram of the copolymer, in THF.

Synthesis of polymer conjugates using IX

Linear polymers with protected CRC-motifs were synthesized by modification of the linear polymer precursors with **IX**. An example is given for **P29**. In a flask, a solution of **IX** (50 mg, 0.03 mmol) in *N*-methylpyrrolidone (1 mL) was added to a solution of **P29** (110 mg, ~0.01 mmol) in *N*-methylpyrrolidone. The flask was sealed with a septum and purged with argon for 20 minutes. The reaction mixture was left for 10 hours at RT. Then the solution was precipitated in cold methanol (150 mL). The polymer was isolated by centrifugation and dried *in vacuo* (102 mg, ~ 70% yield). The purified polymer was characterized by FT-IR and ^{19}F NMR spectroscopies; ^{1}H NMR (400 MHz, CD_2Cl_2), δ (ppm): 8.0-7.7 (m, 4H, -C*H*-C-COO-), 7.53-7.20 (m, 34H, trityl group, -C*H*-CN-), 7.20-6.20 (m, 300H, aromatic *H*), 4.67-3.67 (m, 28H, -C*H*-CH_3, -C*H*$_2$-CH_3, -C*H*$_2$-C*H*$_2$-, -CO-C*H*-NH-, -CO-C*H*$_2$-NH-), 3.60-3.30 (m, 28H, -NH-C*H*$_2$-C*H*$_2$-NH-, -NH-C*H*$_2$-CH_2-CH_2-, -C*H*$_2$-O-C*H*$_2$-, 3.30-2.88 (m, 18H, -C*H*$_2$-S-, -CO-NH-C*H*$_2$-, -C-C*H*-(CH_3)$_3$), 2.74-2.6 (m, 4H, -C-C*H*$_2$-C-), 2.6-2.45 (m, 8H, -CO-C*H*$_2$-C*H*$_2$-CO-), 2.45-2.35 (m, 12H, -SO_2-C-C-C*H*$_3$-), 2.20-1.23 (m, 216H, -C*H*$_2$-C*H*-, -C*H*-C*H*-, -CH-C*H*$_3$, -CO-C*H*$_3$, -C-(C*H*$_3$)$_2$, -O-C-C-C*H*$_3$, -NH-CH_2-C*H*$_2$-C*H*$_2$-), 1.23-1.05 (m, 12H, -CH_2-C*H*$_3$), 1.05-0.60 (m, 36H, -C-(C*H*$_3$)$_3$, -CH-C-(C*H*$_3$)$_3$); and SEC in DMF with 0.1M LiBr: M_n 11250 g·mol^{-1}, M_w/M_n 1.11.

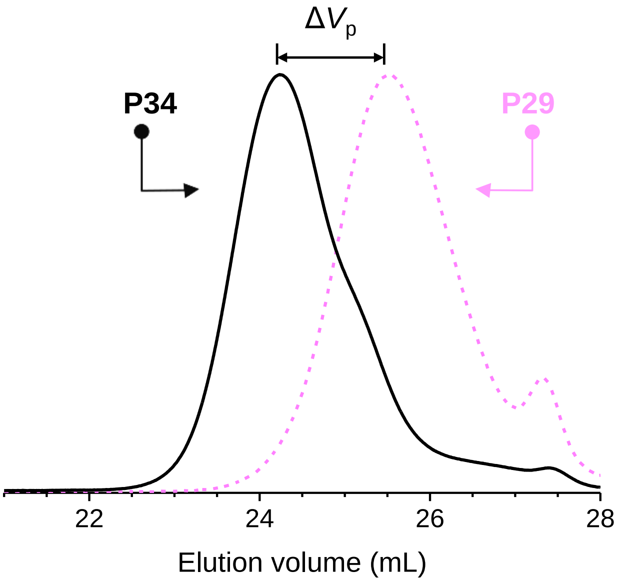

Figure 108 | Size-exclusion chromatograms of **P29** with PFP ester moieties (dashed line) and (**B**) the resulting polymer **P34** after reaction with oligomer **IX** (solid line), in DMF with 0.1 M LiBr.

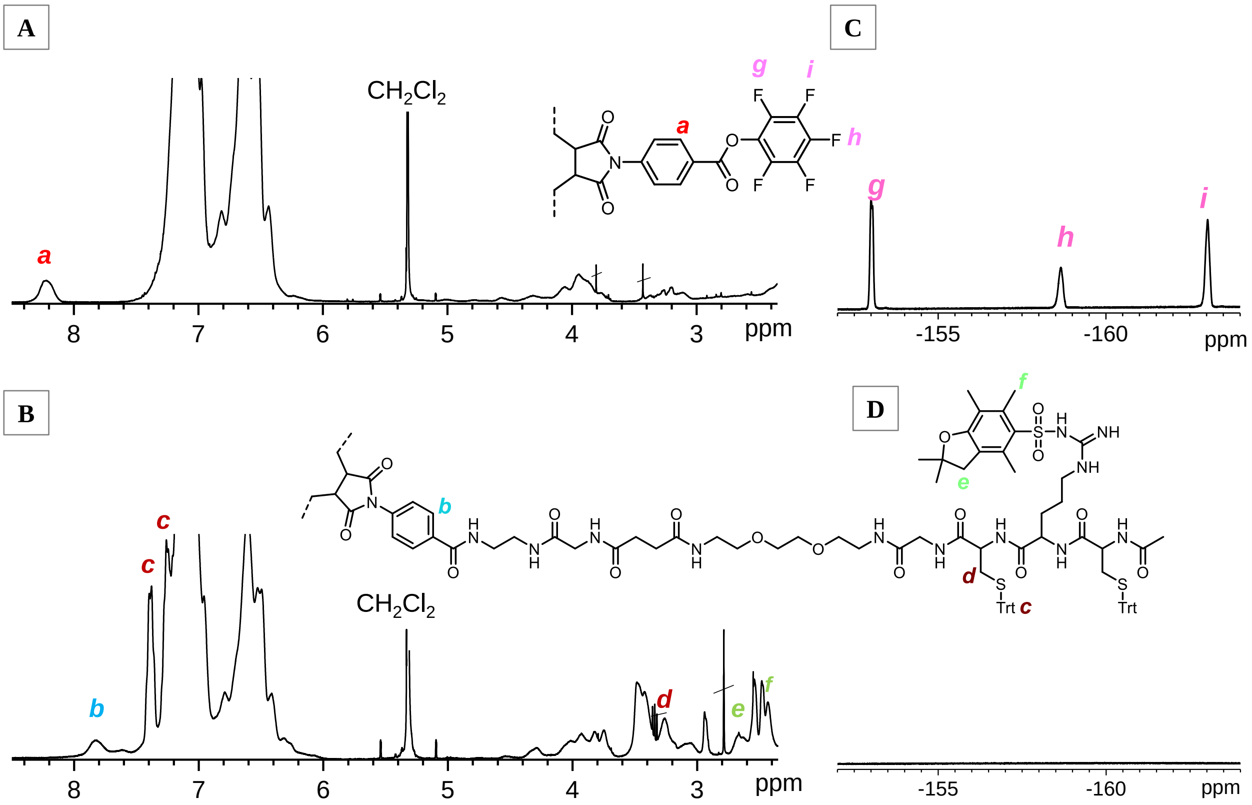

Figure 109 | (A) ^{1}H NMR spectra of **P29** containing pentafluorophenyl ester moieties and (**B**) the resulting polymer **P34** after the reaction with **IX** and (**C**, **D**) the corresponding ^{19}F NMR spectra for **P29** and **P34**, in CD_2Cl_2.

Deprotection of CRC-polymer conjugates

100 mg of CRC-polymer conjugate was dissolved in 1 mL of THF, added into a flask, sealed with a septum and purged with dry argon for 15 minutes. TFA solution was added (1.5 mL: 80% TFA, 10% THF, 6% H_2O, 4% TIS) in a flow of argon. The general composition of the reaction mixture: 60% TFA, 45% THF, 4% H_2O, 1% TIS. After 30 minutes the reaction mixture was precipitated in cold methanol and isolated by centrifugation. 69 mg, ~69% yield. The purified polymer conjugates were characterized by ^{1}H NMR spectroscopy and SEC.

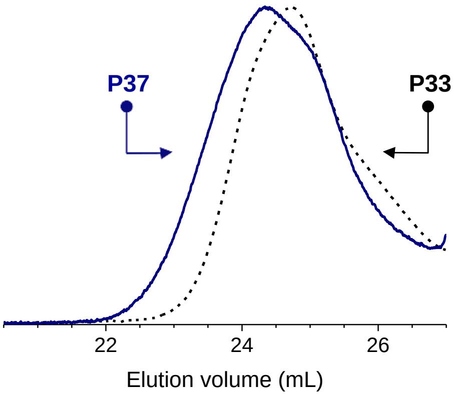

Figure 110 | Size-exclusion chromatograms of the polymers with CRC protected moieties **P33** (dashed line). The resulting polymers **P37** after removal of Trt- and Pbf-protecting groups (solid line), in DMF with 0.1 M LiBr.

Folding of linear polymers containing CRC-motif

A typical procedure for the CRC-polymer conjugates was the following: the polymer was dissolved in *N*-methylpyrrolidone (0.6-0.7 mg/mL) and DIPEA (~0.2% vol.) was added to the solution. After strong air bubbling for 1.5 days, the solution was concentrated, precipitated in a large volume of cold methanol, isolated by centrifugation, and dried *in vacuo*. In some cases, the conditions were slightly modified: DMSO (1-2% vol.) was added to the solution of the polymer.

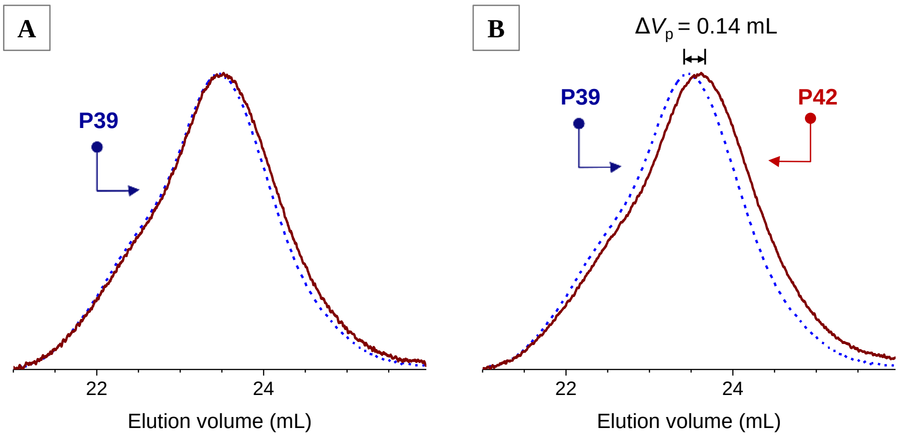

Figure 111 | (**A**), (**B**) Size-exclusion chromatograms of the polymers conjugates with CRC motifs **P39** (dashed line). (**A**) The resulting polymer after the oxidation of thiol groups for 2 days in *N*-methylpyrrolidone (solid line), in CH_2Cl_2. (**B**) The resulting polymer after the oxidation of thiol groups for 2 days in *N*-methylpyrrolidone with added DIPEA (solid line).

Sequence-controlled polymers containing phenanthroline moieties

Copolymers of styrene with symmetrically inserted phenanthroline-bearing maleimides **X** were synthesized by NMP in the presence of **VIII**. The following example corresponds to polymer **P44** in Table 4. 159 mg of **VIII** (0.21 mmol, 1 Eq.) were put in a flask, dissolved in 1.2 mL of anisole. The flask was sealed with a septum and purged with dry argon for 30 minutes. 2.4 mL of degassed styrene (20.9 mmol, 100 Eq.) were added with a degassed syringe. The mixture was then immersed in a preheated oil bath at 120°C. During the copolymerization, aliquots were taken from the mixture with a degassed syringe in order to monitor the incorporation of **X** in the growing copolymer chains. After the conversion of styrene reached approximately 60% (i.e. 50 minutes of reaction), a degassed solution containing 160 mg of **X** (0.42 mmol, 2 Eq.) in degassed DMF was added with a degassed syringe. The reaction mixture was exposed to air after the conversion of styrene reached 80% (90 minutes of the reaction). ~3 mL of THF were added, and the polymer was precipitated in cold methanol. The precipitate was filtered and dried *in vacuo* at RT (1.46 g, 68 % yield). The purified polymer was characterized by ^{1}H NMR (400 MHz, CD_2Cl_2), δ (ppm): 8.98-9.40 (b, 3H, phen –C*H*-N-, -CH-C*H*-C-), 8.01-8.28 (b, 2H, phen -CH-C-C*H*-CH-), 7.55-7.74 (b, 3H, phen -N-C-C*H*-, -C*H*-CH-N-), 6.18-7.43 (m, 400H, PS aromatic *H*), 3.64-4.42 (m, 14H, -C*H*-C-$(CH_3)_3$, -CH_2-CH_2-, -CH_2-CH_3), 1.02-2.38 (m, 262 H, -CH_2-C*H*-CH-CH_3, -C*H*-C*H*-, -N-C-$(CH_3)_3$), 0.60-1.02 (m, 24H, -CH-CH_3, -CH-C-$(CH_3)_3$); and SEC in *N*-methylpyrrolidone with 0.1 M LiBr: M_n 10260 g·mol^{-1}, M_w/M_n 1.60.

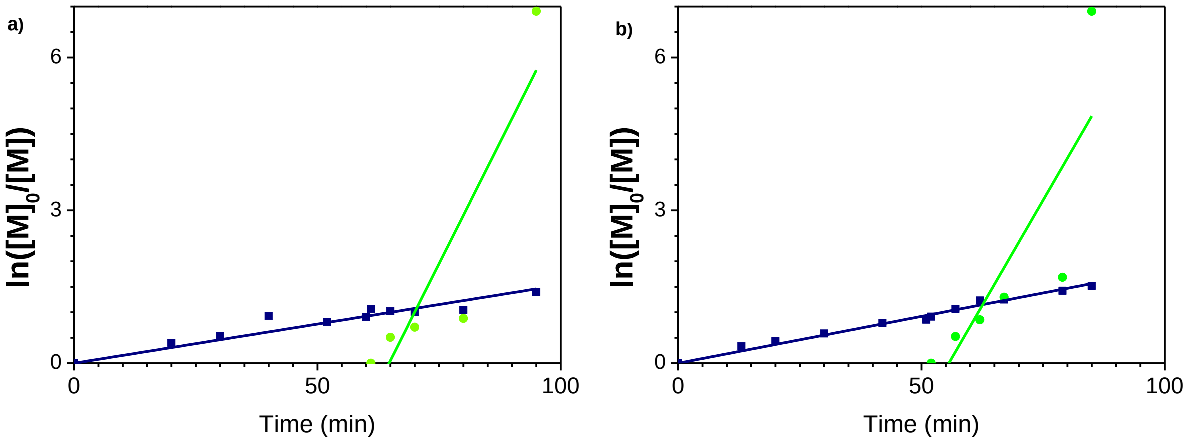

Figure 112 | a) Characterization of **P43**; **b**) Characterization of **P46**. Semi-logarithmic plot of monomer conversion versus time for NMP of styrene (squares) with MI-phen **X** added close to the ends of the polymer chain (dots).

Synthesis of polymer metal complexes

P48. 5.4 mg of [Ru(DMSO)$_4$Cl$_2$] (0.011 mmol, 1 Eq.) were weighted in a round-bottom flask. The flask was sealed with a rubber septum and subsequently degassed with argon. Afterwards 3 mL of anhydrous DMF were added. The mixture was heated at 60 °C in an oil bath. Then a degassed solution of **P43** (90 mg, around 0.01 mmol, 1 Eq. of phen groups) in 15 mL of CHCl$_3$ was added to the mixture and left for 5 hours. After several hours the solution changed colour from yellow to dark brownish. The reaction mixture was left overnight at RT. The solvents were partially removed *in vacuo*. The crude product was dissolved in THF, precipitated in a large volume of cold MeOH (at ice bath), isolated by centrifugation and dried *in vacuo*, yielding a violet powder.

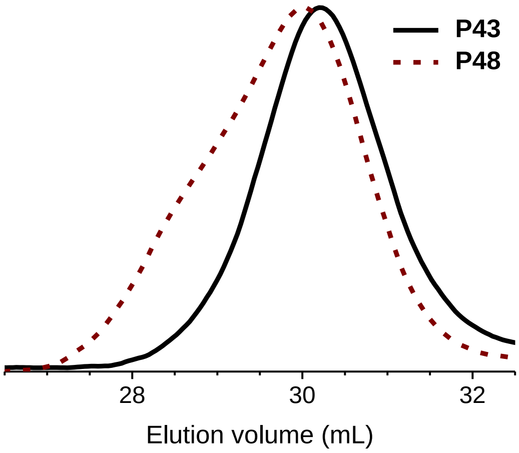

Figure 113 | SEC analysis of Ru(II) polymer complexes. Chromatograms of **P43** (solid) and **P48** (dash), in THF.

P49. 2.9 mg of [Ru(DMSO)$_4$Cl$_2$] (0.006 mmol, 1 Eq.) were weighted in a round-bottom flask. The flask was sealed with a rubber septum and subsequently degassed with argon. Afterwards 3 mL of anhydrous DMF were added. The mixture was heated at 60 °C in an oil bath. Then a degassed solution of **P44** (47 mg, around 0.005 mmol, ~ 2 Eq. of phen groups) in 280 mL of CHCl$_3$ was added slowly to the mixture using a syringe pump (with a speed of 10^{-6} mol/h) during 6 hours. The reaction mixture was left overnight at RT. The solvents were partially removed *in vacuo*. The crude product was dissolved in THF, precipitated in a large volume of cold MeOH (at ice bath), isolated by centrifugation and dried *in vacuo*, yielding a purple (brownish) powder.

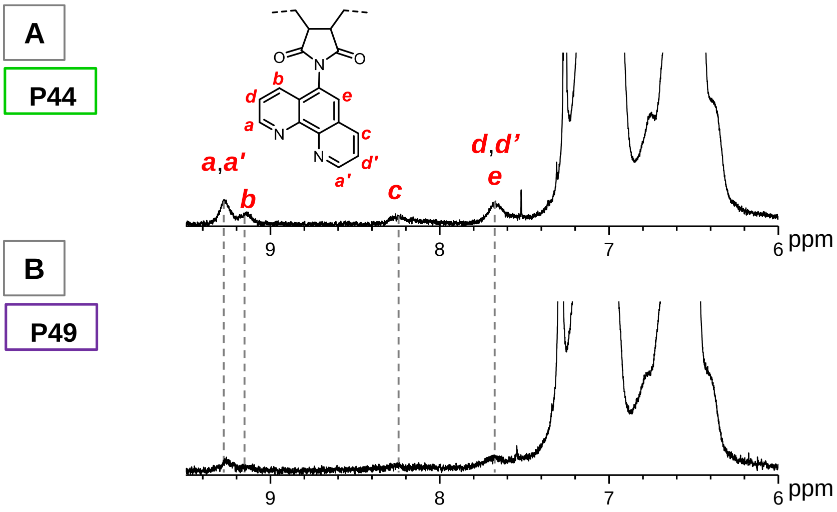

Figure 114 | ^{1}H NMR spectra of **P44** and its complex with Ru(II). (**A**) ^{1}H NMR spectrum of **P44**; (**B**) ^{1}H NMR spectrum of Ru(II) polymer complex **P49**, in $CDCl_3$.

P50. 1 mg of [$Pd(CH_3CN)_4BF_4$] (0.002 mmol, 1 Eq.) were weighted in a round-bottom flask. The flask was sealed with a rubber septum and subsequently degassed with argon. Afterwards 1 mL of CH_3CN was added. Then a degassed solution of **P43** (20 mg, 0.0025-0.003 mmol, 1-1.5 Eq. of phen groups) in 20 mL of CH_2Cl_2 was added to the mixture and left overnight at RT. The solvents were partially removed *in vacuo*, precipitated in a large volume of diethyl ether, isolated by centrifugation and dried *in vacuo*, yielding a yellow powder.

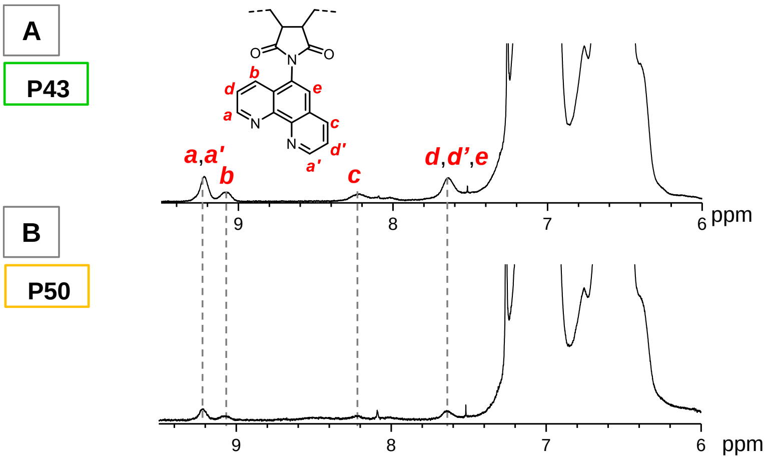

Figure 115 | ^{1}H NMR spectra of **P43** and its complex with Pd(II). (**A**) ^{1}H NMR spectrum of **P43**; (B) ^{1}H NMR spectrum of Pd(II) polymer complex **P50**, in $CDCl_3$.

P51. 0.6 mg of [$Pd(CH_3CN)_4BF_4$] (0.0014 mmol, 1 Eq.) were weighted in a round-bottom flask. The flask was sealed with a rubber septum and subsequently degassed with argon.

Afterwards 1 mL of CH_3CN was added. Then a degassed solution of **P44** (23 mg, 0.0025-0.0028 mmol, ~ 2 Eq. of phen groups) in 130 mL of CH_2Cl_2 was added slowly to the mixture using a syringe pump during 1 day. Then the solvents were partially removed *in vacuo*, precipitated in a large volume of diethyl ether, isolated by centrifugation and dried *in vacuo*, yielding a yellow powder.

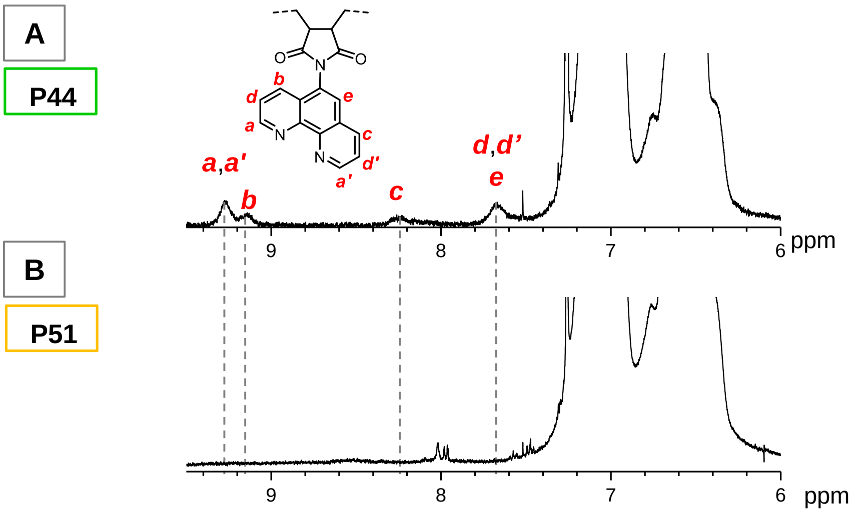

Figure 116 | ^{1}H NMR spectra of **P44** and its complex with Pd(II). (**A**) ^{1}H NMR spectrum of **P44**; (**B**) ^{1}H NMR spectrum of Pd(II) polymer complex **P51**, in $CDCl_3$.

REFERENCES

1. J.F. Lutz, M. Ouchi, D.R. Liu, and M. Sawamoto, *Sequence-controlled polymers.* Science, 2013. **341**(6146): p. 1238149.

2. M. Ouchi, N. Badi, J.F. Lutz, and M. Sawamoto, *Single-chain technology using discrete synthetic macromolecules.* Nat. Chem., 2011. **3**(12): p. 917-924.

3. E. Harth, B.V. Horn, V.Y. Lee, D.S. Germack, C.P. Gonzales, R.D. Miller, and C.J. Hawker, *A facile approach to architecturally defined nanoparticles via intramolecular chain collapse.* J. Am. Chem. Soc., 2002. **124**(29): p. 8653-8660.

4. D. Mecerreyes, V. Lee, C.J. Hawker, J.L. Hedrick, A. Wursch, W. Volksen, T. Magbitang, E. Huang, and R.D. Miller, *A novel approach to functionalized nanoparticles: self-crosslinking of macromolecules in ultradilute solution.* Adv. Mater., 2001. **13**(3): p. 204-208.

5. B.T. Tuten, D. Chao, C.K. Lyon, and E.B. Berda, *Single-chain polymer nanoparticles via reversible disulfide bridges.* Polym. Chem., 2012. **3**(11): p. 3068.

6. S. Mavila, C.E. Diesendruck, S. Linde, L. Amir, R. Shikler, and N.G. Lemcoff, *Polycyclooctadiene complexes of rhodium(I): direct access to organometallic nanoparticles.* Angew. Chem., Int. Ed. Engl., 2013. **52**(22): p. 5767-5770.

7. A. Sanchez-Sanchez, A. Arbe, J. Colmenero, and J.A. Pomposo, *Metallo-folded single-chain nanoparticles with catalytic selectivity.* ACS Macro Lett., 2014. **3**(5): p. 439-443.

8. B.V. Schmidt, N. Fechler, J. Falkenhagen, and J.F. Lutz, *Controlled folding of synthetic polymer chains through the formation of positionable covalent bridges.* Nat. Chem., 2011. **3**(3): p. 234-238.

9. M. Zamfir, P. Theato, and J.F. Lutz, *Controlled folding of polystyrene single chains: design of asymmetric covalent bridges.* Polym. Chem., 2012. **3**(7): p. 1796-1802.

10. G. De Bo, S. Kuschel, D.A. Leigh, B. Lewandowski, M. Papmeyer, and J.W. Ward, *Efficient assembly of threaded molecular machines for sequence-specific synthesis.* J. Am. Chem. Soc., 2014. **136**(15): p. 5811-5814.

11. B. Lewandowski, G. De Bo, J.W. Ward, M. Papmeyer, S. Kuschel, M.J. Aldegunde, P.M. Gramlich, D. Heckmann, S.M. Goldup, D.M. D'Souza, A.E. Fernandes, and D.A. Leigh, *Sequence-specific peptide synthesis by an artificial small-molecule machine.* Science, 2013. **339**(6116): p. 189-193.

12. M. Zamfir and J.F. Lutz, *Ultra-precise insertion of functional monomers in chain-growth polymerizations.* Nat. Commun., 2012. **3**: p. 1138.

13. C. Wu, J.C. Leroux, and M.A. Gauthier, *Twin disulfides for orthogonal disulfide pairing and the directed folding of multicyclic peptides.* Nat. Chem., 2012. **4**(12): p. 1044-1049.

14. O. Shishkan, M. Zamfir, M.A. Gauthier, H.G. Borner, and J.F. Lutz, *Complex single-chain polymer topologies locked by positionable twin disulfide cyclic bridges.* Chem. Commun., 2014. **50**(13): p. 1570-1572.

15. R.B. Merrifield, *Solid phase peptide synthesis. I. The synthesis of a tetrapeptide.* J. Am. Chem. Soc., 1963. **85**(14): p. 2149-2154.

16. E. Brule, J. Guo, G.W. Coates, and C.M. Thomas, *Metal-catalyzed synthesis of alternating copolymers.* Macromol. Rapid Commun., 2011. **32**(2): p. 169-185.

17. M. Verswyvel, J. Steverlynck, S. Hadj Mohamed, M. Trabelsi, B. Champagne, and G. Koeckelberghs, *All-conjugated ABC-block-copolymer formation with a varying sequence via an unassociated catalyst.* Macromolecules, 2014. **47**(14): p. 4668-4675.

18. K. Satoh, S. Ozawa, M. Mizutani, K. Nagai, and M. Kamigaito, *Sequence-regulated vinyl copolymers by metal-catalysed step-growth radical polymerization.* Nat. Commun., 2010. **1**: p. 6.

19. K. Satoh, M. Mizutani, and M. Kamigaito, *Metal-catalyzed radical polyaddition as a novel polymer synthetic route.* Chem. Commun., 2007(12): p. 1260-1262.

20. S. Pfeifer and J.F. Lutz, *A facile procedure for controlling monomer sequence distribution in radical chain polymerizations.* J. Am. Chem. Soc., 2007. **129**(31): p. 9542-9543.

21. S. Pfeifer and J.F. Lutz, *Development of a library of N-substituted maleimides for the local functionalization of linear polymer chains.* Chem. Eur. J., 2008. **14**(35): p. 10949-10957.

22. K. Satoh, M. Matsuda, K. Nagai, and M. Kamigaito, *AAB-sequence living radical chain copolymerization of naturally occurring limonene with maleimide: an end-to-end sequence-regulated copolymer.* J. Am. Chem. Soc., 2010. **132**(29): p. 10003-10005.

23. S. Ida, T. Terashima, M. Ouchi, and M. Sawamoto, *Selective radical addition with a designed heterobifunctional halide: a primary study toward sequence-controlled polymerization upon template effect.* J. Am. Chem. Soc., 2009. **131**(31): p. 10808-10809.

24. F.S. Bates, M.A. Hillmyer, T.P. Lodge, C.M. Bates, K.T. Delaney, and G.H. Fredrickson, *Multiblock polymers: panacea or Pandora's box?* Science, 2012. **336**(6080): p. 434-440.

25. G. Gody, T. Maschmeyer, P.B. Zetterlund, and S. Perrier, *Rapid and quantitative one-pot synthesis of sequence-controlled polymers by radical polymerization.* Nat. Commun., 2013. **4**: p. 2505.

26. K. Nakatani, Y. Ogura, Y. Koda, T. Terashima, and M. Sawamoto, *Sequence-regulated copolymers via tandem catalysis of living radical polymerization and in situ transesterification.* J. Am. Chem. Soc., 2012. **134**(9): p. 4373-4383.

27. M. Szwarc, M. Levy, and R. Milkovich, *Polymerization initiated by electron transfer to monomer. A new method of formation of block polymers.* J. Am. Chem. Soc., 1956. **78**(11): p. 2656-2657.

28. J.G. Kim, C.D. Cowman, A.M. LaPointe, U. Wiesner, and G.W. Coates, *Tailored living block copolymerization: multiblock poly(cyclohexene carbonate)s with sequence control.* Macromolecules, 2011. **44**(5): p. 1110-1113.

29. S. Guo, J. Rzayev, T.S. Bailey, A.S. Zalusky, R. Olayo-Valles, and M.A. Hillmyer, *Nanopore and nanobushing arrays from ABC triblock thin films containing two etchable blocks.* Chem. Mater., 2006. **18**(7): p. 1719-1721.

30. A.H. Soeriyadi, C. Boyer, F. Nystrom, P.B. Zetterlund, and M.R. Whittaker, *High-order multiblock copolymers via iterative Cu(0)-mediated radical polymerizations (SET-LRP): toward biological precision.* J. Am. Chem. Soc., 2011. **133**(29): p. 11128-11131.

31. J.F. Lutz, *Writing on polymer chains.* Acc. Chem. Res., 2013. **46**(11): p. 2696-2705.

32. S. Srichan, D. Chan-Seng, and J.F. Lutz, *Influence of strong electron-donor monomers in sequence-controlled polymerizations.* ACS Macro Lett., 2012. **1**(5): p. 589-592.

33. J. Willenbacher, Altintas, O., Roesky, P. W., Barner-Kowollik, C., *Single-chain self-folding of synthetic polymers induced by metal-ligand complexation.* Macromol. Rapid Commun., 2014. **35**(1): p. 45-51.

34. J.F. Lutz, *Sequence-controlled polymerizations: the next Holy Grail in polymer science?* Polym. Chem., 2010. **1**(1): p. 55.

35. R.B. Merrifield, *Solid phase synthesis (Nobel lecture).* Angew. Chem., Int. Ed. Engl., 1985. **24**(10): p. 799-810.

36. T.J. Dickerson, N.N. Reed, and K.D. Janda, *Soluble polymers as scaffolds for recoverable catalysts and reagents.* Chem. Rev., 2002. **102**(10): p. 3325-3344.

37. C. Cho, E. Moran, Cherry, J. Stephans, S. Fodor, C. Adams, A. Sundaram, J. Jacobs, and P. Schultz, *An unnatural biopolymer.* Science, 1993. **261**(5126): p. 1303-1305.

38. K. Burgess, H. Shin, and D.S. Linthicum, *Solid-phase syntheses of unnatural biopolymers containing repeating urea units.* Angew. Chem., Int. Ed. Engl., 1995. **34**(8): p. 907-909.

39. T.M. Fyles, C.W. Hu, and H. Luong, *Solid-phase synthesis of oligoester ion channels.* J. Org. Chem., 2006. **71**(22): p. 8545-8551.

40. K. Rose and J. Vizzavona, *Stepwise solid-phase synthesis of polyamides as linkers.* J. Am. Chem. Soc., 1999. **121**(30): p. 7034-7038.

41. J. Li, R.M. Stayshich, and T.Y. Meyer, *Exploiting sequence to control the hydrolysis behavior of biodegradable PLGA copolymers.* J. Am. Chem. Soc., 2011. **133**(18): p. 6910-6913.

42. H. Colquhoun and J.F. Lutz, *Information-containing macromolecules.* Nat. Chem., 2014. **6**(6): p. 455-456.

43. H. Mutlu and J.F. Lutz, *Reading polymers: sequencing of natural and synthetic macromolecules.* Angew. Chem., Int. Ed. Engl., 2014.

44. G.M. Church, Y. Gao, and S. Kosuri, *Next-generation digital information storage in DNA.* Science, 2012. **337**(6102): p. 1628.

45. C.K. Lyon, A. Prasher, A.M. Hanlon, B.T. Tuten, C.A. Tooley, P.G. Frank, and E.B. Berda, *A brief user's guide to single-chain nanoparticles.* Polym. Chem., 2014.

46. D.J. Hill, M.J. Mio, R.B. Prince, T.S. Hughes, and J.S. Moore, *A field guide to foldamers.* Chem. Rev., 2001. **101**(12): p. 3893-4012.

47. O. Altintas and C. Barner-Kowollik, *Single chain folding of synthetic polymers by covalent and non-covalent interactions: current status and future perspectives.* Macromol. Rapid Commun., 2012. **33**(11): p. 958-971.

48. S. Ida, T. Terashima, M. Ouchi, and M. Sawamoto, *Selective single monomer addition in living cationic polymerization: sequential double end-functionalization in combination with capping agent.* J. Polym. Sci., Part A: Polym. Chem., 2010. **48**(15): p. 3375-3381.

49. J. Vandenbergh, G. Reekmans, P. Adriaensens, and T. Junkers, *Synthesis of sequence controlled acrylate oligomers via consecutive RAFT monomer additions.* Chem. Commun., 2013. **49**(88): p. 10358-10360.

50. X. Tong, B.H. Guo, and Y. Huang, *Toward the synthesis of sequence-controlled vinyl copolymers.* Chem. Commun., 2011. **47**(5): p. 1455-1457.

51. S. Ida, M. Ouchi, and M. Sawamoto, *Designer template initiator for sequence regulated polymerization: systems design for substrate-selective metal-catalyzed radical addition and living radical polymerization.* Macromol. Rapid Commun., 2011. **32**(2): p. 209-214.

52. S. Ida, M. Ouchi, and M. Sawamoto, *Template-assisted selective radical addition toward sequence-regulated polymerization: lariat capture of target monomer by template initiator.* J. Am. Chem. Soc., 2010. **132**(42): p. 14748-14750.

53. M. Ouchi, Y. Hibi, T. Arima, D. Hayata, and M. Sawamoto, *Selective single monomer radical addition via template-assisted ring closure: A feasibility study toward sequence control in vinyl polymers with peptide templates,* in *Sequence-controlled*

polymers: Synthesis, self-assembly, and properties. American Chemical Society, 2014. P. 149-160.

54. K.A. Davis and K. Matyjaszewski, *ABC triblock copolymers prepared using atom transfer radical polymerization techniques.* Macromolecules, 2001. **34**(7): p. 2101-2107.

55. K. Takahashi, H. Hasegawa, T. Hashimoto, V. Bellas, H. Iatrou, and N. Hadjichristidis, *Four-phase triple coaxial cylindrical microdomain morphology in a linear tetrablock quaterpolymer of styrene, isoprene, dimethylsiloxane, and 2-vinylpyridine.* Macromolecules, 2002. **35**(13): p. 4859-4861.

56. A. Hasneen, H.S. Han, and H.-J. Paik, *Synthesis of linear tetrablock quaterpolymers via atom transfer radical polymerization and a click coupling approach.* React. Funct. Polym., 2009. **69**(9): p. 681-687.

57. C. Boyer, A.H. Soeriyadi, P.B. Zetterlund, and M.R. Whittaker, *Synthesis of complex multiblock copolymers via a simple iterative Cu(0)-mediated radical polymerization approach.* Macromolecules, 2011. **44**(20): p. 8028-8033.

58. J. Vandenbergh, T. de Moraes Ogawa, and T. Junkers, *Precision synthesis of acrylate multiblock copolymers from consecutive microreactor RAFT polymerizations.* J. Polym. Sci., Part A: Polym. Chem., 2013. **51**(11): p. 2366-2374.

59. J.M.G. Cowie, *Alternating copolymers*. Plenum Press, 1985.

60. J.F. Lutz, B.V. Schmidt, and S. Pfeifer, *Tailored polymer microstructures prepared by atom transfer radical copolymerization of styrene and N-substituted maleimides.* Macromol. Rapid Commun., 2011. **32**(2): p. 127-135.

61. M. Hisano, K. Takeda, T. Takashima, Z. Jin, A. Shiibashi, and A. Matsumoto, *Sequence-controlled radical copolymerization of N-substituted maleimides with olefins and polyisobutene macromonomers to fabricate thermally stable and transparent maleimide copolymers with tunable glass transition temperatures and viscoelastic properties.* Macromolecules, 2013. **46**(19): p. 7733-7744.

62. D. Benoit, C.J. Hawker, E.E. Huang, Z. Lin, and T.P. Russell, *One-step formation of functionalized block copolymers.* Macromolecules, 2000. **33**(5): p. 1505-1507.

63. D. Chan-Seng, M. Zamfir, and J.F. Lutz, *Polymer-chain encoding: synthesis of highly complex monomer sequence patterns by using automated protocols.* Angew. Chem., Int. Ed. Engl., 2012. **51**(49): p. 12254-12257.

64. N. Baradel, O. Gok, M. Zamfir, A. Sanyal, and J.F. Lutz, *Sequence-controlled polymerization using dendritic macromonomers: precise chain-positioning of bulky functional clusters.* Chem. Commun., 2013. **49**(66): p. 7280-7282.

65. N. Baradel, S. Fort, S. Halila, N. Badi, and J.F. Lutz, *Synthesis of single-chain sugar arrays.* Angew. Chem., Int. Ed. Engl., 2013. **52**(8): p. 2335-2339.

66. S. Srichan, H. Mutlu, N. Badi, and J.F. Lutz, *Precision PEGylated polymers obtained by sequence-controlled copolymerization and postpolymerization modification.* Angew. Chem., Int. Ed. Engl., 2014. **53**(35): p. 9231-9235.

67. D. Moatsou, C.F. Hansell, and R.K. O'Reilly, *Precision polymers: a kinetic approach for functional poly(norbornenes).* Chem. Sci., 2014. **5**(6): p. 2246.

68. T. Aida and S. Inoue, *Catalytic reaction on both sides of a metalloporphyrin plane - alternating copolymerization of phthalic-anhydride and epoxypropane with an aluminum porphyrin quaternary salt system.* J. Am. Chem. Soc., 1985. **107**(5): p. 1358-1364.

69. R.C. Jeske, A.M. DiCiccio, and G.W. Coates, *Alternating copolymerization of epoxides and cyclic anhydrides: an improved route to aliphatic polyesters.* J. Am. Chem. Soc., 2007. **129**(37): p. 11330-11331.

70. J.W. Kramer, D.S. Treitler, E.W. Dunn, P.M. Castro, T. Roisnel, C.M. Thomas, and G.W. Coates, *Polymerization of enantiopure monomers using syndiospecific catalysts: a new approach to sequence control in polymer synthesis.* J. Am. Chem. Soc., 2009. **131**(44): p. 16042-16044.

71. N.V. Tsarevsky, B.S. Sumerlin, and K. Matyjaszewski, *Step-growth “click” coupling of telechelic polymers prepared by atom transfer radical polymerization.* Macromolecules, 2005. **38**(9): p. 3558-3561.

72. R.P. Cheng, S.H. Gellman, and W.F. DeGrado, *β-Peptides: from structure to function.* Chem. Rev., 2001. **101**(10): p. 3219-3232.

73. L. Hartmann and H.G. Borner, *Precision polymers: monodisperse, monomer-sequence-defined segments to target future demands of polymers in medicine.* Adv. Mater., 2009. **21**(32-33): p. 3425-3431.

74. E. Uhlmann, A. Peyman, G. Breipohl, and D.W. Will, *PNA: synthetic polyamide nucleic acids with unusual binding properties.* Angew. Chem., Int. Ed., 1998. **37**(20): p. 2797-2823.

75. J. Sun, C. Proulx, and R.N. Zuckermann, *Precision sequence control in bioinspired peptoid polymers*, in *Sequence-controlled polymers: Synthesis, self-Assembly, and properties*. American Chemical Society, 2014. P. 35-53.

76. J. Sun and R.N. Zuckermann, *Peptoid polymers: a highly designable bioinspired material.* ACS Nano, 2013. **7**(6): p. 4715-4732.

77. T.T. Trinh, L. Oswald, D. Chan-Seng, and J.F. Lutz, *Synthesis of molecularly encoded oligomers using a chemoselective "AB + CD" iterative approach.* Macromol. Rapid Commun., 2014. **35**(2): p. 141-145.

78. M.I. Amrane, D. Chouikhi, N. Badi, and J.F. Lutz, *Synthesis of well-defined polystyrene rink amide soluble supports and their use in peptide synthesis.* Macromol. Chem. Phys., 2014. **215**(20): p. 1984-1990.

79. J.J. Yan, D. Wang, D.C. Wu, and Y.Z. You, *Synthesis of sequence-ordered polymers via sequential addition of monomers in one pot.* Chem. Commun., 2013. **49**(54): p. 6057-6059.

80. M. Porel and C.A. Alabi, *Sequence-defined polymers via orthogonal allyl acrylamide building blocks.* J. Am. Chem. Soc., 2014. **136**(38): p. 13162-13165.

81. S.C. Solleder and M.A. Meier, *Sequence control in polymer chemistry through the Passerini three-component reaction.* Angew. Chem., Int. Ed. Engl., 2014. **53**(3): p. 711-714.

82. P. Dawson, T. Muir, I. Clark-Lewis, and S. Kent, *Synthesis of proteins by native chemical ligation.* Science, 1994. **266**(5186): p. 776-779.

83. S.H. Gellman, *Foldamers: a manifesto.* Acc. Chem. Res., 1998. **31**(4): p. 173-180.

84. T.B. Yu, J.Z. Bai, and Z. Guan, *Cycloaddition-promoted self-assembly of a polymer into well-defined beta sheets and hierarchical nanofibrils.* Angew. Chem., Int. Ed. Engl., 2009. **48**(6): p. 1097-1101.

85. J.P. Schneider, D.J. Pochan, B. Ozbas, K. Rajagopal, L. Pakstis, and J. Kretsinger, *Responsive hydrogels from the intramolecular folding and self-assembly of a designed peptide.* J. Am. Chem. Soc., 2002. **124**(50): p. 15030-15037.

86. E. Yashima, K. Maeda, H. Iida, Y. Furusho, and K. Nagai, *Helical polymers: synthesis, structures, and functions.* Chem Rev, 2009. **109**(11): p. 6102-6211.

87. J.J. Cornelissen, J.J. Donners, R. de Gelder, W.S. Graswinckel, G.A. Metselaar, A.E. Rowan, N.A. Sommerdijk, and R.J. Nolte, *beta-Helical polymers from isocyanopeptides.* Science, 2001. **293**(5530): p. 676-680.

88. S. Hecht, *Construction with macromolecules.* Mater. Today, 2005. **8**(3): p. 48-55.

89. J.F. Lutz, *Controlled compaction of atactic polymer chains: another approach to macromolecular folding.* Kobunshi, 2013. **62(9)**: p. 509-510.

90. J. Pyun, C. Tang, T. Kowalewski, J.M.J. Fréchet, and C.J. Hawker, *Synthesis and direct visualization of block copolymers composed of different macromolecular architectures.* Macromolecules, 2005. **38**(7): p. 2674-2685.

91. C.T. Adkins, J.N. Dobish, S. Brown, and E. Harth, *Water-soluble semiconducting nanoparticles for imaging.* ACS Macro Lett., 2013. **2**(8): p. 710-714.

92. P.G. Frank, B.T. Tuten, A. Prasher, D. Chao, and E.B. Berda, *Intra-chain photodimerization of pendant anthracene units as an efficient route to single-chain nanoparticle fabrication.* Macromol. Rapid Commun., 2014. **35**(2): p. 249-253.

93. B.S. Murray and D.A. Fulton, *Dynamic covalent single-chain polymer nanoparticles.* Macromolecules, 2011. **44**(18): p. 7242-7252.

94. J.A. Pomposo, I. Perez-Baena, F. Lo Verso, A.J. Moreno, A. Arbe, and J. Colmenero, *How far are single-chain polymer nanoparticles in solution from the globular state?* ACS Macro Lett., 2014. **3**(8): p. 767-772.

95. R.K. Roy and J.F. Lutz, *Compartmentalization of single polymer chains by stepwise intramolecular cross-linking of sequence-controlled macromolecules.* J. Am. Chem. Soc., 2014. **136**(37): p. 12888-12891.

96. P. Lutz, C. Strazielle, and P. Rempp, *Synthesis and solution properties of macrocyclic polymers*, in *Proceedings of the International Symposium on Recent Advances in Anionic Polymerization*, 1987. P. 403-410.

97. M. Schappacher and A. Deffieux, *Imaging of catenated, figure-of-eight, and trefoil knot polymer rings.* Angew. Chem. Int. Ed. Engl., 2009. **48**(32): p. 5930-5933.

98. H.R. Kricheldorf, M. Al-Masri, and G. Schwarz, *Macrocycles. 20. Cyclic poly(ethylene glycol) phthalates via ring-exchange substitution.* Macromolecules, 2002. **35**(24): p. 8936-8942.

99. S. Gooßen, A.R. Brás, W. Pyckhout-Hintzen, A. Wischnewski, D. Richter, M. Rubinstein, J. Roovers, P.J. Lutz, Y. Jeong, T. Chang, and D. Vlassopoulos, *Influence of the solvent quality on ring polymer dimensions.* Macromolecules, 2015. **48**(5): p. 1598-1605.

100. J. Roovers and P.M. Toporowski, *Synthesis of high molecular weight ring polystyrenes.* Macromolecules, 1983. **16**(6): p. 843-849.

101. Z.F. Jia and M.J. Monteiro, *Cyclic polymers: methods and strategies.* J. Polym. Sci., Part A: Polym. Chem., 2012. **50**(11): p. 2085-2097.

102. P.E. Milan M. Stamenović, Eisuke Baba, Takuya Yamamoto, Yasuyuki Tezuka and Filip E. Du Prez *Straightforward synthesis of functionalized cyclic polymers in high yield via RAFT and thiolactone–disulfide chemistry.* Polym. Chem., 2013. **4**: p. 184-193.

103. G.B. McKenna, G. Hadziioannou, P. Lutz, G. Hild, C. Strazielle, C. Straupe, P. Rempp, and A.J. Kovacs, *Dilute solution characterization of cyclic polystyrene molecules and their zero-shear viscosity in the melt.* Macromolecules, 1987. **20**(3): p. 498-512.

104. M. Schappacher and A. Deffieux, *Atomic force microscopy imaging and dilute solution properties of cyclic and linear polystyrene combs.* J. Am. Chem. Soc., 2008. **130**(44): p. 14684-14689.

105. B. Chen, K. Jerger, J.M. Frechet, and F.C. Szoka, Jr., *The influence of polymer topology on pharmacokinetics: differences between cyclic and linear PEGylated poly(acrylic acid) comb polymers.* Journal of controlled release : official journal of the Controlled Release Society, 2009. **140**(3): p. 203-209.

106. B.A. Laurent and S.M. Grayson, *An efficient route to well-defined macrocyclic polymers via "click" cyclization.* J. Am. Chem. Soc., 2006. **128**(13): p. 4238-4239.

107. J. Xu, J. Ye, and S.Y. Liu, *Synthesis of well-defined cyclic poly(N-isopropylacrylamide) via click chemistry and its unique thermal phase transition behavior.* Macromolecules, 2007. **40**(25): p. 9103-9110.

108. A.S. Goldmann, D. Quemener, P.E. Millard, T.P. Davis, M.H. Stenzel, C. Barner-Kowollik, and A.H.E. Wuller, *Access to cyclic polystyrenes via a combination of reversible addition fragmentation chain transfer (RAFT) polymerization and click chemistry.* Polymer, 2008. **49**(9): p. 2274-2281.

109. J.N. Hoskins and S.M. Grayson, *Synthesis and degradation behavior of cyclic poly(ε-caprolactone).* Macromolecules, 2009. **42 (17)**: p. 6406-6413.

110. M.R. Whittaker, Y.K. Goh, H. Gemici, T.M. Legge, S. Perrier, and M.J. Monteiro, *Synthesis of monocyclic and linear polystyrene using the reversible coupling/cleavage of thiol/disulfide groups.* Macromolecules, 2006. **39**(26): p. 9028-9034.

111. D.E. Lonsdale and M.J. Monteiro, *Synthesis and self-assembly of amphiphilic macrocyclic block copolymer topologies.* J. Polym. Sci., Part A: Polym. Chem., 2011. **49**(21): p. 4603-4612.

112. H. Li, A. Debuigne, R. Jerome, and P. Lecomte, *Synthesis of macrocyclic poly(epsilon-caprolactone) by intramolecular cross-linking of unsaturated end groups of chains precyclic by the initiation.* Angew. Chem., Int. Ed. Engl., 2006. **45**(14): p. 2264-2267.

113. H. Li, R. Riva, R. Jerome, and P. Lecomte, *Combination of ring-opening polymerization and "click" chemistry for the synthesis of an amphiphilic tadpole-shaped poly(ε-caprolactone) grafted by PEO.* Macromolecules, 2007. **40**(4): p. 824-831.

114. D.E. Lonsdale and M.J. Monteiro, *Various polystyrene topologies built from tailored cyclic polystyrene via CuAAC reactions.* Chem. Commun., 2010. **46**(42): p. 7945-7947.

115. N. Sugai, H. Heguri, T. Yamamoto, and Y. Tezuka, *A programmed polymer folding: click and clip construction of doubly fused tricyclic and triply fused tetracyclic polymer topologies.* J. Am. Chem. Soc., 2011. **133**(49): p. 19694-19697.

116. J.-M. Lehn, *Supramolecular chemistry — scope and perspectives molecules, supermolecules, and molecular devices (Nobel lecture).* Angew. Chem., Int. Ed. Engl., 1988. **27**(1): p. 89-112.

117. J.M. Lehn, *Toward self-organization and complex matter.* Science, 2002. **295**(5564): p. 2400-2403.

118. C.M. Dobson, *Protein folding and misfolding.* Nature, 2003. **426**: p. 884-890.

119. E.B. Berda, Foster, E. J., Meijer, E. W., *Toward controlling folding in synthetic polymers: fabricating and characterizing supramolecular single-chain nanoparticles.* Macromolecules, 2010. **43**(3): p. 1430-1437.

120. J. Romulus and M. Weck, *Single-chain polymer self-assembly using complementary hydrogen bonding units.* Macromol. Rapid Commun., 2013. **34**(19): p. 1518-1523.

121. A.J. Thomson and H.B. Gray, *Bio-inorganic chemistry.* Curr. Opin. Chem. Biol., 1998. **2**(2): p. 155-158.

122. A. Sigel and H. Sigel, *Metal complex derivatives of peptide nucleic acids (PNA)*, in *Metal ions in biological systems, interactions of metal ions with nucleotides: nucleic acids, and their constituents*. Springer, 1996. P. 319-339.

123. M. Chiper, R. Hoogenboom, and U.S. Schubert, *Toward main chain metallo-terpyridyl supramolecular polymers: "the metal does the trick".* Macromol. Rapid Commun., 2009. **30**(8): p. 565-578.

124. C. Mugemana, P. Guillet, S. Hoeppener, U.S. Schubert, C.A. Fustin, and J.F. Gohy, *Metallo-supramolecular diblock copolymers based on heteroleptic cobalt(III) and nickel(II) bis-terpyridine complexes.* Chem. Commun., 2010. **46**(8): p. 1296-1298.

125. E.A. Appel, J. Dyson, J. del Barrio, Z. Walsh, and O.A. Scherman, *Formation of single-chain polymer nanoparticles in water through host-guest interactions.* Angew. Chem., Int. Ed. Engl., 2012. **51**(17): p. 4185-4189.

126. T. Mes, R. van der Weegen, A.R. Palmans, and E.W. Meijer, *Single-chain polymeric nanoparticles by stepwise folding.* Angew. Chem., Int. Ed. Engl., 2011. **50**(22): p. 5085-5089.

127. N. Hosono, A.R. Palmans, and E.W. Meijer, *"Soldier-Sergeant-Soldier" triblock copolymers: revealing the folded structure of single-chain polymeric nanoparticles.* Chem. Commun., 2014. **50**(59): p. 7990-7993.

128. N. Hosono, P.J. Stals, A.R. Palmans, and E.W. Meijer, *Consequences of block sequence on the orthogonal folding of triblock copolymers.* Chem. Asian J., 2014. **9**(4): p. 1099-1107.

129. N. Hosono, M.A. Gillissen, Y. Li, S.S. Sheiko, A.R. Palmans, and E.W. Meijer, *Orthogonal self-assembly in folding block copolymers.* J. Am. Chem. Soc., 2013. **135**(1): p. 501-510.

130. T. Terashima, Mes, T., De Greef, T. F. A., Gillissen, M. A. J., Besenius, P., Palmans, A. R. A., Meijer, E. W., *Single-chain folding of polymers for catalytic systems in water.* J. Am. Chem. Soc., 2011. **133**(13): p. 4742-4745.

131. N. Giuseppone and J.F. Lutz, *Materials chemistry: catalytic accordions.* Nature, 2011. **473**(7345): p. 40-41.

132. O. Altintas, E. Lejeune, P. Gerstel, and C. Barner-Kowollik, *Bioinspired dual self-folding of single polymer chains via reversible hydrogen bonding.* Polym. Chem., 2012. **3**(3): p. 640-651.

133. K. Matyjaszewski and J. Xia, *Atom transfer radical polymerization.* Chem. Rev., 2001. **101**(9): p. 2921-2990.

134. H.R. Kricheldorf, O. Nuyken, and G. Swift, in *Handbook of polymer synthesis: second edition*. CRC Press, 2005. P. 895-898.

135. M.K. Georges, R.P.N. Veregin, P.M. Kazmaier, and G.K. Hamer, *Narrow molecular weight resins by a free-radical polymerization process.* Macromolecules, 1993. **26**(11): p. 2987-2988.

136. M. Klapper, Brand, T., Steenbock, M., Müllen, K., *Triazolinyl radicals: toward a new mechanism in controlled radical polymerization*, in *Controlled/living radical polymerization* American Chemical Society 2000. P. 152-166.

137. Y.G. Julien Nicolas, Catherine Lefay, Denis Bertin, Didier Gigmes, Bernadette Charleux, *Nitroxide-mediated polymerization.* Prog. Polym. Sci., 2013. **38**: p. 63-235.

138. R.B. Grubbs, *Nitroxide-mediated radical polymerization: limitations and versatility.* Polym. Rev., 2011. **51**(2): p. 104-137.

139. D. Mardare and K. Matyjaszewski, *Thermal polymerization of styrene in the presence of stable radicals and inhibitors.* Abstr. Pap. Am. Chem. S., 1994. **207**: p. 267.

140. C.J. Hawker, *Molecular-weight control by a living free-radical polymerization process.* J. Am. Chem. Soc., 1994. **116**(24): p. 11185-11186.

141. H. Fischer, *The persistent radical effect in controlled radical polymerizations.* J. Polym. Sci., Part A: Polym. Chem., 1999. **37**(13): p. 1885-1901.

142. C.J. Hawker, A.W. Bosman, and E. Harth, *New polymer synthesis by nitroxide mediated living radical polymerizations.* Chem. Rev., 2001. **101**(12): p. 3661-3688.

143. S. Grimaldi, J.-P. Finet, F. Le Moigne, A. Zeghdaoui, P. Tordo, D. Benoit, M. Fontanille, and Y. Gnanou, *Acyclic β-phosphonylated nitroxides: a new series of counter-radicals for "living"/controlled free radical polymerization.* Macromolecules, 2000. **33**(4): p. 1141-1147.

144. M. Kamigaito, *Recent developments in metal-catalyzed living radical polymerization.* Polym. J., 2010. **43**(2): p. 105-120.

145. M. Kamigaito, T. Ando, and M. Sawamoto, *Metal-catalyzed living radical polymerization.* Chem. Rev., 2001. **101**(12): p. 3689-3746.

146. M. Kato, M. Kamigaito, M. Sawamoto, and T. Higashimura, *Polymerization of methyl-methacrylate with the carbon-tetrachloride dichlorotris(triphenylphosphine)ruthenium(II) methylaluminum bis(2,6-di-tert-*

butylphenoxide) initiating system - possibility of living radical polymerization. Macromolecules, 1995. **28**(5): p. 1721-1723.

147. J.-S. Wang and K. Matyjaszewski, *Controlled/"living" radical polymerization. atom transfer radical polymerization in the presence of transition-metal complexes.* J. Am. Chem. Soc., 1995. **117**(20): p. 5614-5615.

148. J. Xia and K. Matyjaszewski, *Controlled/“living” radical polymerization. Atom transfer radical polymerization using multidentate amine ligands.* Macromolecules, 1997. **30**(25): p. 7697-7700.

149. B.E. Woodworth, Z. Metzner, and K. Matyjaszewski, *Copper triflate as a catalyst in atom transfer radical polymerization of styrene and methyl acrylate.* Macromolecules, 1998. **31**(23): p. 7999-8004.

150. K. Matyjaszewski, S. Coca, S.G. Gaynor, M. Wei, and B.E. Woodworth, *Zerovalent metals in controlled/“living” radical polymerization.* Macromolecules, 1997. **30**(23): p. 7348-7350.

151. J. Tom, B. Hornby, A. West, S. Harrisson, and S. Perrier, *Copper(0)-mediated living radical polymerization of styrene.* Polym. Chem., 2010. **1**(4): p. 420.

152. M.E. Levere, N.H. Nguyen, X. Leng, and V. Percec, *Visualization of the crucial step in SET-LRP.* Polym. Chem., 2013. **4**(5): p. 1635.

153. D. Konkolewicz, Y. Wang, P. Krys, M. Zhong, A.A. Isse, A. Gennaro, and K. Matyjaszewski, *SARA ATRP or SET-LRP. End of controversy?* Polym. Chem., 2014. **5**(15): p. 4409.

154. R. Huisgen, *Centenary lecture - 1,3-dipolar cycloadditions.* Proc. Chem. Soc., 1961(October): p. 357.

155. H.C. Kolb, M.G. Finn, and K.B. Sharpless, *Click chemistry: diverse chemical function from a few good reactions.* Angew. Chem., Int. Ed., 2001. **40**(11): p. 2004-2021.

156. R.B. Corey and L. Pauling, *Molecular models of amino acids, peptides, and proteins.* Rev. Sci. Instrum., 1953. **24**(8): p. 621.

157. M.P. Cava, A.A. Deana, K. Muth, and M.J. Mitchell, *N-Phenylmaleimide.* Org. Synth., 1961. **41**: p. 93.

158. K.F. Lin, J.S. Lin, and C.H. Cheng, *High temperature resins based on allylamine/bismaleimides.* Polymer, 1996. **37**(21): p. 4729-4737.

159. K. Kamahori, S. Tada, K. Ito, and S. Itsuno, *Optically active polymer synthesis by Diels−Alder polymerization with chirally modified Lewis acid catalyst.* Macromolecules, 1999. **32**(3): p. 541-547.

160. B.S. Rao, R. Sireesha, and A.R. Pasala, *Preparation and thermal properties of bismaleimide blends based on hydroxyphenyl maleimide.* Polym. Int., 2005. **54**(8): p. 1103-1109.

161. Y. Kita, K. Sakamoto, M. Baba, and A. Okubo, *Method for production of maleimides.* US 4786738 A, 1988.

162. O. Mitsunobu and M. Yamada, *Preparation of esters of carboxylic and phosphoric acid via quaternary phosphonium salts.* Bull. Chem. Soc. Jpn., 1967. **40**(10): p. 2380-2382.

163. D.L. Hughes, R.A. Reamer, J.J. Bergan, and E.J.J. Grabowski, *A mechanistic study of the Mitsunobu esterification reaction.* J. Am. Chem. Soc., 1988. **110**(19): p. 6487-6491.

164. M.A. Walker, *A high yielding synthesis of N-alkyl maleimides using a novel modification of the Mitsunobu reaction.* J. Org. Chem., 1995. **60**(16): p. 5352-5355.

165. W.S. B. Neises, *Simple method for the esterification of carboxylic acids.* Angew. Chem. Int. Ed., 1978. **17**: p. 522-524.

166. M.M. Joullie and K.M. Lassen, *Evolution of amide bond formation.* Arkivoc, 2010: p. 189-250.

167. J. Coste, E. Frerot, and P. Jouin, *Coupling N-methylated amino acids using PyBroP and PyCloP halogenophosphonium salts: mechanism and fields of application.* J. Org. Chem., 1994. **59**(9): p. 2437-2446.

168. S.Y. Han and Y.A. Kim, *Recent development of peptide coupling reagents in organic synthesis.* Tetrahedron, 2004. **60**(11): p. 2447-2467.

169. M.W. Pennington and M.E. Byrnes, *Procedures to improve difficult couplings.* Methods Mol. Biol., 1994. **35**: p. 1-16.

170. E. Frerot, J. Coste, A. Pantaloni, M.N. Dufour, and P. Jouin, *PyBOP® and PyBroP: two reagents for the difficult coupling of the α,α-dialkyl amino acid, Aib.* Tetrahedron, 1991. **47**(2): p. 259-270.

171. R. Adams and L.H. Ulich, *The use of oxalyl chloride and bromide for reproducing acid chlorides, acid bromides or acid anhydrides.* J. Am. Chem. Soc., 1920. **42 (3)**: p. 599-611.

172. J.A. Opsteen and J.C. van Hest, *Modular synthesis of block copolymers via cycloaddition of terminal azide and alkyne functionalized polymers.* Chem. Commun., 2005(1): p. 57-59.

173. J.A. Opsteen and J.C. van Hest, *Modular synthesis of ABC type block copolymers by “click” chemistry.* J. Polym. Sci., Part A: Polym. Chem., 2007. **45**(14): p. 2913-2924.

174. A.K. Nanda and K. Matyjaszewski, *Effect of [PMDETA]/[Cu(I)] ratio, monomer, solvent, counterion, ligand, and alkyl bromide on the activation rate constants in atom transfer radical polymerization.* Macromolecules, 2003. **36**(5): p. 1487-1493.

175. S. Faucher, P. Okrutny, and S. Zhu, *Catalyst solubility and experimental determination of equilibrium constants for heterogeneous atom transfer radical polymerization.* Ind. Eng. Chem. Res., 2007. **46**(9): p. 2726-2734.

176. V. Jaacks, *A novel method of determination of reactivity ratios in binary and ternary copolymerizations.* Macromol. Chem. Phys., 1972. **161**(1): p. 161-172.

177. E. H. Immergut and J. Brandrup, in *Polymer handbook, 3rd edition*. Wiley-Interscience, 1989. P. 221.

178. V. Aucagne and D.A. Leigh, *Chemoselective formation of successive triazole linkages in one pot: "click−click" chemistry.* Org. Lett., 2006. **8**(20): p. 4505-4507.

179. S. Higashibayashi, K. Shinko, T. Ishizu, K. Hashimoto, H. Shirahama, and M. Nakata, *Selective deprotection of t-butyldiphenylsilyl ethers in the presence of t-butyldimethylsilyl ethers by tetrabutylammonium fluoride, acetic acid, and water.* Synlett, 2000. **2000**(09): p. 1306-1308.

180. T.D. Nelson and R.D. Crouch, *Selective deprotection of silyl ethers.* Synthesis, 1996. **1996**(09): p. 1031-1069.

181. R.D. Crouch, *Selective monodeprotection of bis-silyl ethers.* Tetrahedron, 2004. **60**(28): p. 5833-5871.

182. I.E. Valverde, A.F. Delmas, and V. Aucagne, *Click à la carte: robust semi-orthogonal alkyne protecting groups for multiple successive azide/alkyne cycloadditions.* Tetrahedron, 2009. **65**(36): p. 7597-7602.

183. J.F. Lutz and K. Matyjaszewski, *Nuclear magnetic resonance monitoring of chain-end functionality in the atom transfer radical polymerization of styrene.* J. Polym. Sci., Part A: Polym. Chem., 2005. **43**(4): p. 897-910.

184. M.A. Berthet, Z. Zarafshani, S. Pfeifer, and J.F. Lutz, *Facile synthesis of functional periodic copolymers: a step toward polymer-based molecular arrays.* Macromolecules, 2010. **43**(1): p. 44-50.

185. G. Guichard and I. Huc, *Synthetic foldamers.* Chem. Commun., 2011. **47**(21): p. 5933-5941.

186. K.J. Woycechowsky and R.T. Raines, *The CXC motif: a functional mimic of protein disulfide isomerase.* Biochemistry, 2003. **42**(18): p. 5387-5394.

187. M. Rauschenberg, S. Bomke, U. Karst, and B.J. Ravoo, *Dynamic peptides as biomimetic carbohydrate receptors.* Angew. Chem., Int. Ed. Engl., 2010. **49**(40): p. 7340-7345.

188. M.P. Lutolf, N. Tirelli, S. Cerritelli, L. Cavalli, and J.A. Hubbell, *Systematic modulation of michael-type reactivity of thiols through the use of charged amino acids.* Bioconjugate Chem., 2001. **12**(6): p. 1051-1056.

189. D.J. Craik, J.E. Swedberg, J.S. Mylne, and M. Cemazar, *Cyclotides as a basis for drug design.* Expert Opin. Drug Discov., 2012. **7**(3): p. 179-194.

190. D.J. Craik, N.L. Daly, T. Bond, and C. Waine, *Plant cyclotides: A unique family of cyclic and knotted proteins that defines the cyclic cystine knot structural motif.* J. Mol. Biol., 1999. **294**(5): p. 1327-1336.

191. D.J. Craik, *Chemistry. Seamless proteins tie up their loose ends.* Science, 2006. **311**(5767): p. 1563-1564.

192. N. Fujii, S. Oishi, K. Hiramatsu, T. Araki, S. Ueda, H. Tamamura, A. Otaka, S. Kusano, S. Terakubo, H. Nakashima, J.A. Broach, J.O. Trent, Z.X. Wang, and S.C. Peiper, *Molecular-size reduction of a potent CXCR4-chemokine antagonist using orthogonal combination of conformation- and sequence-based libraries.* Angew. Chem., Int. Ed. Engl., 2003. **42**(28): p. 3251-3253.

193. C. Heinis, T. Rutherford, S. Freund, and G. Winter, *Phage-encoded combinatorial chemical libraries based on bicyclic peptides.* Nat. Chem. Biol., 2009. **5**(7): p. 502-507.

194. P. Theato, *Synthesis of well-defined polymeric activated esters.* J. Polym. Sci., Part A: Polym. Chem., 2008. **46**(20): p. 6677-6687.

195. K. Nilles and P. Theato, *Synthesis and polymerization of active ester monomers based on 4-vinylbenzoic acid.* Eur. Polym. J., 2007. **43**(7): p. 2901-2912.

196. M.A. Gauthier, M.I. Gibson, and H.A. Klok, *Synthesis of functional polymers by post-polymerization modification.* Angew. Chem., Int. Ed. Engl., 2009. **48**(1): p. 48-58.

197. J.-M. Noy, M. Koldevitz, and P.J. Roth, *Thiol-reactive functional poly(meth)acrylates: multicomponent monomer synthesis, RAFT (co)polymerization and highly efficient thiol–para-fluoro postpolymerization modification.* Polym. Chem., 2014.

198. K. Nilles and P. Theato, *Sequential conversion of orthogonally functionalized diblock copolymers based on pentafluorophenyl esters.* J. Polym. Sci., Part A: Polym. Chem., 2010. **48**(16): p. 3683-3692.

199. R. Kakuchi, M. Zamfir, J.F. Lutz, and P. Theato, *Controlled positioning of activated ester moieties on well-defined linear polymer chains.* Macromol. Rapid Commun., 2012. **33**(1): p. 54-60.

200. P.D. White and W.C. Chan, in *Fmoc solid phase peptide synthesis: A practical approach*. Oxford University Press, 2000. P. 52-59, 91-109.

201. L.A. Carpino, H. Shroff, S.A. Triolo, E.-S.M.E. Mansour, H. Wenschuh, and F. Albericio, *The 2,2,4,6,7-pentamethyldihydrobenzofuran-5-sulfonyl group (Pbf) as arginine side chain protectant.* Tetrahedron Lett., 1993. **34**(49): p. 7829-7832.

202. I. Photaki, J. Taylor-Papadimitriou, C. Sakarellos, P. Mazarakis, and L. Zervas, *On cysteine and cystine peptides. Part V. S-trityl- and S-diphenylmethyl-cysteine and -cysteine peptides.* J. Chem. Soc. C, 1970(19): p. 2683.

203. A. Isidro-Llobet, M. Alvarez, and F. Albericio, *Amino acid-protecting groups.* Chem. Rev., 2009. **109**(6): p. 2455-2504.

204. B.S. Mamathambika and J.C. Bardwell, *Disulfide-linked protein folding pathways.* Annu. Rev. Cell Dev. Biol., 2008. **24**: p. 211-235.

205. G.L. Ellman, *Tissue sulfhydryl groups.* Arch. Biochem. Biophys., 1959. **82**(1): p. 70-77.

206. J.P. Badyal, A.M. Cameron, N.R. Cameron, D.M. Coe, R. Cox, B.G. Davis, L.J. Oates, G. Oye, and P.G. Steel, *A simple method for the quantitative analysis of resin bound thiol groups.* Tetrahedron Lett., 2001. **42**(48): p. 8531-8533.

207. J.-F. Lutz and H.G. Börner, *Modern trends in polymer bioconjugates design.* Prog. Polym. Sci., 2008. **33**(1): p. 1-39.

208. M.A. Gauthier and H.A. Klok, *Peptide/protein-polymer conjugates: synthetic strategies and design concepts.* Chem. Commun., 2008(23): p. 2591-2611.

209. S. Srichan, L. Oswald, M. Zamfir, and J.F. Lutz, *Precision polyelectrolytes.* Chem. Commun., 2012. **48**(10): p. 1517-1519.

210. B.G.G. Lohmeijer and U.S. Schubert, *Expanding the supramolecular polymer LEGO system: Nitroxide-mediated living free-radical polymerization as a tool for mono- and telechelic polystyrenes.* J. Polym. Sci., Part A: Polym. Chem., 2004. **42**(16): p. 4016-4027.

211. L. Trouillet, A. De Nicola, and S. Guillerez, *Synthesis and characterization of a new soluble, structurally well-defined conjugated polymer alternating regioregularly alkylated thiophene oligomer and 2,2‘-bipyridine units: metal-free form and Ru(II) complex.* Chem. Mater., 2000. **12**(6): p. 1611-1621.

212. K. Peter and M. Thelakkat, *Synthesis and characterization of bifunctional polymers carrying tris(bipyridyl)ruthenium(II) and triphenylamine units.* Macromolecules, 2003. **36**(6): p. 1779-1785.

213. P.K. Ng, X. Gong, S.H. Chan, L.S.M. Lam, and W.K. Chan, *The role of ruthenium and rhenium diimine complexes in conjugated polymers that exhibit interesting opto-electronic properties.* Chem. Eur. J., 2001. **7**(20): p. 4358-4367.

214. M. Chiper, A. Winter, R. Hoogenboom, D.A.M. Egbe, D. Wouters, S. Hoeppener, C.-A. Fustin, J.-F. Gohy, and U.S. Schubert, *Synthesis and micellization of*

coil−rod−coil ruthenium(II) terpyridine assemblies. Macromolecules, 2008. **41**(22): p. 8823-8831.

215. A.O. Moughton and R.K. O'Reilly, *Noncovalently connected micelles, nanoparticles, and metal-functionalized nanocages using supramolecular self-assembly.* J. Am. Chem. Soc., 2008. **130**(27): p. 8714-8725.

216. E. Alessio, *Synthesis and reactivity of Ru-, Os-, Rh-, and Ir-halide-sulfoxide complexes.* Chem. Rev., 2004. **104**(9): p. 4203-4242.

217. S.M. Zakeeruddin, M.K. Nazeeruddin, R. Humphry-Baker, M. Grätzel, and V. Shklover, *Stepwise assembly of tris-heteroleptic polypyridyl complexes of ruthenium(II).* Inorg. Chem., 1998. **37**(20): p. 5251-5259.

218. G. Anderegg and H. Wanner, *Pyridine derivatives as complexing agents. XIII. The stability of the palladium(II) complexes with pyridine, 2,2'-bipyridyl, and 1,10-phenanthroline.* Inorg. Chim. Acta, 1986. **113**(2): p. 101-108.

219. G.C. Nwokogu, L.F. Silva, and R.S. Vasconcelos, *Tetrakis(acetonitrile) palladium tetrafluoroborate*, in *e-EROS Encyclopedia of Reagents for Organic Synthesis*, 2008.

220. B. Milani, A. Anzilutti, L. Vicentini, A. Sessanta o Santi, E. Zangrando, S. Geremia, and G. Mestroni, *Bis-chelated palladium(II) complexes with nitrogen-donor chelating ligands are efficient catalyst precursors for the CO/styrene copolymerization reaction.* Organometallics, 1997. **16**(23): p. 5064-5075.

221. M. Calligaris, E. Zangrando, and A.M.B. Milani, *Stereochemical investigation of palladium(II) complexes with phenanthroline ligands: a molecular mechanics approach.* Eur. J. Inorg. Chem., 2005. **2005**(4): p. 704-712.

222. A. Bencini and V. Lippolis, *1,10-Phenanthroline: A versatile building block for the construction of ligands for various purposes.* Coord. Chem. Rev., 2010. **254**(17-18): p. 2096-2180.

223. P.G. Sammes and G. Yahioglu, *1,10-Phenanthroline: a versatile ligand.* Chem. Soc. Rev., 1994. **23**(5): p. 327.

224. G. Accorsi, A. Listorti, K. Yoosaf, and N. Armaroli, *1,10-phenanthrolines: versatile building blocks for luminescent molecules, materials and metal complexes.* Chem. Soc. Rev., 2009. **38**(6): p. 1690-1700.

225. S.A. Trammell, H.M. Goldston, P.T. Tran, L.M. Tender, D.W. Conrad, D.E. Benson, and H.W. Hellinga, *Synthesis and characterization of a ruthenium(II)-based redox conjugate for reagentless biosensing.* Bioconjugate Chem., 2001. **12**(4): p. 643-647.

226. M.A.R. Meier, B.G.G. Lohmeijer, and U.S. Schubert, *Characterization of defined metal-containing supramolecular block copolymers.* Macromol. Rapid Commun., 2003. **24**(14): p. 852-857.

227. M. Eberhardt, R. Mruk, R. Zentel, and P. Théato, *Synthesis of pentafluorophenyl(meth)acrylate polymers: New precursor polymers for the synthesis of multifunctional materials.* Eur. Polym. J., 2005. **41**(7): p. 1569-1575.

228. S. Grimaldi, J.P. Finet, F. Le Moigne, A. Zeghdaoui, P. Tordo, D. Benoit, M. Fontanille, and Y. Gnanou, *Acyclic β-phosphonylated nitroxides: a new series of counter-radicals for "living"/controlled free radical polymerization.* Macromolecules, 2000. **33**(4): p. 1141-1147.

229. O. Guerret, J.L. Couturier, J.F. Lutz, C. Le Mercier, S. Robin, and B. Vuillemin, *Polyalkoxyamines obtained from β-substituted nitroxides.* N° US 6657043, 2003.

230. K. Matyjaszewski, S. Gaynor, and S. Coca, *Improvements in atom or group transfer radical polymerization.* WO1998040415 A1, 1998.

231. A. Soriano, R. Ventura, A. Molero, R. Hoen, V. Casado, A. Cortes, F. Fanelli, F. Albericio, C. Lluis, R. Franco, and M. Royo, *Adenosine A2A receptor-antagonist/dopamine D2 receptor-agonist bivalent ligands as pharmacological tools to detect A2A-D2 receptor heteromers.* J. Med. Chem., 2009. **52**(18): p. 5590-5602.

ADDITIONAL DATA (ANNEX)

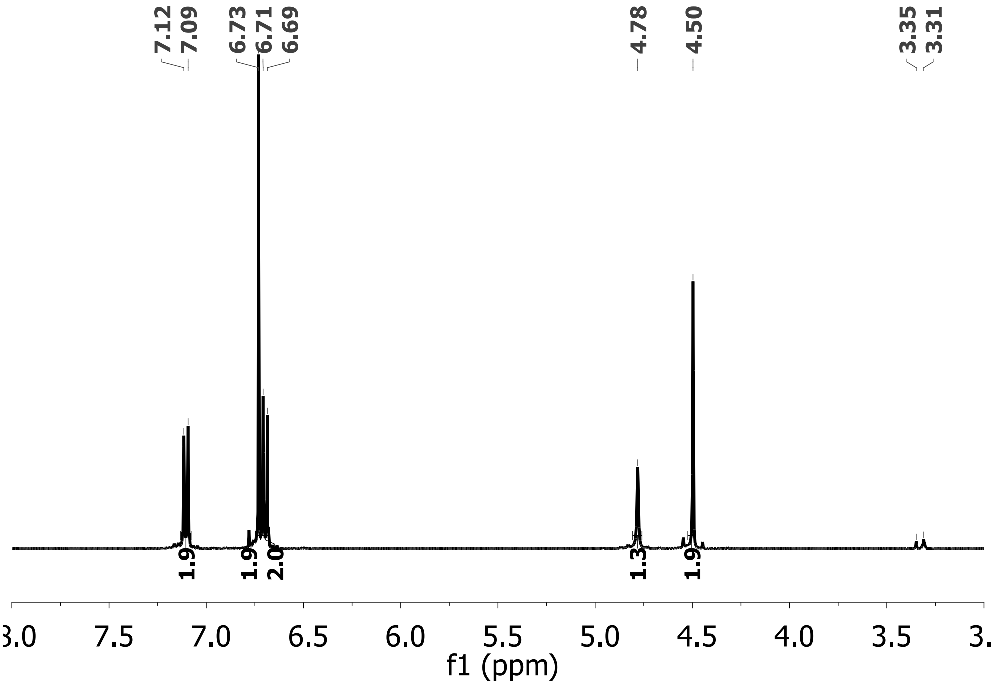

Figure 117 | ^{1}H NMR spectrum of **I**, in CD_3OD.

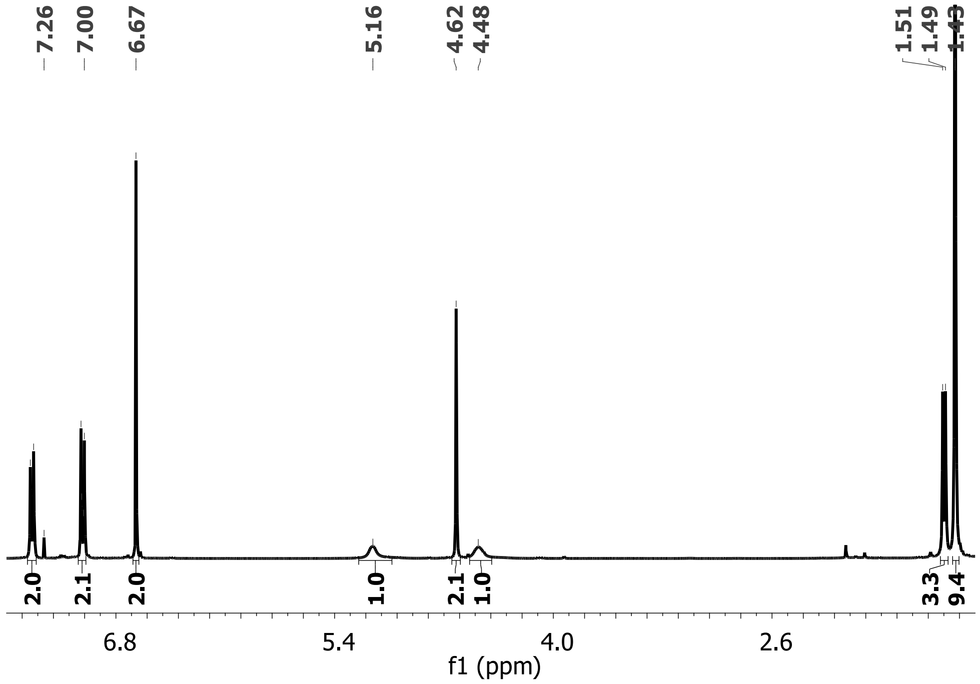

Figure 118 | ^{1}H NMR spectrum of **II**, in $CDCl_3$.

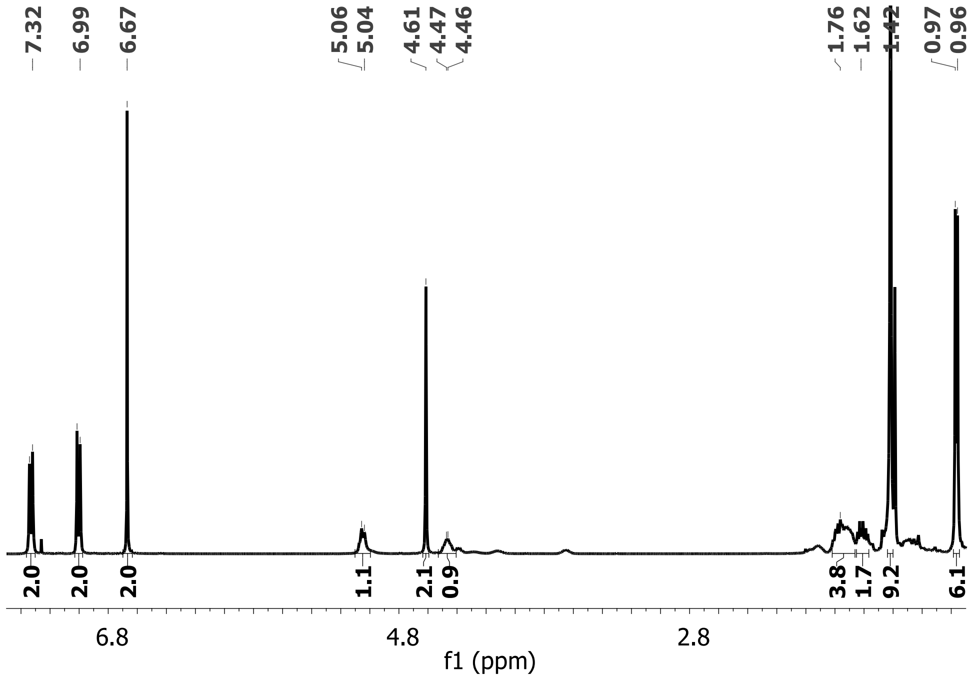

Figure 119 | ^{1}H NMR spectrum of **III** in $CDCl_3$.

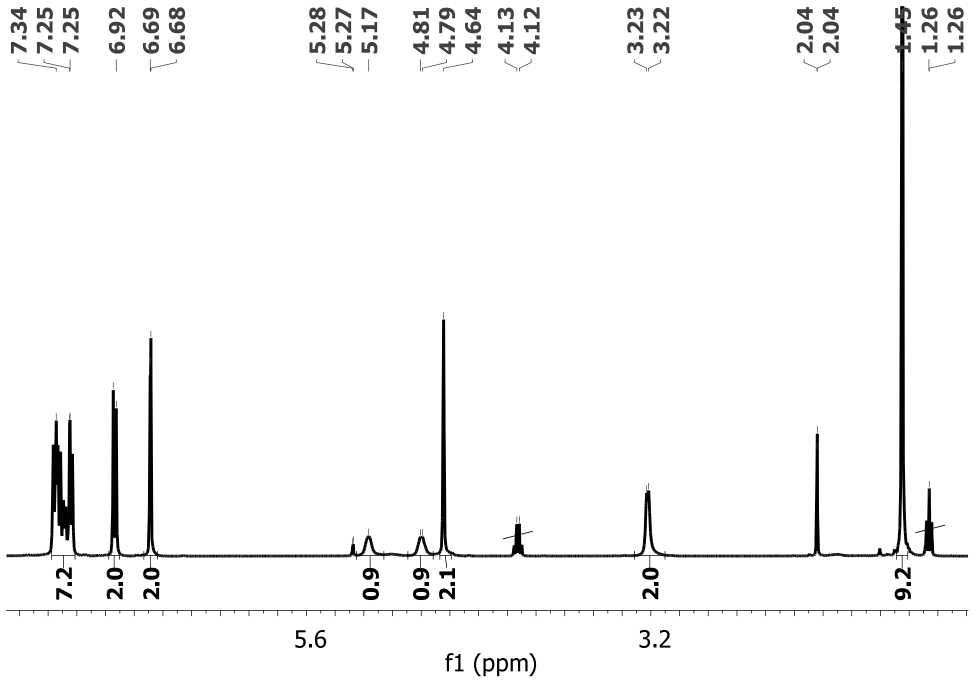

Figure 120 | ^{1}H NMR spectrum of **IV**, in $CDCl_3$.

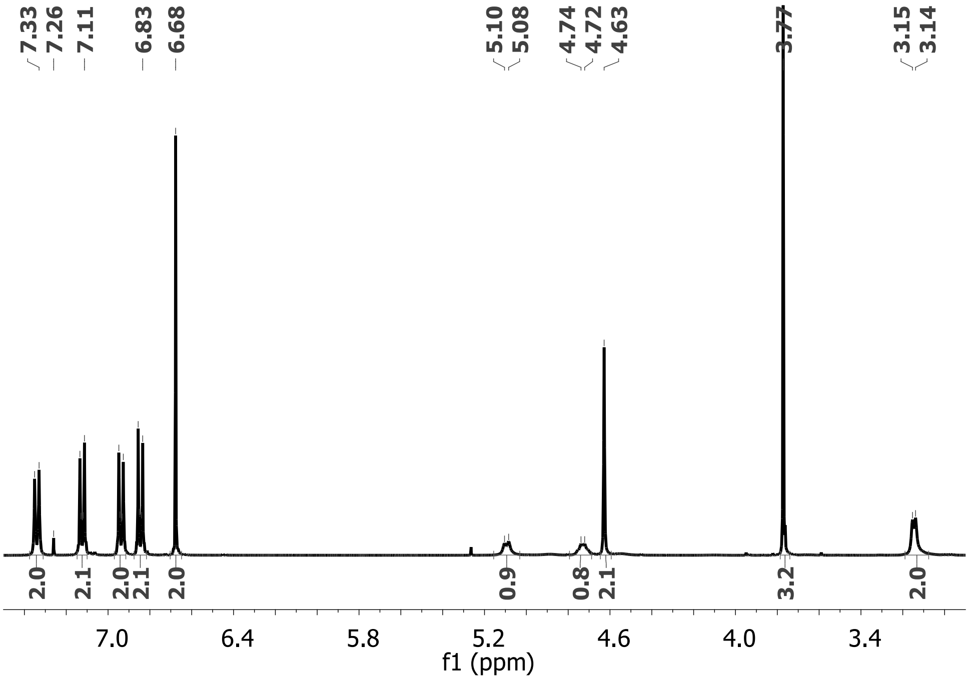

Figure 121 | ^{1}H NMR spectrum of **V**, in $CDCl_3$.

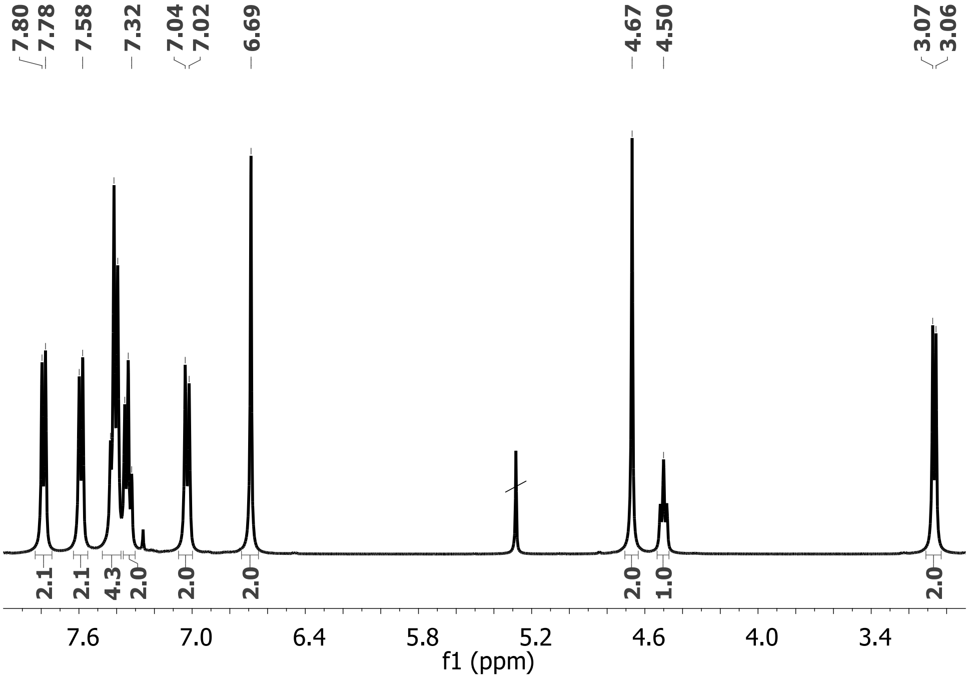

Figure 122 | ^{1}H NMR spectrum of **VI**, in $CDCl_3$.

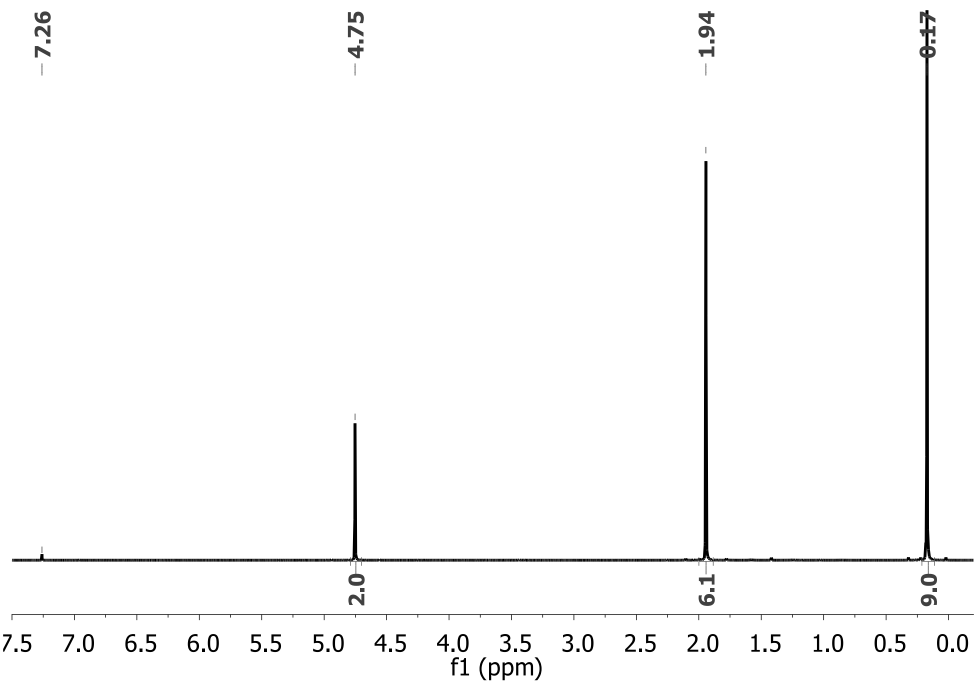

Figure 123 | ^{1}H NMR spectrum of **VII** in $CDCl_3$.

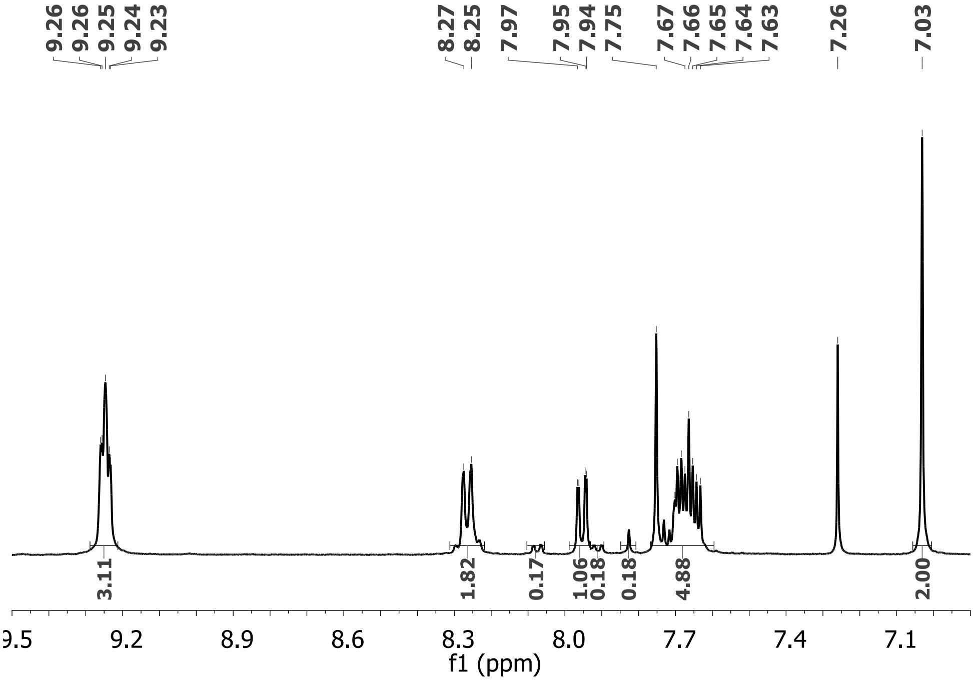

Figure 124 | ^{1}H NMR spectrum of **X,** in $CDCl_3$.

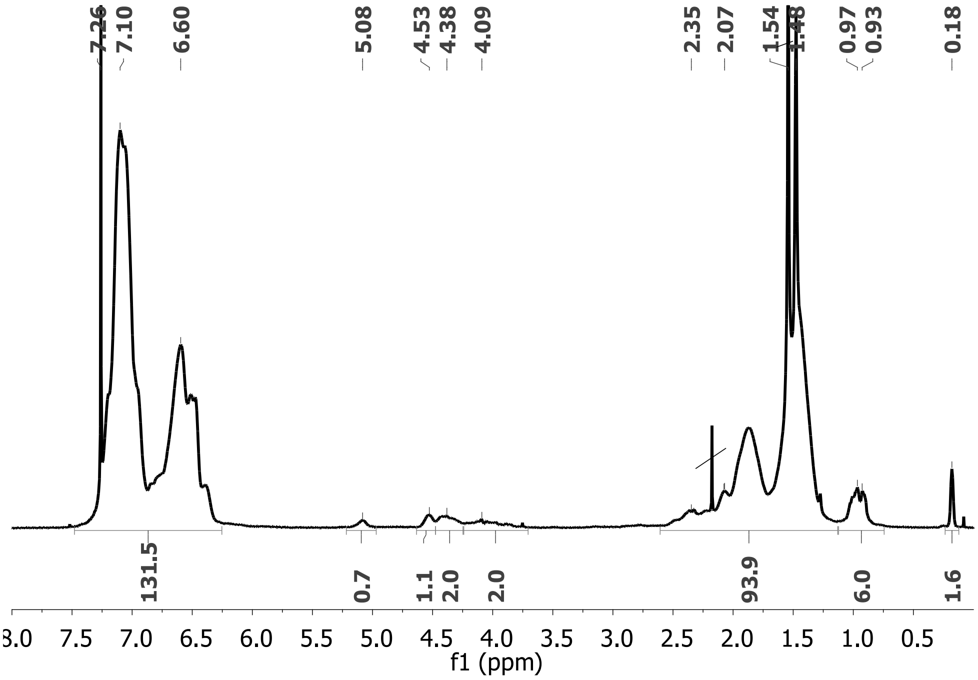

Figure 125 | ^{1}H NMR spectrum of **P7**, in $CDCl_3$.

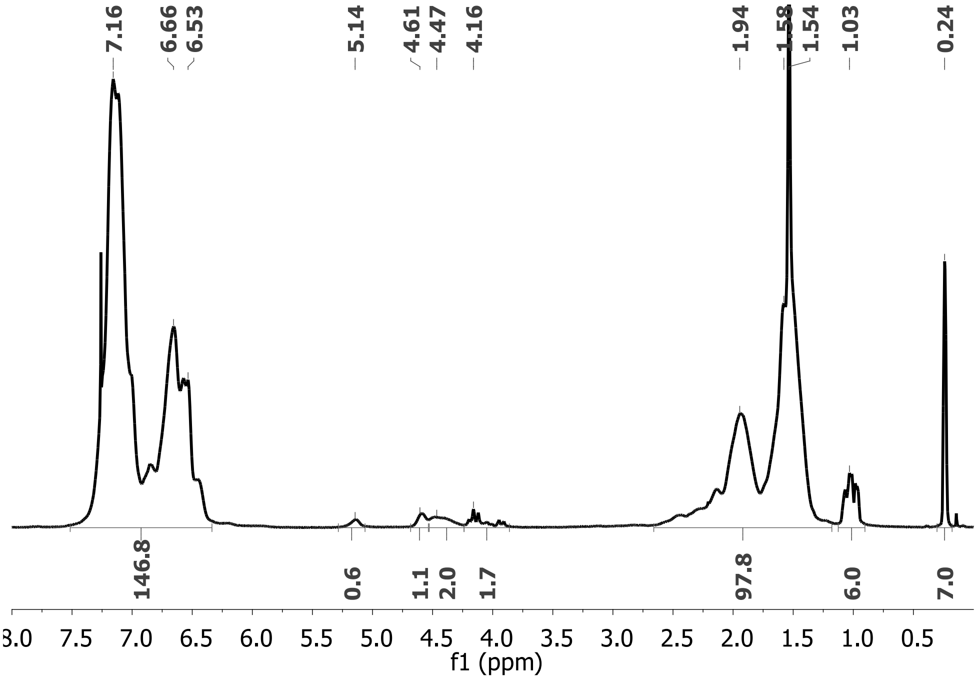

Figure 126 | ^{1}H NMR spectrum of **P8**, in $CDCl_3$.

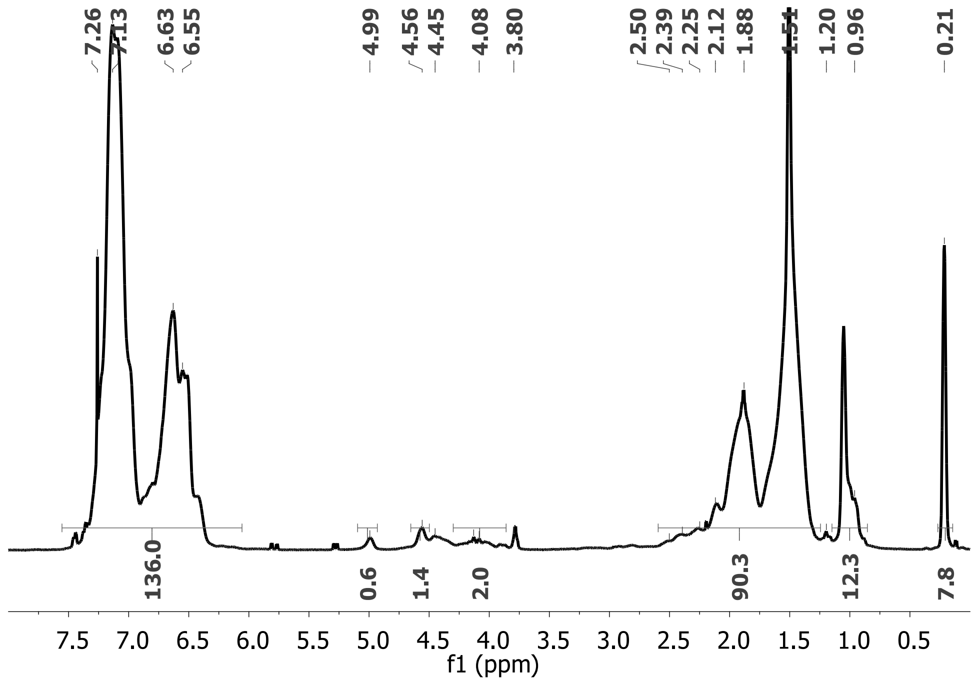

Figure 127 | ^{1}H NMR spectrum of **P9** in $CDCl_3$.

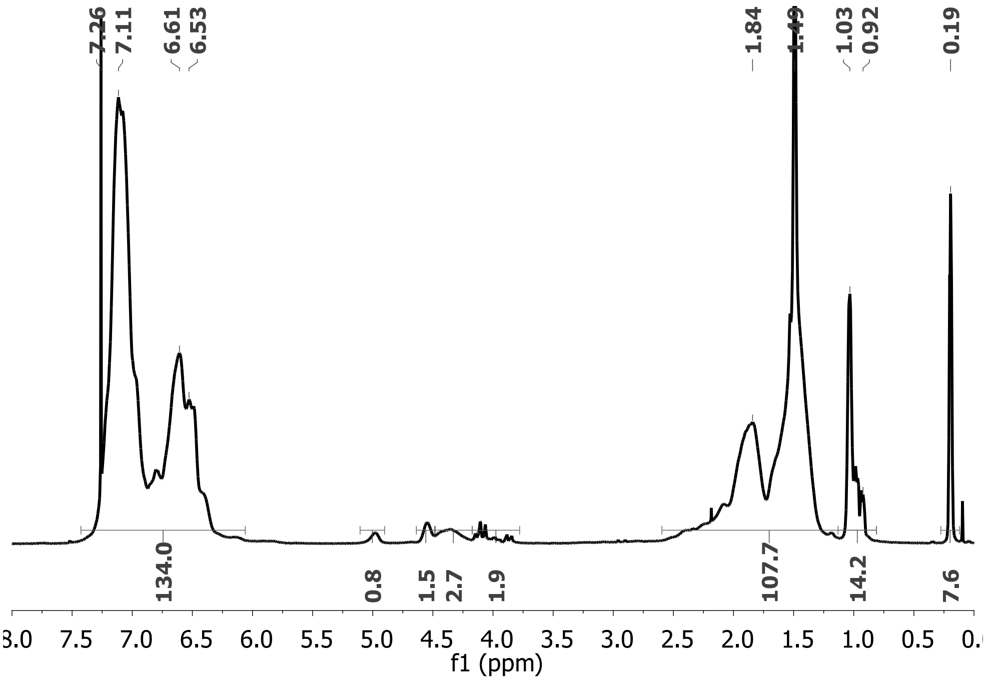

Figure 128 | ^{1}H NMR spectrum of **P10**, in $CDCl_3$.

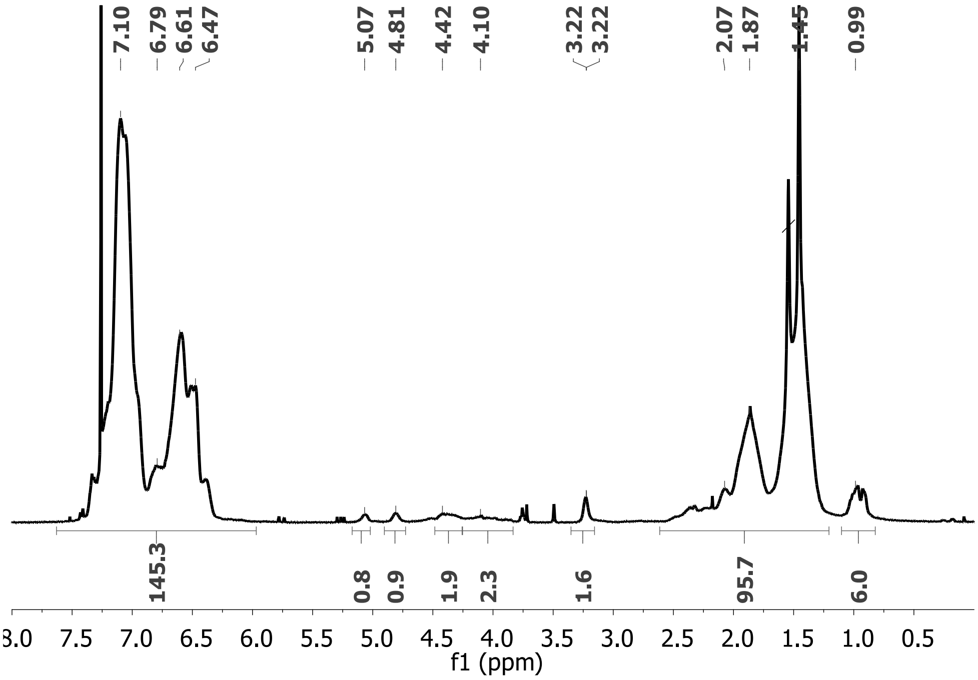

Figure 129 | ^{1}H NMR spectrum of **P11**, in CDCl$_3$.

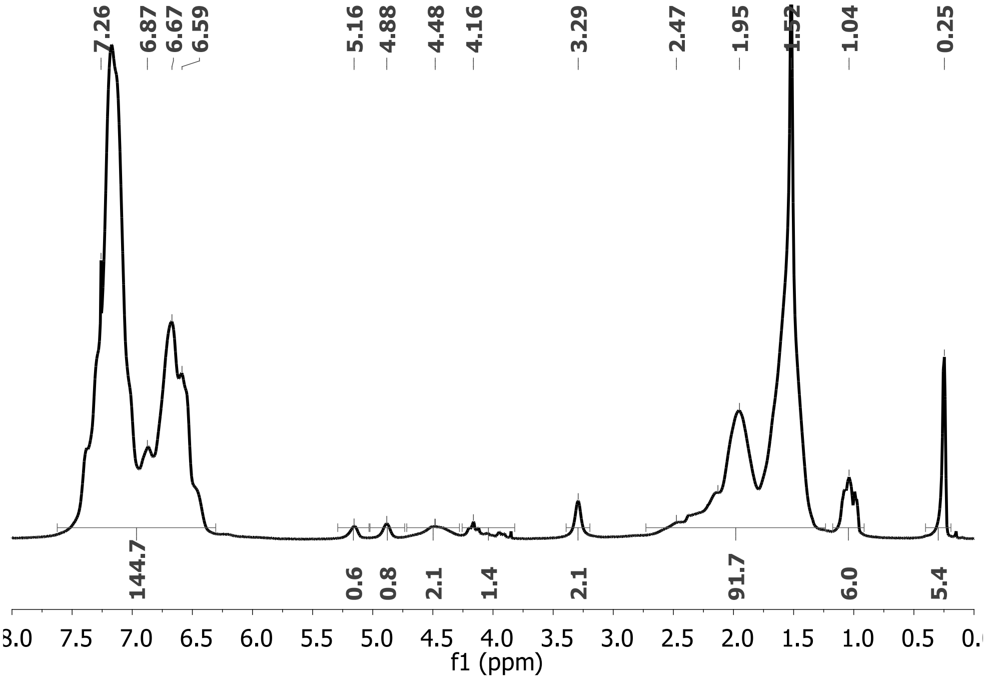

Figure 130 | ^{1}H NMR spectrum of **P12**, in CDCl$_3$.

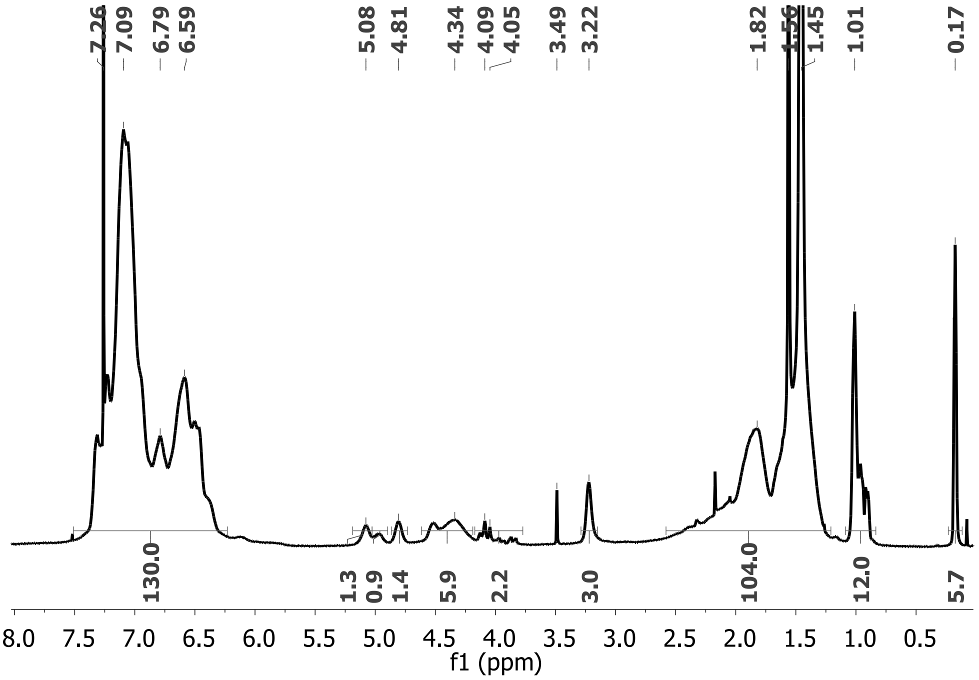

Figure 131 | ^{1}H NMR spectrum of **P16**, in $CDCl_3$.

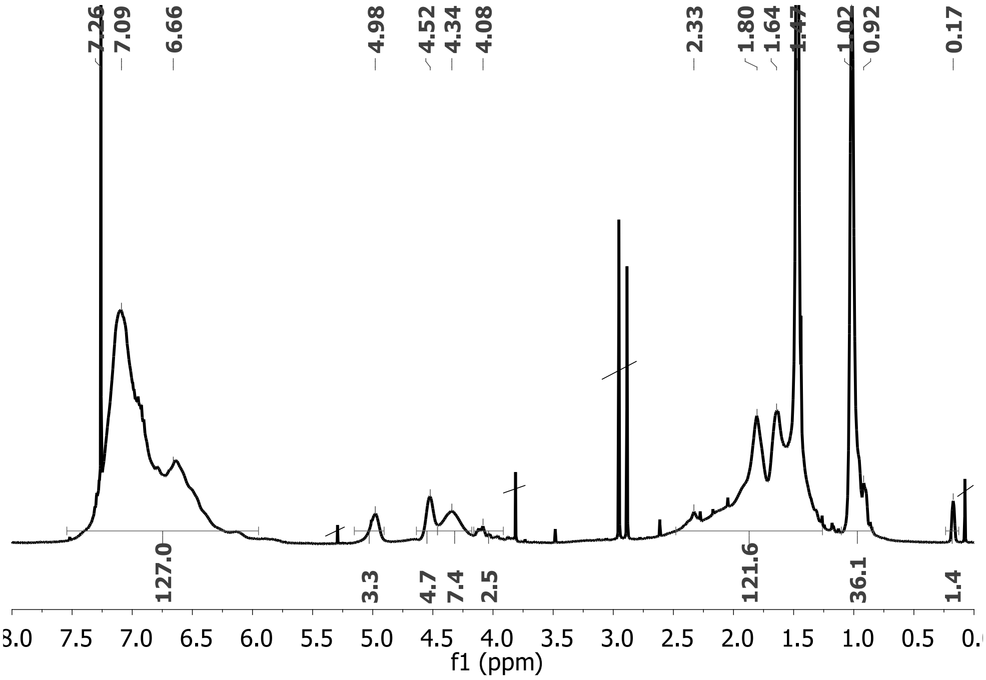

Figure 132 | ^{1}H NMR spectrum of **P17**, in $CDCl_3$.

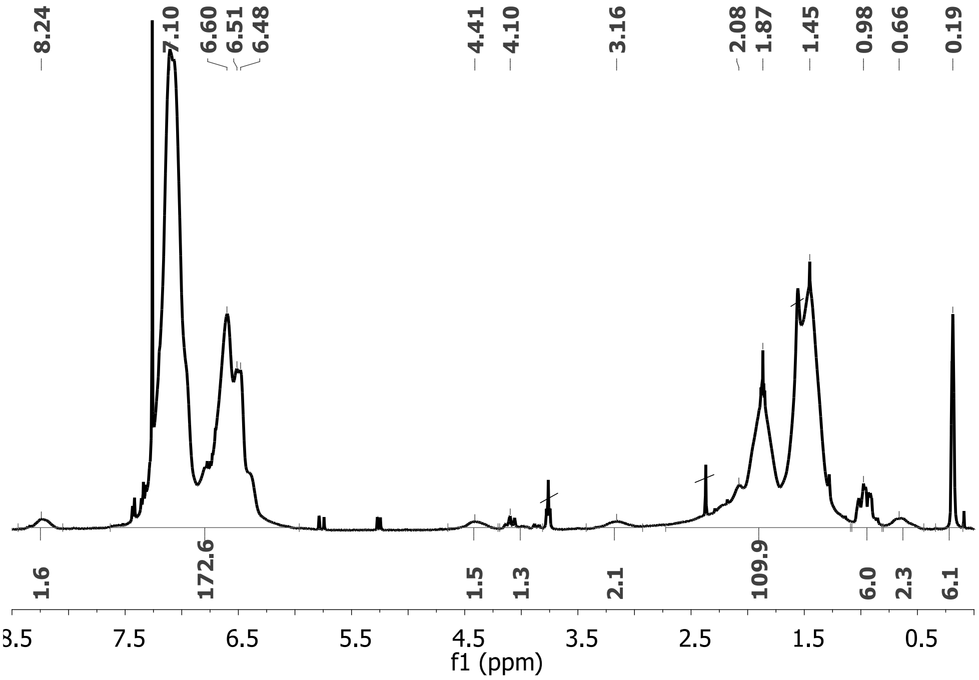

Figure 133 | ^{1}H NMR spectrum of **P20**, in $CDCl_3$.

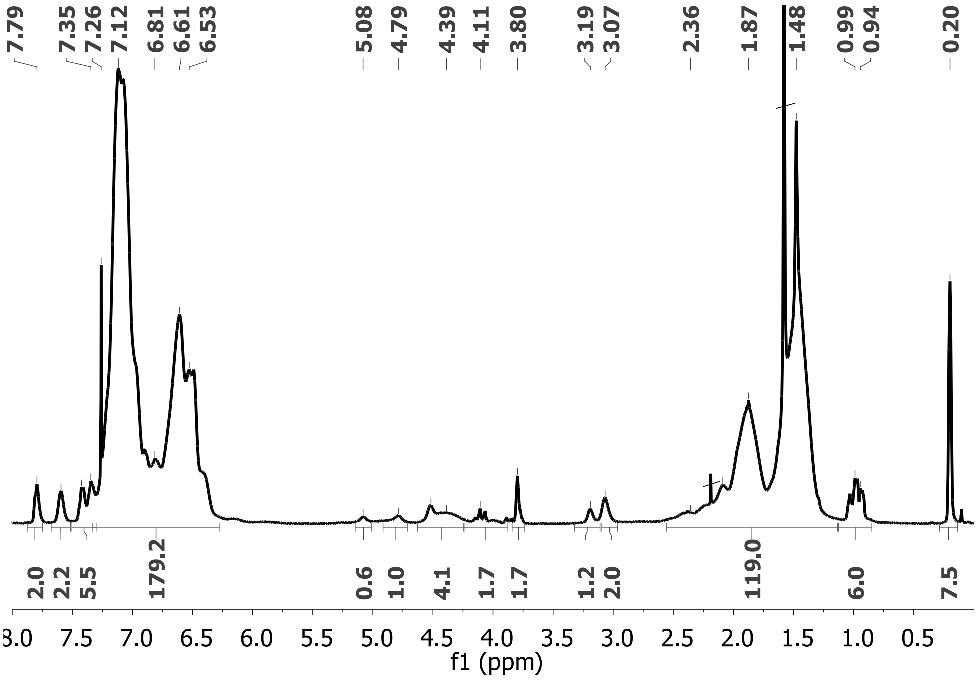

Figure 134 | ^{1}H NMR spectrum of **P22**, in $CDCl_3$.

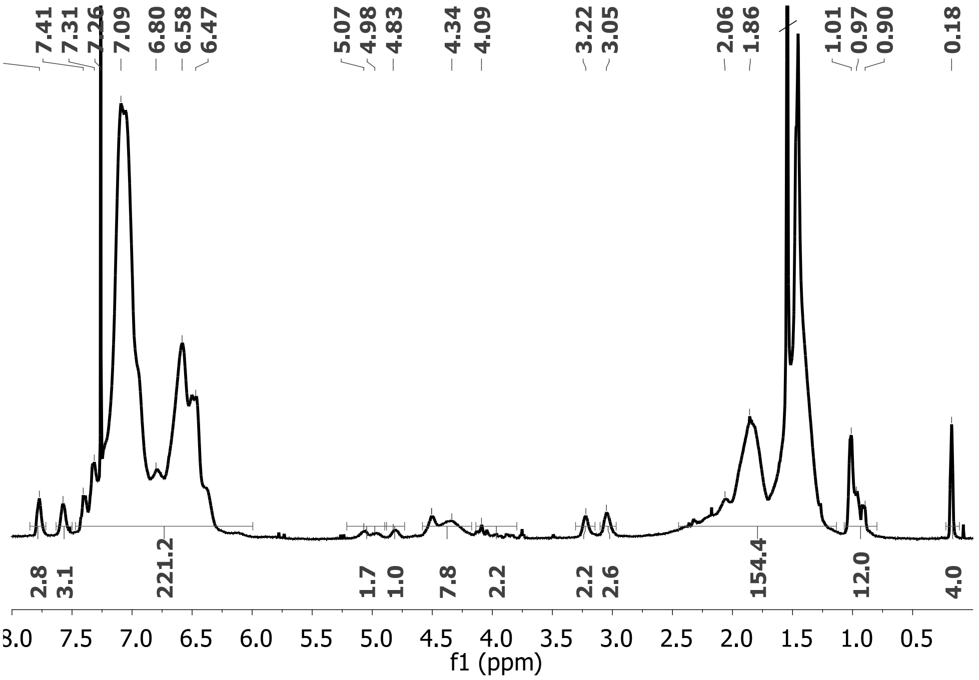

Figure 135 | ^{1}H NMR spectrum of **P23**, in $CDCl_3$.

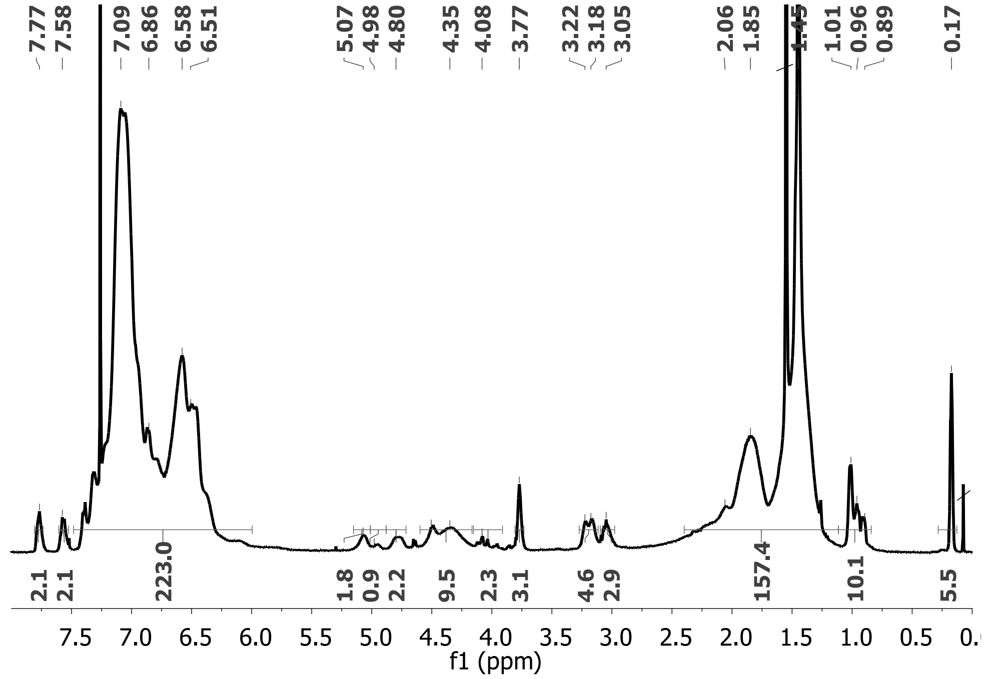

Figure 136 | ^{1}H NMR spectrum of **P24**, in $CDCl_3$.

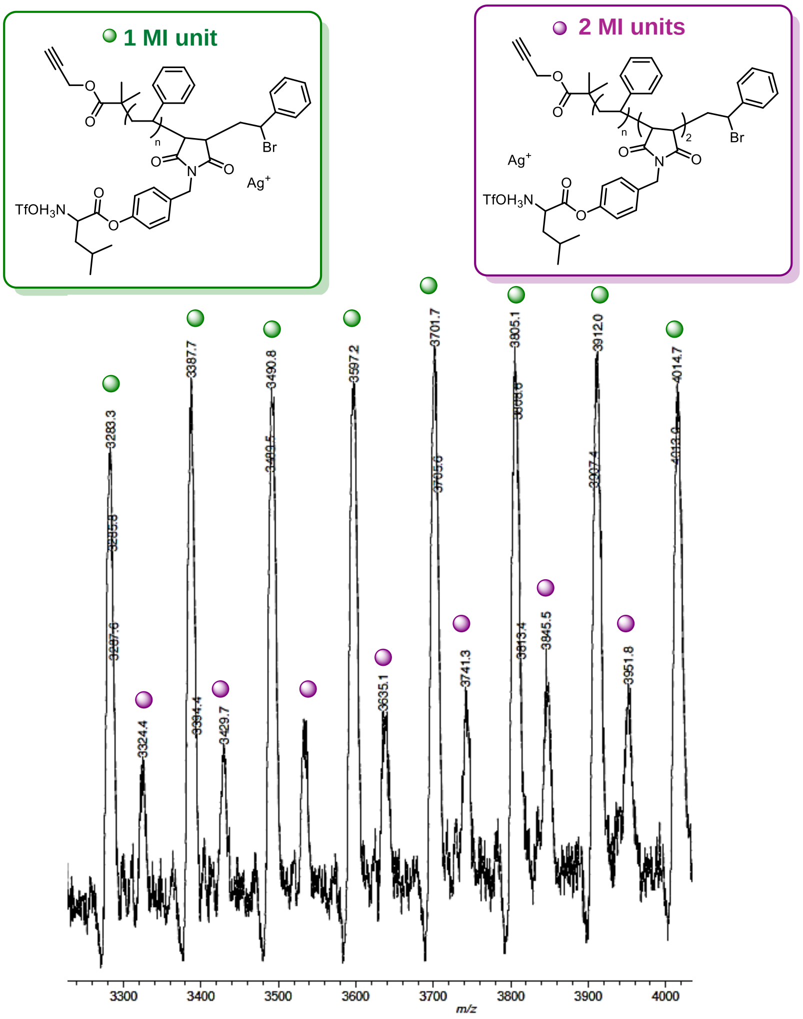

Figure 137 | MALDI-TOF spectrum of the deprotected polymer **P10**.

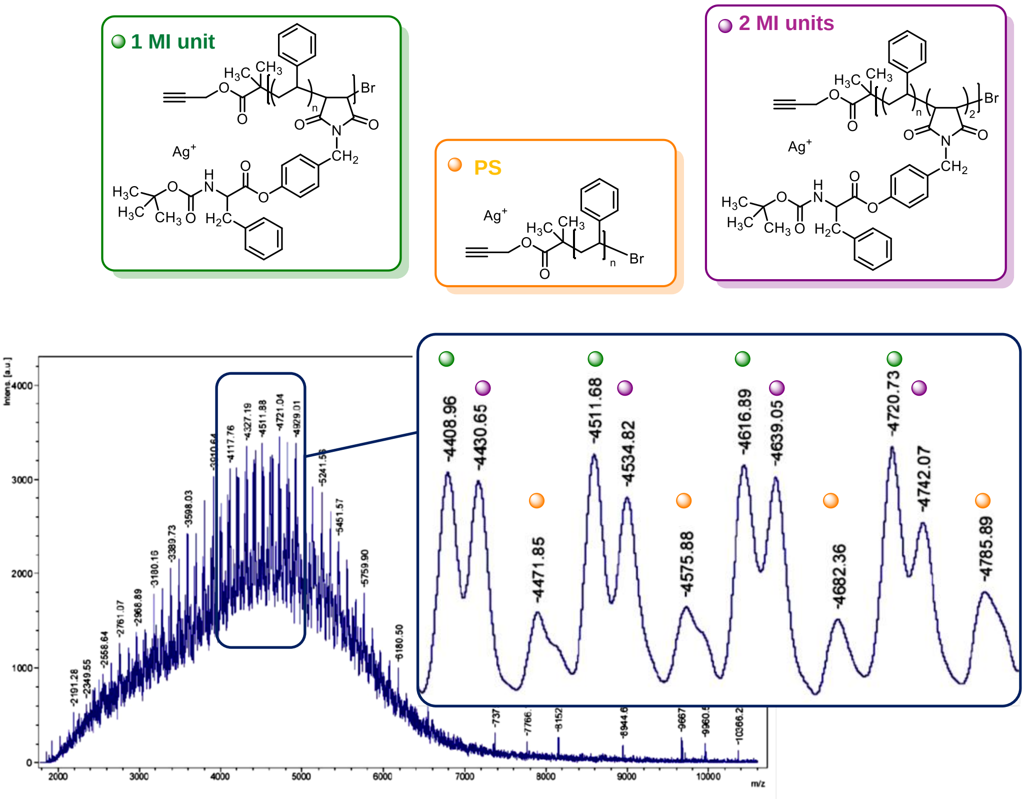

Figure 138 | MALDI-TOF spectrum of **P11**.

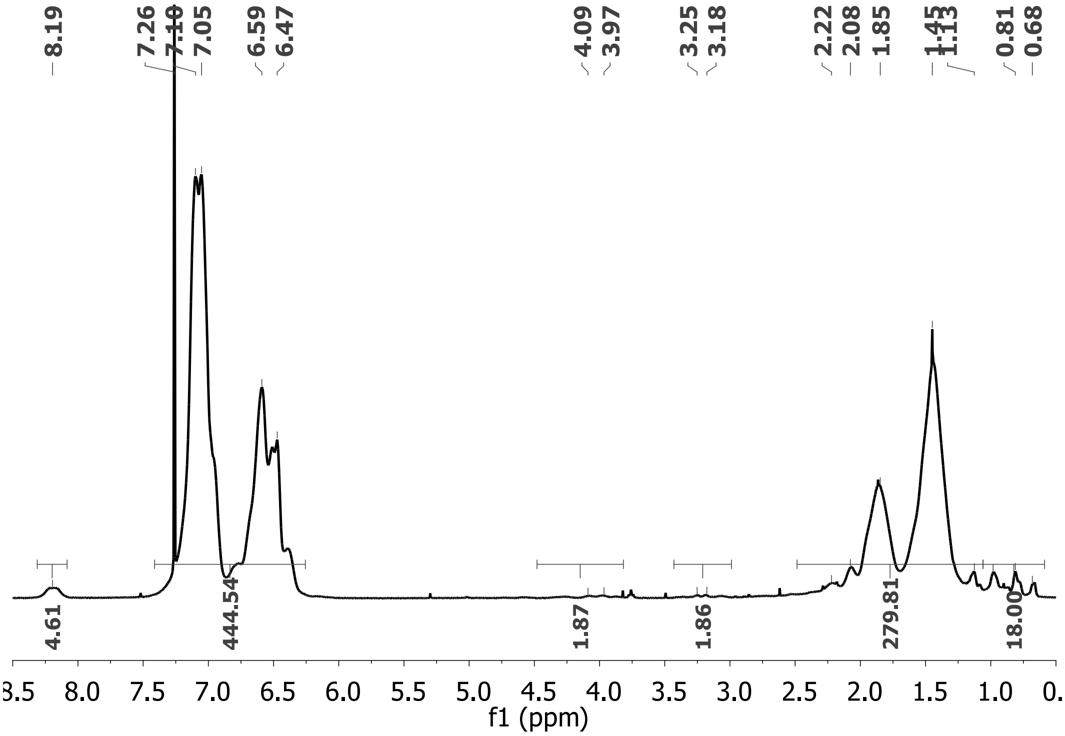

Figure 139 | ^{1}H NMR spectrum of **P26**, in $CDCl_3$.

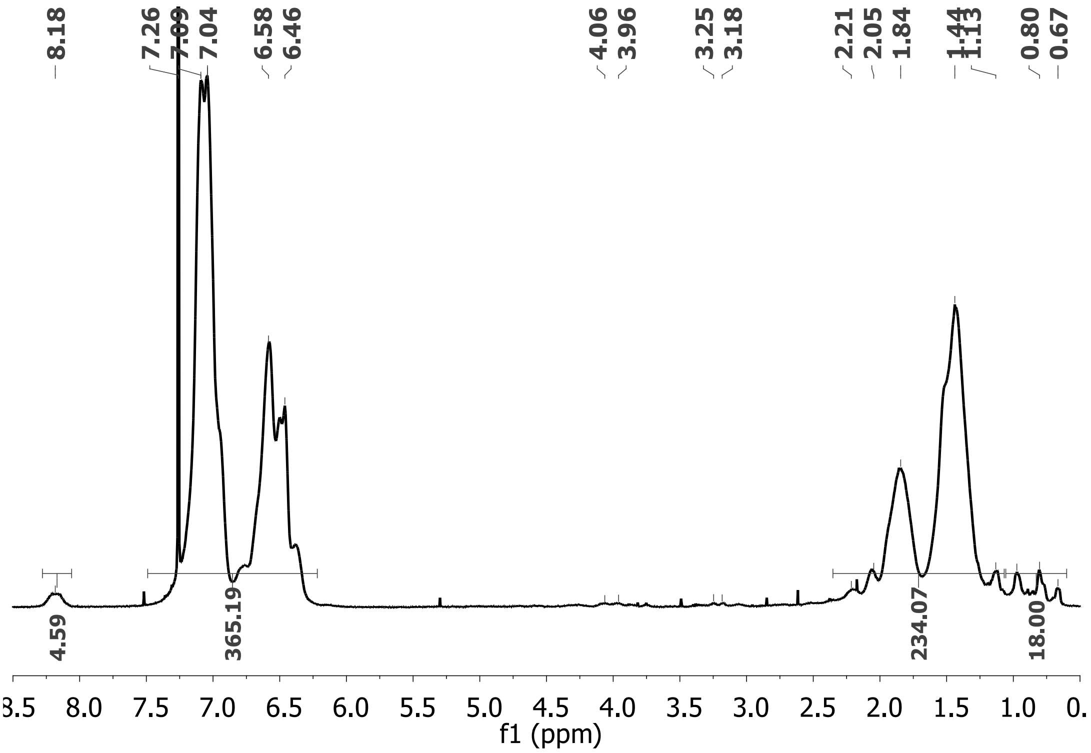

Figure 140 | ^{1}H NMR spectrum of **P27,** in CDCl$_3$.

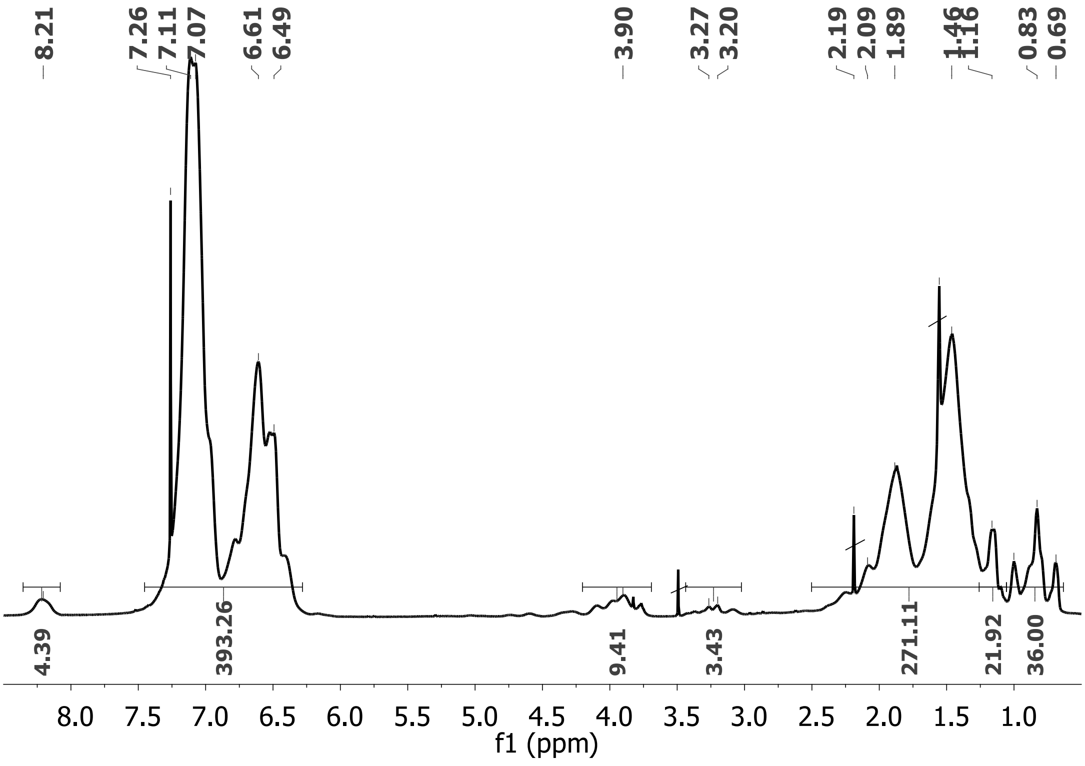

Figure 141 | ^{1}H NMR spectrum of **P29**, in CDCl$_3$.

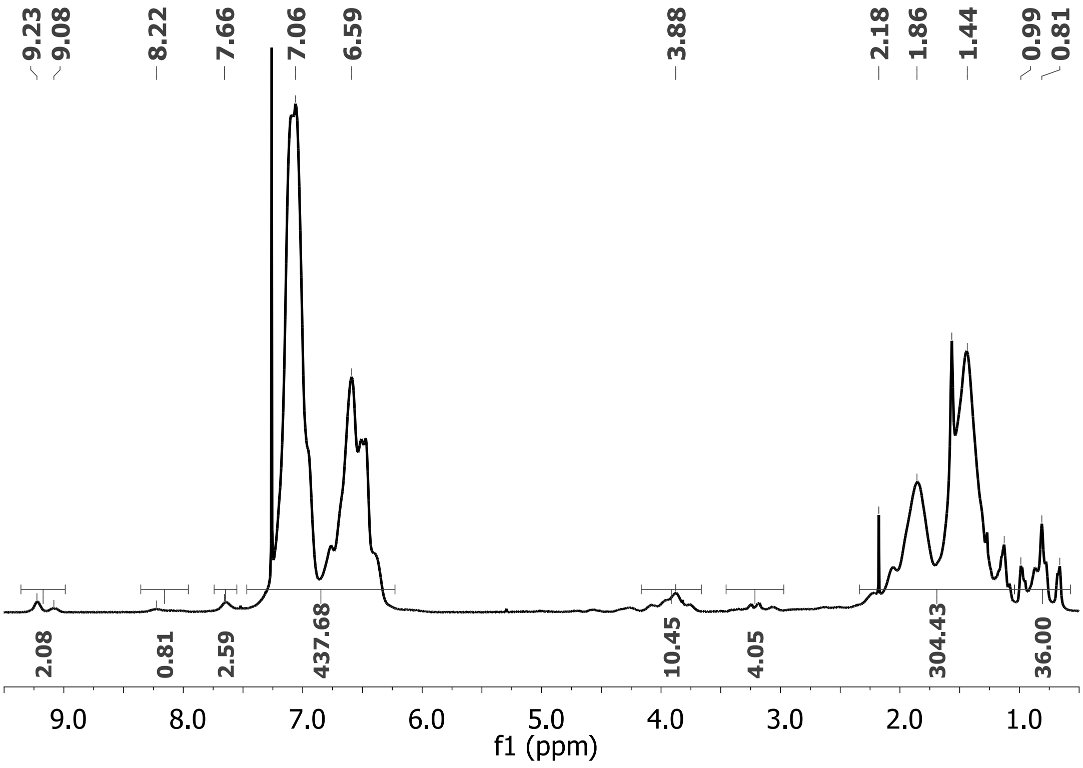

^{1}H NMR spectrum of **P43**, in CDCl$_3$.

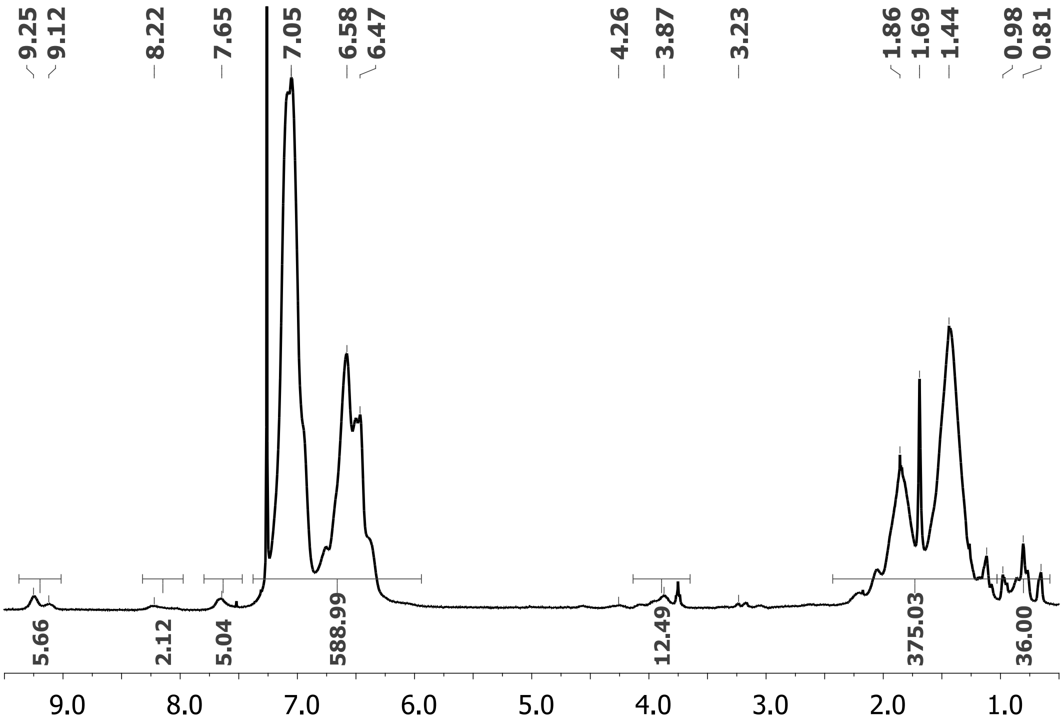

^{1}H NMR spectrum of **P44**, in CDCl$_3$.

Olga SISCAN

Single-chain technology using sequence-controlled precursors

Résumé

Dans cette thèse, de nouveaux systèmes macromoléculaires ont été conçus et synthétisés dans le but de former de nouvelles structures complexes basées sur des systèmes à chaîne polymère unique. Dans la première partie de ce projet, des chaînons contenant des groupements fonctionnels positionnés de manière précise ont été préparés avec succès dans le but de former des machines moléculaires de type rotaxane. Dans la seconde étude, des origamis macromoléculaires repliés ont été étudiés, et plus particulièrement des chaînes uniques à topologies complexes telles que des composés pseudocycliques ou noué. Ces topologies ont été obtenus en utilisant des ponts disulfures pouvant être positionnés à divers endroits de la chaîne polymère et grâce à des auto-associations intramoléculaires de type métal-ligand. Le placement des groupements fonctionnels et des ponts intramoléculaires dans les chaînes polymères a été rendu possible par le contrôle des séquences de monomères, en s'appuyant sur la cinétique de copolymérisation de monomères styrèniques (donneurs d'électrons) avec des monomères de type maléimides *N*-substitués (accepteurs). En effet, l'ajout de maléimides *N*-substitués à des temps contrôlés dans la chaîne de polystyrène en croissance, au moyen de techniques de polymérisations radicalaires contrôlées (vivantes) s'est avéré être une stratégie efficace et rapide pour la régulation de la séquence de monomères dans la chaîne polymère.

Mot clés : polymérisation en chaîne, compression de chaînes, polymérisation radicalaire contrôlée, approche cinétique, polymères à séquence contrôlée, contrôle de la topologie

Résumé en anglais

In this thesis, new macromolecular systems for single-chain technology were designed and synthesized. In the first study, tracks containing precisely positioned functional groups for single-chain rotaxane-based molecular machines were successfully prepared. In the second study, folded macromolecular origami were investigated, and specifically single-chain complex topologies such as pseudocyclic (Q-shaped) and knotted (α-shaped) using positionable disulfide bridges and intramolecular metal-ligand self-associations. The placement of functional moieties and intramolecular bridges in polymer chains was possible due to the monomer sequence control, by relying on the kinetics of copolymerization of donor styrenic monomer with acceptor *N*-substituted maleimide monomers. Indeed, time-controlled monomer additions of *N*-substituted maleimides into growing polystyrene chains by means of controlled/living radical polymerization techniques proved to be a convenient, rapid and scalable strategy for sequence regulation.

Keywords: chain-growth polymerization, compaction, controlled radical polymerization, kinetic approach, sequence control, sequence-controlled polymer, single-chain folding, topology control